STUDIES IN THE EXPRESSION AND MODULATION OF MUCOSAL ADDRESSIN CELL ADHESION MOLECULE-1 (MAdCAM-1)

Thesis submitted for the degree of Doctor of Philosophy

Aftab Ala MB BS FRCP

2010

Centre for Hepatology
Division of Medicine
UCL Medical School
Royal Free Campus
University College London

SUPERVISORS

Professor HJF Hodgson **DM, FRCP, FMedSci**
Sheila Sherlock Chair of Medicine
Centre for Hepatology
Division of Medicine
UCL Medical School
Royal Free Campus
University College London

Professor AP Dhillon **MA MD FRCP FRCPath**
Professor of Histopathology
Department of Cellular Pathology
Royal Free Hospital, London

Abstract

Introduction: The endothelial mucosal cell adhesion molecule (MAdCAM-1) is considered to be critically important in recruiting lymphocytes expressing the α4β7 cell surface integrin. In addition to its well-characterised role in the normal gastrointestinal tract, there is emerging evidence of its role in liver and gastrointestinal inflammation. The ability to detect MAdCAM-1 has thus far been challenging, hindering progress into studies to explore its modulation.

Aims*:* (i) To characterise MAdCAM-1 in the liver and gut, (ii) establish an *in vitro* model system of MAdCAM-1 and (iii) investigate the factors leading to its expression and subsequent modulation.

Methods: I have described novel methods of detecting MAdCAM-1 by:

1. Characterising its presence in the human liver, gut and associated tissues e.g. pancreas.
2. Developing a reverse transcriptase–polymerase chain reaction (RT-PCR) technique so as to detect MAdCAM-1 in the gastrointestinal system and thus quantify its expression using Real-Time RT-PCR analysis.
3. Developing an *in vitro* cell culture system using the endothelial SVEC4-10 cells to express and subsequently modulate the expression of MAdCAM-1.

Results: Using immunohistochemical methodology I found that in end stage chronic liver disease, MAdCAM-1 is expressed primarily on the peribiliary plexus and lymphoid aggregates, where it may facilitate lymphocyte egress. MAdCAM-1's constitutive expression was confirmed in histologically normal gut tissue and its upregulation was demonstrated in ulcerative colitis and Crohn's disease, particularly localised to the venular endothelium of the lamina propria and follicular dendritic cells. MAdCAM-1 mRNA from human gut was measured by a RT-PCR technique in which a 94 base pair product consistent with human mucosal vascular MAdCAM-1 was detected in normal large bowel. Real Time analysis confirmed that MAdCAM-1 was upregulated in end stage liver disease. In a cell culture system MAdCAM-1 was shown to be upregulated by TNFα on SVEC4-10 using immunofluoresence studies and its expression was further modulated by steroids and anti-sense oligonucleotides.

Conclusion: The importance of MAdCAM-1 in the gastrointestinal system is emphasised throughout. Our *in vitro* culture system utilising the SVEC endothelial cell line provides the basis for studying the modulation of MAdCAM-1 expression.

Ethical Approval

Approval for parts of the study involving human patients was obtained from The Royal Free Hospital, Ethics Committee

(Ethics ID 5441, Project ID 5441)

Acknowledgments

I am deeply indebted to my mentor Professor Humphrey Hodgson for supporting me. His guidance, knowledge, patience and wisdom have been invaluable before, during and after the project.

I wish to thank Professor Amar Dhillon for his enormous enthusiasm, supervision and expertise. I am thankful to David Brown, Korsa Khan and Ruth Jacobs for their invaluable laboratory assistance, advice, and experience, all members of the Centre for Hepatology, Royal Free Campus and Department of Histopathology for their assistance whenever it was needed. I also wish to thank Dr Joseph Odin, Dr Swann Thung and Dr Scott Friedman, for their help, advice and the use of laboratory space and materials during my Advanced Hepatology Fellowship 2003-4, at Mount Sinai Hospital Medical Center and Mount Sinai School of Medicine, New York, USA.

I am grateful to the Wellcome Trust, Digestive Diseases Foundation, The Tana Trust, The British Transplant Society and The St John's Ambulance Trust who supported me and the study.

Finally, I thank my family without whom none of this would have been possible.

Table of Contents

Abstract 1

Ethical Approval 4

Acknowledgments 5

List of figures 11

List of tables 14

Publications and presentations related to research 15

List of Abbreviations 16

Synopsis 19

Chapter 1 The role of cell adhesion molecules in leukocyte recruitment in the liver and gut 21 21

1.1 Background 22

1.1.1 Leukocyte trafficking 22

1.1.2 Adhesion molecules, cell trafficking & recruitment 23

1.1.2.1 Tethering and rolling 25

1.1.2.2 Activation of integrins 25

1.1.2.3 Firm adhesion and migration 27

1.1.3 Leukocyte migration into the liver and gut 27

1.2 Classes of cell adhesion molecules in the liver and gut 29

1.2.1 Selectins 29

1.2.1.1 E- selectin (expressed on endothelial cells) 31

1.2.1.2 P-selectin (expressed on endothelial cells and platelets) 31

1.2.1.3 L-selectin (expressed on leukocytes) 32

1.2.2 The Immunoglobulin (Ig) Superfamily 32

1.2.2.1 Intercellular adhesion molecule-1 and 2 (ICAM-1, ICAM-2) 34

1.2.2.2 Vascular cell adhesion molecule-1 (VCAM-1) 34

1.2.2.3 Platelet endothelial cell adhesion molecule-1(PECAM-1) 34

1.2.2.4 Mucosal addressin cell adhesion molecule-1 (MAdCAM-1) 35

1.2.2.4.1 Expression of MAdCAM-1 during development 36

1.2.2.4.2 Regulation of MAdCAM-1 expression 40

1.2.2.5 Carcinoembryonic antigen-related cell adhesion molecule (CEACAM-1) 41

1.2.3 Integrins 42

1.2.4 E-Cadherin 43

1.2.5 CD44 43

1.2.6 Vascular adhesion protein (VAP-1) 44

1.3 Chemokines 45

1.4 Regulation and synthesis of endothelial adhesion molecules 49

1.5 Adhesion molecules in gastrointestinal disease 50

1.5.1 Gastrointestinal infection 50

1.5.2 Coeliac Disease 51
1.5.3 Radiation enteritis 51
1.5.4 Inflammatory bowel disease 52
1.6 Entero-hepatic recirculation & extra-intestinal manifestations of IBD 54
1.6.1 Extraintestinal intestinal manifestations of IBD 54
1.7 Modulating adhesion molecule expression and therapeutic applications of anti-adhesion therapy in IBD 56
1.8 Adhesion molecules in liver disease 57
1.9 Liver allograft rejection 60
1.10 Ischaemia/Reperfusion 61
1.11 Aims of the Study 62
Chapter 2 MAdCAM-1 expression in the liver, gut and associated tissues 63
2.1 Overview of MAdCAM-1 expression in the gastrointestinal tract 64
2.2 Experiment 1: Morphological survey of MAdCAM-1 expression in the human liver 65
2.2.1 Background 65
2.2.2 Hypothesis and Aims 65
2.2.3 Material and Methods 66
2.2.3.1 Alkaline Phosphatase Anti-Alkaline Phosphatase (APAAP) methodology 67
2.2.3.2 Trilogy methodology as a form of antigen retrieval 67
2.2.3.3 Immunoperoxidase staining 68
2.2.3.4 Dendritic cell and lymphatic vessel staining 69
2.2.3.5 Immunofluoresence Microscopy 69
2.2.3.6 Immunohistochemical Assessment 70
2.2.4 Results 70
2.2.5 Discussion 80
2.3 Experiment 2: Expression of MAdCAM-1 in IBD 85
2.3.1 Background 85
2.3.2 Hypothesis and Aims 85
2.3.3 Methods 85
2.3.3.1 Immunohistochemistry 86
2.3.3.2 Morphometric analysis 86
2.3.4 Results 87
2.3.5 Discussion 92
2.4 Experiment 3: Expression of MAdCAM-1 in the human pancreas 96
2.4.1 Background 96
2.4.2 Methods 97
2.4.2.1 Morphological analysis 98
2.4.3 Results 98
2.4.4 Discussion 103

Chapter 3 Developing an *in vitro* model of MAdCAM-1 expression.....105

3.1 Overview 106

3.2 Developing an *in vitro* model of MAdCAM-1 expression (8 chamber well)..107

3.2.1 Background 107
3.2.2 Aims 107
3.2.3 Methods 108
3.2.3.1 SVEC, bEND cells and Culture Medium 108
3.2.3.2 Subculture procedure and trypsinising cells 108
3.2.3.3 Immunofluoresence staining of MAdCAM-1.....109
3.2.3.4 MAdCAM-1 and time course of its expression on SVEC and Bend.3.....110
3.2.3.5 Image Analysis 110
3.2.3.6 Statistical analysis.....110
3.2.4 Results 111
3.2.4.1 Cell viability 111
3.2.4.2 Morphology and immunofluoresence 111
3.2.4.3 Time course of MAdCAM-1 immunofluoresence induction by TNFα.....115
3.3 Developing an *in vitro* model of MAdCAM-1 expression (96 well plate).....117

3.3.1 Background 117
3.3.2 Aims.....116
3.3.3 Method..... 118
3.3.3.1 Image Analysis.....118
3.3.4 Results 119
3.3.5 Discussion..... 120

Chapter 4 Qualitative and Quantitative measurement of MAdCAM-1 expression in cells 122

4.1 Experiment 1: Development of a Reverse Transcriptase-Polymerase Chain Reaction (RT-PCR) assay to assess MAdCAM-1 expression in gastrointestinal tissues.....123

4.1.1 Background..... 123
4.1.1.1 Human and Mouse MAdCAM-1 123
4.1.1.2 Polymerase chain reaction 128
4.1.2 Aim 128
4.1.3 Methods 128
4.1.3.1 Reverse Transcription.....129
4.1.3.2 Polymerase Chain Reaction 130
4.1.3.4 Gel extraction of PCR DNA 131
4.1.3.4 DNA sequencing 132
4.1.4 Results 132
4.1.5 Discussion..... 135

4.2 Experiment 2: Developing a real time RT-PCR method to quantify gut and liver tissue MAdCAM- 1 137

4.2.1 Introduction - Real time PCR 137
4.2.1.1 Quantitation 137

4.2.2 Quantitation of Mouse tissue MAdCAM-1 mRNA by RT-PCR 138
4.2.2.1 Isolation of Total RNA from tissue 138
4.2.2.2 Reverse Transcription 139
4.2.2.3 Quantitative Polymerase Chain Reaction 139
4.2.3 Results 140
4.2.4 Discussion 141
4.3 Development and use of a Real Time PCR assay to quantify MAdCAM-1 mRNA in human disease 144
4.3.1 Isolation of Total RNA from tissue 144
4.3.2 Reverse Transcription 144
4.3.3 Quantitative Polymerase Chain Reaction 144
4.3.4 Results 149
4.3.5 Discussion 151
Chapter 5 Modulation of MAdCAM-1 expression 154
5.1 Overview 155
5.2 Experiment 1: Effect of modulating MAdCAM-1 using an *in vitro* model 156
5.2.1 Introduction 156
5.2.2 Methods 157
5.2.3 Results 157
5.2.4 Discussion 161
5.3 Experiment 2 Modulating mouse MAdCAM-1 expression using specific antisense oligonucleotides 163
5.3.1 Introduction 163
5.3.1.1 Binding to complementary mRNA 164
5.3.1.2 Utilization of *Rnase H* 164
5.3.1.3 Intracellular Anti-S degradation 164
5.3.1.4 Non-antisense effects 165
5.4 Methods 166
5.4.1 Generation and design of antisense oligonucleotides 166
5.4.2 Oligonucleotide treatment 167
5.4.3 Oligonucleotide Uptake in endothelial cells 167
5.4.4 Quantifying the effect of different oligonucleotides and varying concentrations on MAdCAM-1 expression 168
5.5 Results 169
5.6 Discussion 172
Chapter 6 General Discussion 176
6.1 Role and expression of MAdCAM-1 in tissues 177
6.2 Other observations on MadCAM-1 179
6.3 Detection of MAdCAM-1 expression in fluids 182
6.4 Potential of imaging MAdCAM-1 expression in inflammation 182

6.5 MAdCAM-1 as a therapeutic target 183
6.5.1 Modulating MAdCAM-1 and $\alpha 4\beta 7$ axis. 183
6.5.2 Modulating MAdCAM-1 using Anti-MAdCAM-1 antibodies 185
6.5.3 Modulating MAdCAM-1 protein synthesis: applications of oligonucleotides-silencing MAdCAM-1 RNA 186
6.5.4 Chemokines and emerging relationships with MAdCAM-1 and its modulation 188
6.5.5 VAP and its emerging relationship in the expression MAdCAM-1 190
6.5.6 Other MAdCAM-1 related targets 191
6.6 Future work 193
References 194

List of figures

Chapter 1

Figure 1.1 Transmigration of leukocytes through vascular endothelium

Figure 1.2 Adhesion molecules involved in leukocyte emigration

Figure 1.3 Schematic diagram adapted from Briskin et al (1996) demonstrating murine & human MAdCAM-1 superimmunoglobulin protein structure.

Figure 1.4 Ribbon drawing demonstrating Human MAdCAM-1 N-terminal 2 domain structure

Figure 1.5 Human MAdCAM-1 and its relationship with aspartate 42 and arginine 70

Figure 1.6 Expression of CCL25 and MAdCAM-1 in the human liver

Chapter 2

Figure 2.1 MAdCAM-1 immunoreactivity patterns in vessels and lymphoid aggregates from cirrhotic liver explants of PSC and PBC

Figure 2.2 Immunohistochemical localisation of the lymphatic phenotypic marker podoplanin in PSC and PBC

Figure 2.3 Dual immunofluoresence micrographs showing representations of MAdCAM-1, CD34 and CD 21 immunoreactivity

Figure 2.4 Immunohistochemical localisation of MAdCAM-1 in the gastrointestinal tract and inflammatory bowel disease

Figure 2.5 MAdCAM-1 immunoreactivity in inflamed colonic mucosa from a patient with advanced Crohn's disease

Figure 2.6 MAdCAM-1 immunoreactivity in venules in normal colon and uninvolved and highly inflamed gut in Crohn's disease

Figure 2.7 MAdCAM-1 immunoreactivity in venules in normal colon and in uninvolved and highly inflamed ulcerative colitis

Figure 2.8 Percentage of CD 34 positive vessels coexpressing MAdCAM-1 in IBD

Figure 2.9 MAdCAM-1 staining patterns of periductal and intra acinar capillary vessels in human pancreas using peroxidase methodology

Figure 2.10 APAAP methodology of immunostaining demonstrating pancreatic islet capillaries and islet cells primarily devoid of MAdCAM-1 with very weak expression within normal islet cells

Chapter 3

Figure 3.1a Phase contrast image analysis of SVEC4-10 endothelial cells at near confluence prior to stimulation with TNFα

Figure 3.1b Phase contrast image of bEnd.3 endothelial cells at near confluence, prior to stimulation with TNFα

Figure 3.2 Immunofluorescent staining of MAdCAM-1 on SVEC cells demonstrating MAdCAM-1 surface expression after 0-48 hours incubation with TNFα

Figure 3.3 Immunofluorescent staining of MAdCAM-1 on bEnd.3 cells demonstrating surface expression after 0-20 hours incubation with TNFα

Figure 3.4 Surface expression and time course of MAdCAM-1 after 20ng/ml TNFα stimulation of Bend.3 cells in an 8 chamber system.

Figure 3.5 Surface expression and time course of MAdCAM-1 after 20ng/ml TNFα stimulation of SVEC cells in an 8 chamber system

Figure 3.6 Surface expression of MAdCAM-1 from SVEC4-10 cells after 24 hours stimulation with varying doses of TNFα in a 96 well plate.

Chapter 4

Figure 4.1 Schematic diagram representing genomic organisation of the Human MAdCAM-1 gene and comparisons with the Mouse homologue on Chromosome 19 (p13.3) close to ICAM-1/3 genes (p13.2-p13.3)

Figure 4.2 Human MAdCMA-1 cDNA

Figure 4.3 Identification of human MAdCAM-1

Figure 4.4 Electrophoretogram and sequence of human MAdCAM-1 using specific PCR primer sequences

Figure 4.5 Relative expression of MAdCAM-1 in mouse tissues.

Figure 4.6 The fluorescence profile for the standard concentrations of Human MAdCAM-1 DNA using real time PCR

Figure 4.7 A standard curve for the serial dilutions of MAdCAM-1

Figure 4.8 Expression of MAdCAM-1 mRNA in the human liver as determined by real-time PCR

Chapter 5

Figure 5.1 The dose response studies on the effect of stimulating a monolayer of SVEC4-10 cells with Interleukin 1L-1β(1-100ng/ml) or LPS (1-500ng/ml) compared to 20ng/ml TNFα

Figure 5.2 The effect of different doses of dexamethasone and hydrortisone on mouse SVEC4-10 cells pre-stimulated with 20ng/ml mouse TNFα

Figure 5.3 The effect of 5-ASA and IL-10 on SVEC4-10 endothelial cells stimulated with 20ng/ml TNFα

Figure 5.4 Uptake and intracellular localisation of Antisense Oligonucleotides

Figure 5.5 The Effect of Antisense Oligonucleotides on MAdCAM-1 expression

List of tables

Table 1.1 The ligands, localisation, expression and functions of the selectins

Table 1.2 Adhesion super immunoglobulin glycoproteins involved in leukocyte-endothelial interactions in the liver and gut

Table 2.1 Primary sclerosing cholangitis MAdCAM-1 immunostaining

Table 2.2 Primary Biliary Cirrhosis MAdCAM-1 immunostaining

Table 2.3 Alcohol liver disease MAdCAM-1 immunostaining

Table 2.4 Hepatitis C and MAdCAM-1 immunostaining

Table 2.5 Differential MAdCAM-1 expressions on vascular endothelium in normal gut and IBD gut

Table 2.6 MAdCAM-1 immunoreactivity in normal pancreas, pancreatic carcinoma and chronic pancreatitis

Table 4.1 Design of MAdCAM-1 Oligonucleotide Primers

Table 4.2 Real time RT-PCR methodology to quantify levels of mouse MAdCAM-1/18S RNA expression in different mouse tissues(n=1)

Table 4.3 Human hepatic MAdCAM-1 cDNA assay from normal liver tissues and a range of liver diseases

Publications and presentations related to research

Articles

1. Ala A, Dhillon AP, Hodgson HJ. 2003. Role of cell adhesion molecules in leukocyte recruitment in the liver and gut. *Int J Exp Pathol* 84:1-16.

Abstracts

1. Ala A, Standish R Khan K, Prasad N, Hillon K, Hodgson HJF, Dhillon AP. Expression of the Mucosal Addressin Cell Adhesion molecule-1 (MAdCAM-1) in Primary Sclerosing Cholangitis and Primary Biliary Cirrhosis. American Association Study of Liver Disease (AASLD). Basic Research Single Topic Conference. The Pathobiology of the Biliary Epithelia. Virginia, USA. June 2001. *(Awarded Poster of Distinction).*
2. Ala A, Standish R, Khan K, Hillon K, Dhillon AP, Hodgson HJF. 2002. Mucosal addressin cell adhesion molecule-1 and podoplanin localisation in primary sclerosing cholangitis and primary biliary cirrhosis. MAdCAM-1 in PSC and PBC. *Journal of Hepatology*. 36(1). *(Young Investigators Award-European Association for the Study of Liver Diseases)*
3. Ala A, Brown D, Stubbs M, Hodgson HJ. 2001. An *in vitro* model of MAdCAM-1. Cell adhesion molecules in health and disease. Falk symposium, Berlin, Germany.(Poster and Travel Award)
4. Ala A, Brown D, Stubbs M, Jacobs R, Hodgson HJ. 2003. Mucosal addressin cell adhesion molecule in chronic liver disease and development of an *in vitro* model to investigate therapeutic modulation. *Hepatology* 38 (suppl i), 648A
5. Ala A, Stubbs M, Coward S, Brown D, Hodgson HJ. 2003. Characterisation of mucosal addressin cell adhesion molecule in inflammatory bowel disease. Gut 52 (suppl i)A121*(BSG Annual Scientific Meeting, Glasgow Poster Plenary)*
6. Ala A, Brown D, Hodgson HJ. Studies in the expression and modulation of MAdCAM-1. British Society of Gastroenterology and American Gastroenterology Association Symposium. Gastrointestinal Inflammation. Oxford. Poster Plenary, September 2004.

List of Abbreviations

aHSCT	Allogeneic hematopoietic stem cell transplantation
AIH	Autoimmune hepatitis
ALD	Alcohol Liver Disease
Anti-S	Antisense oligonucleotide
APAAP	Alkaline Phosphatase Anti-Alkaline Phosphatase
APES	3-aminopropy triethoxysiline
5ASA	5Aminosalicylic acid
AS1-4	Antisense oligonucleotides 1-4
AT1R	Angiotensin II type 1 receptor
BGP-I	Biliary glycoprotein1
Bp	Base pairs
CEACAM-1	Carcinoembryonic antigen-related cell adhesion molecules
CCL	CC-Chemokine ligand
CCR	CC-Chemokine receptor
CD	Crohn's Disease
CNS	Central nervous system
CXCL	CXC-Chemokine ligand
CXCR	CXC-Chemokine receptor
DNA	Deoxyribose nucleic acid
dNTP's	Deoxy-nucleotide-triphosphates
DMEM	Dulbecco's Modified Eagle Medium
EAE	Experimental autoimmune encephalomyelitis
E-cadherin	Endothelial cadherin
EDTA	Ethylenediaminetetraacetic acid
ELISA	Enzyme-linked immunosorbent assay
E-Selectin	Endothelial Selectin
FCS	Fetal Calf Serum
FITC	Fluorescein Isothiocyanate
GALT	Gut-associated lymphoid tissue
GCSF	Granulocyte colony stimulating factor
HBV	Hepatitis B virus

HCV	Hepatitis C virus
HEC	Hepatic endothelial cells
HEV	High endothelial venules
HIMEC	Human intestinal microvascular endothelial cells
HRP	Horseradish Peroxidase
HUVEC	Human umbilical vein endothelial cells
H_20_2	Hydrogen peroxide
IBD	Inflammatory bowel disease
ICAM-1,-2,-3	Intracellular adhesion molecule-1,-2,-3
IDDM	Insulin dependent diabetes mellitus
IELs	Intraepithelial lymphocytes
IFNγ	Interferon gamma
Ig	Immunoglobulin
IL	Interleukin
IL-1	Interleukin -1
IL-10	Interleukin-10
LFA-1	Leukocyte function associated antigen-1
LPAM	lymphocyte Peyer's patch adhesion molecule integrin $\alpha_4\beta_7$
LPL	Lamina propria lymphocytes
LPS	Lipopolysaccharide
L-selectin	Leukocyte – selectin
MAdCAM-1	Mucosal addressin cellular adhesion molecule-1
MALT	Mucosa associated lymphoid tissue
MB	Microbubbles
MEC	Mucosal-associated epithelial chemokine
mRNA	Messenger ribose nucleic acid
NK	Natural killer cells
NF-κβ	Nuclear factor kappa-β
NO	Nitric oxide
NOD	Non-obese diabetic mice
OLT	Orthotopic liver transplant
PBC	Primary Biliary Cirrhosis
PBP	Peribiliary plexus

PCR	Polymerase chain reaction
PECAM-1	Platelet endothelial cellular adhesion molecule -1
P13K	Phosphoinositide 3-kinase
PSC	Primary Sclerosing Cholangitis
PKC	Protein Kinase C
PLN	Peripheral lymph node
PNAd	Peripheral lymph node addressin
PP	Peyer's patches
P-selectin	Platelet-selectin
RA	Retinoic acid
RT-PCR	Reverse Transcriptase Polymerase Chain Reaction
RNA	Ribosenucelic acid
SV40	Simian Virus 40
S.D.	Standard Deviation
SFM	Serum free media
TBS	Tris –buffered saline
TECK	Thymus-expressed chemokines
TNFα	Tumour necrosis factor α
TNBS	Trinitrobenzesulfonic acid
TRIS	Tris (hydroxymethyl) aminomethane
UC	Ulcerative Colitis
UTR	Untranslated region
VAP-1	Vascular adhesion protein-1
VCAM-1	Vascular cellular adhesion molecule-1

Synopsis

Chapter 1 acts a general introduction to adhesion molecules, leukocyte recirculation and the role of adhesion molecules in the pathogenesis of diseases affecting the closely related tissues of the liver and gut, which offer novel opportunities for treatment. The focus of attention is mucosal addressin cell adhesion molecule (MAdCAM-1) as this is now considered to be the major adhesion molecule involved in directing leukocytes to the gut and related tissues.

Chapter 2 describes the detection of MAdCAM-1 in liver disease, inflammatory bowel disease (IBD) and pancreatic disease. The liver disease included primary sclerosing cholangitis and those unrelated to gut inflammation e.g. primary biliary cirrhosis, alcoholic liver disease and hepatitis C. Immunohistochemistry was used to characterise the specific MAdCAM-1 immunoreactivity patterns in endothelium lined vessels and lymphoid aggregates. Blood vessel endothelium expresses MAdCAM-1 in immune mediated chronic cholestatic diseases (PBC and PSC). The expression of MAdCAM-1 in vascular beds of the peribiliary plexus and lymphoid aggregates in end-stage liver cirrhosis of PSC and PBC may contribute to the localisation and recruitment of $\alpha 4\beta 7$ lymphocytes to the bile ducts during the pathogenesis of these conditions. Furthermore, there was lack of MAdCAM-1 in pre-cirrhotic liver tissues. The differential expression of MAdCAM-1 in IBD unrelated to liver disease is also described, where the findings confirm the upregulation of MAdCAM-1 venules in IBD and shows Crohn's disease to be characterised by MAdCAM-1 venules in the deeper layers of the intestinal tissue, reflecting the transmural nature of the inflammation.

Chapter 3 describes the development of an in vitro model of MAdCAM-1 expression utilising the murine endothelial cell lines SVEC4-10 and bEND3 to investigate mechanisms leading to its upregulation and detection of expression using immunofluoresence. TNF-α stimulation caused MAdCAM-1 upregulation, demonstrated with a dose response curve and time course analysis. Maximal MAdCAM-1 expression occurred at 24 and 72 hours after stimulating bEND3 and SVEC4-10 cells respectively.

Chapter 4 describes the development of reverse transcriptase polymerase chain reaction (RT-PCR) of murine and human MAdCAM-1 in cell culture and tissues MAdCAM-1 was present constitutively in histologically normal gut tissues. Real time RT-PCR allowed quantification of MAdCAM-1 mRNA and confirmed its upregulation in end stage cirrhotic liver tissues. Therefore, the ability to detect the presence of MAdCAM-1 and quantify its expression could be useful in the diagnosis and management of other chronic inflammatory diseases e.g. IBD.

Chapter 5 studies the effect of modulating MAdCAM-1 using the SVEC 4-10 cell culture system (previously described in chapter 3). The model allowed efficient testing of specifically designed strategies to modulate expression MAdCAM-1 in an *in vitro* setting. Such potential strategies include administration of anti-inflammatory cytokines such as IL-10, dexamethasone, and anti-sense oligonucleotide sequences targeted to MAdCAM-1. The principles underlying antisense therapies and their utility as potential therapeutic targets are described.

Chapter 6 discusses the overall contribution of MAdCAM-1 to gastrointestinal inflammation thus far and the role of existing and newer agents to its modulation.

Chapter 1

The role of cell adhesion molecules in leukocyte recruitment in the liver and gut

1.1 Background

This chapter summarises the evidence that adhesion molecules (including MAdCAM-1) are critical in lymphocyte recirculation and pathogenesis of diseases affecting the closely related tissues of the liver and gut, which offer novel opportunities for modulation and treatment.

1.1.1 Leukocyte trafficking

Leukocytes continuously recirculate between the blood and tissues. They traffic to organs and subsequently leave the circulation via lymph nodes. Some are naïve, others have been programmed to recognise antigens and interact with endothelium and thus disseminate preferentially (i.e. "home") to the site of original antigen exposure.

In the absence of inflammation, circulating virgin leukocytes traffic preferentially in a physiological circulation to secondary lymphoid tissue e.g. lymph nodes, spleen and gut-associated lymphoid tissue (GALT), where requirements for effective antigen presentation and differentiation are fulfilled. The exit from the blood mainly takes place in unique post-capillary venules high endothelial venules (HEV) (Girard *et al* 1995). These are near-cuboidal cells displaying functional modifications to facilitate leukocyte extravasation. Migration through HEV's appears to be very specific. Leukocytes circulating in the blood are able to discriminate between the HEV endothelium and endothelium lining non-lymphoid tissues. It has been estimated that approximately 1.4 x 10^4 lymphocytes extravasate from blood into a single lymph node via HEV's every second and that 25% of lymphocytes circulating in HEV's will bind and emigrate (Butcher *et al* 1991). If lymphocytes are presented with antigens, they proliferate by clonal expansion. Lymphocytes can exit from lymphoid tissues via efferent lymphatics to re-enter the systemic circulation.

When tissues become inflamed, leukocytes including lymphocytes are recruited to those sites. The mechanisms of recruitment involve combinations of molecules expressed on the leukocytes and on the endothelium. Addressins are key partners in these processes, being tissue molecules that provide a unique molecular address, allowing leukocytes expressing the corresponding molecular ligands to target to particular organs (Vidal-

Vanaclocha *et al* 1993) (Salmi *et al* 1998). Granulocytes and monocytes also emigrate from the blood stream in response to molecular changes on the surface of blood vessels that signal injury or infection; they cannot recirculate. The processes governing emigration of cells from the circulation into tissues were first defined for neutrophils, but similar processes pertain for lymphocyte homing as well, although the latter process is more complex.

1.1.2 Adhesion molecules, cell trafficking & recruitment

Adhesion molecule is a general term for the molecules involved in the recruitment process, which are surface bound glycoprotein molecules expressed on leukocytes and/or endothelial cells. They share common characteristics acting as a molecular link between the external and internal milieu of the cell. They are all trans-membrane proteins with different domains, the largest of which is extracellular, attached to an intra-membranous segment linked to a cytoplasmic functional domain, through which they can influence cell function e.g. modulating the cytoskeleton of the cell and activating secondary messenger systems.

The molecular mechanisms of leukocyte extravasation are well characterised in a "multistep paradigm" *(Figure 1.1 and 1.2)*. This describes the overall process of extravasation as a three-step mechanism consisting of i) tethering and rolling of leukocytes on the endothelium ii) activation of integrins iii) firm adhesion and transmigration.

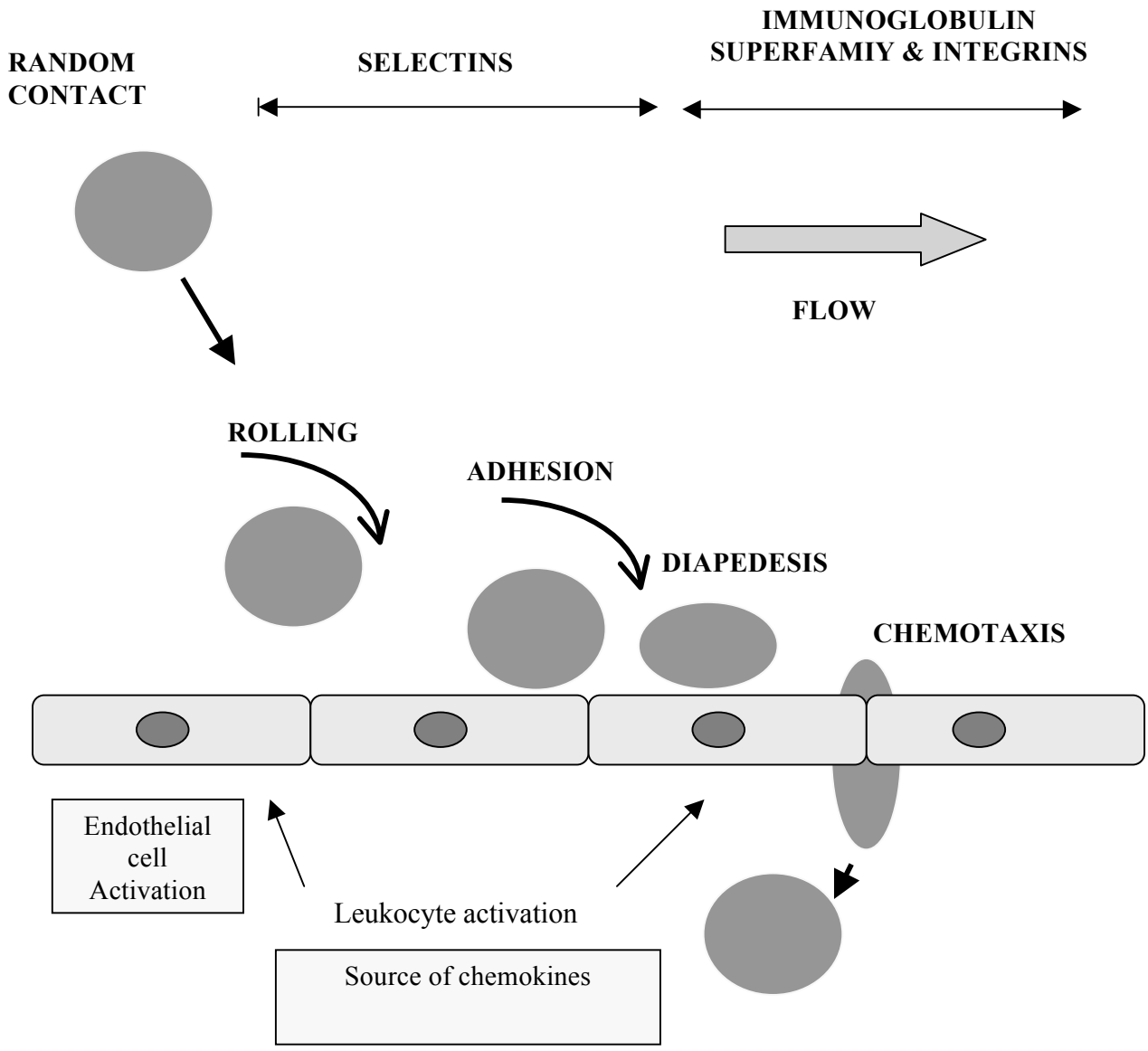

Fig 1.1 Transmigration of leukocytes through vascular endothelium. Normally, there is random contact between leukocytes and vascular endothelium. However, following vascular endothelium activation, leukocytes roll on to it, adhere and transmigrate between the endothelial cells to reach the areas of inflammation.

The main classes of adhesion molecules are integrins, selectins, and cadherins. As already mentioned, endothelial adhesion molecules with a dominant role in tissue-specific migration are often called "vascular addressins"; their counter-receptors on leukocytes are called "homing receptors". Cells can express adhesion molecules constitutively (e.g. endothelial cells of the HEV in lymph nodes), or up-regulate them on exposure to cytokines, chemokines, or other pro-inflammatory molecules such as activated complement products and microbial metabolites. There are several families of adhesion molecules, which participate variously in immune and inflammatory processes, based on structure, function, and location.

1.1.2.1 Tethering and rolling

Blood borne leukocytes are displaced from the central flow of the vessel, largely in regions of the microvasculature i.e. post-capillary venules. These tethering contacts lead to cells rolling at an estimated velocity of 10-50μm/s, slower than the erythrocyte which is typically 4000μm/s (Springer 1990). Adhesion molecules called selectins mediate these readily reversible contacts, controlling both tethering and rolling (Pachynski *et al* 1998). These molecules are constitutively active and presented on the tip of microvillus projections, considerably higher than the planar surface, making them suitable candidates for initial contacts. The patterns of leukocyte recirculation depend upon the combinations of molecules expressed on the leukocyte and the combinations of addressins and other molecules providing individual tissues with a unique molecular address.

1.1.2.2 Activation of integrins

The integrin activation step is thought to involve binding of chemotactic cytokines (called chemokines) immobilized by glycoaminoglycans on the endothelial glycocalyx (Gunn *et al* 1998). Chemokines binding to specific G protein–coupled receptors on the lymphocyte trigger cytoskeletal rearrangement and thus activation of the leukocyte. The lymphocyte is therefore able to bind to the endothelium, resist the high shearing forces imposed on it and stop within the vessel (Berlin *et al* 1993).

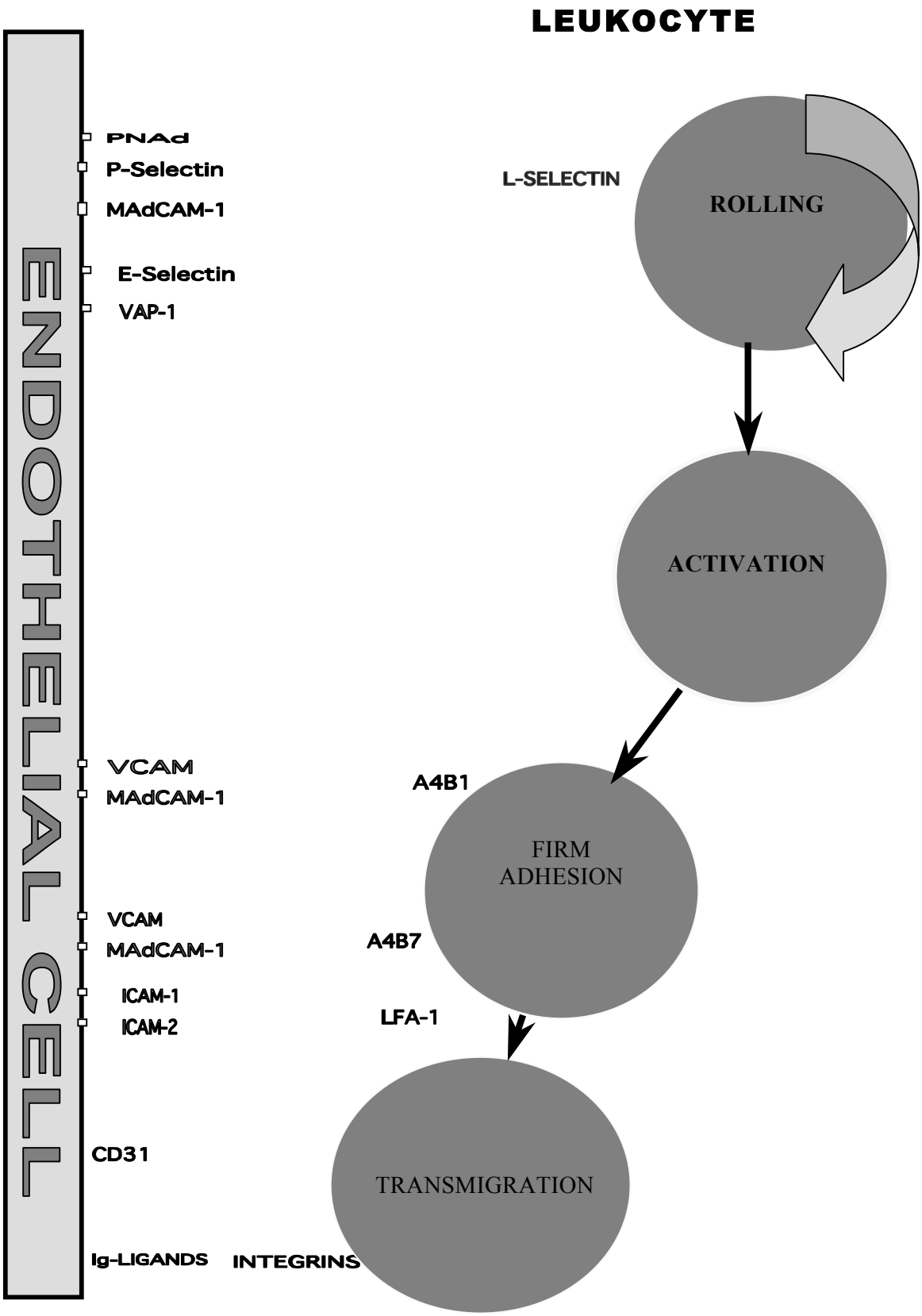

***Figure 1.2** Adhesion molecules involved in leukocyte emigration*

1.1.2.3 Firm adhesion and migration

The "stable" cell then seeks inter-endothelial cell junctions through which it can migrate within tissues and adhesion molecules expressed on the surface of endothelial cells ensure orderly sequence of cell-cell interactions.

1.1.3 Leukocyte migration into the liver and gut

The gut has a specialised immune system appropriate to its exposure to the major antigen challenge from the lumen, consisting of food products and bacteria. Antigen enters intestinal mucosa via 'M' (microfolded) cells, the specialised epithelium above the lymphoid follicles. Peyer's patches represent organised lymphoid structures, appearing different from lymphoid follicles because they lack afferent lymphatics. Within Peyer's patches the mucosal immune response is initiated by the uptake and processing of antigenic material by macrophages, follicular dendritic cells and its presentation to T and B cells. Here, lymphocytes bind to specialised HEV's. If the naïve lymphocyte is not exposed to antigen it leaves Peyer's patches and returns into the systemic circulation via efferent lymphatics. However, if the lymphocyte makes contact with its antigen it divides and differentiates into effector or memory cells. These immunoblasts are transported via the lymphatics into mesenteric lymph nodes and eventually into the blood with wide dispersion throughout the body.

The liver shares a common embryological origin with the gut (from the endoderm), and it too has a distinct endothelial phenotype characterised by expression of several adhesion molecules. Furthermore, the liver like the gut epithelium is an important site of exposure to foreign antigens, particularly through the portal vein and thus needs to be able to respond efficiently to pathogens. Mechanisms by which the liver may modify gut-derived antigens range from conceptually simple filter functions of the reticulo-endothelial system to complex processes such as induction of systemic tolerance.

The resident leukocytes within normal liver include natural killer lymphocytes and a large number of functional memory/effector T cells which are removed from the circulation by the liver and continue to provide ongoing immune surveillance. Common mechanisms for leukocyte homing to both the gut and liver would make good sense in

evolutionary terms as the first port of call for the blood from the gut carrying nutrients (and potentially hazardous compounds), is the liver. However, unlike the gut, lymphocyte recirculation in the liver is less well defined and the exact route of entry for lymphocytes into portal tracts remains unclear.

There are three vascular routes by which T cells may enter the liver. Firstly, via portal vessels in the portal tracts; secondly, directly into the parenchyma from the hepatic sinusoids and finally via the central vein of the lobule. The sinusoids comprise a unique vascular bed which has a low velocity blood flow and which unlike other vascular beds does not require capture mediation by selectins. Lymphocytes are seen in portal tracts in the normal liver and heavy infiltration is observed in inflammatory liver diseases e.g. Hepatitis C. The portal vessels empty into sinusoids but do not normally appear to have morphological evidence of post-capillary venules (high endothelial venules). However, the presence of new vessels at sites of lymphocytic infiltration is intriguing. These vessels appear to have phenotypic similarities with high endothelial venules; they have been described within portal tracts in chronic viral hepatitis where they could facilitate the recruitment of lymphocytes and may be important in regulating T-cell recirculation to the liver (Garcia-Monzon *et al* 1995).

1.2 Classes of cell adhesion molecules in the liver and gut

1.2.1 Selectins

The selectin family consists of three closely related cell-surface molecules: P-selectin, E-selctin and L-selectin The selectin family shares a common mosaic structure consisting of a lectin, carbohydrate and single epidermal growth factor-like domains, including a series of 2-9 short repeats similar to those found in complement regulatory proteins. The lectin domain is the central structure of the molecule concerned with receptor binding because it interacts efficiently with molecules containing fucosylated, sialylated and related sulphated carbohydrate ligands (Lasky 1995). Selectin function is uniquely restricted to the vascular system and expression of individual selectins varies in the different inflammatory conditions summarised in *Table 1.1*

The ligands for selectins are glycoproteins and include P-selectin glycoprotein-1 (PSGL-1), E-selectin ligand-1 (ESL-1) and CD44. Both ESL-1 and CD44 are ligands for E-selectin. Glycosylation-dependant cell adhesion molecule-1(GlyCAM-1) and CD34 are both members of the peripheral node addressin family (PNAd) which serve as ligands for L-selectin. Mucosal addressin cell adhesion molecule-1 (MAdCAM-1), a member of the immunoglobulin superfamily, may also serve as a ligand for L-selectin, when it is appropriately glycoslyated. Specifically, PSGL-1 has the ability to bind to all three selectins when appropriately glycosylated; binding of PSGL-1 to L-selectin (both expressed on leucocytes) can mediate a secondary tethering process, so that leucocytes expressing PSGL-1 can adhere to leukocytes already rolling on L-selectin.

Table 1.1 The ligands, localisation, expression and functions of the selectin family

Selectin (Receptor)	Ligand(s)	Location	Expression	Functions
E-selectin	E-selectin ligand-1 (ESL-1), CD44, cutaneous lymphocyte ligand (CLA)	Vascular endothelial surface	Transcriptionally induced by pro-inflammatory mediators and LPS	Eosinophils, neutrophils and monocyte adhesion during acute inflammation. Facilitates migration of T cells to skin
P-selectin	P-selectin glycoprotein-1 (PSGL-1)	Plateletα granules & endothelial cell Weibel-Palade bodies	Granule/plasma membrane fusion in response to thrombin, histamine,substance P	Eosinophils, neutrophils monocytes, adhesion during acute inflammation and thrombosis
L-selectin	Peripheral node addressin (PNAd), MAdCAM-1	Leukocytes	Expressed until leukocytes are activated, then shed	Acute neutrophil mediated inflammation, peripheral lymph node homing

1.2.1.1 E- selectin (expressed on endothelial cells)

E-selectin is also known as endothelium leukocyte molecule ELAM-1 or CD62E. E-selectin is barely expressed by the inactivate endothelium, but its expression is upregulated during inflammation when vascular endothelium becomes activated by pro-inflammatory cytokines or lipopolysaccharides. As well as facilitating the emigration of leukocytes into tissues, most notably neutrophils, it also promotes adhesion of resting CD4 memory cells to activated endothelium (Shimizu *et al*. 1991). Interferon γ (IFNγ) appears to stabilise E-selectin expression without prolonging its duration of synthesis (Doukas *et al* 1990).

While the majority of endothelial cell surface E-selectin is thought to be removed from the cell surface by internalisation, some of it is shed in a circulating soluble form (Patel *et al* 1995). The expression of E-selectin as a circulating soluble adhesion molecule is up-regulated by transcription from TNF-α, IL-1 and LPS in inflammatory bowel disease (IBD).

E-selectin is not expressed in the normal liver. (Bevilacqua *et al*. 1989). However, during endotoxaemia or septic shock its mRNA expression is seen in large vessel endothelial cells but also to a lesser degree on the sinusoidal lining (Adams *et al* 1994). Similar induction is found in liver from alcoholic hepatitis, primary biliary cirrhosis (PBC) and acute allograft rejection (Mueller *et al.* 1996) (Wong *et al.* 1997).

1.2.1.2 P-selectin (expressed on endothelial cells and platelets)

P-selectin is stored in Weibel–Palade bodies of endothelial cells and produced by alpha granules of platelets (Diacovo 1996). It is released after activation of platelets with histamine or thrombin, during clotting and mediates adhesion between leukocytes and platelets. During inflammation, endothelial P-selectin acts to recruit leukocytes into postcapillary venules, while platelet associated P-selectin promotes aggregation of leukocytes with platelets to form thrombi. Endothelial cells can also synthesise and express P-Selectin in response to endotoxin or cytokines. However, important species differences have been observed in response to these stimuli. TNF α and endotoxin increase expression of P-selectin in murine endothelial cells, but do not do so in human

endothelial cells (Gotsch *et al.* 1994). This differential response may be related to differences in the P-selectin promoter among species. (Weller *et al* 1992)

1.2.1.3 L-selectin (expressed on leukocytes)

The majority of B cells, virgin T cells, most neutrophils, monocytes and eosinophils express L-selectin (also known as LECAM-1, LAM-1, Mel-14 antigen, $gp90^{mel}$, and Leu8/TQ-1 antigen). L-selectins are the smallest of the vascular selectins and are important in lymphocyte homing and adhesion to high endothelial venules of peripheral lymph nodes contributing largely to the capture of leukocytes during the early phases of the cell adhesion cascade (Berg et al 1993) (Collett *et al* 1999). The broad expression of L-selectin explains its critical role in the trafficking of all leukocyte lineages into secondary lymphoid tissues and peripheral sites of injury and inflammation. Following capture, L-selectins are shed from the leukocyte surface after chemo-attractant stimulation, which limits the ability of these cells to roll on endothelial cells. They have been implicated in the binding and tethering of neutrophils to activated endothelium via different vascular adhesion molecules (Sitrin *et al* 2001). Interferon α is the only cytokine reported to increase surface density of L-selectin, correlating with increased m-RNA levels (Evans *et al* 1993).

1.2.2 The Immunoglobulin (Ig) Superfamily

The Ig superfamilies are calcium independent transmembrane glycoproteins. Each Ig superfamily has extra-cellular domains, which contains several Ig-like disulphide bonded loops with condensed cysteine residues, a transmembrane and an intracellular domain, which interacts with the cytoskeleton. The Ig superfamily includes ICAM-1, ICAM-2, VCAM-1, and MAdCAM-1 *(Table 1.2)*. All members of this family are expressed or inducible on vascular endothelium and only ICAM-1 and ICAM-2, very rarely VCAM (but not MAdCAM-1) may also be expressed by leukocytes.

Table 1.2 Adhesion super immunoglobulin glycoproteins involved in leukocyte-endothelial interactions in the liver

ADHESION MOLECULE	ALTERNATIVE NAME	LOCALISATION	CONSTITUTIVE	INDUCIBLE	LIGAND	FUNCTION
ICAM-1	CD54	Endothelium	Yes	Yes	LFA-1 Mac-1 CD43	Adherence/Emigration
VCAM-1	CD106	Endothelium	Very small	Yes	VLA-4	Adherence
MAdCAM-1		Endothelium	Yes (gut only)	Yes	Lselectin $\alpha 4\beta 7$	Adherence/Emigration

1.2.2.1 Intercellular adhesion molecule-1 and 2 (ICAM-1, ICAM-2)

Both ICAM-1 and ICAM-2 are receptors for LFA-1. They are either constitutively present on capillary endothelium or may be induced by the cytokines TNFα, IL-1, IFN-γ and LPS (Ayers *et al* 1993). ICAM-1 is also expressed on activated T cells, B cells, and monocytes. In these cells ICAM-1 contributes to the adhesion between interacting lymphocytes, and between lymphocytes and antigen presenting cells or other target cells. ICAM-1 may be up-regulated at sites of immune reaction where it controls the enhanced movement of lymphocytes into sites of inflammation. ICAM-1 binds to the β2 integrins, lymphocyte function-associated antigen-1 (LFA) and also has a binding site for certain viruses e.g. rhinovirus (Tian *et al* 1997).

1.2.2.2 Vascular cell adhesion molecule-1 (VCAM-1)

VCAM-1 appears to be important in controlling lymphocyte migration. VCAM-1 is less widely distributed than ICAM-1 and is expressed by germinal centre dendritic cells, interdigitating cells, Kupffer cells, synovial lining cells and renal proximal tubule cells. VCAM-1 is induced on the endothelium by cytokines with a similar time course to E-selectin showing maximal transcript levels for both VCAM-1 and E-selectin at 3-6 hours with a decline to low, constitutive levels of expression at 48 hours (Fries *et al* 1993). VCAM-1 is primarily involved in lymphocyte and monocyte-endothelial cell interactions and binds to an integrin of the VLA4 class expressed on all leukocytes except neutrophils. T cell activation leads to kinase-induced conformational changes of VLA-4, increasing the avidity of binding with VCAM-1.

1.2.2.3 Platelet endothelial cell adhesion molecule-1(PECAM-1)

PECAM-1 is found on platelets, leukocytes and endothelial cells. Its expression is stimulated by cytokines e.g. TNFα, IL-1 and IFN-γ (Bujan *et al* 1999). Endothelial cells express PECAM-1 on their lateral cell membranes. This distribution suggests three main functions involvement in endothelial cell junction, mediation of leukocyte movement between endothelial cells and binding of platelets to injured endothelium.

1.2.2.4 Mucosal addressin cell adhesion molecule-1 (MAdCAM-1)

Human MAdCAM-1 is a 60-kDa endothelial cell adhesion molecule, which combines two immunoglobulin-like domains and a mucin like region between Ig domain 2, and the endothelial surface *(Figure 1.3)* (Tan *et al* 1998) (Streeter *et al* 1988). It can bind two distinct lymphocyte receptors, L-selectin and the α4β7 integrin (Erle *et al* 1994). Thus, within Peyer's patches MAdCAM-1 is covered with unique oligosaccharide determinants, which allow it to serve as a ligand to L-selectin and mediate rolling of naïve lymphocytes. This is in contrast to the vasculature of the lamina propria where initial rolling interactions between activated lymphocytes and endothelial cells are apparently mediated by binding of α4β7 and immunoglobulin like domains of MAdCAM-1 *(Figure 1.3).*

In the study by Dando *et al* (2002) a dimeric form of MAdCAM-1 was observed created by two symmetry-related full-length molecules within the srystal lattice, through an extensive interface formed by residues from the edge of a B-sandwich in domain 1. Such edge-to-edge dimerisations of Ig domains have also been reported for human ICAM-1. In addition the fact that the two Ig domains of MAdCAM-1 project approximately 22nm away from the cell surface by an extended domain indicates that there are no steric restrictions for the formation of a dimmer. It is interesting to note that the arginine (Arg)70 residue important for integrin recognition also contributes to the formation of the MAdCAM-1 via formation of bifurcated charged hydrogen bonds across the dimmer interface. *(Figures 1.4 and 1.5).* Mutational analysis experiments that identified the significance of (Arg)70 in integrin binding might suggest that the diminished integrin binding of the mutants could well be a consequence of dimeric structure discruption, thus suggesting that the arrangement of MAdCAM-1 in a dimeric form is essential for activity.

MAdCAM-1's important role is in regulating lymphocyte trafficking to both normal and inflamed mucosal tissues, specifically in the maintenance of mucosal immunity and the regulation of inflammation of the gastrointestinal tract (Briskin *et al* 1997). It has been shown to participate in directing lymphocyte traffic into the lamina propria of the small and large intestine, the inflamed pancreas and the lactating mammary gland. Its constitutive expression is restricted to endothelium lining a subset of blood vessels and

mucosal associated lymphoid tissue in stomach, small intestine, large bowel, pancreas, marginal zone of the spleen, inflamed choroid plexus and gall bladder (Auth *et al* 1993).

1.2.2.4.1 Expression of MAdCAM-1 during development

Up to 20% of thymocytes are CD4 or CD8, reacting with soluble MAdCAM-1, via α4β7. However, after birth soluble MAdCAM-1 reactive thymocytes are rapidly down regulated and MAdCAM-1 expression in thymic blood vessels disappears. In the developing gastrointestinal tract of rodents MAdCAM-1 is expressed widely in the venules of lamina propria and follicular dendritic cells in neonatal Peyer's patches (Iizuka *et al* 2000). It is also expressed transiently in non-mucosal tissues during fetal life of rats e.g. vascular endothelial cells in the skin. Immune cell trafficking *in utero* and early human life is dominated by MAdCAM-1 (Salmi *et al* 2001a). During this period there are interestingly age dependant switches and species dependant class switches in the molecular mechanisms of lymphocyte migration MAdCAM-1 is widely expressed from week seven onwards of embryogenesis found to be present in microvessels of many extraintestinal tissues e.g. peripheral lymph nodes, thymus, spleen, pancreas, skin, muscle, kidney. Gradually MAdCAM-1 becomes polarised to mucosal vessels after birth until adulthood, where it is the most tissue-specific endothelial adhesion molecule known. *In utero* MAdCAM-1 functionally governs lymphocyte adhesion to vessels both in the gut and peripheral lymph nodes binding to α4β7 integrin. MAdCAM-1-α4β7 pathways are fully operative *in utero* and MAdCAM-1 mediated binding shows a more prevalent role both at the mucosal/non mucosal sites *in utero* and in newborns than in adults. Fetal MAdCAM-1 may be involved in the immigration of bone marrow T-lymphocytes precursors into thymus or in a population of splanchnic mesoderm during development. Induction of peripheral node addressin gradually starts to dominate the binding of lymphocytes to PLN during childhood.

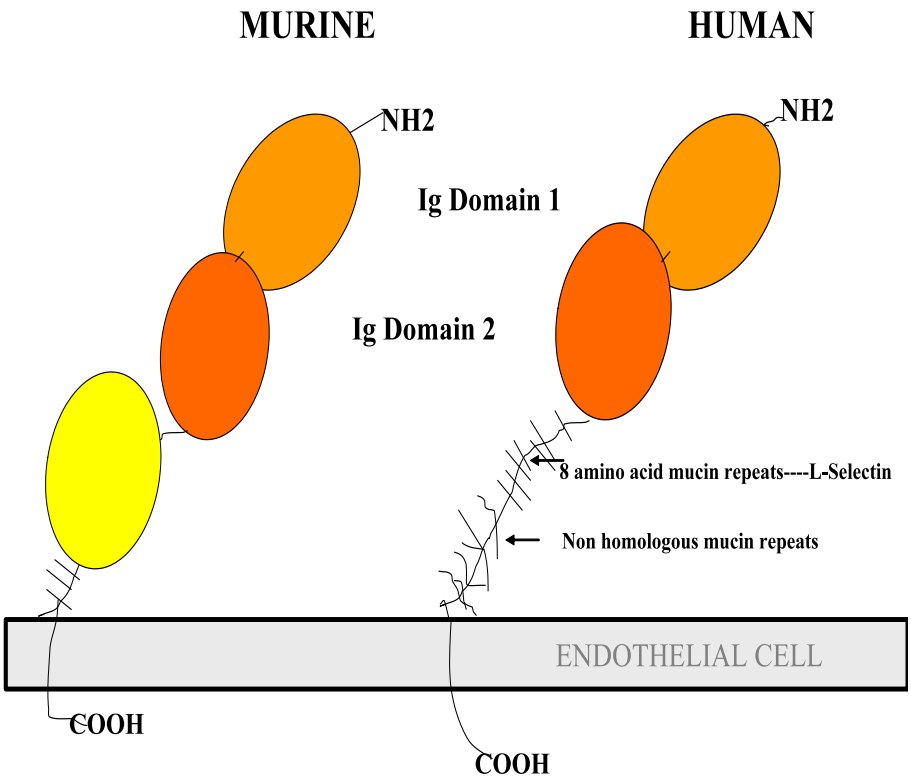

Figure 1.3 Schematic diagram adapted from Briskin et al (1996) demonstrating murine & human MAdCAM-1 superimmunoglobulin protein structure. The encoded MAdCAM-1 protein is a 40kDa protein, which is extensively post-transcriptionally; modified in vivo, through 0-linked glycosylation leading to the formation of 60kDa mature glycoprotein. MAdCAM-1 comprises two N-terminal Ig domains of 52 and 71 amino acids and both separated from the cell surface by a mucin like region. Human MAdCAM-1 is made up of a transmembrane domain of 20 hydrophobic residues and a 43 amino acid tail, which is longer than the murine homologue. The extracellular domain of murine MAdCAM-1 contains an additional Ig domain, adjacent to the transmembrane segment that displays high homology to IgA1 and is separated from the second Ig domain by a mucin-like region. In humans MAdCAM-1 has compensated for the lack of a third Ig domain (present in murine and other species) by extending its mucin domain as two separate regions (major & minor domain) so as to hold the two N-terminal ligand-binding domains above the glycocalyx for presentation to αβ47.

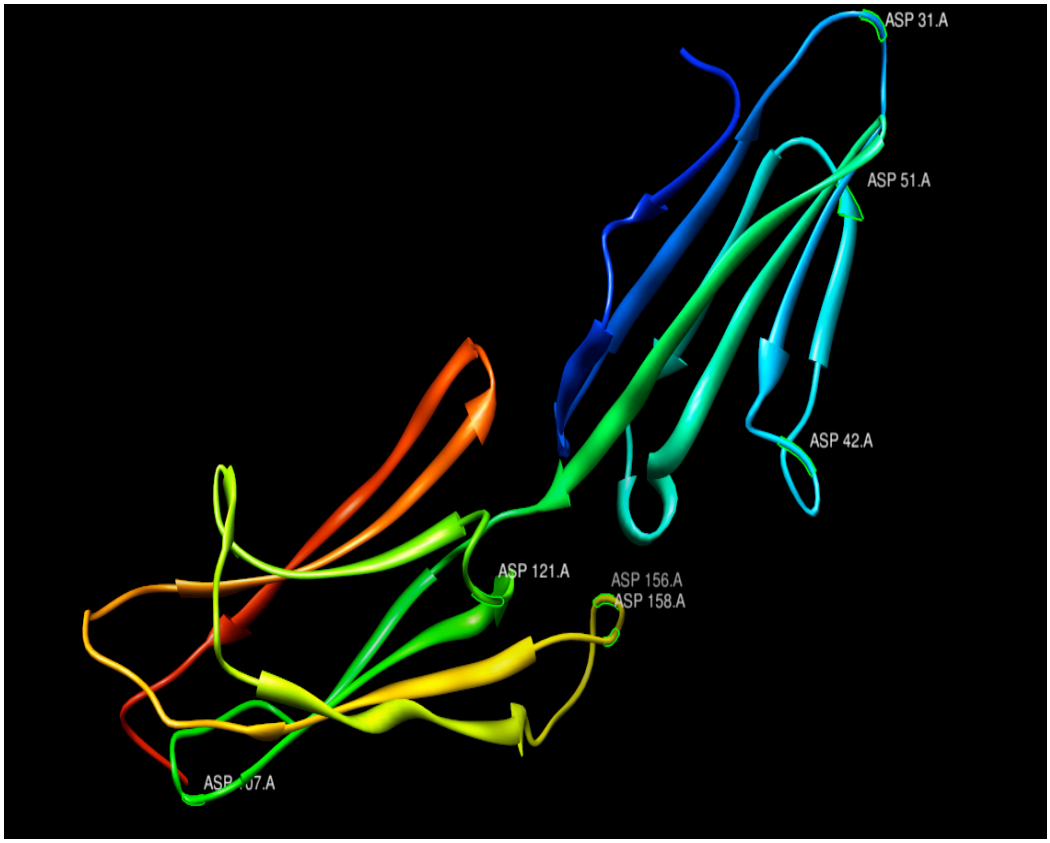

***Figure 1.4 Ribbon representation of the N-terminal two-domain crystal structure of human MAdCAM*-1 (PDB id 1GSM).** The pivotal elements for α4β7 integrin recognition and binding to human MACAM-1 are aspartate residue (Asp42) in the CD loop of domain 1, a negatively charged B-ribbon on the DE loop of domain 2 which actually stretches out far from the body of domain 2 and optimally orientates domains 1 and 2 for recognition of integrin and an arginine (Arg)70 in domain 2, critical for formation of a MAdCAM-1 dimeric form. This figure has been produced by UCSF CHIMERA package (Dando et al 2002).

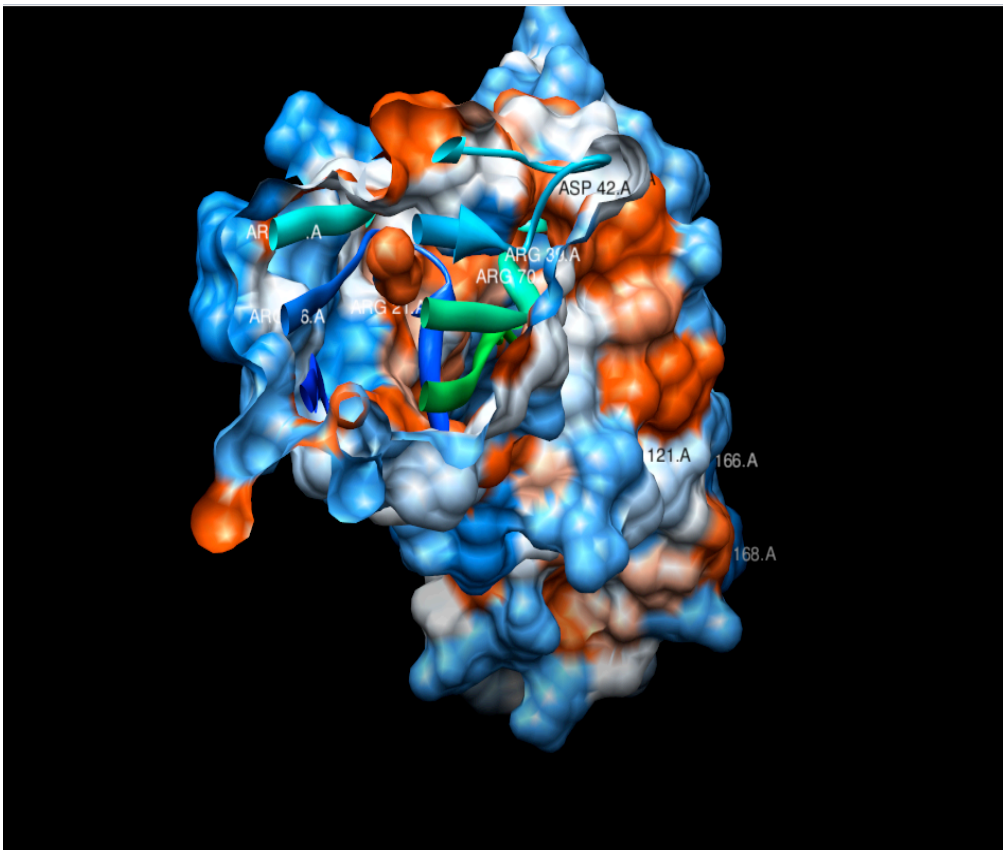

Figure 1.5 Surface structure of human MAdCAM-1 showing the relationship of aspartate residue (Asp42) in the CD loop of domain 1 and arginine (Arg70) in domain 2 **(PDB id 1GSM).** The binding site for α4β7 is buried in domain 1 surrounded by seven hydrophobic residues with no evidence of negatively charged residues in the vicinity to neutralise the strong positive charge critical for formation of a MAdCAM-1 dimeric form. In the monomeric form of MAdCAM-1, this leaves the arginine surface accessible and potentially free to interact with ligand. This and other figures have been produced by UCSF CHIMERA package (Dando et al 2002).

1.2.2.4.2 Regulation of *MAdCAM-1 expression*

The micro environmental factors which maintain preferential expression of MAdCAM-1 on gut endothelial cells are elusive. Human microvasculature endothelial cell cultures (HIMEC) established from the small intestine appear to lose their expression of MAdCAM-1 within a few days *in vitro* (Haraldsen *et al* 1996). Two endothelial cell lines bEND.3 (brain) and SVEC (high endothelium) have been used to study the signal pathways which regulate MAdCAM-1 in response to TNFα (Takeuchi *et al* 1995), which induces MAdCAM-1 mRNA and protein in a dose and time-dependant manner (Oshima *et al* 2001a). This induction is tyrosine kinase (TK), p42/44, p38 mitogen-activated protein kinase (MAPK) and nuclear factor (NF)-κB/poly-ADP ribose polymerase (PARP) dependent. MAdCAM-1 expression requires NF-κB translocation through both p42/44 and p38 MAPK pathways in high endothelial cells.

MAdCAM-1 is induced in both gut and liver inflammation. In the gut, MAdCAM-1 is expressed in the flat walled endothelial vessels of the non-lymphoid tissues of the lamina propria and the follicular dendritic cells of the organised lymphoid tissues of Peyer's patches and mesenteric lymph nodes. MAdCAM-1 has been found to be expressed in primary sclerosing cholangitis (PSC) in which portal inflammation may be a prominent feature (Hillan *et al* 1999) (Grant *et al* 2001). Its expression has been described to be restricted to the portal vasculature, particularly the portal veins and the specialised but not exclusively the HEV's as well as at sites of portal tract lymphoid follicle formation where it may be localised to dendritic cells, similar to its related super Ig family member VCAM-1. These observations suggest that MAdCAM-1 may be important in inflammation where it is involved in the recruitment of lymphocytes to the liver.

1.2.2.5 Carcinoembryonic antigen-related cell adhesion molecule (CEACAM-1)

Carcinoembryonic antigen (CEA) is a glycosyl phosphatidyl inositol (GPI)-cell surface anchored glycoprotein involved in cell adhesion. It is normally produced during fetal development with its production ceasing before birth. Therefore, it is not usually present in the blood of healthy adults, although levels are raised in heavy smokers. CEA serves as a functional ligand for colon carcinoma L-selectin and E-selectin receptors which may be critical to the metastatic dissemination of colon carcinoma cells.

Carcinoembryonic Antigen-related Cell Adhesion Molecule-1 (CEACAM-1), formely known as CD66a and biliary glycoprotein-1 (BGP-I) is a 115 kDa transmembrane glycoprotein. It is a member of the CEA family, which belongs to the immunoglobulin superfamily. Two subgroups of the CEA family, the CEA cell adhesion molecules and the pregnancy-specific glycoproteins, are located within a 1.2 Mb cluster on the long arm of chromosome 19. In humans, the CEA family consists of 29 genes, 18 of which are normally expressed.

The CECAM-1 combines structural features of the immunoglobulin superfamily with functional properties of the cadherin adhesion molecules *(section 1.2.4)*. CEACAM-1 is expressed in a variety of normal human tissues including epithelial, endothelial, and hematopoietic cells. CEACAM-1 mediates cell–cell adhesion and regulates cell proliferation, apoptosis, tumor growth, differentiation/polarisation of epithelial cells, NK cell cytotoxicity, and T-cell-mediated immune response. CEACAM-1 has been suggested as putative tumor suppressor and its expression is reduced in malignant tissues as compared with corresponding normal tissues deriving from breast, prostate, colon and endometrium. These findings indicate that CEACAM-1 may play a role in suppression of carcinogenesis. In contrast, Thies *et al* (2007) recently provided evidence that CEACAM-1 expression in primary tumors of malignant melanoma patients is associated with subsequent development of metastatic relapse. This observation raised the possibility that CEACAM-1 might facilitate metastatic tumor spread. In endothelial cells, CEACAM1 exhibits properties of an angiogenic factor and acts as a major effector of VEGF, suggesting that CEACAM-1 expression may promote metastasis by the induction of angiogenesis.

1.2.3 Integrins

Integrins form a diverse family of proteins which mediate cell-matrix and cell-cell interactions. Integrins are constitutively expressed molecules on un-stimulated lymphocytes (LFA-1, α4β1, VLA-4, α4β7, αEβ7) and/or up-regulated on rolling lymphocytes in response to chemokines on endothelial surfaces. They become activated to enhance rolling and lead to tethering of the cells. Integrins consist of two heterodimers, with non-covalently associated αβ chains and short cytoplasmic tails (Berman *et al* 2000). They "integrate" the activation of the cytoskeleton with the extracellular matrix by transducing messages via classical signal pathways and are important in cellular processes e.g. proliferation, apoptosis and differentiation (Arao *et al* 2000) (Masumoto *et al* 1999).

Naïve lymphocytes express low levels of α4β7 integrin but upon activation significant amount appears on the lymphocyte surface in a functionally active form. α4β7 positivity defines a discrete subpopulation of memory T cells ($CD4^+$, $CD8^+$) and probably B cells involved in mucosal immunity (Schweighoffer *et al* 1993). Monoclonal antibodies to MAdCAM-1 or α4β7 effectively inhibit migration of gut-derived thoracic duct blasts and memory/effector T cells to the intestine. Unlike naïve lymphocytes gut homing blasts and memory cells express very low levels of L-selectin or lack it completely and do not need L-selectin to home to Peyer's patches or the appendix. Instead, they can bind directly to endothelium via an activated α4β7. Of interest, the principal function of α4β7 appears to be interaction with MAdCAM-1 where it acts as a rolling receptor and mediates firm adhesion to endothelium (Wagner *et al* 1996).

LFA-1 appears to be instrumental in the contact between cytotoxic T lymphocytes and target cells where it binds to ICAM-1 (Sigal *et al* 2000); in the gut (Peyer's patches and the lamina propria) the combination of α4β7-MAdCAM-1 interaction and possibly LFA –1 ensure firm lymphocyte adhesion.

1.2.4 E-Cadherin

E-cadherin is a member of the large cadherin superfamily. It is the predominant intercellular adhesion molecule expressed by intestinal epithelial cells. It is a calcium dependent transmembrane protein, which forms a key component of the zone adherens. E-cadherin molecules form dimers at the cell surface which interdigitate with other E-cadherin molecules on adjacent epithelial cells. The functions of E-cadherin are mediated through actin cytoskeleton linkage via a number of cytoplasmic catenin plaque proteins, leading to signal transduction. E-cadherin gene knockout mice have confirmed (Schon *et al* 1999) its critical importance to normal development and tissue function. Low or absent levels of E-cadherin are associated with a variety of epithelial malignancies arising from mutations in the E-cadherin promoter (Palmer *et al* 2001). These abnormalities are accompanied with increased tumour invasion, metastasis and poor survival. Decreased membranous expression of E-cadherin molecules have been found in a number of gastrointestinal solid organ malignancies in humans e.g. gastric, oesophageal, pancreas, liver, colon as well as breast, bladder and prostate. Direct correlation between E-cadherin and grade of tumour differentiation has been observed in some gastric tumours e.g. in a multivariate retrospective study, E-cadherin positive tumours had significantly better survival rates than E-cadherin negative tumours (Grabsch *et al* 2001).

E-cadherin is thought to be exclusively involved in cell-cell adhesion and hence cancer cell metastasis and invasion. However, evidence also suggests a heterophilic interaction with $\alpha 4\beta 7$ integrin, which is on the surface of predominately intra-epithelial lymphocytes and only on a minority of circulating lymphocytes (Taraszka *et al* 2000). This receptor ligand interaction may therefore be important in mediating the retention of lymphocytes within the mucosal epithelium.

1.2.5 CD44

CD44 is a multifunctional adhesion proteoglycan molecule able to mediate lymphocyte rolling on hyaluronate and activate LFA-1 *(figure 1.2)*. Lymphocyte binding to mucosal endothelium can be partially blocked by anti-CD44 antibodies *in vitro* (Shepley *et al* 1994); CD44 may not be central in the homing of lymphocytes to normal

mucosal sites as CD44 deficient mice do not have abnormalities in their mucosa associated lymphatic tissues (Steeber *et al* 1996).

1.2.6 Vascular adhesion protein (VAP-1)

VAP-1 was discovered in the early 1990's (Salmi *et al* 1992). It is an inducible human endothelial protein, which supports shear-dependant lymphocyte binding to HEV in peripheral and mesenteric lymph nodes. It has a dual role as it has also been shown to act as a semicarbazide-sensitive mono-amine oxidase (SSAO) in addition to its adhesive function which involves binding to an uncharacterised lymphocyte counter-receptor by the oligosaccharide moiety of VAP-1. It is interesting to note that as an enzyme, VAP-1 can convert soluble primary amines into corresponding aldehydes and hydrogen peroxide, in a reaction that results in the formation of biologically active products (Kurkijarvi *et al* 2000). At high concentrations these compounds are cytotoxic and may contribute to the pathogenesis of different vasculopathies, as indicated by studies demonstrating that SSAO inhibition ameliorates the development of atherosclerotic lesions in diabetic models (Obata 2006).

The molecular characterisation and cloning of VAP-1 shows it to be a homodimeric 170-180 kDa glycoprotein, consisting of two 90-kDa subunits, held together by disulphide bonds (Salmi *et al* 1997). VAP-1 has a large extracellular domain, a single transmembrane domain, and a short cytoplasmic tail. The molecule has abundant sialic acid decorations that are essential to its adhesive function. *In vivo* studies support its involvement in rolling mechanisms on mesenteric vessels.

VAP-1 has been found to be expressed constitutively in high concentrations on hepatic endothelium, which normally fails to express adhesion molecules such as selectins, and mediates capture of lymphocytes in the liver. The expression of VAP-1 under normal conditions is most prominent in endothelium of lymph nodes, although in the setting of chronic inflammation it is up-regulated in vessels from a variety of tissues including synovium, tonsil, gut and skin. Its constitutive expression in the liver (particularly the sinusoidal and vascular endothelia), as well as its absence or relatively low expression in other non-lymphoid sites, suggests that it could function as an addressin, to direct T cells onto hepatic endothelium, where in the absence of selectins and CD31, it may play

a specific role in lymphocyte recruitment. This has been confirmed from recent evidence which suggests that under conditions of physiological shear stress, VAP-1 supports transendothelial migration, as well as lymphocyte adhesion across hepatic sinusoidal endothelial cells in directing T cell recirculation to the liver (Lalor *et al* 2002).

Although VAP-1 is only expressed at low concentrations within vessels in the non-inflamed gut, it is also up-regulated in active IBD, which suggests that lymphocytes using VAP-1 to enter the liver (Kurkijarvi *et al* 1998) could also use VAP-1 to enter inflamed mesenteric vessels. Thus, a proportion of mucosal T cells as well as T cells activated in the liver also have the ability to migrate to the gut, thereby providing immune surveillance to both these sites. Interestingly, since prolonged VAP-1 blockade causes a significant decrease in the inflammatory response, e.g. in rat allograft rejection, this could be used for therapeutic benefit (Martelius *et al* 2004). Furthermore, due to the restricted tissue expression of VAP-1, targeting its expression may favour future possibilities for more liver-specific immunosuppression.

1.3 Chemokines

We have seen that whereas selectins are constitutively active, integrins must be activated to mediate adhesion. Specifically, rolling T cells activate integrins when they receive signals from chemokines on endothelial surfaces. Chemokines are a family of small closely related c*hem*otactic pro-inflammatory cyto*kine* proteins secreted by cells. They share structural characteristics such as small size (they are all approximately 8-10 kilodaltons in size) and the presence of four cysteine residues in conserved locations are crucial to their three dimensional morphology.

There are more than 18 chemokine receptors and 50 chemokines identified and the family is rapidly increasing. There are four major groups of chemokines (CXC, CC, C and CX_3C), based on the the number and spacing of conserved cysteine residues in the NH2-terminus.

Specifically, the CXC chemokine group are important in angiogenesis and angiostasis e.g. wound healing and development. They are further subdivided into two subclasses based on the presence of the glutamic acid, leucine and arginine group at the N-terminus. These include CXCL8/1L-8, with strong neutrophil chemoattractant properties i.e. chemotaxis. Absence of these specific amino acid related chemokines recruit mainly lymphocytes and exert angiostatic effects.

The CC chemokines have two adjacent cysteines near their amino terminus. There have been at least 27 distinct members of this group reported for mammals, namely CC chemokine ligands (CCL) 1 to 28. Chemokines of this subfamily usually contain four cysteines (C4-CC chemokines) but a small number of CC chemokines possess six cysteines (C6-CC chemokines). The C6-CC chemokines include CCL1, CCL15, CCL21, CCL23 and CCL28. CC chemokines are known to induce the migration of monocytes and other cell types such as natural killer (NK) cells and dendritic cells. The CC chemokine includes monocyte chemoattractant protein-1 (MCP-1) or CCL2. They stimulate monocytes to enter the surrounding tissues from the bloodstream which transforms them into tissue macrophages. Another important member of the CC chemokine subfamily is CCL5 (or RANTES). They are known to interact with different cell types such as T cells, eosinophils and basophils that express the receptor CCR5.

In the C chemokine group, lymphotactin attracts lymphocytes and NK cells but not monocytes. The chemokine fractalkine defines the CX_3 .

Activated endothelial cells, leukocytes and epithelial cells produce chemokines. Virtually any cell is capable of chemokine generation upon stimulation with lipopolysaccharide or pro-inflammatory cytokines. After secretion, chemokines can bind to heparin-like glycoaminoglycans on the cell surface, helping leukocytes to track down these ‘immobilised’ chemokines in a process named haptotaxis. The binding of chemokines to glycosaminoglycans not only prevents them from being washed away, but also maintains them in mono/dimeric forms, which increases their affinity for their individual receptors. The immobilised chemokines can persist at high concentrations in

tissues for longer than freely diffusible chemokines, allowing them to exert their specific effects.

Specifially, chemokines bind to precise G-protein receptors on the lymphocyte leading to cytoskeletal rearrangement and *activation* of integrins essential for lymphocyte recruitment. The combination of such unique chemokines and adhesion molecule interactions within different tissues are comparable to postal addresses. Thus, lymphocytes bearing the appropriate receptors are able to respond to such addresses. In addition to high concentrations of surface L-selectin essential for lymphocyte capture, naïve lymphocytes also express the chemokine receptor CCR7 thereby facilitating interaction with the L-selectin ligand PNAd and the chemokine SLC (CCL21), (both restricted to endothelium in secondary lymphoid tissues). CCL21 activates α4β7 dependant adhesion to MAdCAM-1 and plays an important role in recruiting naïve lymphocytes to the Peyer's patches of the gut (Pachynskil *et al* 1998). By contrast, surface L-selectin and CCR7 are reported to disappear from most memory lymphocytes, thereby preventing them from re-entering lymph nodes. The recruitment and localisation of memory T cells to the gut is also helped by two important chemokines with restricted expression at mucosal sites. The gut associated chemokine CCL25 (thymus-expressed chemokines 'TECK') is mainly concentrated to the small intestine, where it is expressed by endothelial, epithelial cells and the mucosal-associated epithelial chemokine (MEC) is identified at most mucosal sites including the colon (Kunkel *et al* 2000). It is interesting that ligation of CCR9 by the chemokines ligand CCL25 promotes conformational changes in the α4β7 integrins and firm adhesion of MAdCAM-1 *(figure 1.6)*.

Chemokines can be divided into homeostatic and inflammatory types based on their functional properties. Inflammatory chemokines are up-regulated by inflammatory stimuli in inflamed tissues by resident and infiltrating immune cells, and mainly regulate the recruitment of neutrophil, moncytes, NK cells and effector lymphocytes into effector sites. Homeostatic chemokines are constitutively expressed at high levels in lymphoid organs as well as in non-lymphoid tissues such as skin and mucosa where they mediate the naïve and memory lymphocytes trafficking to lymphoid and effector tissues as well as their guidance to the correct microenvironment within the tissue.

Figure 1.6 Expression of CCL25 and human MAdCAM-1 by vascular endothelium promotes recruitment of gut-derived lymphocytes and binding of CCR9 and α4β7 respectively

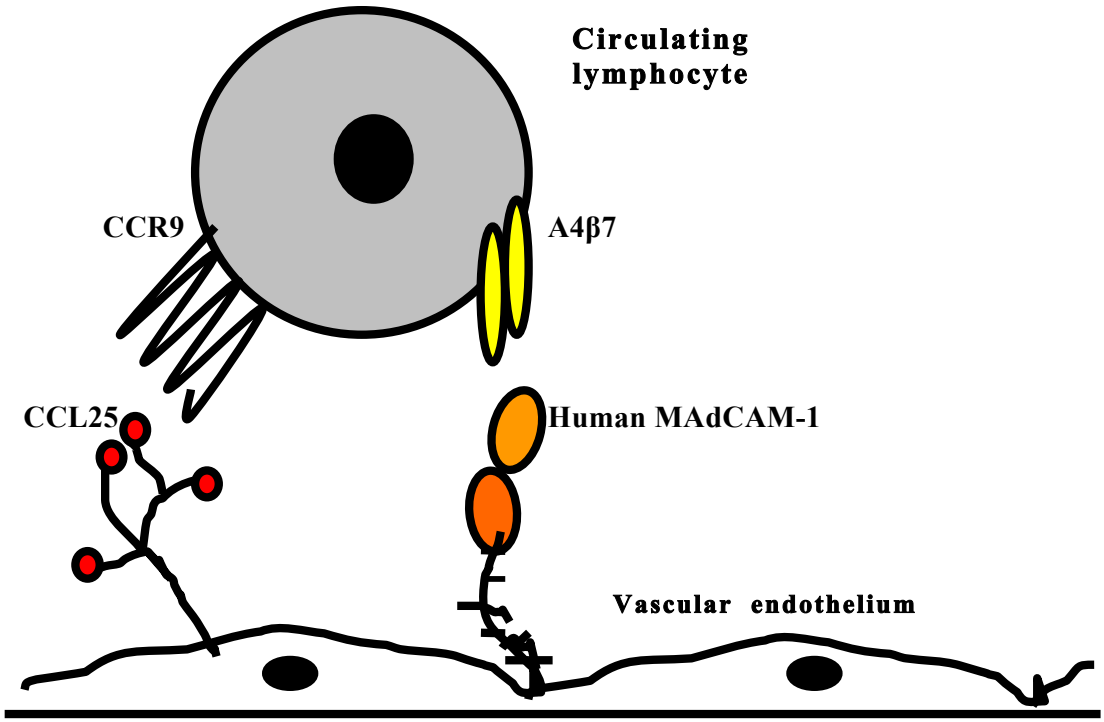

1.4 Regulation and synthesis of endothelial adhesion molecules

Stimuli such as lipopolysaccharide (LPS) and pro-inflammatory cytokines enhance expression of different endothelial cell adhesion molecules. For example, LPS and the cytokines TNF-α, IL-1β, Il-4 and IFN-γ can substantially enhance the transcription of genes for ICAM-1, V-CAM-1, P-selectin, E-selectin (Lidington *et al* 1999). P-and E-selectin expression on HUVEC mono-layers and *in vivo* usually reach a maximal level at 3-5 hours in comparison to VCAM-1 which peaks at 6 hours and ICAM-1 at 12 hours after endothelial cell stimulation. E-selectin expression returned to basal values within a few hours after stimulation whereas P-selectin, VCAM-1 and ICAM-1 persisted for 24-48 hours after a single stimulus.

NF-κB transcription factors appear to be the most relevant in inflammatory bowel and liver diseases, as they are important in the regulation of endothelial cell adhesion molecules (Schreiber *et al* 1998). Unlike most transcription factors, NF-κB normally resides in the cytoplasm and must translocate into the nucleus to elicit a response. Many signals, including bacterial and viral pathogens and inflammatory cytokines elicit NF-κB translocation.

Binding sites for NF-κB have been identified in the promoter regions of the genes for VCAM-1, ICAM-1 and E-selectin. Activation of VCAM-1 requires two tandem binding sites for NF-κB, which are located on the basal VCAM-1 promoter. Of the four positive regulatory domains identified in the promoter region of the E-selectin gene, three require NF-κB binding for induction.

The majority of the functional role of adhesion molecules arises from their surface expression, although a small amount is cleaved from sites of expression with a presense in biological fluids. This is probably by enzymatic action since mRNA encoding alternatively spliced soluble forms of adhesion molecules have not been reported in man. The first molecule to be recognised in soluble form was ICAM-1 and soluble forms of other molecules including E-selectin and VCAM-1 were later identified. The shed molecules may represent only a small proportion of the total expression of E-selectin, as most of the molecules are internalised and subsequently degraded or recycled. The circulating isoforms of the adhesion molecules retain their ability to bind

to their respective ligands in spite of lacking transmembrane and intra-cytoplasmic domains, however little is known about their function.

1.5 Adhesion molecules in gastrointestinal disease

Many different families of adhesion molecules are upregulated during inflammation in gastrointestinal and liver diseases accompanied by the coordinated recruitment of leukocytes. In the gastrointestinal tract, lymphocytes are localised in the lamina propria, Peyer's patches, and are increased in number, particularly in the lamina propria and epithelial cells in ulcerative colitis, Crohn's disease, coeliac disease and many other conditions. The liver has a massive population of leukocytes principally lymphocytes, which are recruited in response to insults such as injury, infection, and inflammation in viral hepatitis, primary biliary cirrhosis (PBC), autoimmune hepatitis (AIH) and alcoholic liver diseases (ALD) in which the predominant infiltrating leukocyte is the neutrophil.

The evidence discussed thus far suggests that recruitment of lymphocytes is identified by their critical ability to bind and subsequently migrate across the endothelium lining vessels within target tissues. The process involves a sequence of interactions with different adhesion molecules and chemokines which act synergistically to capture, bind and then direct the migration of the lymphocyte into tissues.

1.5.1 Gastrointestinal infection

Bacterial products initiate or amplify gastrointestinal inflammation with the recruitment and activation of leukocytes during inflammation of the colon (e.g. *Clostridium difficile)* and stomach (e.g. *Helicobacter pylori).*

There is an accumulation of neutrophils in the lamina propria in response to an acute gastrointestinal infection with invasive bacteria (Huang *et al* 1996). Intestinal epithelial cells play an important role in the recruitment of these inflammatory cells to the site of infection through the secretion of adhesion molecules. ICAM-1 may function to maintain neutrophils, which have transmigrated through the epithelium in close contact with the intestinal epithelium, thereby reducing further invasion of colonic mucosa by

invading pathogens. Activation of the leukocyte adhesion glycoproteins LFA-1 and subsequent interaction with constitutively expressed endothelial ICAM-1 may help this, causing increased vascular permeability further aided by leukocyte-platelet aggregation. The infiltration of leukocytes caused by *Clostridium difficile* toxin A is protracted if the LFA-1 and P-selectin expression induced indirectly by the toxin is blocked.

Penetration of the gut mucosa by pathogens expressing invasive genes occurs prominently through M cells, located in Peyer's patches. However, alternative mechanisms exist for bacterial uptake in mucosal tissues such as that proposed by dendritic cells (Rescigno *et al* 2001). Dendritic cells appear to open the tight junction between epithelial cells, send dendrites outside the epithelium and directly sample bacteria. This mechanism may involve interactions with the tight junctions, the transmembrane protein occludin and other cell adhesion related molecules including E-cadherin and B-catenin. It will be of interest to know if similar mechanisms exist in the liver.

1.5.2 Coeliac Disease

In coeliac disease, a T-cell mediated response to dietary gluten causes chronic inflammation, increased epithelial cell proliferation and architectural distortion in the small upper bowel. Lymphocytes accumulate within the lamina propria, and also a distinct subpopulation within the epithelial cell layer. ICAM-1 and LFA-1 are expressed in the former site but not the latter in active disease, although on short term gluten challenge in treated coeliac patients ICAM-1 expression was not altered whilst VCAM-1 and E-selectin expression increased over hours. (Sturgess *et al* 1990) (Kelleher D *et al* 1994).

1.5.3 Radiation Enteritis

Radiation enterocolitis is a sequel to radiotherapy for pelvic and abdominal malignancy. Early changes after exposure include increased cell death, loss of villous height, and the extensive loss of intestinal function leading to fluid and electrolyte imbalance. Late complications develop from endarteritis obliterans leading to intestinal ischaemia and gangrene.

Cellular adhesion molecules may play an important role in the pathogenesis of radiation enteropathy. After gamma radiation, the nuclear transcription factor NFκB induces oxygen radicals causing endothelial cell activation and the release of inflammatory mediators. There follows up-regulation of CD11/CD18 on leucocytes accompanied by NF-κB dose dependent increase expression of ICAM-1 and E-selectin (Zouki *et al* 2000). This increase occurs by binding p50 and p65 nuclear proteins, with release of proteases and reactive oxygen metabolites accounting for most of the neutrophil mediated radiation induced tissue damage (Handschel *et al* 1999).

As a result of endothelial adhesion molecule upregulation there is recruitment of adherent and emigrating leucocytes in post-capillary venules. *In vitro* studies show cultured monolayers of endothelial cells respond to ionising radiation by increasing mRNA and cell surface expression of ICAM-1 and E-selectin (Panes *et al* 1995) (Heckmann *et al* 1998). Indeed, ICAM-1 may remain elevated as long as 10 days after one single dose of radiation.

Medical therapy of radiation enteritis is limited. Antibiotics may be of use for bacterial overgrowth and local topical therapy to patients with proctitis. Anti-adhesion molecule therapy could have a therapeutic role in controlling the local inflammatory processes e.g. blocking LFA-1 and ICAM-1 has been shown to be beneficial in treating post irradiation syndrome in rats (Horie *et al* 1996).

1.5.4 Inflammatory Bowel Disease

Mucosal changes in ulcerative colitis (UC) and Crohn's disease (CD) are characterised by the development of ulcerative lesions and prominent inflammatory infiltrates of leukocytes in the bowel wall consisting of B and T lymphocytes, macrophages, plasma cells and granulocytes. The aetiology is unknown but a failure to control mucosal immune responses to antigens in the lumen is likely to play a role. Recruitment of cells to diseased gut mucosa appears essential to the initiation and perpetuation of IBD. The recruitment involves activation of a number of adhesion molecules and their ligands, on leukocytes and vascular endothelium.

MAdCAM-1 plays a central role in the aetiology of IBD through its ability to direct circulating lymphocytes to enter gut-associated lymphoid tissue and the gut interstitum. Furthermore, although MAdCAM-1 is constitutively expressed in some regions of the gut and mesenteric lymph nodes, the expression of MAdCAM-1 in these tissues is significantly increased during active colitis. Briskin *et al (1997)* reported that in small intestine and colon from patients with Crohn's disease, the pattern of MAdCAM-1 expression paralleled that found constitutively in normal intestinal tract, but the relative area of endothelium expressing MAdCAM-1was greater in IBD.

In active IBD, ICAM-1 expression is increased on the cell membranes primarily by activated endothelial venular cells at the base of ulcerations with dense cellular infiltration. ICAM-1 is also expressed by infiltrating leukocytes and is upregulated in early lesions of CD e.g. aphthous ulcerations. The blocking of β2 integrins may initiate some intracellular mechanisms, which make neutrophils insensitive to ICAM-1, and these mechanisms seem to be impaired in UC in which integrins have also been shown to show inhibit ICAM-1 induced neutrophil locomotion (Nielsen *et al* 2000). The chemotactic properties of ICAM-1 have been further explored in UC where the effect of prednisolone was shown to include both anti-chemotactic effects towards ICAM-1 and pro-chemokinetic properties, which might explain the rebound symptoms of UC during the tapering of prednisolone therapy.

In IBD VCAM-1 is found to be membrane bound on endothelial cells, monocyte/macrophages, lymphoid and non-lymphoid tissues. VCAM-1 is functionally active in the chronic inflammation of UC and CD. It is important in the trafficking of recirculating lymphocytes into inflamed bowel mucosa but does not appear to be active in the acute inflammatory response.

Expression of PECAM-1 is greater in normal colonic tissue than small intestine. A significant increase in PECAM-1 positive vessels is seen in active UC (Vainer *et al* 2000) as compared with non inflamed areas adjacent to the inflamed tissue, indicating that PECAM-1 is involved in the earliest phases of IBD; its upregulation seems to a preconditioning for the development of inflammatory lesions. It is significantly increased in mucosal vessels of uninvolved UC compared with healthy volunteers.

E-selectin may prove useful for *in vivo* detection and quantitation of disease activity in IBD as its expression is limited to activated endothelium. Interestingly, radiolabelled E-selectin has been used to image IBD-affected bowel by scintigraphy, which appear to show good correlation with results of colonoscopy and barium studies (Bhatti *et al* 1998). This study and others (Nielson *et al* 1996) also report a positive correlation between disease activity in IBD and serum levels of soluble, presumed shed E-selectin, although other studies (Goggins *et al* 2001) have not confirmed this relationship.

There is the increasing appreciation of the role of *E.coli* in IBD as 'mildly pathogenic' by virtue of their possession of adhesion mechanisms and secretion of proteases. In Crohn's disease *E.coli* probably invade the tissue, perhaps as a result of defective clearance by neutrophils, and chronically infect macrophages, where they may have a more superficial relationship with the mucosal surface in ulcerative colitis. There is already considerable interest on how uropathogenic *Ecoli* interact with epithelial cells and much of this may be relevant in the colon. This may include interaction with members of the CEACAM family that are present in the glycocalyx.

1.6 Entero-hepatic recirculation & extra-intestinal manifestations of Inflammatory Bowel Disease

1.6.1 Extraintestinal intestinal manifestations of Inflammatory Bowel Disease

Inflammatory bowel disease may be associated with a variety of extraintestinal manifestations. Some are transient and generally associated with active disease (e.g. joint, skin and eye inflammation). Other conditions may preceed or follow episodes of inflammation e.g liver involvment with sclerosing cholangitis.

Grant *et al* (2002) proposed an attractive rationale for simultaneous expression of $\alpha 4\beta 7$ mediated responses in gut and liver which therefore allow the entero-hepatic recirculation of lymphocytes and provides surveillance to protect the liver against gut derived organisms; this pathway could well promote the development of liver

inflammation in association with IBD. Effector lymphocytes would have the capacity to migrate to both the gut and liver due to the common expression of adhesion molecules. T cell activation in the gut during episodes of IBD would thus lead to the production of primed lymphocytes, with the ability to bind both hepatic and mucosal endothelium. Furthermore, some of these cells will persist as long-lived memory T cells even after resolution of IBD. Such a mechanism could involve VAP-1 and/or MAdCAM-1 acting as common addressins shared by the liver and bowel. If hepatic inflammation subsequently develops in response to an appropriate insult or infection, these memory cells will be rapidly recruited via interactions with MAdCAM-1 or VAP-1 on portal endothelium and with VAP-1 on hepatic sinusoidal endothelium. If cross-reactive self antigens in the liver activate these cells, they could presumably survive and promote the development of chronic inflammation, in liver diseases such as primary sclerosing cholangitis (PSC) or autoimmune hepatitis.

The involvement of long-lived memory T cells from the gut in the pathogenesis of PSC could explain why IBD and PSC do not always occur at the same time and why PSC can present for the first time in patients with quiescent UC and in people whose colons were removed many years before. However, although this model is attractive it still does not explain all the features of PSC i.e. why the activity of the PSC liver disease does not parallel bowel inflammation and indeed why the association is greater with UC than Crohn's disease. It has been postulated that similar numbers of activated mucosal memory T cells are present in Crohn's disease as in ulcerative colitis. Moreover, the fact that the association with Crohn's disease is predominant in Crohn's colitis suggests that colonic inflammation may be a critical factor. The explanation could lie in the nature of the auto antigens which activate mucosal lymphocytes in the PSC liver or the differences between the homing potential of colonic and small bowel memory T cells.

Other extraintestinal complications may arise and in whom leucocytes may infiltrate organs e.g. eyes and joints. It is certainly apparent that the extraintestinal manifestations may occur during a flare of IBD, as circulating effector lymphocytes activated in the gut have been shown to express high concentrations of adhesion molecules e.g. VLA-4 and LFA-1, which subsequently promote recruitment of effector lymphocytes to tissues in which low concentrations of endothelial ligands VCAM-1 and ICAM-1 are expressed This mechanism could apply to the eye, a mucosal surface where increased expression

of ICAM-1 and VCAM-1 have been recorded in people with uveitis where VAP-1 have been detected in conjunctival follicle vessels.

About 25% of IBD patients suffer from extraintestinal inflammatory complications, of which arthropathy is the commonest. The manifestations have been attributed to the presence of putative cross-reactive antigens between gut and liver, shared susceptibility genes, and to circulating immune complexes or lipopolysacharide. Leukocyte trafficking between gut and joints suggests an alternative mechanism. Salmi *et al* (2001b) showed that mucosal T cells bind to inflamed synovial high endothelial venules *in vitro*, an occurrence which is not just a result of inflammation because the same activated mucosal T cells bind poorly to inflamed peripheral lymph nodes. MAdCAM-1 is absent from synovial vessels. Activated IBD gut immunoblasts may rely on VAP-1 for synovial recognition, as blocking VAP-1 significantly inhibits binding of these leukocyte subsets to joint vessels (Salmi *et al* 2001).

1.7 Modulating adhesion molecule expression and therapeutic applications of anti-adhesion therapy in IBD

Interrupting inflammatory cell recruitment into IBD lesions is an important therapeutic aim. Several approaches have been used to probe the role of adhesion molecules *in vivo*, including blocking antibodies (Podolsky *et al* 1993) (Briskin *et al* 1997) chimeric selectin-immunoglobulin proteins (Dietsh *et al* 1993) and the study of human and animals with genetically determined cell adhesion deficiencies. These studies demonstrate that blocking one or more adhesion molecules can effectively inhibit inflammation; however, there appear to be clear differences in the adhesion requirements for particular types of inflammation.

Anti-α4 monoclonal antibodies with recognition of α4β7 and α4β1 relieved gut inflammation and reduced leukocyte accumulation in a cotton-top tamarin model of inflammatory colitis (Podolsky *et al* 1993). Studies of transgenic mice have shown that α4 deficient transgenic mice are unable to recruit T-cells to Peyer's patches and similarly, Peyer's patches are absent in β7 integrin deficient animals, suggesting that both these integrins are essential for the formation of gut-associated lymphoid tissue.

Studies of other animal models of colitis have also shown intravenous administration of monoclonal antibodies to α4, or β7 integrin significantly attenuates colonic inflammation. (Picarella *et al* 1993).

More recently, following the positive therapeutic effect of anti-α4 antibodies in experimental colitis, a trial of humanised monoclonal antibody to α4 integrin was performed. Although therapeutic efficacy was low there was evidence of interaction with endothelial VCAM-1 as shown by reduced serum soluble VCAM-1 concentrations after antibody blockade of α4 integrins (Gordon *et al* 2001) (Gordon *et al* 2002).

In other approaches, antisense oligonucleotides (Anti-S) have been used to prevent the synthesis of adhesion molecule proteins in IBD patients. The concept of modulating gastrointestinal inflammation using Anti-S to therapeutic effect e.g. targeted to adhesion molecules and in particular MAdCAM-1 will be discussed in chapter 5.

1.8 Adhesion molecules in liver disease

Lymphocyte-endothelial interactions take place in sinusoidal vessels under conditions of low-velocity blood flow*)*. Normal liver sinusoids contain large granular lymphocytes, which are intimately associated with other sinusoidal (pit) cells. Lymphocyte interactions with sinusoidal endothelium differ from those involved with postcapillary venules in e.g. lymphoid tissue in some important aspects. The characteristic rolling phase of primary adhesion seen in HEV is not observed, and adhesion to sinusoidal endothelium is unaffected in animals lacking endothelial selectins. Retention of leukocytes in the hepatic sinusoids is however greatly reduced, although not abolished, in animals some lacking certain cellular adhesion molecules e.g. ICAM-1. Inflammation in the liver causes portal vessels to express P-selectin, E-selectin, VCAM-1 and high levels of ICAM-1.

In some forms of chronic liver diseases particularly that associated with ductopenia such as primary biliary cirrhosis (PBC) and primary sclerosing cholangitis (PSC), immunological mechanisms involving lymphocyte-mediated damage are important in the characteristic bile duct damage. The bile-duct damage characteristic of early PBC

mainly affects the septal and larger interlobular ducts, while the smaller interlobular ducts remain intact until later. The epithelium of the affected ducts becomes irregular and is infiltrated with lymphocytes. The basement membrane becomes disrupted and the duct may rupture. An inflammatory infiltrate is seen around the ducts which may form lymphcytes aggregates or follicles. Elsewhere, there are a mixture of plasma cells, eosinophils and neutrophils. The eosionphils contribute to bile duct damage and granuoloma formation by releasing mediators which are located with in their granules. With progressive PBC the disease extends beyond the confines of the portal tracts and there is increasing fibrosis and alteration of the acinar architecture. There is ductular reaction and progressive fall in duct numbers.

Primary sclerosing cholangitis is characterised by inflammation, strictures and saccular dilatations in the biliary tree. The features on liver biopsy depend in part on the location of strictures in relation to the biopsy site. There is periductal oedema, concentric fibrosis, ductular proliferation, portal inflammation, atrophy or disappearance of the ducts. Loss of the ducts is the common finding in the smallest portal tracts, while periductal fibrosis is typical of medium-sized tracts.

Primary biliary cirrhosis closely resembles PSC in the more later stages. Notably, the typical granulomatous cholangitis of PBC is not a feature of PSC. Substantive chronic inflammation of the portal tracts with or without lymphoid follicles favours PBC. Conversely, fibrous obliteration of ducts is characteristic of PSC, with dense portal fibrosis and relatively little inflammation.

PSC and PBC are both characterised by the relative increase in cytotoxic T-lymphocytes compared to healthy adults. (Lindor *et al* 1987) (Whiteside *et al* 1985) (Yamada *et al 1985).* The possibility however that T cells mediate biliary epithelial cell injury in PSC by a direct cytotoxic effect appears less likely in view of the observations showing the inability to detect any normal cytotoxic activity among liver derived T lymphocytes from these patients (Bo *et al* 2001). In both PBC and PSC there is increased expression of class II antigens. Infiltrating T cells have been shown to be closely associated with areas of bile duct destruction in both diseases. Recent studies have revealed enhanced T helper type 17 (Th17) response and weakened T regulatory cell (T_{reg}) response in some autoimmune diseases such as PBC; thus indicating a role of

Th17/T_{reg} imbalance in the pathogenesis of autoimmunity and its potential function in the breakdown of immune self-tolerance, with Interleukin-23 characterising the disproportionate cytokine profile pivotal in Th17-related human autoimmunity (Rong *et al* 2009).

ICAM-1 is strongly expressed on inflammatory interlobular bile ducts in PSC and PBC, in contrast to bile ducts in normal livers, which do not express ICAM-1 (Adams *et al* 1991) (Volpes *et al* 1990) (Bloom *et al* 1995). In PBC, medium sized ducts, which are spared by the disease, do not express ICAM-1. Whether ICAM-1 expression on biliary epithelia cells is an early event in the pathogenesis of bile-duct damage or a secondary response to inflammation is not clear. This is highlighted by Bloom *et al (1995)* who showed ICAM-1 expression only in advanced PSC making a primary role for ICAM-1 in early disease less likely.

A soluble isoform of ICAM-1 can be detected in the bile as well as sera of normal subjects with greatly elevated levels detected in chronic liver disease (Adams *et al* 1992). Soluble ICAM-1 from bile samples may arise as a result of increased production by hepatocytes, bile epithelial cells or from changes in ICAM-1 elimination. The use of soluble isoforms of ICAM-1, as systemic markers of endothelial cell ICAM-1 expression from work on murine and human endothelial cells has been proposed, but suggest that they may not be directly related. Messenger RNA which specifically encodes soluble isoforms of ICAM-1 in mouse plasma after TNFα administration may be dissociated from ICAM-1 expression on endothelial cells of lung , intestine and other organs. Serum ICAM-1 levels are increased in intra and extra hepatic cholestasis (Polzien *et al* 1996). The rise appears to be dependant on the degree of disease. Serum ICAM-1 concentrations in advanced PBC seems to be more reliably correlated to the histologically proven degree of intrahepatic cholestatsis than any of the other classical parameters of cholestasis.

In alcoholic cirrhosis, there is activation of the immune response with increased expression of adhesion molecules e.g ICAM-1 , LFA-3 and MAC-1, on the surface of circulating lymphocytes which is more intense in patients with advanced disease (Luna-Casada *et al* 1997).

There is emerging evidence of MAdCAM-1's role in inflammatory liver disease. Grant *et al 2001* demonstrated, using adhesion assays, that leukocytes would specifically adhere via α4β7 receptors to human PSC liver, and that α4β7 lymphocytes could be demonstrated adjacent to MAdCAM-1 on portal vessels. These findings indicate that the MAdCAM-1/α4β7 system is likely to be of functional significance in the inflammatory pathophsiology of PSC.

1.9 Liver allograft rejection

Acute (cellular) rejection, the most common form of rejection, is a cell-mediated immune injury. The characteristic histological triad of cellular rejection includes portal inflammation, bile duct damage and endothelialitis, although the latter is not present in all cases. During acute liver allograft rejection there is upregulation of ICAM-1 expression on bile ducts, endothelium and perivenular hepatocytes compared to donor livers, patients with stable transplants, or those with non-rejection complications (Adams *et al* 1989). The tissue distribution of ICAM-1 during rejection resembles that seen for HLA-DR although ICAM-1 expression rather than MHC antigen expression seems more specific for rejection. The upregulation of ICAM-1 on tissues may be an important step in the development of acute rejection determining which cells are the targets of immune damage. Most patients with acute cellular rejection will respond to treatment with high dose immunosuppression but approximately 15% do not and progress to chronic irreversible rejection. On the other hand, whilst VCAM-1 is constitutively expressed on kupffer cells with extremely week portal vein endothelia expression in the normal liver, acute rejection is associated with up regulation of VCAM-1 on most portal venous and arterial vessels, mainly in infiltrated portal tracts.

Chronic (ductopenic) rejection ("vanishing bile duct syndrome") is defined as obliterative vasculopathy and loss of bile ducts occurring 60 days or longer after transplantation. The expression of VCAM-1 is upregulated on central vein endothelia in chronic rejection and additional focal expression on hepatocytes, whilst the expression of ICAM-1 on bile ducts and hepatocytes is greatest in chronic, irreversible rejection. Persistent expression of VCAM-1 and ICAM-1 may promote a continuing inflammatory response resulting in their destruction. However, why these patients fail to respond to immunosuppression is unknown and the reduction of VCAM-1 and ICAM-1

expression seen after successful treatment with high-dose corticosteroids suggests that the action of these drugs may in part be mediated by their regulation.

1.10 Ischaemia/Reperfusion

Ischaemia/Reperfusion (I/R) has been implicated in the pathogenesis of a number of gastrointestinal disorders such as IBD and necrotising enterocolitis. Leukocytes are key mediators of I/R injury in several splanchnic organs, including stomach, intestine, liver, and pancreas (Dulkanchainum *et al* 1998). Leukocytes accumulate in the post ischaemic gut, and I/R induced inflammatory responses (leukocyte adhesion, increased vascular permeability) may be mimicked *in vitro* by exposing endothelial cell monolayers to hypoxia and oxygenation. I/R also results in the upregulation and activation of the P65/P50 heterodimer of NF-κB in endothelial monolayers. The firm adhesion and emigration of leukocytes elicited by I/R involves an interaction between Mac-1 on leucocytes and ICAM-1 on endothelial cells. Antibody blocking studies show that P-selectin contributes to the rapid rolling of leukocytes. There is a biphasic response that peaks at 30 minutes with a second peak in surface expression at 4-6hrs after reoxygenation. A similar biphasic response occurs with very rapid increase in E-selectin. Several chemical mediators have been implicated in the increased expression of P and E-selectin, with leukotrienes, histamine and reactive oxygen metabolites all postulated mediators.

1.11 Aims of the Study

MAdCAM-1 is now thought to be the major adhesion molecule linking liver and gut, providing the main route by which lymphocytes gain access to the normal and inflamed gut. The lymphocyte integrin $\alpha 4\beta 7$ is the major ligand receptor for MAdCAM-1, which is thus critically placed to mediate the homing of these lymphocytes to mucosal organs. Modulation of other adhesion molecules has been used for therapeutic advantage.

The overall aim of this project was to determine the expression of MAdCAM-1 in tissues/cell culture systems and investigate effects of modulating MAdCAM-1 expression.

In order to achieve this, we have followed the following sequence:

a) To characterise the expression of MAdCAM-1 using immunohistochemical analysis.

- The first chapter deals with the broad concept of adhesion molecules including MAdCAM-1.
- The second chapter describes the detection of MAdCAM-1 in liver, gut and related tissues e.g. pancreas in a variety of diseases using immunohistochemical analysis.

b) To develop an in vitro model of MAdCAM-1 as a basis of investigating its expression.

- The third and fourth chapters deal with further characterisation of MAdCAM-1 with detection and quantification of MAdCAM-1 in tissues and cell culture.

c) To modulate MAdCAM-1 using an in vitro model.

- The fifth chapter deals with investigating the effects of modulating MAdCAM-1 using a variety of strategies including Anti-S. In principle the results of this work could then be applied to animal models of MAdCAM-1 expression to determine which agents have effective modulatory capabilities on MAdCAM-1 expression, thereby attenuating inflammatory and immune mediated diseases associated with MAdCAM-1.
- The sixth and final chapter summarises the findings from characterising MAdCAM-1 and the effect of modulating its expression including the role of existing and newer agents

Chapter 2

MAdCAM-1 expression in the liver, gut and associated tissues

2.1 Overview of MAdCAM-1 expression in the gastrointestinal tract

We have seen from chapter 1 that the recruitment of leukocytes from the circulation is a pivotal step in inflammation. The ligand-receptor interactions mediating the emigration of specific cell-types into individual organs affected by inflammation are crucial to our understanding of gastrointestinal disease. Such interactions are important as they have the potential ability to act as targets for therapeutic gain. The critical role of one such interaction in the gut is MAdCAM-1 and its ligand, the lymphocyte integrin $\alpha4\beta7$.

MAdCAM-1 was first recognised on murine endothelial cells in the gut lamina propria, mesenteric nodes, mammary gland, and on follicular dendritic cells of mucosal lymphoid organs (Peyer's patches) but not peripheral lymph nodes. The expression of MAdCAM-1 in experimental gut inflammation increases (Kato *et al* 2000) and $\alpha4\beta7$ is therefore decisively placed to mediate the homing of these lymphocytes to mucosal organs.

The intriguing concept that lymphocytes programmed to home to the gut may also home to the liver constitutes an attractive hypothesis linking chronic IBD with liver associated inflammation affecting medium to large bile ducts e.g. primary sclerosing cholangitis. Grant *et al (2002)* proposed an interesting hypothesis involving the entero-hepatic recirculation of lymphocytes, providing surveillance to protect the liver against gut derived organisms, a pathway which may help the development of liver inflammation in association with IBD.

In this part of the work we have therefore set out to characterise the immunohistochemical expression of MAdCAM-1 in gastrointestinal tissues, liver and related organs e.g. pancreas. The ability to detect the presence of MAdCAM-1 and ultimately quantify its expression could be potentially useful in the diagnosis and subsequent management of chronic inflammatory diseases affecting these organs.

2.2 Experiment 1: Morphological survey of MAdCAM-1 expression in the human liver

2.2.1 Background

Immunological mechanisms are important in the development of liver cirrhosis. In this regard, recruitment and regulation of lymphocytes entering from the circulation into areas of inflammation are crucial. Lymphocyte trafficking is dependent on the interaction of ligands on cell surfaces and adhesion molecules on the surface of blood and lymphatic vessels. The endothelium thus provides a molecular address which is recognised by T lymhocytes subsets. The liver, placed astride the portal venous circulation, plays a major role in modifying the systemic immune response to gut-derived antigens, by mechanisms ranging from conceptually simple filter functions of the reticulo-endothelial system to complex processes such as induction of systemic tolerance (Sumpter *et al* 2007).

In the human gut, MAdCAM-1 is predominantly expressed on vascular endothelium in the lamina propria, high endothelial venules in lymphoid aggregates and follicular dendritic cells in lymphoid follicles (Briskin *et al* 1997). Potential functions in these sites are the recruitment of antigen-specific cells (Waidmann *et al* 2002), recruitment of naïve lymphocytes, antigen presentation/processing, (Feuerer *et al* 2004) modulation of maturation of antibody responses (van der Feltz *et al* 2001) and provision of growth and survival signals to B cells (Krtaz *et al* 1996).

2.2.2 Hypothesis and Aims

Our hypothesis is that inflammatory processes within the liver upregulate local MAdCAM-1 expression to enhance those functions and in particular, the regional vascular distribution of MAdCAM-1 upregulation is related to distribution of disease within the liver lobule/portal tract. Since the expression of MAdCAM-1 in the liver remains poorly characterised the aim of this study was to compare semi-quantitatively compare the expression of MAdCAM-1 in normal liver, in relation to inflammation in a variety of liver disease.

It is already established that the peribiliary vascular plexus supplies the intrahepatic bile ducts; around the larger ducts the plexus is two layered with a rich inner subepithelia layer of fine capillaries and an outer capillary venous network which receives blood from the inner layer (Burt *et al* 2007) (Koda *et al* 2000). Small bile ducts have only a single layer of fine capillaries. Specifically, our object was to define the fine structure of vascular plexuses and lymphatics in the portal tract, particularly the peribiliary plexus, and the bile ducts in liver on which MAdCAM-1 may be expressed and to determine the presence/distribution of MAdCAM-1 in normal, mild, moderate and severely affected livers in a range of immune and non-immune mediated liver disease, with and without co-existing gut inflammation i.e. to compare the expression of MAdCAM-1 in a variety of liver diseases, so as to better understand its role in the liver.

2.2.3 Material and Methods

MAdCAM-1 expression was determined by immunohistochemistry on human liver from a total of 29 patients with chronic liver disease who underwent orthotopic liver transplant (OLT): 9 patients (5 male, 4 female, age range 22-57, median 53 yrs) with PSC, 7 female subjects (age range 36-51, median 50 yrs) with PBC; 7 explants with alcoholic liver disease (ALD 5 males and 2 females) age range 33-64 yrs, median 48 yrs, 5 with chronic hepatitis C virus infection (all males, age range 44-57, median 51 yrs) 3 liver biopsies from chronic rejection after OLT, normal liver tissue obtained from 3 liver biopsy, 4 partial hepatectomies performed for colorectal metastasis with wide resection margins and 4 sections of extra hepatic biliary obstruction were obtained from trucut liver biopsies during staging laparoscopy for pancreatic adenocarcinoma associated with obstructive jaundice. The diagnoses of PBC, PSC, ALD, HCV, HBV and chronic ductopenic rejection were made on established criteria (Lefkowitch 2010). Pre-cirrhotic liver tissues were taken from needle biopsy specimens of PBC stages 1-2 (5 females), HCV stages 1-2 (3males, 2 females), and explants from hepatitis B fulminant liver failure (2 males). There were 2 specimens of non cirrhotic portal hypertension obtained from transjugular liver biopsies; the first was from a 48 year man on long term azathioprine therapy for Crohn's disease and the second from a 52 year lady with myeloproliferative disease and portal venous thrombosis. The controls for MAdCAM-1 expression were taken from samples of normal colon tissue, which constitutively expresses MAdCAM-1.

All tissues were fixed in 10% buffered formalin and embedded in paraffin. Four micron sections were cut on to APES (3-aminopropy triethoxysiline) coated slides, one section being stained with haematoxylin and eosin. Two methods of immunohistochemical staining were used (i) three stage immuno-alkaline phosphatase (APAAP) (ii) three stage immunoperoxidase techniques, whilst also comparing antigen retrieval methods using *Trilogy,* an EDTA based solution with EDTA only

2.2.3.1 Alkaline Phosphatase Anti-Alkaline Phosphatase (APAAP) methodology

Sections were deparaffinised in xylene, dehydrated in alcohol, re-hydrated in water, and immersed in 15% acetic acid for 20mins to block endogenous alkaline phosphatase. They were then treated for target antigen retrieval using 1mmol/L EDTA (pH 8) in a pressure cooker followed by cooling in running water. After rinsing in TRIS buffered saline (TBS) pH 7.6, slides were incubated in 10% normal goat serum (Dako) for 20minutes followed by polyclonal rabbit anti-human MAdCAM-1 (2µg/ml, a gift from Genetech, San Francisco, USA) overnight at 4^0C. Sections were then thoroughly washed in TBS, and incubated with alkaline phosphatase conjugated goat anti-rabbit IgG antibody (1:50 Sigma Aldrich, Poole, UK) for 1 hour at room temperature. The sections were washed with TBS again and incubated with fast red substrate (diazotised 5-nitroanisidine 1-5-naphthalene disulphonate, Dako, UK) for 30 minutes, followed by brief counter staining with Mayer's hematoxylin (Sigma Aldrich, Poole, UK). The slides were mounted in DPX (ProSciTech) and observed using light microscopy.

2.2.3.2 *Trilogy* methodology as a form of antigen retrieval

Trilogy (Cell Marque, Rocklin, CA, USA) is a commercial EDTA based solution used by laboratories as a universal solution to unmask antibodies and has the apparent advantages of lack of refrigeration, expiry and dilution not being required as compared to EDTA on its own.

The sections were deparaffinised and re-hydrated as before. They were rinsed in distilled water twice for 5 minutes each. Antigen retrieval included preheating with

Trilogy (pH 8) at 99^0C for 30 minutes in a water bath. The sections were transferred to new preheated *Triology* for another 30minutes at 99^0 C and rinsed with PBS for 5minutes. Endogenous peroxidase activity was quenched with KPL Blocking Solution and diluted concentrate at 1:10 in hydrogen peroxide at room temperature for 4minutes. The slides were then rinsed with PBS for a further 5minutes, followed by blocking with avidin biotin with Vector Avidin Biotin Kit and rinsed with PBS for 5 minutes. The endogenous immunoglobulin binding sites were blocked with 10% normal goat serum in 3% BSA/PBS for 30 minutes and then the sections were incubated with primary antibody rabbit-antihuman MAdCAM-1 (concentration 2ug/ml) in blocking serum for 30 minutes at room temperature. A negative control in which primary antibody was replaced by mouse IgG antibody (DAKO; Code X0931) was performed for each tissue specimen to assess non specific staining. Dilution of antibodies and duration of incubation at individual stages of the test were adjusted experimentally in laboratory conditions (dilution of anti-mouse MT antibodies, 1:100; incubation duration, 30 minutes). The slides were washed twice with PBS for 5 minutes and then incubated with diluted biotinolated goat-ant-rabbit IgG diluted 1:200 in blocking serum for 30 minutes at room temperature. This was followed by an ABC reagent for 30 minutes and further rinsing with PBS. The sections were further incubated with Pierece Metal Enhanced DAB for 5mins, rinsed with tap water and counterstained with Mayer's hematoxlin for 1 minute and finally washed in distilled water. They were dehydrated, cleared and mounted in synthetic mounting media.

2.2.3.3 Immunoperoxidase staining

After dewaxing, the slides were incubated in 0.3% hydrogen peroxide in methanol followed by microwave treatment in citrate buffer for 5 minutes. They were then incubated in Normal Goat serum (1:10 dilution) for 20 minutes, followed by anti-human MAdCAM-1 for 1 hour. The sections were washed with PBS and incubated with biotinylated goat anti-rabbit IgG (1:200 dilution) for 30 minutes and washed again with PBS. They were then incubated with PAP complex for 30 minutes and washed repeatedly with PBS. DAB substrate was added and left for 10 minutes, washed again with PBS, counterstained with haematoxylin, mounted and visualized by light microscopy.

2.2.3.4 Dendritic cell and lymphatic vessel staining

A panel of adjacent serial sections from tissue were also immunostained for a subset of dendritic cells, including CD21, CD68 and S100 to elucidate the site of the MAdCAM-1 immunoreactivity in the lymphoid aggregates using the APAAP methodology as described above.

Monoclonal antibodies to CD21 were used to identify follicular dendritic cells, CD68 stains to recognise monocyte/macrophage and dendritic cell. Antibody to S100 proteins stains antigen presenting cells such as interdigitating dendritic cells.

Sections were incubated with primary antibody for one hour. Blocking was performed with normal goat serum (1:10, DAKO UK Ltd) followed by incubation with rabbit anti-mouse antibody (1:25, DAKO UK Ltd) for 45 minutes and then with alkaline phosphatase-conjugated mouse anti-alkaline phosphatase (1:50, DAKO UK Ltd) for a further 45 minutes.

Some sections were stained to demonstrate lymphatic endothelium using anti-podoplanin (a gift from Dr Kershaki, Austria). Microwave pre-treatment was followed by labeling with rabbit anti-human podoplanin IgG for 60 minutes at room temperature and washing in PBS biotinylated goat anti-rabbit antibodies (Vector). The staining was visualised using a streptavidin–peroxidase complex (Vector), diamino-benzidine and H_2O_2. Sections incubated without primary antibodies were used as negative controls.

2.2.3.5 Immunofluoresence Microscopy

After pre-treatment, sections were incubated with anti-human MAdCAM-1 (1:150) and antiCD34 (1:100) primary antibodies. They were then washed in PBS and incubated with secondary antibody (goat anti-rabbit FITC and goat anti-mouse Texas Red, both 1:50 in PBS) for 1 hour at room temperature, and examined by fluorescence microscopy.

Representative sections were incubated with anti-CD21(1:100), anti-CD68(1:50), anti-S100(1:50) and anti-human MAdCAM-1(1:150) primary antibodies. They were

subsequently washed in PBS and incubated with secondary antibody (goat ant-rabbit FITC and goat anti-rabbit FITC and goat anti-mouse Texas Red, both 1:50 in PBS) for 1 hour at room temperature and examined by flouorescence microscopy.

2.2.3.6 Immunohistochemical Assessment

Two observers (Aftab Ala and Richard Standish) independently assessed the sections semi-quantitatively and scored the staining on a scale of 0-3 according to the intensity of MAdCAM-1 immunoreactivity (0-no staining, 1-mild staining, 2- moderate staining and 3 marked staining). The staining methods were repeated twice to validate the scoring system. Particular attention was paid to areas of lymphoid aggregation and vascular endothelium, specifically in the vessels of the PBP. The sections were also examined for staining of hepatocytes, biliary epithelium and sinusoid lining cells. The bile ducts were analysed in three categories according to size: proliferating bile ductules (the smallest duct branches with a generally inconspicuous lumen, usually confined to marginal zones in portal areas), interlobular ducts (small ducts, diameter 20-100um), and large ducts of greater than 100um in diameter, usually septal or trabecular ducts.

2.2.4 Results

Both APAAP and immunoperoxidase techniques showed similar levels of MAdCAM-1 immunostaining, but immunoperoxidase gave rather higher background staining than APAAP as did using the Triology method of antigen retrieval. MAdCAM-1 immunoreactivity was seen in all cirrhotic sections of explant liver tissue expression being localised primarily to septal areas mainly within the (i) endothelium of the peribiliary vascular plexus and (ii) septal-hepatic lymphoid aggregates.

The sections taken from normal livers and non cirrhotic portal hypertension failed to demonstrate any immunoreactivity to MAdCAM-1.Positive ontrols were taken from sections of normal colonic tissue, which demonstrated MAdCAM-1 expression on vascular endothelium within the lamina propria and submucosa.

2.2.4.1 Peribiliary vascular plexus (fig 2.1, tables 2.1-2.4)

Around the large to medium bile ducts, 2 layers of vessels showed MAdCAM-1 immunoreactivity representing the inner and outer layers of peribiliary vascular plexus (PBP). MAdCAM-1 expression was seen in vessels around large to medium sized ducts in PSC. In PSC most (7/9) showed MAdCAM-1 expression in vessels around medium sized bile ducts; 3 showed moderate staining of the PBP and in the remaining 4 staining was weaker. Overall. moderate staining in the PBP appeared to be more frequently present arounds ducts in PSC, compared to the other disease states. In PBC, over half of MAdCAM-1 expressing PBP vessels showed only weak immunoreactivity (4/6) with the remainder (2/6) showing moderate staining. Double staining with anti-MAdCAM-1 and anti-CD34 demonstrated co-localisation of CD-34 and MAdCAM-1 in structures resembling PBP capillaries *(figure 2.4)*.

There were similar levels of MAdCAM-1 immunoreactivity of the PBP in other cirrhotic liver sections.

2.2.4.2 Intrahepatic lymphoid aggregates (figure 2.1, tables 2.1 to 2.4)

Most patients expressed MAdCAM-1 within septal lymphoid aggregates (6/9 PSC and all 7 PBC cases). This appeared as 2 distinct forms, (i) away from the aggregate centre in a "peripheral" pattern (3/9 PSC and 6/7 PBC) or (ii) in vessel endothelium - "central" pattern of MAdCAM-1 staining (6/7 PSC and 3/9 PBC). 4 of 7 had moderate to marked MAdCAM-1 staining intensity conforming to the "peripheral" pattern compared to only 2/7 in a central pattern of similar intensity. Most of the PSC cases had light MAdCAM-1 immunoreactivity (5/9) and only one had moderate staining to MAdCAM-1. Localisation of MAdCAM-1 to lymphoid aggregates in PSC and PBC was confirmed by immunofluoresence microscopy, which showed both the "peripheral" and "central" staining patterns.

Focal staining was seen with S100, CD68 and CD21 antibodies but these did not correspond to the observed pattern of MAdCAM-1 immunoreactivity. Dual immunostaining was also performed with anti-MAdCAM-1 and anti-S100, CD68 and CD21, but these did not co-localise with MAdCAM-1. An example of this has been illustrated with CD21 in figure 2.3(G-I).

We explored the possibility that the 'central' cells within lymphoid aggregates were CD 34 positive. There was focal staining evident with CD34 that matched the 'central' pattern of MAdCAM-1 staining in lymphoid aggregates.

All the sections taken from Hepatitis C showed similar immunoreactivity.

2.2.4.3 Lymphatic endothelium and podoplanin localisation in lymphoid aggregates and the peribiliary vascular plexus (figures 2.2 to 2.4)

Podoplanin was located in vessels with morphological features of lymphatic channels that were surrounding, immediately adjacent to, and separate from lymphoid aggregates. These vessels were characterised by flattened endothelium without evidence of erythrocytes within their lumen and were spatially distinct from vessels expressing MAdCAM-1, including the PBP. Co-localisation of CD34 and MAdCAM-1 with a different pattern of staining than the podoplanin suggests that the vessels are capillaries of the PBP.

There was no evidence of MAdCAM-1 expression in hepatocytes, biliary epithelium, hepatic artery, septal connective tissue or sinusoids from any of the liver sections. Only one patient with PSC had weak staining of two small vessels at the edge of parenchymal nodules.

2.2.4.4 Negative controls

MAdCAM-1 was not present in normal liver, specimens from extra-hepatic duct obstruction, or chronic rejection after liver transplantation. Negative controls incubated without primary antibody or with isotype matched anti-IgG were included in all experiments.

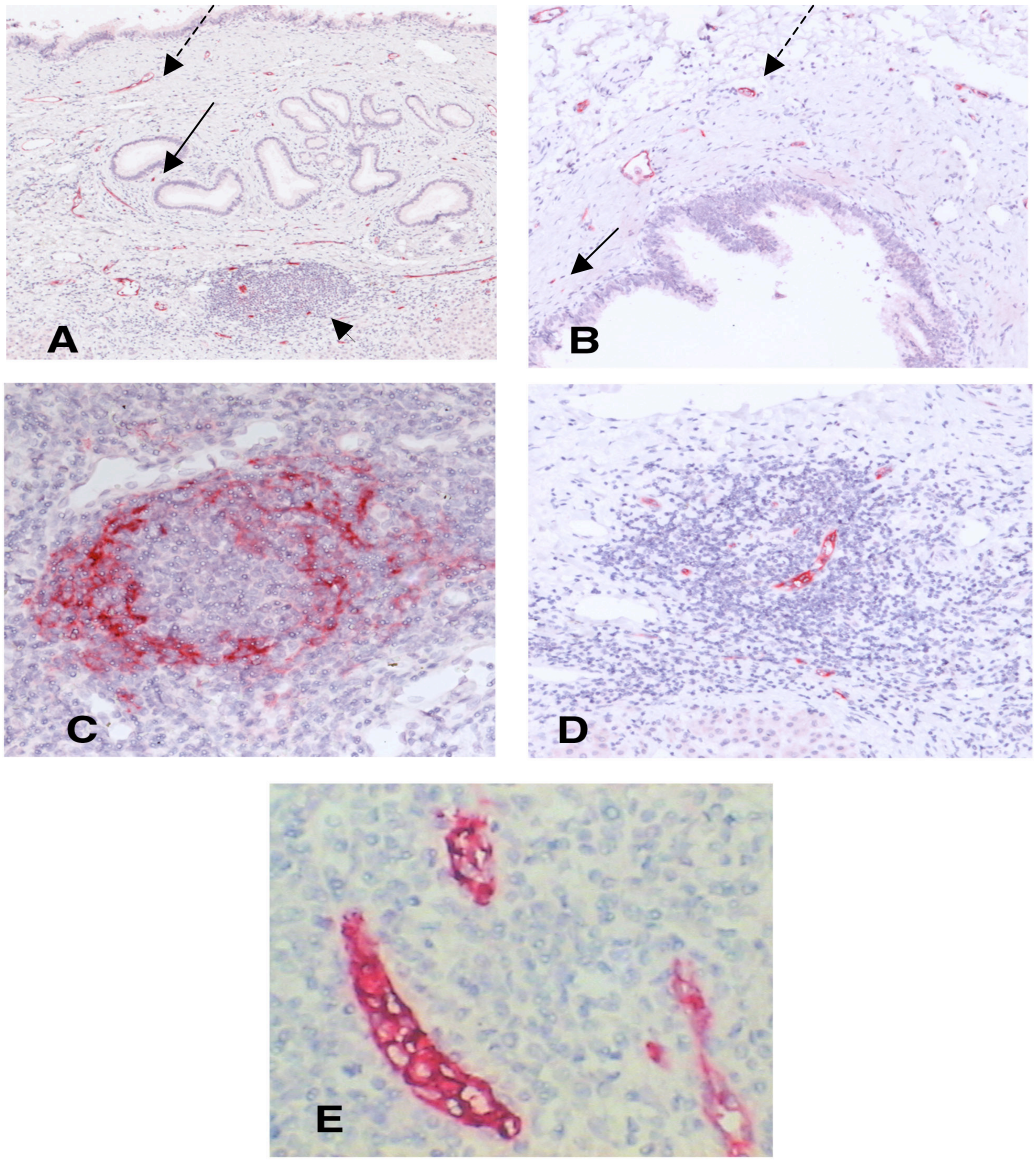

Figure 2.1 (A-E) MAdCAM-1 immunoreactivity patterns in vessels and lymphoid aggregates from cirrhotic liver explants of PSC and PBC. Plate A and B show MAdCAM-1 immunostaining of vessels around peribiliary glands, adjacent to a lymphoid aggregate(arrow head). These vessels represent the inner (continous arrow) and outer layers (broken arrow)of the peribiliary plexus (Plate B higher magnification x10 objective). The pattern of staining of the lymphoid aggregate (plate C) appears to correspond to follicular dendritic cells. The lymphoid aggregates have two main MAdCAM-1 immunoreactivity patterns: "peripheral" (plate C) and "central" (plate D). The high endothelial venules are MAdCAM-1 immunoreactive vessels (plate E) within lymphoid aggregates, which are likely to represent areas of lymphocyte egress. (Alkaline phosphatase/Fast Red immunostaining: Magnification x5 objective A; x10 objective B, C and D; x20 objective E).

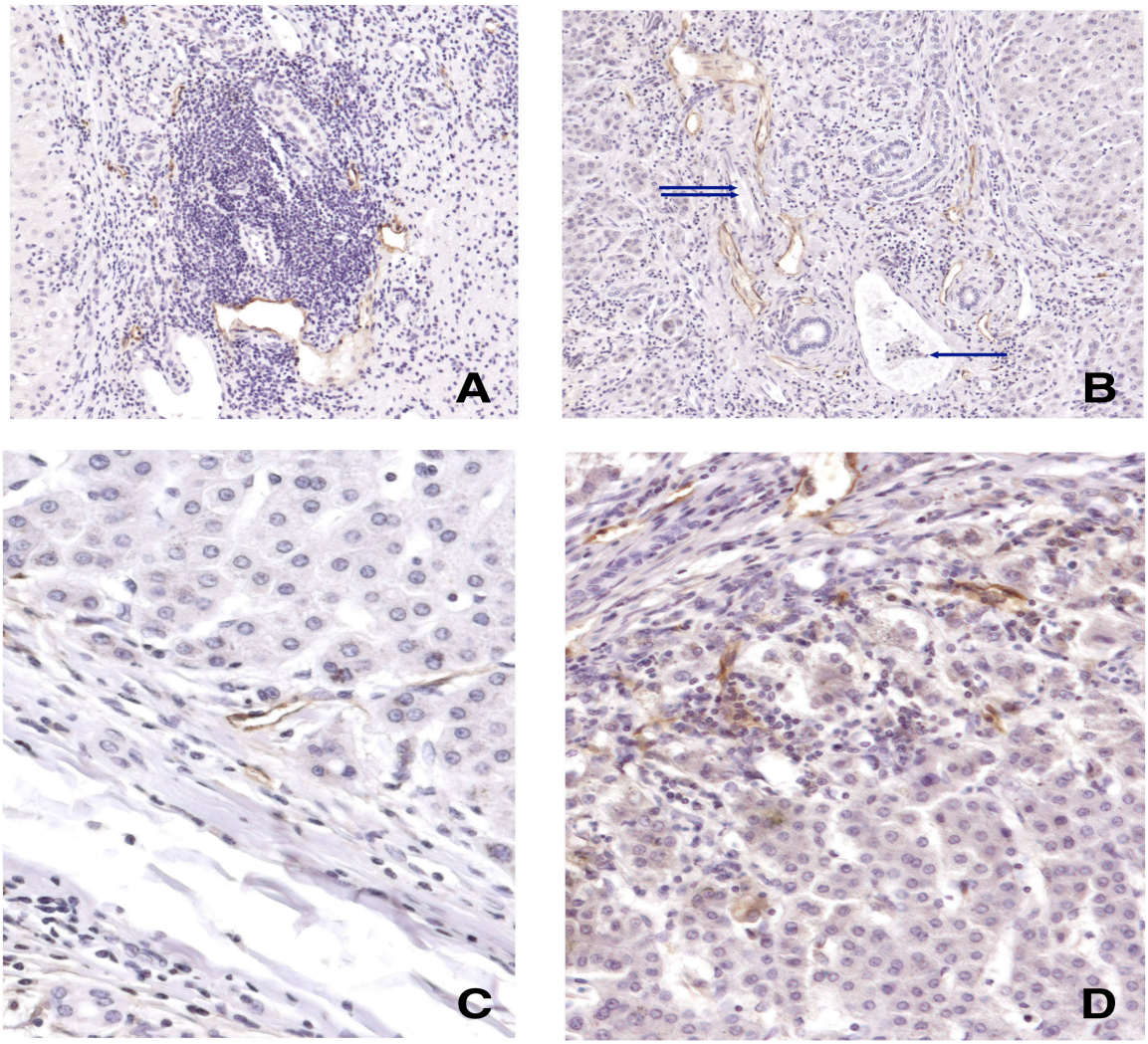

Figure 2.2 (A-D) Immunohistochemical localisation of the lymphatic phenotypic marker podoplanin in PSC and PBC. Plates A and B demonstrate podoplanin staining patterns of vessels around a lymphoid aggregate, but not conforming to "peripheral" or "central" MAdCAM-1 immunoreactivity. Note the portal vein (single arrow) containing red blood cells is identifiable, as is the muscular wall of the hepatic artery (double arrow), and neither shows podoplanin immunoreactivity. Plates C and D show podoplanin staining into lymphatic channels, which extend a short distance into the parenchyma from porto-septal areas, both in the presence and absence of inflammatory cells. (Alkaline phosphatase immunostaining: Magnification x10 objective A&B, x20 Objective C&D)

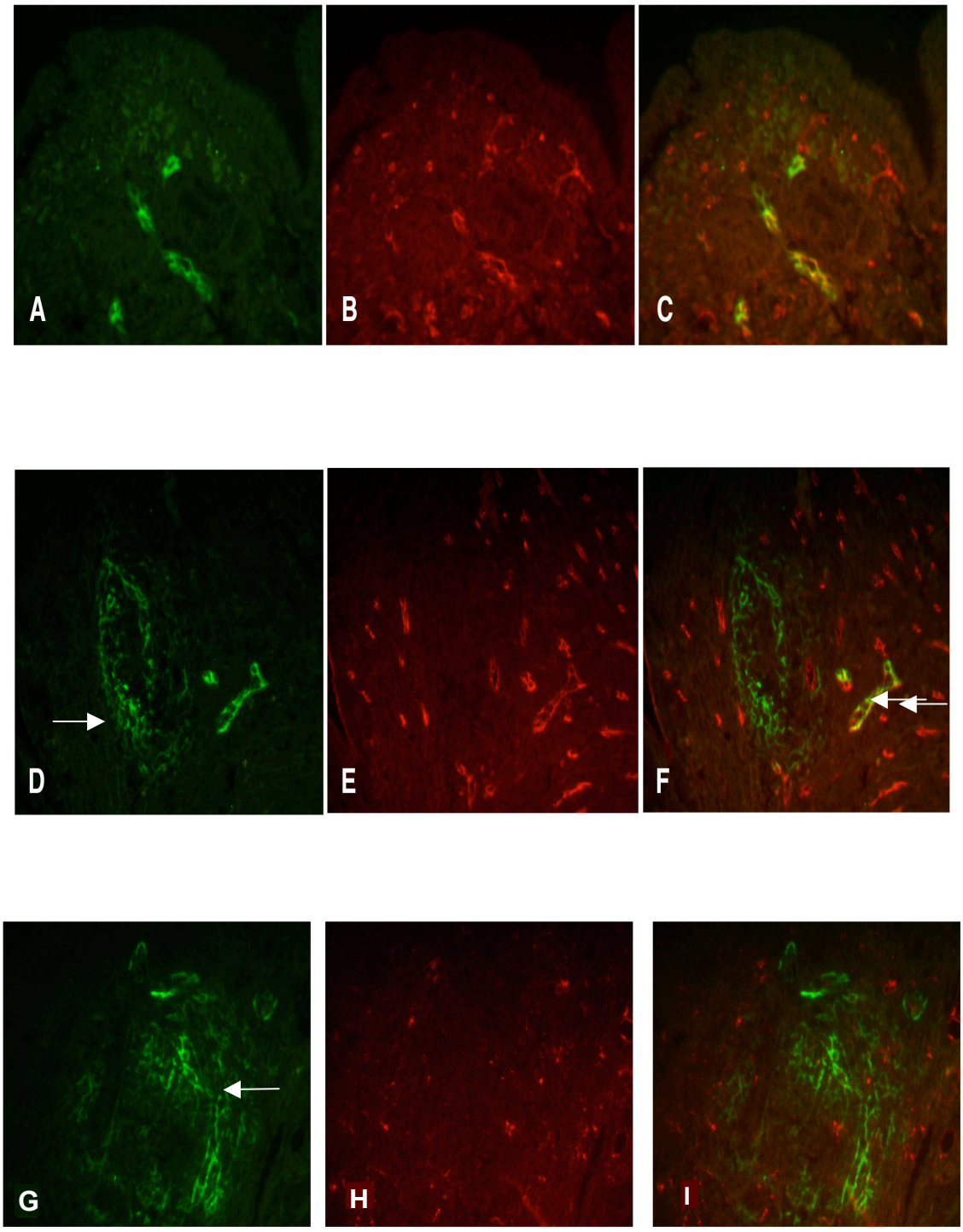

Figure 2.3(A-I) Dual immunofluoresence micrographs showing representations of MAdCAM-1 (Panel A and D –green), CD34 (Panel B and E-red) and CD 21(Panel H-red) immunoreactivity. Panel A demonstrates MAdCAM-1 immunofluoresence of a peribiliary plexus around a large sized bile duct. Panel B confirms the presence of CD34 immunoreactive vessels around these ducts. Panel C shows dual colour co-localisation (yellow) of MAdCAM-1 and CD34 fluorescence within the peribiliary plexus. Plate D-F shows a lymphoid aggregate with a 'peripheral' pattern of MAdCAM-1 immunolocalisation (Panel D maked with single arrow) which fails to co-localise with CD34 (Panel E) in double staining (Panel F) but colocalises an adjacent vessel endothelium (yellow-marked with double arrow). Panels G-I shows a different lymphoid aggregate from the same tissue with a 'peripheral' pattern of MAdCAM-1 immunoreactivity (Panel G), Focal staining was performed to exclude a dendritic cell morphology e.g CD21(Panel H) but did not correspond to the observed pattern of MAdCAM-1 immunoreactivity. Dual immunostaining with anti-MAdCAM-1 did not co-localise with anti-CD21(Panel I) (Magnification x20 objective).

Table 2.1 (Primary sclerosing cholangitis: n=9) MAdCAM-1 immunostaining score

PATIENT	AGE	HISTOLOGY	LYMPHOID AGGREGATE STAINING PATTERN		PERIBILIARY PLEXUS-BILE DUCT SIZE		
			'Peripheral'	'Central'	Large	Medium	Small
1M	**22**	**Cirrhosis**	**2+**	**1+**	**0**	**0**	**0**
2F	**47**	**Cirrhosis**	**2+**	**1+**	**0**	**1+**	**0**
3F	**28**	**Cirrhosis**	**0**	**0**	**0**	**2+**	**0**
4F	**35**	**Cirrhosis**	**1+**	**1+**	**0**	**2+**	**0**
5M	**38**	**Cirrhosis**	**0**	**1+**	**0**	**2+**	**0**
6F	**47**	**Cirrhosis**	**1+**	**1+**	**1+**	**1+**	**2+**
7M	**50**	**Cirrhosis**	**0**	**0**	**0**	**0**	**0**
8M	**43**	**Cirrhosis**	**3+**	**3+**	**2+**	**1+**	**1+**
9M	**34**	**Cirrhosis**	**0**	**0**	**0**	**1+**	**0**

MAdCAM-1 Immunostaining score

No staining	**0**
Light staining	**1+**
Moderate staining	**2+**
Marked staining	**3+**

Table 2.2 (Primary Biliary Cirrhosis: n=12) MAdCAM-1 immunostaining score

PATIENT	AGE	HISTOLOGY	LYMPHOID AGGREGATE *STAINING PATTERN*		PERIBILIARY PLEXUS- BILE DUCT SIZE		
			'Peripheral'	*'Central'*	*Large*	*Medium*	*Small*
1F	**61**	**Cirrhosis**	**1+**	**2+**	**0**	**1+**	**1+**
2F	**57**	**Cirrhosis**	**2+**	**3+**	**0**	**1+**	**1+**
3F	**51**	**Cirrhosis**	**1+**	**0**	**0**	**1+**	**0**
4F	**57**	**Cirrhosis**	**2+**	**0**	**0**	**1+**	**0**
5F	**36**	**Cirrhosis**	**0**	**1+**	**0**	**2+**	**0**
6F	**57**	**Cirrhosis**	**3+**	**0**	**0**	**0**	**0**
7F	**47**	**Cirrhosis**	**2+**	**0**	**0**	**1+**	**0**
8F	**49**	**Stage1**	**0**	**0**	**N/A**	**0**	**0**
9F	**52**	**Stage2**	**0**	**1+**	**N/A**	**0**	**0**
10F	**49**	**Stage2**	**0**	**0**	**N/A**	**0**	**0**
11F	**59**	**Stage1**	**0**	**0**	**N/A**	**0**	**0**
12F	**61**	**Stage1**	**0**	**0**	**N/A**	**0**	**0**

MAdCAM-1 immunostaining score

No staining 0
Light staining 1+
Moderate staining 2+
Marked staining 3+

Large ducts were not present in the needle biopsy sprecimens. They are classified as a N/A

Table 2.3 (Alcohol liver disease: n=7) MAdCAM-1 immunostaining score

PATIENT	*AGE*	HISTOLOGY	PERIBILIARY PLEXUS-BILE DUCT SIZE		
			Large	Medium	Small
1M	61	Cirrhosis	0	1+	0
2F	57	Cirrhosis	0	1+	0
3M	51	Cirrhosis	0	1+	0
4F	57	Cirrhosis	0	1+	0
5M	36	Cirrhosis	0	1+	1+
6M	48	Cirrhosis	0	1+	0
7M	57	Cirrhosis	0	0	0

MAdCAM-1 immunostaining score

No staining	**0+**
Light staining	**1+**
Moderate staining	**2+**
Marked staining	**3+**

Table 2.4 (Hepatitis C: n=10) MAdCAM-1 immunostaining score.

PATIENT	*AGE*	HISTOLOGY	*LYMPHOID AGGREGATE* *STAINING PATTERN*		PERIBILIARY PLEXUS-BILE DUCT SIZE		
			'Peripheral'	'Central'	Large	Medium	Small
1M	51	Cirrhosis	1+	2+	0	1+	1+
2M	52	Cirrhosis	2+	1+	0	1+	0
3M	49	Cirrhosis	1+	2+	0	1+	0
4M	55	Cirrhosis	1+	0	0	1+	0
5M	48	Cirrhosis	1+	1+	0	1+	0
6M	48	Stage2	0	0	N/A	0	0
7F	54	Stage2	0	1+	N/A	0	0
8M	52	Stage2	0	0	N/A	0	0
9M	53	Stage1	0	0	N/A	0	0
10F	48	Stage1	0	0	N/A	0	0

MAdCAM-1 immunostaining score

No staining 0
Light staining 1+
Moderate staining 2+
Marked staining 3+

Large ducts were not present in the needle biopsy sprecimens. They are classified as a N/A

2.2.5 Discussion

My results have demonstrated significant up-regulation of MAdCAM-1 expression in chronic liver disease i.e. cirrhosis. Specifically, I found MAdCAM-1 to be localised to septal areas primarily within: i) endothelium of the PBP and ii) intra-hepatic (septal) lymphoid aggregates. I confirmed the presence of MAdCAM-1 expression in liver disease characterised by portal inflammation e.g. PSC and PBC and extended these observations to show its presence in a number of other chronic liver diseases which are not necessarily associated with portal inflammation e.g. ALD, as well as those which are unrelated to gastrointestinal inflammation e.g. HCV.

The peribiliary plexus (PBP) is a network of delicate small vessels surrounding the intrahepatic bile ducts supplied by branches of the hepatic artery, which drain into hepatic sinusoids or branches of the portal vein (Kobatashi *et al* 1994). The PBP is the main vascular supply of the biliary epithelium (Takasaki S *et al* 2001). It functions in supporting the secretory and absorptive properties of the biliary epithelium. I found MAdCAM-1 to be expressed in the PBP in a range of bile duct sizes in PSC and PBC explants. The specificity of MAdCAM-1 staining is indicated by the fact that bile ducts are not stained. The vascular endothelial nature of these structures was confirmed by dual immunofluoresence with MAdCAM-1 and CD34. The distribution of MAdCAM-1 around the bile ducts differed between PSC and PBC. The smaller single capillary layer ducts showed similar levels in both conditions but only large sized bile ducts expressed MAdCAM-1 in PSC, an observation which is particularly interesting since PSC involves large ducts than PBC i.e. the absence of large duct inflammation in PBC and lack of MAdCAM-1 expression around these ducts may reflect regional distribution of disease, which was further supported by MAdCAM-1 staining around its small bile ducts. In addition, MAdCAM-1 expression on the PBP around medium and large ducts is increased in the cirrhotic PSC and PBC liver. Moreover, moderate staining appeared more frequently in the PBP of the cirrhotic PSC liver compared to the other disease states. These vessels of the PBP might represent transformed high-endothelial venules which in other sites are well characterised for their role in leukocyte trafficking (Miyasaka *et al* 2004) (Hayasaka H *et al* 2010). That is, there is some evidence to suggest that HEV neogenesis and the development of the high endothelial venules which may mediate lymphocyte trafficking can appear ectopically for instance in

chronically inflamed tissues.

There is little previous evidence on the expression of vascular adhesion molecules on the PBP. Yasoshima *et al* (1995) showed some of these vessels to express ICAM-1 in PBC but did not study MAdCAM-1. The vascular endothelium can secrete proinflammatory cytokines e.g. TNFα and this is a likely amplification step leading to the upregulation of adhesion molecules on the endothelium of the peribiliary vascular plexus.

The presence of MAdCAM-1 on the endothelium of the PBP is presumptive of a role in lymphocyte emigration and recruitment, suggesting MAdCAM-1 acts as a local addressin at these sites, using the endothelium of the PBP for egress and as a recirculatory pathway to areas of inflammation such as those around bile ducts. The possibility that this egress occurs in capillaries is exciting because this lymphocyte-endothelium interaction could occur in low velocity flow states. The functional significance of the expression of MAdCAM-1 on the PBP is uncertain as they are also present in cases of HCV and ALD cirrhosis, where bile duct injurt is not a major feature. It is possible that the structures immunoeactive to MAdCAM-1 on the PBP are functionally post-capillary sinuses which are ideal sites for lymphocyte egress.

Whether MAdCAM-1 upregulation is a late event in the pathogenesis of chronic liver disease or a secondary response to inflammation is not known. Cholestasis alone is unlikely to be responsible for MAdCAM-1 upregulation due to the lack of expression in extrahepatic obstruction. We studied early stage specimens (pre-cirrhotic) in other biliary tract diseases e.g. PBC, and non-biliary tract liver disease, unrelated to gastrointestinal inflammation such as. HCV, and acute fulminant hepatitis B, to characterise the time course of MAdCAM-1 and assess its expression in relation to degree of inflammation and bile duct loss. In PBC other adhesion molecules such as ICAM-1 appear to be expressed commensurate with the level of inflammation (Adams *et al* 1991). Interestingly, there was minimal evidence of MAdCAM-1 expression in any pre-cirrhotic specimens, (PBC, HCV). I detected MAdCAM-1 in nearly all cirrhotic liver but not in non cirrhotic liver (non-cirrhotic portal hypertension and normal liver).

It therefore follows that the upregulation of MAdCAM-1 was not due to the effects of portal hypertension.

The observation that the majority of MAdCAM-1 was upregulated on cirrhotic liver suggests that its upregulation might be related to the fibrogenesis or neovascularisation of cirrhosis. Certainly, TNFα activation of fibroblasts reportedly induces expression of MAdCAM-1 (Leung *et al* 2003). The possibility that some of the endothelium-lined vessels showing immunoreactivity to MAdCAM-1 were actually lymphatic in origin was considered using the novel endothelial cell-surface glycoprotein podoplanin, originally observed in rat and human kidney as a marker for the endothelium of lymphatic vessels (Breitender-Geleff *et al* 1997). I have demonstrated podoplanin expression on vessels with morphological features of lymphatic vasculature, subjacent to and separate from lymphoid aggregates but these were morphologically distinct from vessels expressing MAdCAM-1. They were characterised by a single layer of flattened endothelium without erythrocytes and with intraluminal lymphocytes. There were occasional thin-walled branches originating from larger lymphatic vessel in portal-septal areas extending a short distance between hepatocyte plates. Thus, those areas that express MAdCAM-1 in and around septal lymphoid aggregates appear not to be lymphatic channels.

There appeared to be two populations of MAdCAM-1 positive cells in the lymphoid aggregates. I described the pattern of MAdCAM-1 expression in lymphoid aggregates as "peripheral" or "central" with immunoreactivity in vessel endothelium likely to be the HEV. Although definitive conclusions could not be made from our experiments regarding the nature of the peripheral staining pattern, it may represent MAdCAM-1 expression on the specialised dendritic cells e.g. interdigitating reticular cells, follicular dendritic cells (FDC) (Szabo *et al* 1997), or macrophages (Stagg *et al* 2002).

We explored the possibility that the 'central' cells within lymphoid aggregates were CD 34 positive. There was focal staining evident with CD34 that matched the 'central' pattern of MAdCAM-1 staining in lymphoid aggregates. Dual immunostaining with MAdCAM-1 and CD 34 to extend these experiments would have been useful to confirm whether these cells were vascular endothelial in origin e.g. HEV.

The inflammatory processes within the liver may up-regulate MAdCAM-1 locally, enhancing recruitment of antigen specific cells. Although there was focal staining seen with S100, CD68 and CD21 antibodies, surprisingly this did not correspond to the pattern seen for MAdCAM-1. Dual immunostaining was also performed with anti-MAdCAM-1 and anti-S100, CD68, CD21 but these did not co-localise with MAdCAM-1.The morphology of some of the lymphoid MAdCAM-1 staining pattern appeared similar to dendritic cells e.g. FDC present in Peyer's patch and also resembled VCAM-1 immunoreactivity in lymphoid aggregates from end stage viral hepatitis (García-Monzón *et al* 1995) and ICAM-1 (Koopman *et al* 1991), through which they can support antigen presentation to α4β1 and LFA-1 expressing B cells, respectively in germinal centres, thus leading to their maturation and differentiation into memory cells. Hepatic expression of MAdCAM-1 on dendritic cells could serve as a signal for retention of α4β7 lymphocytes in the liver. The possibility of HEV within lymphoid aggregates raises the further possibility of its importance in lymphocyte egress and effective recirculation to areas of inflammation. Unfortunately, the dendritic cell markers used in our study did not appear to give any comparable immunoreactivity. Certainly more extensive dual staining using specific markers for further dendritic cell subsets is required to define exactly where MAdCAM-1 protein is expressed. If MAdCAM-1 appears to be expressed in dendritic cells within the liver then this would suggest that it has a more extensive role then acting as an addressin in chronic liver disease.

The activation of α4β7 mucosal lymphocytes recruited from the gut to the PSC liver is a possible mechanism by which hepatic inflammation is maintained in some patients with IBD. The concept that lymphocytes programmed to home to the gut may also home to the liver constitutes an attractive hypothesis linking chronic IBD with liver inflammation. These results concur with those by Grant *et al* (2001) confirming MAdCAM-1 expression in liver cirrhosis secondary to PSC. We have extended these observations to demonstrate MAdCAM-1 in other cirrhotic liver diseases e.g. PBC, (where we see similar patterns of MAdCAM-1 expression in the vascular beds of the PBP) as well as ALD and HCV. We did not see MAdCAM-1 expression in normal liver, extra-hepatic biliary obstruction and very little in the way of pre-cirrhotic stages

of liver disease. In all cases the isotype-matched control used displayed no reactivity, suggesting that the stain with anti-MAdCAM-1 was real.

In conclusion, we have provided evidence to suggest that MAdCAM-1 may contribute to the pathogenesis of end stage immune mediated liver disease. Furthermore these observations have been extended to include other non-cholestatic bile duct chronic liver diseases. Further investigation of the expression and modulation of MAdCAM-1 expression could lead to improved understanding of the pathophysiology of end-stage liver disease and provide the basis for the development of new therapeutic modalities.

2.3 Experiment 2: Expression of MAdCAM-1 in inflammatory bowel disease

2.3.1 Background

Crohn's disease (CD) and ulcerative colitis (UC) comprise chronic inflammatory bowel disease, the aetiology of which still remains unclear. Crohn's disease is characterised by non caseating granulomas, lymphoid aggregates and extension of inflammation through all layers of the bowel wall. Ulcerative Colitis is characterised by mucosal inflammation and extensive formation of ulcers which are usually confined to the submucosa.

Briskin *et al (1997)* report a ubiquitous over expression of MAdCAM-1 in venules in mucosal inflammation sites in CD and UC. However, differences in immunological backgrounds suggest different expression patterns of cell adhesion molecules between UC and CD. Cytokine analysis in CD demonstrates an increased expression of IL-2, IFN-y and IL-12 (produced by antigen presenting cells), which suggests the predominance of the T-helper type 1 (Th1)response. Ulcerative colitis seems to be an atypical Th2 disorder, in which the Tcell-profile has been more difficult to characterise. This disease was considered to have Th2 profile but the concentrations of 1L-4 and IL-5 which are normally elevated in Th2 mediated diseases have been variable in UC tissues.

2.3.2 Hypothesis and Aims

Our hypothesis is that there are regional differences in MAdCAM-1 expression between Crohn's disease and ulcerative colitis and this reflects the distribution of the disease. With this in mind, we set out to characterise the expression of MAdCAM-1 in inflammatory bowel disease by immunohistochemical analysis.

2.3.3 Methods

Surgically resected tissue specimens were prospectively obtained immediately after removal from seven patients with Crohn's disease (five men and two women, median age 34.1 years) and six with ulcerative colitis (four men and two women, median age 29.7 years). The patients with Crohn's disease included four ileocolitis and three with terminal ileal diseases. Patients with ulcerative colitis included four with pancolitis and two with left sided disease. All the patients were treated with corticosteroids before the

operation. Control tissue consisting normal appearing colon and small intestine tissue was obtained from 5 patients with colorectal carcinoma. Tissue samples were collected from either macrospically uninvolved areas at a distance of 2-4 cms from the inflamed area or from centres of severely affected tissue. The indications for surgery included disease refractory to treatment, chronic stenosis or both in Crohn's disease, long standing pancolitis or those individuals with left sided colitis in UC. In all cases, diagnosis was confirmed by histopathological examination of the resected specimen.

2.3.3.1 Immunohistochemistry

The tissue samples were collected immediately after elective surgical resection and formalin fixed. Immunohistochemistry was performed as described earlier in this chapter. The negative control consisted replacement of the primary antibody with isotype-matched negative control antibodies *(DAKO UK*).

2.3.3.2 Morphometric analysis

Two observers (Aftab Ala and Richard Standish) independently assessed the sections semiquantively and scored the staining on a scale of 0-3 according to the degree of MAdCAM-1 immunoreactivity (0-no staining, 1-mild staining, 2-moderate staining and 3- marked staining, without knowledge of the histological diagnosis. The staining methods were repeated twice to validate the scoring system. To quantify the expression of MAdCAM-1 whole areas of the ulcer base and active inflammation from each slide in 5 representative fields per high power field (at a magnification of x40 objective) were studied. The average numbers of vessels immunoreactive to MAdCAM-1 were calculated in the lamina propria, submucosa or mucosa. Five visual fields within the mucosa, submucosa and muscularis mucosa were chosen randomly from each section for semi-quantitative light microscopic analysis (x40 objective) so as to assess the extent of the endothelial expression of MAdCAM-1 positive vessels and then quantify the number of MAdCAM-1 positive vessels on a section serial stained for CD34. The percentage of CD34 positive vessels that co-expressed MAdCAM-1 vessels was estimated and the results were expressed as semi-quantitative scores. Only tissues without histological signs of inflammation were included as 'uninvolved'. There was no

relationship between the presence of granuloma formation in CD and associated nearby or focal MAdCAM-1 immunoreactivity upregulation or intensity of staining.

The distinction between capillaries and venules were made on the following criteria: capillaries consist of a single layer of endothelial cells; they have a luminal diameter from 4-10 μm; they do not have a tunica media and little or no tunica adventitia; they are predominantly localised to the lamina propria. Venules are initially formed by the confluence of a number of capillaries. These are distinguished by size from capillaries, being 20-30 μm in diameter with a muscular wall.

Comparisons between groups were made using the Mann-Whitney two tailed test for unpaired samples. Correlations were tested using Spearman's rank correlation test.

2.3.4 Results

2.3.4.1 Control mucosal tissues (Figure 2.4 i to ii)

MAdCAM-1 was expressed sporadically in the endothelial cells of venules in the lamina propria and submucosa compared to relative paucity in the subserosa or muscularis mucosa in control large intestine. There was absence of immunoreactivity on arteries and very little on arterioles and veins. MAdCAM-1 immunoreactivity in an individual vessel usually was either very strong or could not be detected at all; only few vessels showed weak staining.

2.3.4.2 MAdCAM-1 in the uninvolved gut adjacent to inflammation (Figure 2.5 to 2.7, table 2.5*)*

In the uninvolved area of CD and UC, MAdCAM-1 showed distribution patterns and staining intensity similar to those seen in the normal gut. As in controls immunoreactivity for MAdCAM-1 was restricted to venules and a few veins, but was not detected on arterial vessels. Vascular endothelium was more often MadCAM-1 positive in the mucosa and submucosa than in the serosa or muscularis propria. Evaluation of semiquantitative analysis showed no significant differences between uninvolved areas of IBD and the normal gut (Table 2.5, figure 2.6 to 2.8).

2.3.4.3 MAdCAM-1 in the inflamed gut (Figures 2.4iii to iv& 2.5 to 2.8, table 2.5)

In highly inflamed areas of CD and UC, there was upregulation of MAdCAM-1. MAdCAM-1 expression was multi-focal i.e. localised to both the luminal and ab-luminal aspect of venular endothelial cells, within the lamina propria but only partially encircled the venular endothelial surface. In CD, MAdCAM-1 was expressed in venular endothelial and gut associated lymphoid tissue *(figure 2.4iii);* there were consistent MAdCAM-1 immunoreactivity patterns on the venular endothelium within the tunica muscularis and serosa in all cases of highly inflamed CD*,* consistent with the pattern of disease i.e. immunoreactivity was observed in all layers of the intestinal wall. There were no clear differences between the intensity of staining patterns in CD and UC in the venular endothelium or the lymphoid aggregates. However, taking into account the ratio of MAdCAM-1 venules to CD34+ vessels in comparison with normal bowel, inflamed colon lesions of Crohn's disease showed a significant increase in MAdCAM-1 immunoreactivity score on venules ($p<0.001$). In ulcerative colitis, the significance between inflamed colon lesions and the normal bowel or uninvolved gut reached a level of $p<0.01$. Overall, comparing active Crohn's disease with ulcerative colitis the level of signifiance was $p<0.05$.

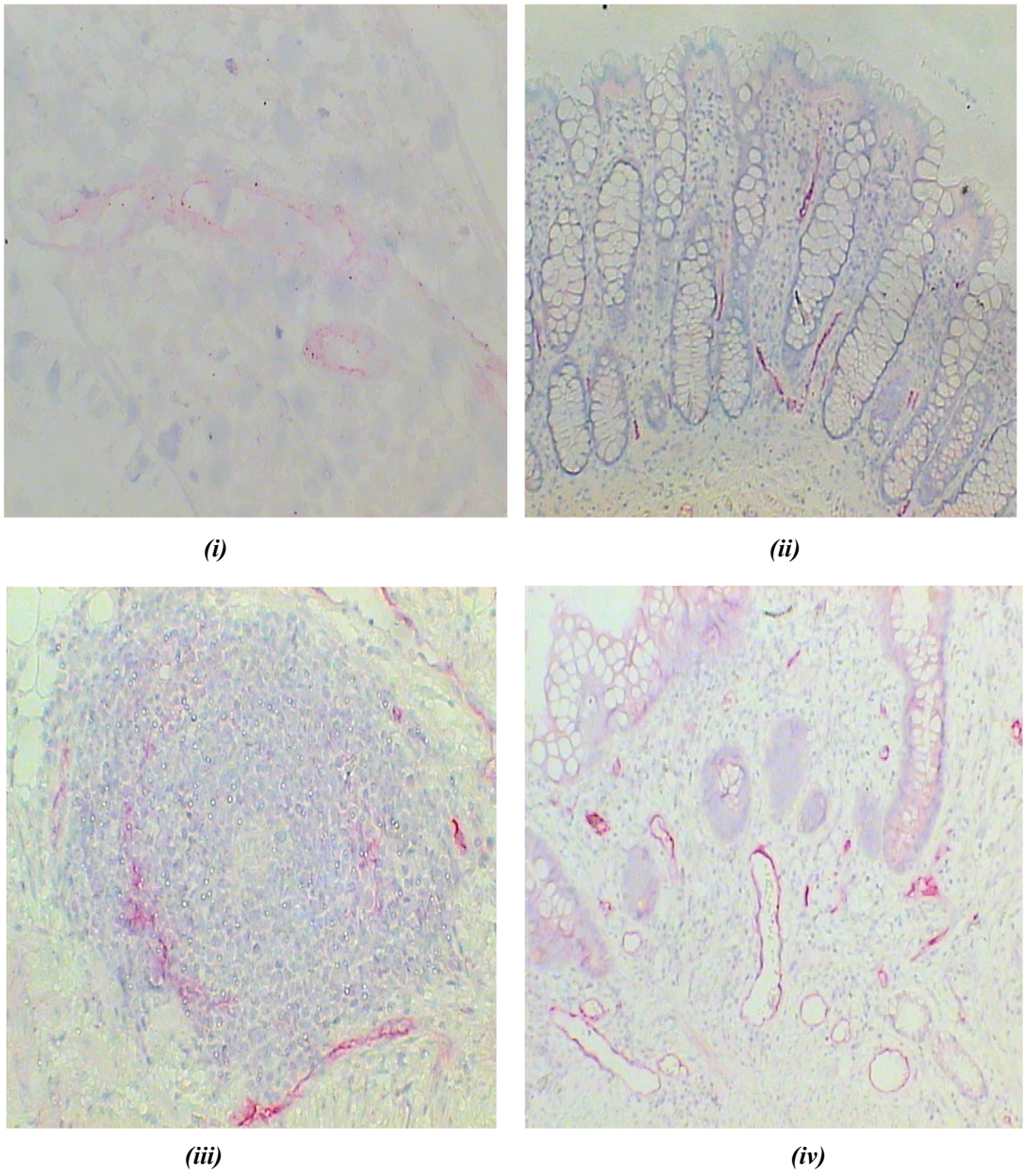

Figure 2.4 Immunohistochemical localisation of MAdCAM-1 in the gastrointestinal tract and inflammatory bowel disease. MAdCAM-1 immunoreactivity (red) in Formalin fixed tissue sections of vascular endothelium from colon explants of histologically normal large bowel tissue(i and ii), where MAdCAM-1 is localised to endothelial lined venules of the lamina propria and submuosa (iii) gut associated lymphoid tissue, with differential expression of MAdCAM-1 in venules within lymphoid aggregates of the submucosa, compared to sub-serosa, suggesting that gut associated tissues are more abundantly involved in Crohn's disease than ulcerative colitis.(iv)advanced Crohn's disease, where MAdCAM-1 was observed in all layers of the intestinal wall and no relationship between MAdCAM-1 immunoreactivity, granulomas or neighbouring blood vessels.

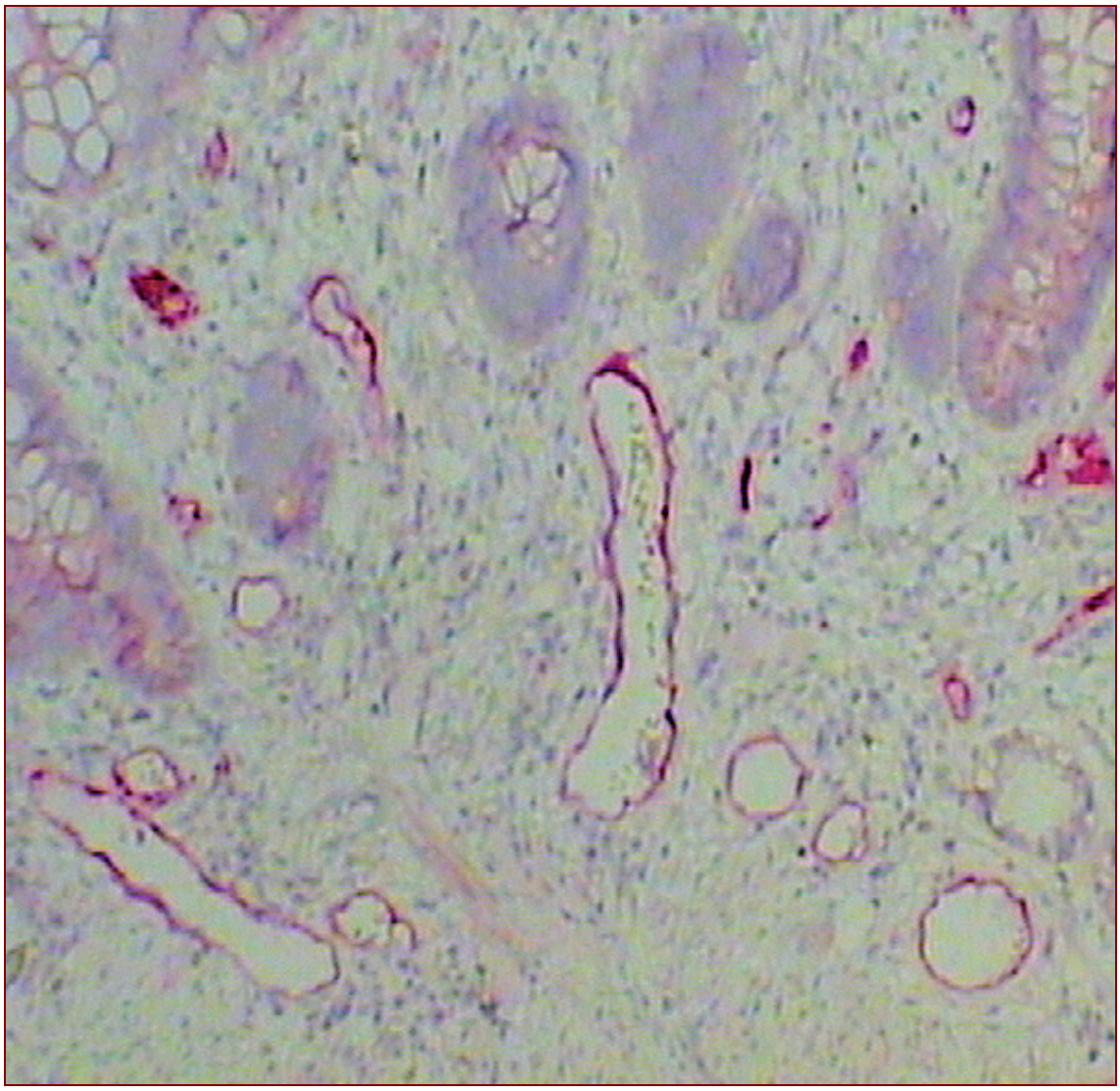

Figure 2.5 MAdCAM-1 immunoreactivity in inflamed colonic mucosa from a patient with advanced Crohns disease taken from a high power view of figure 2.4 (iv). MAdCAM-1 immunolocalisation to both the luminal and abluminal aspect of venular endothelial cells in the lamina propria and submucosa. The abluminal aspect refers to the side away from the lumen of the venular endothelial cells. MAdCAM-1 expression was multifocal, in that there was variation in the distribition of MAdCAM-1 in venular endothelium and did not always encircle the entire venular endothelium.

Table 2.5 Differential MAdCAM-1 expressions in Crohn's disease, ulcerative colitis and normal colon tissues. MAdCAM-1 immunoreactivity on vascular endothelium in normal colon (n=5), un-involved (n=7) and highly inflamed (n=7) gut in Crohn's disease, uninvolved (n=6) and highly inflamed gut (n=6) in Ulcerative Colitis. A=artery, As=arteriole, Vein=vein, Ven=venule, Cap=capillary. Only tissues without histological signs of inflammation were included as 'uninvolved'. There is upregulation of MAdCAM-1 in highly inflamed CD and UC. There was consistant immunoreactivity on the venular endothelium within all layers of the intestinal wall in CD.

MAdCAM-1 immunoreactivity score	***Normal*** ***Colon*** ***(n=5)***					***Uninvolved*** ***CROHN'S DISEASE*** ***(n=7)***					***Highly inflamed*** ***CROHN'S DISEASE*** ***(n=7)***				
	A	*As*	*Vein*	*Ven*	*Cap*	*A*	*As*	*Vein*	*Ven*	*Cap*	*A*	*As*	*Vein*	*Ven*	*Ca*
3+	*0*	*0*	*0*	*0*	*0*	*0*	*0*	*0*	*1*	*0*	*0*	*0*	*2*	*4*	*0*
2+	*0*	*0*	*1*	*1*	*0*	*0*	*0*	*1*	*1*	*0*	*0*	*0*	*0*	*2*	*0*
1+	*0*	*0*	*0*	*1*	*0*	*0*	*0*	*0*	*0*	*0*	*0*	*0*	*0*	*0*	*0*
Nil	*5*	*5*	*4*	*3*	*5*	*7*	*7*	*6*	*5*	*7*	*7*	*7*	*5*	*1*	*7*

MAdCAM-1 immunoreactivity score	***Normal*** ***Colon*** ***(n=5)***					***Uninvolved*** ***ULCERATIVE COLITIS*** ***(n=6)***					***Highly inflamed*** ***ULCERATIVE COLITIS*** ***(n=6)***				
	A	*As*	*Vein*	*Ven*	*Cap*	*A*	*As*	*Vein*	*Ven*	*Cap*	*A*	*As*	*Vein*	*Ven*	*Ca*
3+	*0*	*0*	*0*	*0*	*0*	*0*	*0*	*0*	*1*	*0*	*0*	*0*	*1*	*1*	*0*
2+	*0*	*0*	*1*	*1*	*0*	*0*	*0*	*1*	*0*	*0*	*0*	*0*	*0*	*1*	*0*
1+	*0*	*0*	*0*	*1*	*0*	*0*	*0*	*0*	*0*	*0*	*0*	*0*	*0*	*1*	*0*
Nil	*5*	*5*	*4*	*3*	*5*	*6*	*6*	*5*	*5*	*6*	*6*	*6*	*5*	*3*	*6*

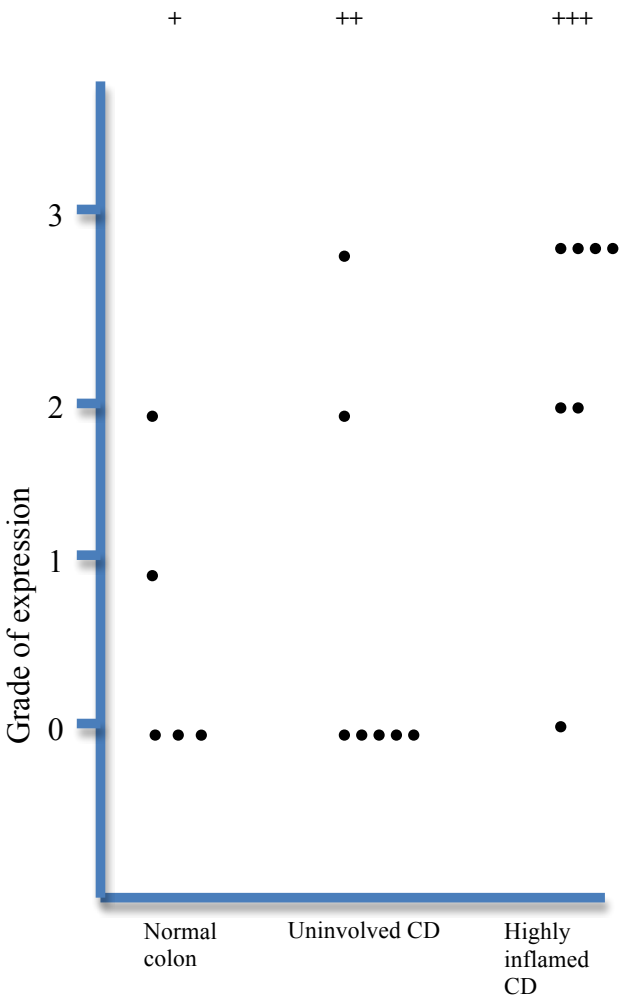

Figure 2.6 MAdCAM-1 immunoreactivity in venules in normal colon(n=5), uninvolved(n=7) and highly inflamed gut in Crohn's disease(CD)(n=7). In comparison with normal colon(+), inflamed lesions of Crohn's disease (+++) showed a significant increase in MAdCAM-1 immunoreactivity scores(p=0.001).

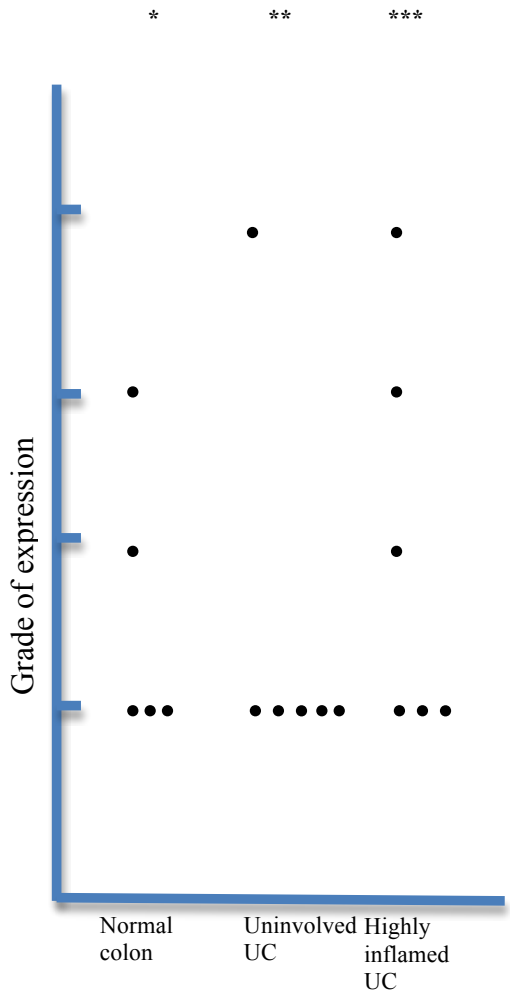

Figure 2.7 MAdCAM-1 immunoreactivity in venules in normal colon(n=5), uninvolved(n=6) and highly inflamed ulcerative colitis (UC) (n=6). MAdCAM-1 expression was upregulated in active ulcerative colitis (***)compared with normal colon(*) and uninvolved colon(**).

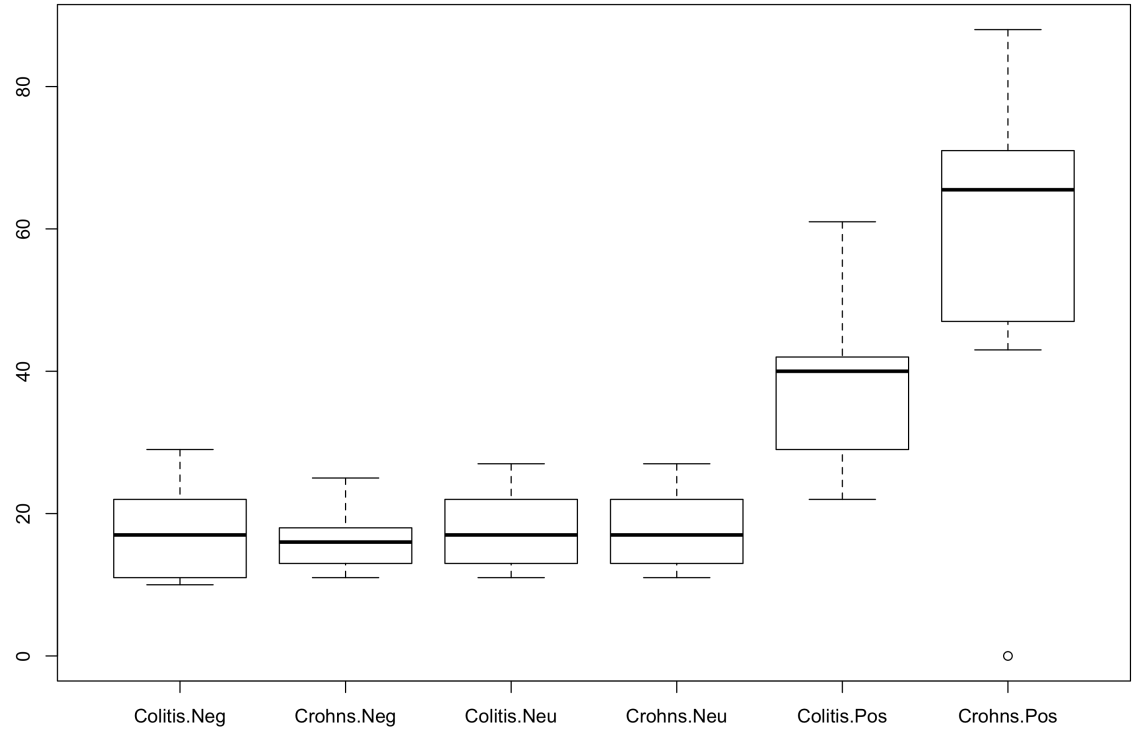

Figure 2.8 Percentage of CD34 positive vessels co-expressing MAdCAM-1 in IBD
There is differential expression MAdCAM-1 in venules in ulcer bases of Crohn's disease and ulcerative colitis . The vertical axis represents the ratio of MAdCAM-1 venules to CD34 total vessels(box-whisker plots). Neg=normal bowel, Neu=unaffected gut, positive inflamed gut. MAdCAM-1 venules appeared to be more frequently observed in the ulcer base in Crohn's disease than normal or unaffected gut tissue as demonstrated by the difference in the ratio of of MAdCAM-1 venules to CD34($p<0.001$). The differences in ulcerative colitis compared to normal and unaffected tissues were relatively less apparent at $p<0.01$. There was an increased expression of Crohn's MAdCAM-1 venules to CD34 in comparison to ulcerative colitis at $p<0.05$

2.3.5 Discussion

Our results demonstrates upregulation of endothelial expression of MAdCAM-1 in CD and UC, where significant MAdCAM-1 expression was found within inflamed areas of colonic IBD, compared to histologically normal mucosa in confirmation of preliminary findings by Briskin *et al* (1997) and Souza *et al* (1999), which suggests that MAdCAM-1 may participate in the recruitment of circulating inflammatory cells into inflammatory lesions.

MAdCAM-1 venules were abundant in inflamed mucosa in both UC and CD. There were however important differences noted between UC and CD. We found immunolocalisation within inflammatory areas at the ulcer base, where MAdCAM-1 venules appeared to be predominant in CD, and interestingly favoring venules within the deeper layers of the intestinal tissue, mainly in lymphoid aggregates. These observations demonstrate a more extensive expression of MAdCAM-1 in CD, which could therefore contribute to transmural inflammation as well as mucosal inflammation, suggesting that MAdCAM-1 is involved not only in the initial phase of inflammation at the mucosal level, but also in the progression phase of CD, towards transmural inflammation and inflammatory reactions in ulcer bases. It is possible that also our observations demonstrating the higher occurrence of MAdCAM-1 laden venules in the submucosa lymphoid aggregates than subserosa suggests that MAdCAM,-1 expression may be upregulated by bacteria in the intestinal tissues or enhancing entry of dietary antigens. Our observations accord with the more extensive nature of MAdCAM-1 immunoreactivity in CD as noted in parallel by Arihiro *et al* (2002). However, these workers used different sets of MAdCAM-1 antibodies i.e monoclonal, different antigen retrieval methodology and tissue samples which had been fixed frozen compared to our formalin fixed materials. It is interesting to note that when taking in account the ratio of MAdCAM-1 venules to CD34+ there is also significant MAdCAM-1 expression in ulcerative colitis with normal/uninvolved tissues (figure 2.8). Dual immunostaining as a method of co-localisation may have been useful as a method of confirming colocalisation of CD34 with MAdCAM-1 in our tissue samples. Our observations on ulcerative colitis contrasts with those from figure 2.7 where the significance was less apparent. A possible reason for this difference may relate to the active angiogenesis and related pre-angiogenic factors critical in ulcer healing in

ulcerative colitis leading to new vessel formation and therefore an increase in the MAdCAM-1 venules to CD34+ ratios (Danese *et al* 2008).

In IBD, perhaps surprisingly, there was no evidence of significant up-regulation of MAdCAM-1 in histologically non-inflamed tissues, adjacent to inflamed lesions. Given the susceptibility of any segment of the gastrointestinal tract to be affected by CD and the continuous spread of UC, areas in the vicinity of inflammation will probably become inflamed in the later course of disease and thus be regarded as 'early' lesions. MAdCAM-1 expression therefore appears to follow the onset of inflammation. Of course, that may be a very low level expression in uninvolved gut, which may not be detected by immunohistochemistry. Alternatively, as these tissues were all previously exposed to corticosteroids, it is possible that the lack of expression is a modulatory effect of corticosteroids on MAdCAM-1. This has been studied in an *invitro* setting in chapter 5.

We found that three out of the four specimens taken from ileo-caecal CD had granulomas that initially appeared to have extremely high expression of MAdCAM-1. We tested the hypothesis that MAdCAM-1 is important in the pathogenesis of granulomas in CD but there was no consistent pattern between granulomas and associated immunoreactive venules. Furthermore, when these sections were stained without the primary antibody there was similar focal concentration of fast red immunoreactivity indicating this was likely to be non-specific, possibly due to FcR expression by granulocytes/macrophages.

The upregulation of MAdCAM-1 during gut inflammation has been suggested to be responsible for the establishment of chronic inflammation via the recruitment of α4β7 lymphocytes. The functional significance of MAdCAM-1 in IBD has been highlighted by studies where immunoneutralisation of either MAdCAM-1 or α4β7 intergrin attenuate inflammation in animal models as well as patients with IBD, which we have already discussed in Chapter 1. Numerous animal models of colitis have been used to study the mechanisms for the development of chronic IBD. As we have observed in normal colon human MAdCAM-1 is constitutively expressed on the venular endothelium of the lamina propria and submucosa, where as in murine experimental colitis models MAdCAM-1 is induced on colonic vascular and on the vessels within

serosa and muscularis propria when compared to control animals. (Viney *et al* 1996). One elegant and important study by Soriano *et al* (2000) using mice from the age of 4 weeks to 40 weeks showed that blockade with MAdCAM-1 antibodies alone during established inflammation was less effective than the combined synergistic blockade of MAdCAM-1 and VCAM-1 (which is also strongly expressed in the SAMP/Yit mice with spontaneous ileitis). Futheremore, since the simultaneous blockade of both cellular adhesion molecules significantly attenuated T-lymphocyte binding to microvessels in the ileal mucosa, it is possible that pathways independent of the α4β7/MAdCAM-1 can also mediate trafficking to inflamed intestine (Matsuazaki *et al* 2005). Furthermore, prophylactic blockade of MAdCAM-1 prevented the development of ileitis, whereas the early administration of VCAM-1 antibodies had no effect supporting the earlier concept that the contribution of MAdCAM-1 is likely to be most pronounced during the early phases of IBD. Thus, it is likely that MAdCAM-1 affects ileal inflammation locally not only in the mucosa but also in the mesenteric lymph node (MLN), as significant amelioration of acute and chronic infiltrates have been observed when both MAdCAM-1 and L-selectin are blocked.

2.4 Experiment 3: Expression of MAdCAM-1 in the human pancreas.

2.4.1 Background

The pancreas is an intriguing organ with a rich blood supply, facilitating the recruitment of lymphocytes. It is already known to express some adhesion molecules constitutively e.g. ICAM-1 and VCAM-1, which are known to be important for lymphocyte recruitment (Komatsu *et al* 2000). MAdCAM-1 is the main vascular addressin responsible for homing of lymphocytes laden with α4β7 to emigrate into the gut and gut-associated lymphatic tissues. However, the expression of MAdCAM-1 in extraintestinal tissues such as the human pancreas has not been fully characterised. We have seen that lymphocyte homing to mucosal associated lymphoid tissue (MALT) such as Peyer's patches and the lamina propria of the intestine is critically dependant on MAdCAM-1. The restricted expression of MAdCAM-1 is acquired during embryonic development. This is supported by early fetal expression (7-17 weeks gestation) of

MAdCAM-1 in the micro vessels of many extraintestinal tissues e.g. peripheral lymph nodes, skin, muscle, spleen and also the pancreas (Salmi *et al* 2001).

Our earliest observations confirm the significant upregulation of MAdCAM-1 in active inflammatory bowel disease, where we have confirmed expression to be localised on endothelia cells in lamina propria of the gastrointestinal tract. It has been reported that MAdCAM-1 becomes expressed on islet cells of non obese diabetic (NOD) mice at a relatively early phase during lymphocyte accumulation (Hänninen *et al* 1998). The NOD mouse is an appropriate model for insulin-dependent diabetes mellitus, since it itself results from destruction of pancreatic beta cells by mononuclear cells infiltrating the islets of Langerhans. As it is well known that MAdCAM-1 preferentially mediates the homing of mucosal lymphocytes, it is conceivable that islet associated MAdCAM-1 favours the accumulation of such mucosal lymphocytes into pancreatic islets, suggesting that MAdCAM-1 may have a role in the pathogenesis of chronic pancreatitis.

The aim of this part of the study was to identify and localise the expression of MAdCAM-1 in the human pancreas.

2.4.2 Methods

MAdCAM-1 expression was determined by immunohistochemistry on human pancreas from a total of 7 patients with chronic pancreatitis (5male, 2 female, age range to 46-64, median 53 yrs) with chronic pancreatitis associated with pancreatic adenocarcinoma. For comparison, we used 4 samples of normal pancreatic tissue, two samples from type I diabetes with chronic pancreatitis and six with pancreatic adenocarcinoma only during staging laparoscopy.

Negative controls included sections without primary antibody and also isotype matched purified IgG.

Positive controls for MAdCAM-1 expression were taken from samples of normal colon tissue, which constitutively expresses MAdCAM-1(as previously described in section 2.2.3). The tissue samples were taken from resection on those patients undergoing

pancreatectomy for pancreatic adenocarcinoma. All these patients had a history of chronic excess alcohol consumption. However, it was impossible to be certain that chronic pancreatitis preceded carcinoma.

All pancreatic tissues were fixed in 10% buffered formalin and embedded in paraffin. Sections were cut at four micron thickness on to APES (3-aminopropy triethoxysiline) coated slides and one section was stained with haematoxylin and eosin. For comparison immunohistochemistry was carried out using both three stage immuno-alkaline phosphatase (APAAP) and three stage immunoperoxidase techniques as described earlier in this chapter.

2.4.2.1 Morphological analysis

Two observers (Aftab Ala and Richard Standish) independently assessed the sections semiquantitativley and scored on a scale of 0-3+ according to the intensity of MAdCAM-1 immunoreactivity: grade 0 did not exhibit staining, grade 1+: light, grade 2+: moderate, grade 3+: marked staining, without knowledge of the histological diagnosis. Particular attention was paid to areas of lymphoid aggregation and vascular endothelium in relationship to the pancreatic islets and acinar cells. The staining methods were repeated twice to validate the scoring system.

2.4.3 Results (Table 2.6, Figure 2.6 to 2.7)

There was very weak constitutive staining of periductal and intracinar capillary vessels in normal pancreas. Intensity of MAdCAM-1 immunoreactivity increased in all cases of chronic pancreatitis, compared to normal and pancreatic carcinoma. On the whole the islets were devoid of immunoreactivity in the normal pancreas. Focal immunostaining of lymphoid aggregates was seen for S100, CD68 and CD21 but the staining pattern did not correspond to the pattern of MAdCAM-1 immunoreactivity

Positive controls: These were taken from sections of normal colonic tissue, which demonstrated MAdCAM-1 expression on vascular endothelium within the lamina propria and submucosa.

Negative controls: MAdCAM-1 was not present in negative controls incubated without primary antibody or with isotope matched anti-IgG.

Characteristic features of chronic pancreatitis with advanced peri- and intralobular fibrosis of pancreatic parenchyma were observed in all study cases. Exocrine acinar cells appeared atrophic. The presence of fibrous connective tissue was observed both in exocrine texture and pancreatic islets. The ducts were dilated and focally proliferated, and some were filled with partially calcified protein plugs. The duct epithelium adjacent to these plugs was flattened or destroyed. In the areas of inflammatory cell infiltration and fibrosis there were lymphoid aggregates with MAdCAM-1 immunoreactivity.

We found MAdCAM-1 upregulation in chronic pancreatitis, compared to slightly weaker evidence of expression in pancreatic carcinoma. MAdCAM-1 expression was immunolocalised to the periductal and intracinar capillary vessels.

In the majority of cases, the islets were devoid of immunoreactivity. Interestingly, in two cases of type 1 diabetes mellitus, there was staining of perineural capillaries in association with inflammatory cell infiltration, adjacent to islets and in one case only there appeared to be immunoreactive capillary vessels within a single islet.

Table 2.6 MAdCAM-1 immunoreactivity in normal pancreas, pancreatic carcinoma and chronic pancreatits The sections were assessed semiquantitativley and scored on a scale of 0-3+ according to the intensity of MAdCAM-1 immunoreactivity: grade 0 did not exhibit staining, grade 1+: light, grade 2+: moderate, grade 3+: marked staining.

NORMAL PANCREAS	**MAdCAM-1 immunoreactivity in Acinar Cells**	**MAdCAM-1 immunoreactivity in Pancreatic Islets**	**MAdCAM-1 in lymphoid aggregates**
PATIENT 1	0	0	0
PATIENT 2	1+	0	0
PATIENT 3	0	0	0
PATIENT 4	1+	0	0
PANCREATIC CARCINOMA			
PATIENT 5	1+	0	0
PATIENT 6	1+	0	0
PATIENT 7	1+	0	0
PATIENT 8	0	0	0
PATIENT 9	0	0	0
PATIENT 10	1+	0	0
CHRONIC PANCREATITIS			
PATIENT 11	1+	0	1+
PATIENT 12	3+	1+	2+
PATIENT 13	1+	0	0
PATIENT 14	1+	0	1+
PATIENT 15	2+	1+	0
PATIENT 16	2+	0	0
PATIENT 17	1+	0	1+

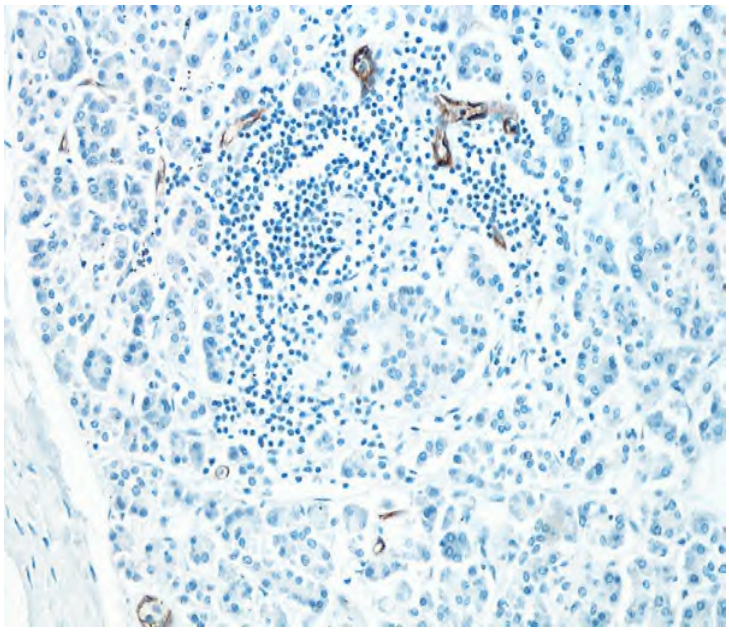

(A)

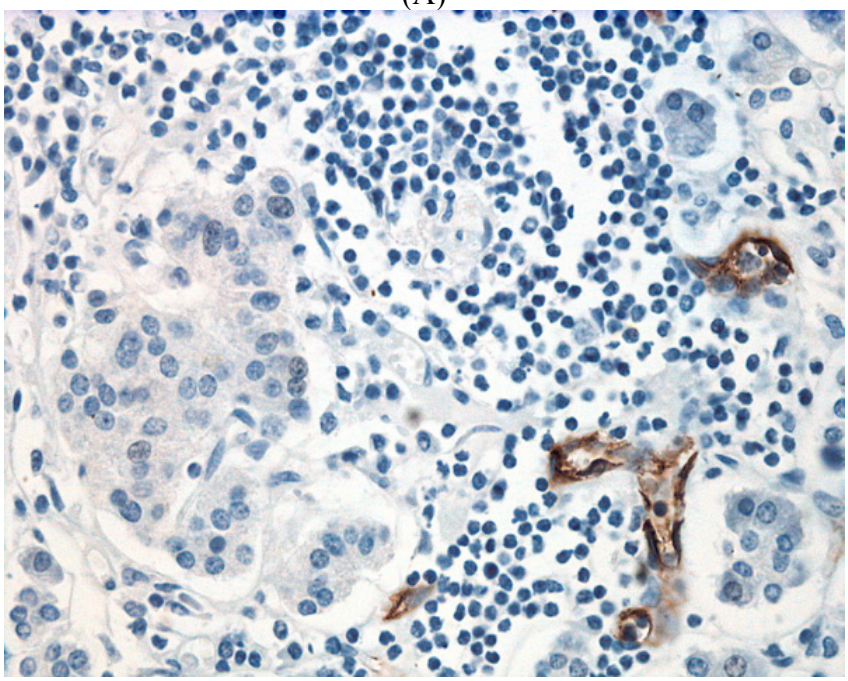

(B)

Figure 2.9 MAdCAM-1 staining patterns in periductal and intra acinar capillary vessels of human pancreas using peroxidase methodology. Plate A and B shows groups of of islet cells lying within a lymphocytic infiltrate including lymphoid aggregates. Although in the majority of chronic pancreatitis cases the islets were devoid of MAdCAM-1 immunoreactivity, MAdCAM-1 staining within the islet cell lymphoid aggregate is typical of the staining as a whole. (Plate A magnification x5 objective, Plate B x20 objective).

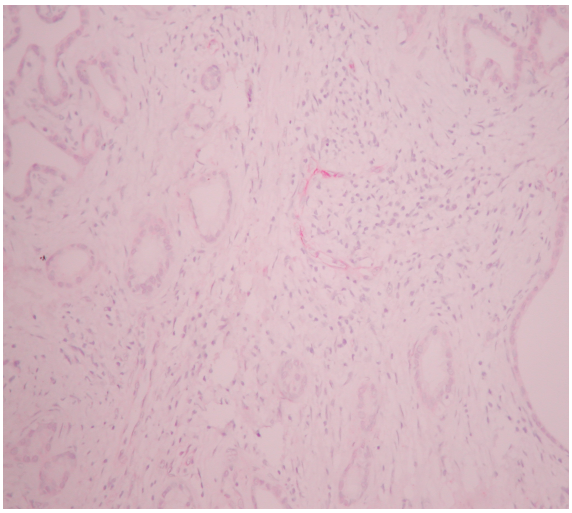

(A)

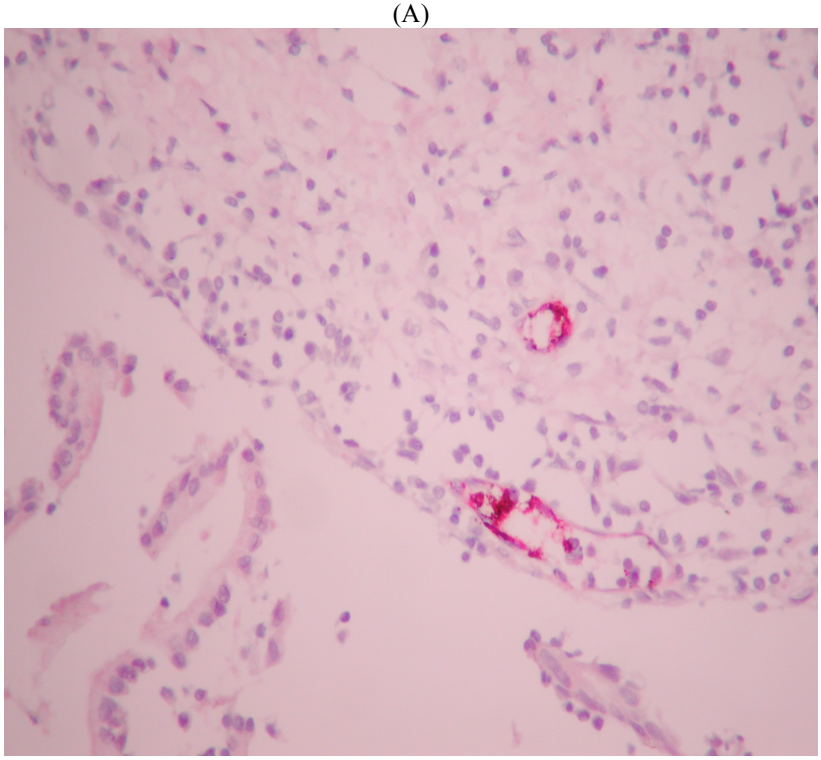

(B)

Figure 2.10 APAAP methodology of immunostaining demonstrating islet capillaries and islet cells. Although there is relatively weak expression within normal islet cells, strong focal MAdCAM-1 expression is found localised to high endothelial venules (mainly in a 'ring pattern') within focal areas of chronic inflammation. (Plate A magnification x5 objective, Plate B x20 objective).

2.4.4 Discussion

Our study shows upregulation of MAdCAM-1 expression in chronic pancreatitis compared to controls from normal and pancreatic carcinoma tissues. Specifically, MAdCAM-1 immunolocalises to the periductal and intra-acinar capillary vessels in the human pancreas with increased intensity of staining in chronic pancreatitis. This observation suggests that endothelial MAdCAM-1 is involved in lymphocyte entry into the tissues of chronic pancreatitis. Chronic pancreatitis is histologically characterized by extended fibrosis and infiltration of leukocytes. Cellular infiltrates are present already in early stages of chronic pancreatitis, but the mechanisms responsible for their recruitment into human pancreas are unknown.

The differences which we have observed in restricted immunolocalisation of MAdCAM-1 in the pancreas suggest a mechanism for controlling cellular traffic in the pancreas. The differential MAdCAM-1 expression in pancreatic parenchyma and infiltrates from patients with chronic pancreatitis strongly suggests an involvement in the initiation and perpetuation of disease. In support of these conclusions it is interesting to note that from our two cases of type I diabetes mellitus and chronic pancreatitis, there was MAdCAM-1 immunoreactivity of vessels, in association with inflammatory cell infiltration, adjacent to islets and in one case there appeared to be MAdCAM-1 immunoreactive capillary vessels within a single islet. The staining of the periductal and intraductal capillary vessels appeared uniform, compared to the differential staining pattern of the venules seen in the colonic tissues described earlier in the chapter. Typically there are groups of islet cells lying within a lymphocytic infiltrate including lymphoid aggregates. Although in the majority of chronic pancreatitis cases the islets were devoid of MAdCAM-1 immunoreactivity, MAdCAM-1 staining within the islet cell lymphoid aggregate is typical of the staining as a whole. In the inflamed pancreas of non-obese diabetic mice, elevated levels of MAdCAM-1 in high endothelial like vessels of the Langerhans is also observed.

There is evidence to suggest these mice develop autoimmune-mediated lymphocytic inflammation of pancreatic islets (insulitis), which leads to beta-cell destruction, and development of diabetes (Xang *et al* 1997). Inflamed islets of these animals show the expression of lymphocyte α4β7 integrin and endothelial MAdCAM-1 adhesion molecules involved in tissue-selective migration of lymphocytes to mucosal lymphoid tissues. The tissue samples used in our study were taken from resection on those patients undergoing pancreatectomy for pancreatic adenocarcinoma. All these patients had a history of chronic excess alcohol consumption. However, it was impossible to be certain that chronic pancreatitis preceded carcinoma. Other aetiologies of chronic pancreatitis include inherited genetic predisposition (hereditary pancreatitis), or autoimmune pancreatitis. In our series, the chronic pancreatitis may have been associated with duct obstruction secondary to the pancreatic adenocarcinoma, which limits the interpretations from the results.

The modest but clear presence of MAdCAM-1 in our samples from pancreatic tumour and the recent observations linking Tregulatory cells and MAdCAM-1 in pancreatic carcinoma may be significant. (Nummer *et al* 2007). The data demonstrate a previously unrecognised role of tumour endothelium for the selective recruitment of Treg cells. Such recruitment involves selective interactions between Treg cells and the tumor vasculature mediated by adhesion molecules and respective ligands e.g. α4β7. These findings suggest that the development of new therapeutic strategies based on targeted endothelial blockade could have merit in therapy.

Chapter 3

Establishing an *in vitro* model to Investigate MAdCAM-1 expression

3.1 Overview

In chapter 2 we demonstrated that MAdCAM-1 is expressed constitutively in the gut, and is upregulated in liver and gastrointestinal inflammation. Specifically, we have shown that MAdCAM-1 is upregulated in the inflamed colonic mucosa of humans with UC and CD, with increased expression in deeper layers of the bowel wall in surgically resected Crohn's tissues. MAdCAM-1 also seems to play critical roles in several chronic immune and inflammatory conditions e.g. chronic pancreatitis. We hypothesised that MAdCAM-1 acts as a local addressin in the gut and liver concerned with the recirculation and homing of lymphocytes to these organs during inflammatory processes.

As we have discussed earlier, the expression of other cell adhesion molecules ICAM-1 and E-selectin on endothelial cells have been well characterised. In marked contrast, the mechanisms underlying the regulation of MAdCAM-1 expression and the effect of MAdCAM-1 modulation from therapies related to IBD have been ill defined, in large part because of the lack of a suitable *in vitro* endothelial cell culture system in which this organ specific adhesion molecule is expressed. Since the original report on MAdCAM-1 regulation by Sikoski *et al* (1993), few other studies have examined the regulation of MAdCAM-1, particularly within high endothelial venules, which are most relevant to chronic gut inflammation and inflammatory bowel disease. Since the entry of lymphocytes into specialised venules appears to regulate chronic gut inflammation an improved understanding of the factors which promote MAdCAM-1 expression will inform modalities for the modulation of MAdCAM-1.

MAdCAM-1 expression *in vitro* has previously been reported in high endothelial venules and brain capillary cell lines (Steffen *et al* 1996). Most experimental studies on MAdCAM-1 expression thus far, have been obtained using an endothelioma cell line bEnd.3, originally derived from brain microvessels. However, bEnd.3-based models do not accurately model high endothelial venules and therefore would not appear to be an attractive model of MAdCAM-1 in this regard. We show in this chapter that a relatively recently characterised endothelial cell line (SVEC4-10) from high endothelial venules of mice may provide the basis for such a model.

3.2 Developing an *in vitro* model of MAdCAM-1 expression in an 8-chamber well system

3.2.1 Background

SVEC are endothelial cell lines derived by simian virus SV40 (strain 4A) transformation of high endothelial venules cells from axillary lymph node vessels of adult male C3H/HeJ mouse (H-2k). These fully transformed, small vessel murine endothelial cells were first cloned in 1987. They grow indefinitely and are well differentiated, responding like normal endothelial cells to some interleukins and to extracellular matrix signals for tube-like differentiation.

The mouse brain endothelial cell line bEnd.3 (strain BALB/c) was transformed by infection with NTKmT retrovirus vector that expresses polyomavirus middle T antigen. The endothelial nature of these cells has been confirmed by the observed expression of von Willebrand factor and uptake of fluorescently labelled low density lipoprotein.

Tumour necrosis factor (TNFα) is one of most potent cytokines capable of stimulating MAdCAM-1 both *in vivo* and *in vitro*. Expression of MAdCAM-1 on endothelial cells and in the colon of mice has been reported after TNFα administration. TNFα also induces the expression of several other adhesion molecules including ICAM-1, VCAM-1 and E-selectin.

3.2.2 Aims

To develop:

(i) An *in vitro* model cell culture system of MAdCAM-1 expression

(ii) Semi-quantitative analysis of MAdCAM-1 expression in this model

3.2.3 Methods

3.2.3.1 SVEC4-10, bEnd.3 cells and Culture Medium

SVEC4-10 (ATCC catalogue number CRL-2181) and bEnd.3 (ATCC catalogue number CRL-2299) were maintained in freshly made culture medium consisting of Dulbecco's modified Essential medium containing 2mM L-glutamine, 1.5 g/L sodium bicarbonate, 4.5 g/L glucose, 1 mM sodium pyruvate, heat inactivated 10% fetal bovine serum, 100U/ml penicillin/streptomycin.

The frozen cells were thawed quickly in a 37^0C water bath. The ampoule was in 70% ethanol at room temperature and each 0.5ml cell suspension was diluted slowly over 5 minutes with 1ml s of filtered HBSS and followed by 2mls of HBSS for a further 5minutes. This was then di1uted with 5 mls of culture medium in a 75 mls flask and incubated at 37^0C in 10 % CO_2/air atmosphere.

3.2.3.2 Subculture procedure and trypsinising cells

The SVEC and bEnd.3 cells were maintained in culture with the medium replenished every 48 hours. When cells reached 70-80% confluence, the monolayer was detached from the flask by trypsinising the cells. Ideally, at this confluence the cells are not piled up or aggregated, but appear in single sheet uniform cells. The culture medium was discarded from the flask and the cells immediately washed three times with warm Ca^{2+} /Mg^{2+} free HBSS to remove residual serum which would inhibit the action of trypsin. One ml warm trypsin (0.25%)–EDTA (0.03%) was filtered-sterilised through a 0.2 μm filter (Minisart, Sartorius) into the flask at room temperature until the cells detached; typically about 5 minutes. The cells were transferred rapidly to warm complete DMEM to inhibit further action of the trypsin and centrifuged at 1200 rpm (300g) at room temperature for 3 minutes. The supernatant was discarded and the resulting pellet resuspended in an appropriate volume of DMEM (175 cm^2 flask, 5mls and 80 cm^2 flask, 2mls) with gentle syringing using a sterile 21G needle to disaggregate cell clumps.

Cell yield and viability were determined by trypan blue exclusion and haemocytometer counting. 20μl of trypan blue solution, 160 μl of HBSS and 20 μl of the cell suspension were mixed sequentially and after 2 minutes the cells were counted in a Neubauer

haemocytometer. Intact membranes of viable cells exclude trypan blue, whereas trypan blue stains dead or injured cells due to loss of membrane integrity. An appropriate cell density was reseeded into fresh flasks for the next cell passage, frozen for storage in a liquid nitrogen cell bank, or used for experimental procedures.

3.2.3.3 Immunofluoresence staining of MAdCAM-1

Fresh culture medium were added, aspirated and dispensed into new culture flasks with a subculture ratio of 1:4 to 1:6. The cells were seeded on to 8 well Falcon^{R} Culture Chambers each consisting of Polystyrene Vessel Treated Glass slides (Becton Dickinson Labware - Catalogue no 354118). Falcon Culture Slides are comprised of a glass slide treated to provide a consistent surface (0.69 cm^2 for cell growth) and compartmentalized chamber molded from medical grade polystyrene. A hydrophobic mask on the slide delineates the location of cells and prevents adhesive from remaining on the Culture Slide after chamber removal.

At 70%-80 % confluence these cells were stimulated by incubating with 20 ng/ml mouse Recombinant TNFα (SigmaAldrich, Poole, UK) in the 8 chamber well slides, initially for 24hours. Thereafter, each chamber well was rinsed carefully three times with 0.5 mls of phosphate buffer saline (PBS) followed by 10 minute incubation with equal volume of Formalin fixative, with further rinsing using 0.5 mls PBS. The cells were incubated at 4^0C overnight with primary antibody using functional grade purified Rat anti-mouse MAdCAM-1 monoclonal antibody-10μg/ml MECA 367 (eBioscience, UK Cat No 16-5997), in 1% Bovine serum albumin in PBS.

Each chamber was rinsed three times with PBS and further incubated for one hour with secondary antibody Goat Anti-Rat IgG (whole molecule) FITC conjugate at 10μg/ml (SigmaAldrich, Poole, UK), followed by further washing three times in PBS. VECTASHIELD^{R} Mounting Medium (Cat No H-100, Vector Laboratories, UK) was applied to prevent rapid photo bleaching. After removal of the chamber wells cover slips were applied.

3.2.3.4 MAdCAM-1 and time course of its expression on SVEC and Bend.3 monolayer

A time course experiment was performed where cells were exposed to TNFα for 2, 5, 9, 23, 48, and 72 hours (SVEC) and 2, 5, 9 and 20 hours (bEnd.3). At the end of the time course cells were fixed with formalin and immunostained for MAdCAM-1 the technique described. Each experiment was repeated three times.

3.2.3.5 Image Analysis

Slides were initially examined by phase contrast imaging to demonstrate the morphology of the two cell types. They were then examined on a Nikon microscope and images captured using a Nikon Coolpix 990 digital camera; the images taken were representative of 2 to 4 fields observed for each time point in each experiment. They were analysed using image analysis software (NIH Image, Bethesda, Maryland, USA) and the mean pixel intensity was measured for each field and a mean ± standard deviation calculated. The time 0 control was subtracted from the other time point values to give a value minus the background fluorescence intensity.

3.2.3.6 Statistical analysis

The results are displayed as the mean ± standard deviation of the sample means ($\mu \pm SD_{n-1}$). Statistical analysis carried out using the two tailed t-test and significance determined if $p<0.05$

3.2.4 Results (figure 3.1 to 3.5)

3.2.4.1 Cell viability

There was an estimated greater than 98% in cell viability in all experiments which were performed.

3.2.4.2 Morphology and immunofluoresence

SVEC cells formed branching tube-like networks. They divided slowly forming sheets of flattened polygonal cells (figure 3.1a), which ceased division at confluence. At near confluence both cell types remained in a monolayer. The monolayer morphology of SVEC cells forms 'nests' of polygonal cells surrounded by elongated bands. Immunofluoresence localisation of MAdCAM-1 in SVEC4-10 endothelial cells showed that TNFα (20 ng/ml) stimulation induced a marked increase in the immunofluoresence localisation of MAdCAM-1 on the surface of SVEC cells (figure 3.2). TNFα stimulation also induced a cell surface expression of MAdCAM-1 on bEnd.3 although there appeared to be less junctional localisation than the SVEC cells(figure 3.3).

Compared to the SVEC cells, the bEnd.3 cells appeared relatively more elongated and 'spindly' at near confluency (figure 3.1b and 3.3). In the control experiments, MAdCAM-1 expression was only faintly detected in the non-stimulated cells and primary antibody deficient controls were consistently negative.

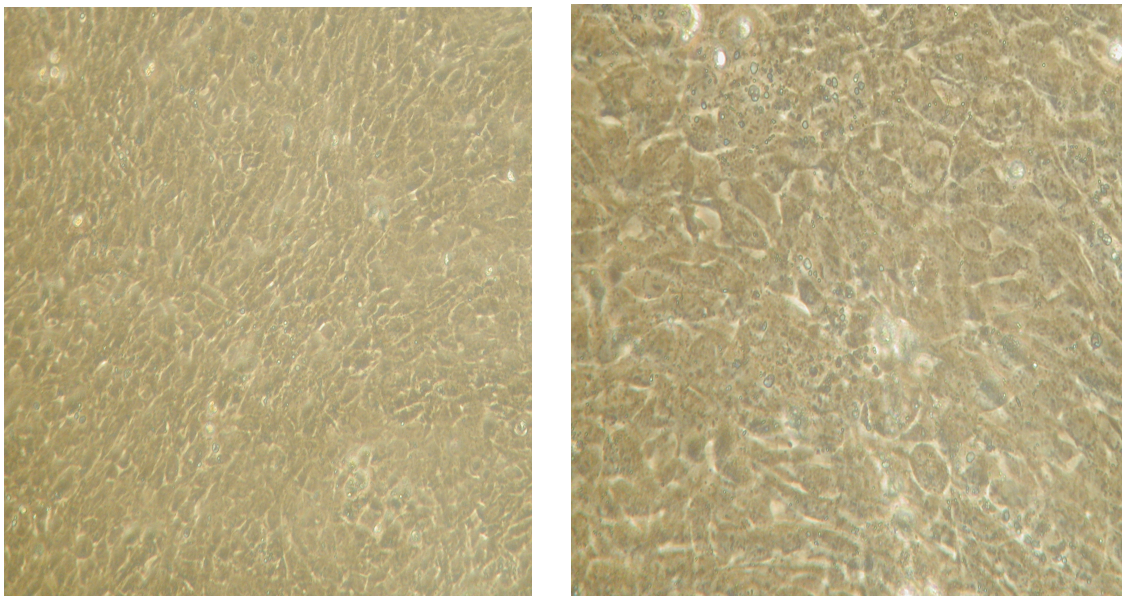

Figure 3.1a Phase contrast image analysis of SVEC4-10 endothelial cells at near confluence prior to stimulation with TNFα. The monolayer of cells form a 'nest' of polygonal like structures (100x and 200x magnification respectively).

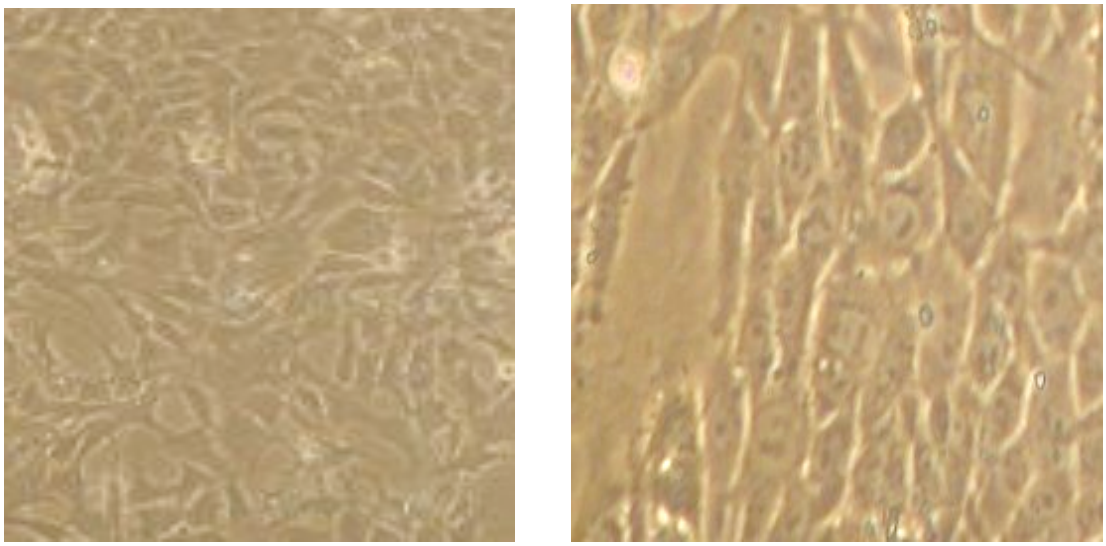

Figure 3.1b Phase contrast image of bEnd.3 endothelial cells at near confluence, prior to stimulation with TNFα. The monolayer of cells appears elongated and 'spindly' (100x and 200x magnification respectively).

.

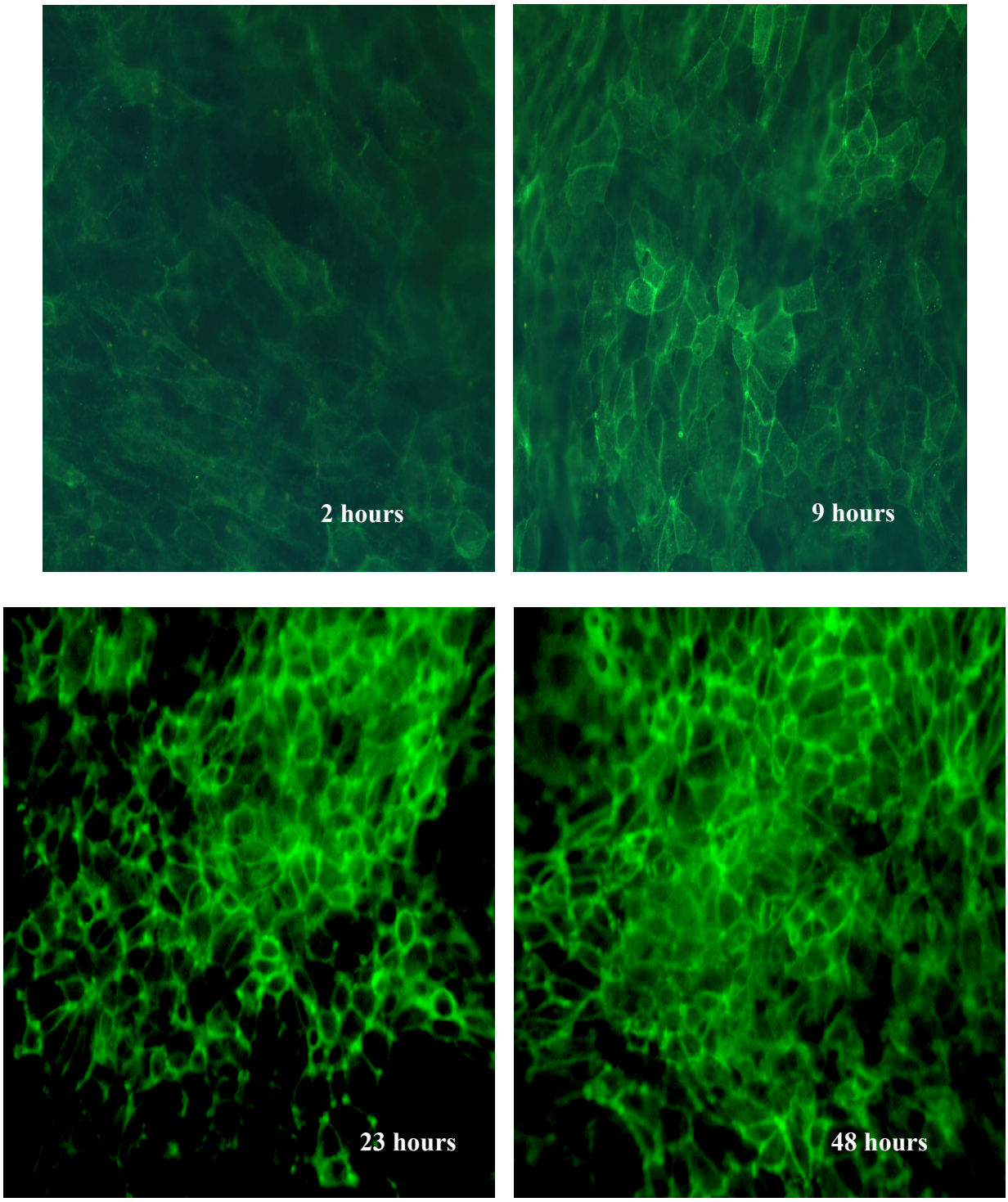

Figure 3.2 Immunofluorescent staining of MAdCAM-1 on SVEC cells demonstrating MAdCAM-1 surface expression after 0-48 hours incubation with TNFα. Following stimulation, there was marked MAdCAM-1 immunostaining expressed on the surface of the cells *particularly at the junctions (200xmagnifiation)*

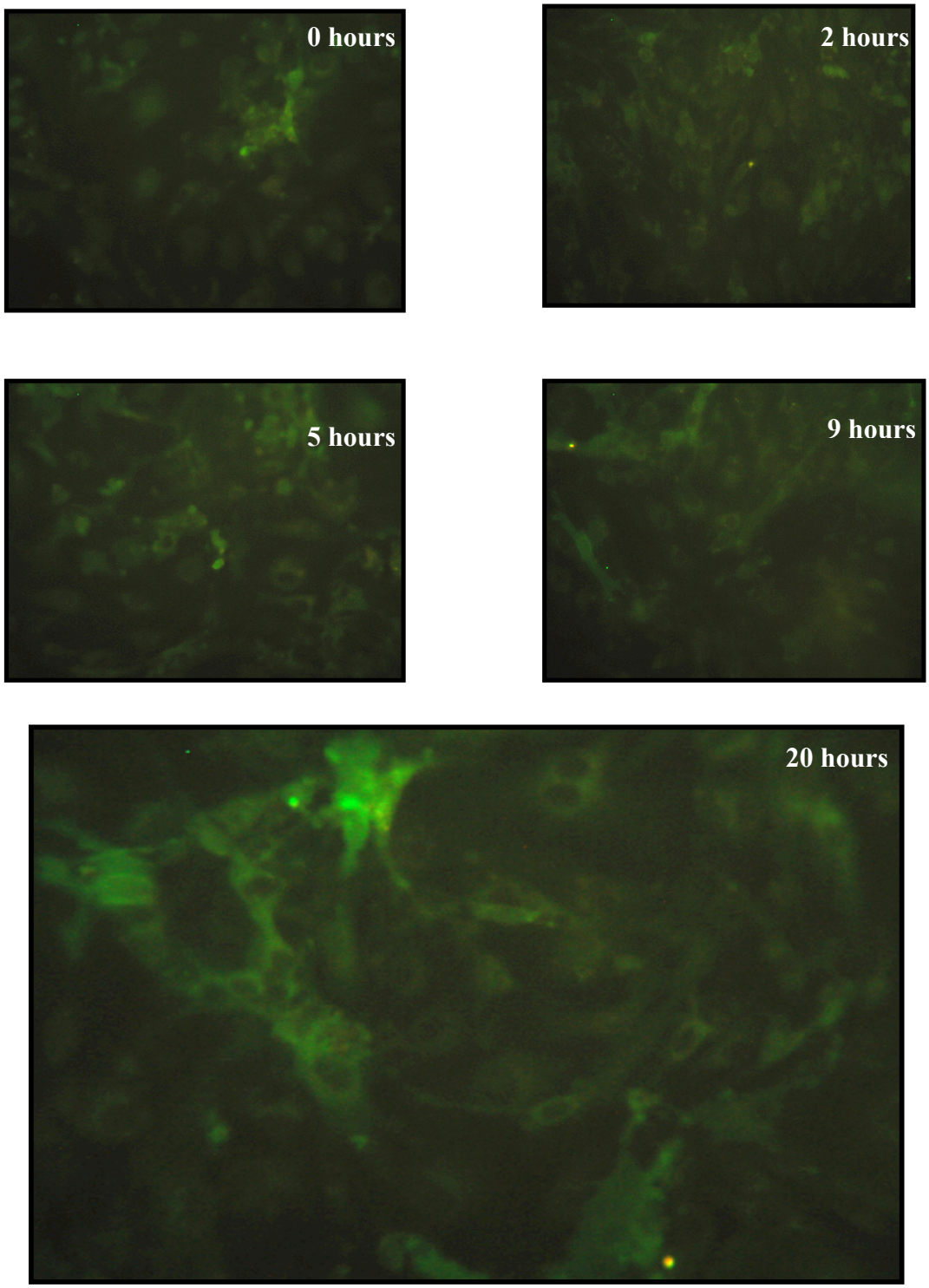

Figure 3.3 ***Immunofluorescent staining of MAdCAM-1 on bEnd.3 cells demonstrating surface expression after 0-20 hours incubation with TNFα.*** The cells appear typically elongated at near confluence (200x magnification).

3.2.4.3 Time course of MAdCAM-1 immunofluoresence induction by 20ng/ml TNFα

In the bEnd.3 cells, the time course experiment was only carried out for 20 hours with maximum stimulation after 20ng/ml TNFα stimulation (figure 3.4).

Cell surface expression of MAdCAM-1 is increased on SVEC high endothelial cells stimulated by 20ng/ml TNFα. Significant MAdCAM-1 fluorescence occured at 23hrs($p<0.01$), which was further sustained up to 72 hrs (figure 3.5). This contrasted with the control experiments without TNFα stimulation where MAdCAM-1 was only faintly detected.

The maximal mean pixel intensity following TNFα stimulation of SVEC cells was higher than that achieved with bEnd.3 cells.

Figure 3.4 Surface expression and time course of MAdCAM-1 after 20ng/ml TNF α stimulation of Bend.3 cells in an 8 chamber system. Significant MAdCAM-1 fluoresence(marked as *) occured at 20hrs ($p<0.05$), contrasted with the control experiments without TNFα stimulation where MAdCAM-1 was only faintly detected. Each cohort was performed in triplicate. (n=9)

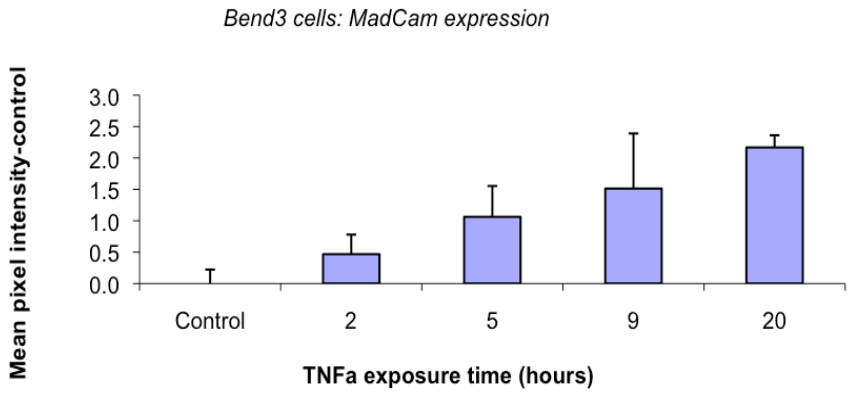

Figure 3.5 Surface expression and time course of MAdCAM-1 after 20ng/ml TNFα stimulation of SVEC cells in an 8 chamber system. Significant MAdCAM-1 fluoresence (marked as *) occured at 23hrs($p<0.01$), which is sustained at 48hrs($p<0.01$ marked as **) and maintained up to 72 hrs($p<0.01$, marked as ***). This contrasted with the control experiments without TNFα stimulation where MAdCAM-1 was only faintly detected. Each cohort was performed in triplicate. (n=9)

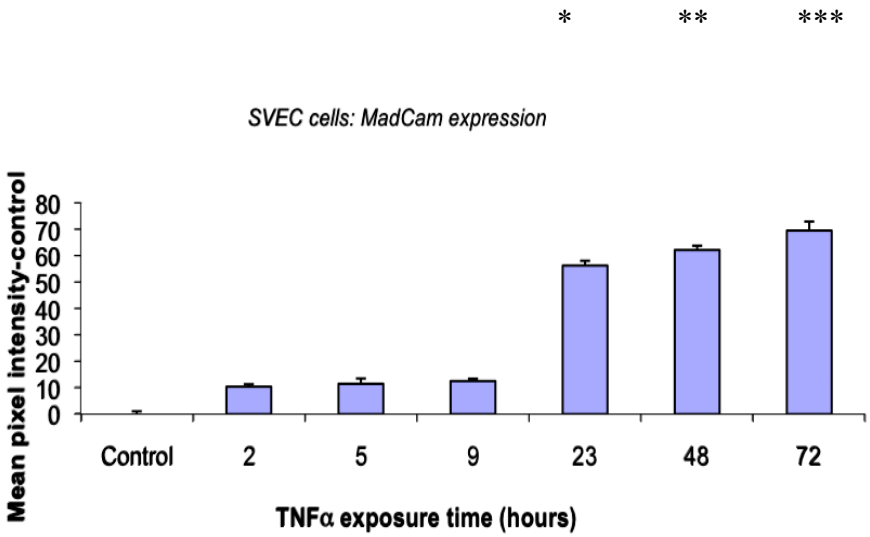

3.3 Developing an *in vitro* model of MAdCAM-1 expression in a 96 well plate system

3.3.1 Background

In the previous experiments we have demonstrated the constitutive surface expression of MAdCAM-1, albeit at low levels, on 2 different types of endothelial cells. Using an *in vitro* 8 chamber well system we showed this level of expression to be influenced by TNFα. Specifically, TNFα in a dose and time dependant manner causes the upregulation of MAdCAM-1 as measured quantitatively. It would therefore make therapeutic sense to quantify MAdCAM-1 expression since this would enable us to accurately study factors governing this expression.

We focused our attention to SVEC 4-10 cells because of its similarities to HEV and the consistent and optimal MAdCAM-1 upregulation with TNFα. Nevertheless, there appeared to be inherent limitations to further use of the 8 chamber well system. The number of experiments, which could be performed at any one time clearly restricted its use. Moreover, there were also severe limitations in the number of variables i.e. experimental conditons which could be designed at a given time point. Finally, there were the innate quantitation biases of image analysis in an 8 chamber system. That is, the quantifiable flouresence value was based on mean pixel intensity following subjective representation of 2 to 4 fields. This inevitably contributed to delayed readings and possible inaccuracies in the final fluorescence and henceforth MAdCAM-1 signal.

A possible solution to overcome these pertinent disadvantages of the 8 chamber system were the introduction of a 96 well plate system. Our ability to stimulate surface expression of MAdCAM-1 in this *in vitro* model will be used to investigate a number of factors which will be used to modulate its expression. This work is described in Chapter 5.

3.3.2 Aims

1. To develop a reproducible *in vitro* model of MAdCAM-1 expression using SVEC 4-10 cells
2. To quantify the level of MAdCAM-1 expression in the *in vitro* model using a 96 well plate reader system

3.3.3 Method

SVEC4-10 cells in fresh DMEM taken at time of subculture were seeded at a ratio 1:4 to 1:6 on to gelatin coated 96 Falcon™ 96-well flexible polyvinyl chloride (PVC) plates.

The plated cells were incubated as previously until they were 70%-80 % confluent and stimulated by incubating with 20 ng/ml mouse Recombinant TNFα (SigmaAldrich, Poole, UK) in for 24hours. Thereafter, each chamber well was washed carefully three times with 0.2 mls of phosphate buffer saline (PBS) followed by ten-minute incubation with equal volume of Formalin fixative, followed by further rinsing with PBS. The cells were incubated overnight at 4^0C functional grade purified Rat anti-mouse MAdCAM-1 monoclonal antibody-10μg/ml MECA 367 (eBioscience, UK Cat No 16-5997) in 1% Bovine serum albumin/PBS. Each chamber well was washed 3x with PBS and further incubated for one hour at room temperature with Goat Anti-Rat IgG (whole molecule) FITC conjugate at 10μg/ml (SigmaAldrich, Poole, UK), followed by a further 3 washes with PBS.

3.3.3.1 Image Analysis

The surface expression of MAdCAM-1 was detected and analysed using the Fluorescent Cytofluor^R 4000 reader at 485/20(excitation) and 530/25(emission). The value for the time 0 (background control) was subtracted from that of the other time points. The value for each time point and TNFα concentration was the mean ± standard error of 6 observations.

3.3.4 Results (figure 3.6)

The SVEC4-10 cells showed maximal fluorescence intensity following 20ng/ml stimulation with TNFα ($p<0.01$). There was generally a dose dependant increase in surface MAdCAM-1 expression with increasing doses of TNFα (0 to 20ng/ml) but a relative fall in fluorescence intensity at higher doses e.g. with 30 ng/ml TNFα ($p<0.05$)

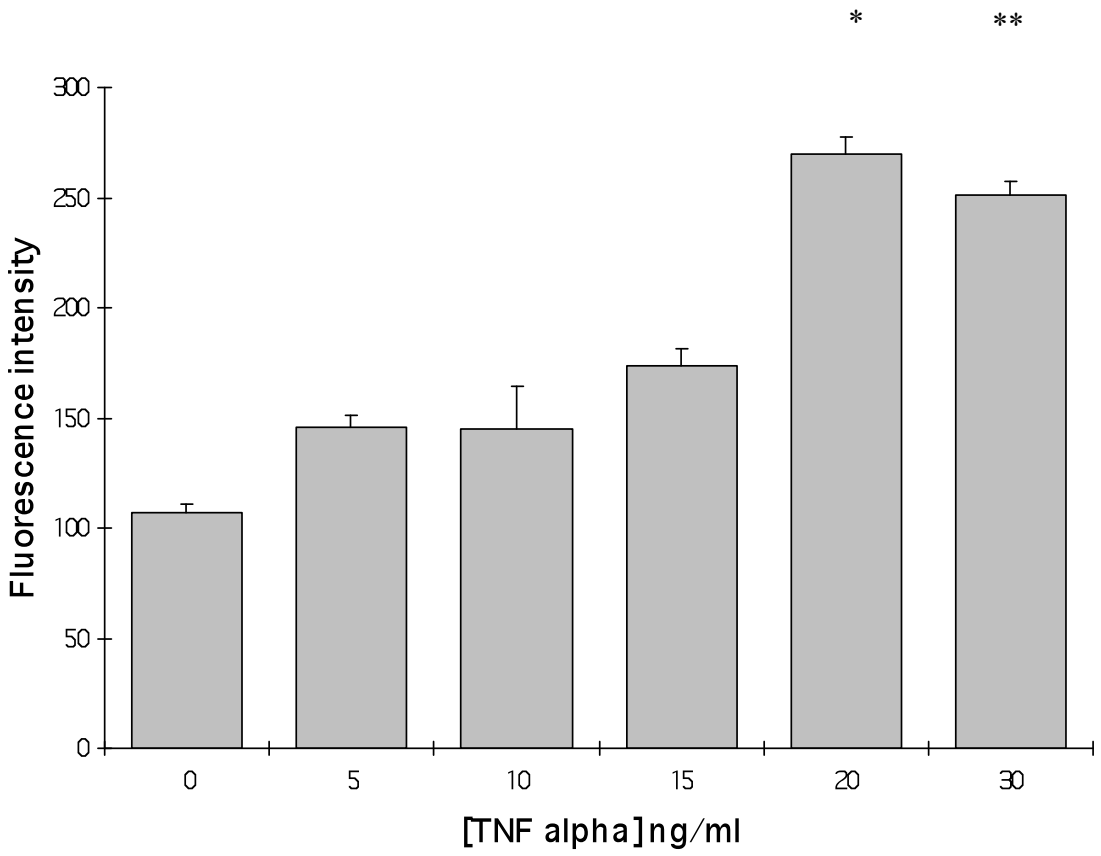

Figure 3.6 Surface expression of MAdCAM-1 from SVEC4-10 cells after 24 hours stimulation with varying doses of TNFα in a 96 well plate **(n=9).** Maximal peak expression occurred with 20ng/ml TNFα with a relative fall in fluorescence intensity at higher doses (30ng/ml)

- * $p<0.01$ compared to control (without TNFα)
- ** $p<0.05$ compared to control (without TNFα)

3.3.5 Discussion

Following the 8 well system studies, in this chapter I have optimised the expression of MAdCAM-1 in SVEC 4-10 cells using immunofluoresence studies, so as to develop a robust *in vitro* mouse model of MAdCAM-1 in a 96 well plate system.

My results related to the time course of MAdCAM-1 appear to be different to the parallel work by Oshima *et al* (also in 2001) using the same SVEC cell line. This group demonstrated maximal MAdCAM-1 expression (later confirmed by Western Blot methodology), also occurred at 24 hours following TNF-α stimulation, although a further time course analysis beyond 24 hours was not included. Like these workers, I wished to confirm the presence of MAdCAM-1 protein from the SVEC 4-10 cells and carried out Western analysis but were unfortunately unable to detect any signal. This could be due to antibody non-specificities or technology failure. We could not detect a signal on multiple occasions for unknown reasons.

My initial results used 8 chamber well slides as opposed to conventional glass slides to assess the morphological characteristics of the endothelial cells. The observed distribution of MAdCAM-1 on the cell surface was interesting, showing that TNFα induced MAdCAM-1 appeared to be concentrated at cell-cell junction, although this junctional appearance of MAdCAM-1 was not uniform on all cells. This could be explained by (i) cell alterations induced by transformation (ii) direct TNFα heterogeneous stimulatory effects on the endothelium or, (iii) the degree of confluence of the culture. It still remains, that the role of MAdCAM-1 at endothelial junctions is ill-defined.

Although bEnd.3-based models are clearly useful, these cells derived from brain capillaries do not accurately model high endothelial venules. The SVEC cells appear to be useful in this regard and could provide a more realistic and relevant model in the investigation of the mechanisms involved in human IBD. It is for this reason that I chose to pursue further experiments with SVEC 4-10 cells rather than bEnd.3

The 96 well system had advantages over the 8 well system. It allowed in one sitting (i) larger numbers of experiments to be performed (ii) greater number of variables and experimental conditions to be adjusted in a consistent manner and (iii) quicker acquistion of results by using a plate reader. Certainly, the 96 well system allowed consistent levels of fluorescence and appeared to be a more reproducible model without the inherent risks of bias associated with mean pixel intensities and subjective representations from areas of maximal fluorescence associated within the 8 well system. This inevitably led to delays and possibilities of inaccuracies in the final fluorescence and therefore MAdCAM-1 signal from the 8 well systems.

From my quantitative immunofluoresence data I have confirmed the ability of this model to demonstrate a TNFα dose dependent increase in MAdCAM-1 expression which was quantifiable by direct measurement of the fluorescence (figure 3.6). This experiment showed a significant maximal fluorescence intensity following 20ng/ml TNFα ($p<0.01$). Although there was a relative fall in fluorescence intensity at higher TNFα doses, this still remained significant, albeit at a level of signifiance of $p<0.05$. I therefore choase 20ng TNF/ml as the concentration of choice in future experiements on MAdCAM-1 modulation.

Using the 96 well system, I repeated the time course series of experiements which I had initially performed in an 8 chamber sytem with 20ng/ml of TNFα. I confirmed MAdCAM-1 expression at 23 hrs which was sustained at 72 hours. My *in vitro* model system was reproducible enabling MAdCAM-1 expression to be formally quantified after endothelial cell activation.

Our ability to stimulate surface expression of MAdCAM-1 in this *in vitro* model will be used to investigate factors, which will be used to modulate its expression. This work is described in Chapter 5.

Chapter 4

Qualitative and Quantitative measurement of MAdCAM-1 expression in cells and tissues

4.1 Experiment 1: Development of a Reverse Transcriptase-Polymerase Chain Reaction (RT-PCR) assay to assess MAdCAM-1 expression in gastrointestinal tissues

4.1.1 Background

Previously, we have semiquantitativley characterised human MAdCAM-1 in gastrointestinal tissues, liver and pancreas by immunohistochemical analysis. The ability to quantitatively assess MAdCAM-1 expression in these tissues may provide not only an assessment critical in evaluating disease activity but also study the response and effect of treatment. The most commonly used methodology to do this is the estimation of MAdCAM-1 mRNA by quantitative RT-PCR (qPCR), although of course this technique provides information at the RNA (gene transcription) rather than the protein level.

Elevated levels of circulating soluble adhesion molecules have been essential in the understanding the pathology of disease. In support of this, there has been an elevated level of soluble ICAM-1 and VCAM-1 in observed malignancy, infection and inflammation. Leung *et al.* showed for the first time the ability of MAdCAM-1 to be secreted as a soluble molecule into serum, urine and other biological fluids. The average level of MAdCAM-1 detected in the serum was 237ng/ml(180-317 ng/mls). These levels are similar to those of ICAM-1 in the serum and levels of soluble MAdCAM-1 in urine ranging from 20-123ng/ml.

4.1.1.1 Human and Mouse MAdCAM-1

The human MAdCAM-1 gene is localised to p13.3 on chromosome 19 in close proximity to the ICAM-1 and ICAM-3 genes (p13.2-13.3). This region is homologous to a region on mouse chromosome 10. Of note, the overall nucleotide protein identity between human and murine MAdCAM-1 is poor (42% and 38%) respectively, although the first Ig domains are highly conserved (59% and 65% respectively).

The coding sequences of the human MAdCAM-1 gene is contained in five exons, under the control of a 717bp 5'flanking promoter region; the signal peptide and the two

Ig and mucin domains (major and minor) are encoded by separate exons (Butcher *et al* 1996), although the transmembrane domain, cytoplasmic domain and 3'untranslated region are themselves encoded on exon 5. The mucin domain contains 8 repeats which are subject to alternative splicing, an observation which has been confirmed by human and mouse cDNA analysis; this inevitably leads to the generation of splice variants which lack all or part of the second Ig domain and all or parts of the mucin domain.

The genomic organisation of the MAdCAM-1 gene correlates well with the subdomain structure of the encoded protein (Grimwood J *et al* 2004). The 5'UTR and the signal peptide are encoded by exon 1; the two N-terminal Ig domains and mucin-like domain are encoded by exons 2, 3 and 4 respectively, and finally the transmembrane and cytoplasmic domains and 3'UTR are combined on exon 5. Several potential transcriptional regulatory elements, including NF-κβ, SP1, AP2, PEA3, NF-E1, Adh1, MYOd, E2A, ENKCRE, IRS sites and a GC box have been identified in the promoter region of the gene. A potential TATA box, 2 NF-κβ sites and one SP1 have been found in the mouse MAdCAM-1 gene promoter region and conserved in position (Leung *et al* 1997). These transcription factor-binding sites including NF-Kb docking may explain the upregulation of MAdCAM-1 following stimulation with cytokines such as TNF-α, which activate NF-KB. DNA methylation occurs naturally in both prokaryotic and eukaryotic organisms. In higher eukaryotes, DNA methylation has been proven to play a central role in a number of biological processes such as X chromosome gene slincing, embryonic development, gene imprinting and cell cycle regulation. DNA methylation usually occurs in CpG islands which are often located around the promoters of housekeeping or other genes frequently expressed in the cell. Human MAdCAM-1 is encoded by a gene on chromosome 19p13. Of note, chromosome 19, which contains the human MAdCAM-1 gene has the highest densities of all human chromosomes and its high G+C content and density of CpG islands and repetitive DNA sequences indicate a chromosome rich in biological and evolutionary significance. The density of CpG islands on this chromosome suggests that MAdCAM-1 gene may be a candidate for regulation by methylation.

Several features of MAdCAM-1 have been conserved between humans and mice including the structure of the Ig ligand-binding domains. Nonetheless, the 3' region

remains relatively divergent between the species. Comparison of the human gene sequence with the mouse homologue shows that the differences in organisation of the 3' region are not simply due to splice variants (Sampaio *et al* 1995). As a consequence, the human MAdCAM-1 gene does not contain sequence equivalents to the 3rd Ig-A homologous domain of mouse MAdCAM-1 adjoining the 3'end of the mucin domain. Certainly, despite this major difference in structure, other regions of the human and mouse MAdCAM-1 remain highly conserved, including positions at three of the four intron-exon splice junctions, further supporting the close evolutionary relationship between these molecules. Alignment of the human and mouse MAdCAM-1 gene shows three of the four intron-exon junctions separating the signal peptide and Ig domain sequences, MAdCAM-1 mucin-like domains and intron-exon splice sites separating the mucin and transmembrane sequences are not conserved between species. For example, in humans, the splice site is nine amino acids N-terminal to the boundary of the extracellular and transmembrane domains, whereas in mouse it is only three amino acids N-terminal.

Sequence and genomic organisation of the human MAdCAM-1 gene provides further evidence that previously isolated MAdCAM-1 cDNA encode human MAdCAM-1 (Leung E *et al* 1997). The identification of an additional cDNA splice variant serves to emphasise that the functions of MAdCAM-1 are likely to be extensively altered by rearrangement of its multi domain structure. At least seven alternatively spliced variants of the human MAdCAM-1 gene have been identified that encode different protein isoforms e.g. Variation 1: lacking major and minor mucin domains, variation 2: lacking entire mucin domain and domain 2, variation 3: lacking some of the major mucin repeats and second immunoglobulin domain. It must be noted that the full –length nature of some variants have not been determined.

Despite the absence of a human counterpart of the third IgA-homologous domain and lack of sequence of conservation of the mucin domain, the genomic organisations of the human and mouse MAdCAM-1 are very similar. An alternatively spliced human MAdCAM-1 variant exists which lacks exon 4, encoding the whole mucin domain; therefore this shorter MAdCAM-1 would be unable to accept and present carbohydrate modifiactions and as a result would have a reduced capacity to support lymphocyte adhesion through binding to L-selectin.

Signal Peptide 5'translated	ICAM-1 VCAM-1 Super Ig domain 1	VCAM-1 Super Ig domain 2	Mucin domain- 8 repeats - alternating slicing	Transmembrane-cytoplasmic domain 3'untranslated

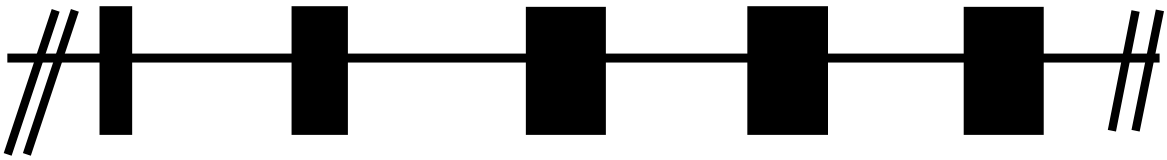

EXON 1 **EXON 2** **EXON 3** **EXON 4** **EXON 5**

Figure 4.1 Schematic diagram representing genomic organisation of the Human MAdCAM-1 gene and comparisons with the mouse homologue on Chromosome 19 (p13.3) close to ICAM-1/3 genes (p13.2-p13.3). The MAdCAM-1 subdomains encoded by the MAdCAM-1 cDNA sequence, organisation of exons and their relationship to the cDNA sequence are described. The human MAdCAM-1 gene contains five exons where the signal peptide, two immunoglobulin domains and mucin domains are each encoded by separate exons. The transmembrane domain, cytoplasmic domain and the 3'' untranslated region are encoded together on exon 5. The mucin domain contains eight repeats in total which are subject to alternate splicing.

ccacgcgtcc gtcacaagac agaggcaggc atggaatcca tcctggccct cctgctggcc

ctggccctag taccctacca gctcagcaga ggacagtcct tccaggtgaa ccccccctgag

tctgaggtag ctgtggccat gggcacatcc ctccagatca cctgcagcat gtcctgtgac

gagggtgtag cccgggtgca ctggcgtggt cgggacacca gcttgggcag tgtacagacc

ctcccaggca gcagtatcct ctctgtacgg ggcatgctgt cagacacagg cactcctgtg

tgtgtgggct cctgcgggag tcgaagcttc cagcactccg tgaagatcct **TGTGTATGCC**

TTCCCAGACC agctggtggt gtccccggag ttccttgtac ctggacagga ccaggtggtg

tcctgcacgg cccacaacat ctggcctgca gacc**CGAACA GTCTCTCCTT TGCC**ctgcta

ctgggagagc agagactgga gggtgcccaa gccctggaac cagagcaaga agaggagata

caagaggctg agggcacacc actgttccga atgacacaac gctggcggtt accctccctg

gggacccctg cccctcctgc ccttcactgc caggtcacca tgcagctgcc caaactggtg

ctgacccata gaaaggagat tccagtacta cagagccaga cctcacctaa gccccccaac

acgacctctg ctgagcccta catcctgacc tcatcaagta ctgctgaggc agtctccact

gggctcaaca tcaccaccct accttctgcc cctccatacc ccaagcttag ccctaggact

ctgagctctg agggaccttg ccgcccgaaa atccaccagg acctggaggc aggctgggag

ctactctgtg aagcatcctg tgggcccgga gttactgtgc gctggacctt ggctcctggc

gacctggcaa cctaccacaa gagggaggct ggggcccagg catggctaag cgtgctgccc

ccaggtccca tggtagaggg ctggttccag tgccgccagg accctggcgg ggaggtgacc

aatctgtatg ttcctggcca ggtgaccccg aattcctcct ccaccgtcgt cctatggatt

ggcagcttgg tgctggggct gcttgcactg gtcttccttg cctaccgcct gtggaaatgc

taccggccag gtcctcgccc agacactagc tcatgtacac acctatgaag ctccattatg

ccagactaaa ggaggcagag agtgaccagc tgcaggattt ggggcatcaa gatgatagtg

tggcctcttt ccttggtggt cagcacatct ataagtttct cctgacttct gggcttttct

gcctgctggc ccagagctaa ataaaagccc cgtatct

Figure 4.2 Human MAdCMA-1 cDNA

4.1.1.2 Polymerase chain reaction

The development of the polymerase chain reaction (PCR) technique in the 1980's has allowed rapid advances in the field of molecular biology. It is an indispensable tool in medical and biological research and diagnostics. The methodology uses thermostable DNA polymerase to replicate a piece of DNA initiated from synthetic oligonucleotides primers complementary to sequences flanking the region of interest recruiting free dNTP's (deoxy-nucleotide-triphosphates) from the reaction mixture. The resulting DNA then becomes a template for further replication and in this way a few copies of target DNA can be exponentially amplified to millions of copies by cycles of denaturation, primer annealing and DNA extension.

In order to utilise PCR for estimation of MAdCAM-1 expression in cells and tissues cDNA is generated which is complimentary to the mRNA of interest. This is carried out by reverse transcription with the aid of reverse transcriptase, an enzyme utilised by certain RNA viruses to convert their genomic RNA to DNA within the host cell. In *in vitro* reverse transcription the enzyme catalyses the synthesis of a single strand of cDNA initiated from oligo dT, sequence specific oligonucleotides primers or random hexamers which anneal to the mRNA.

4.1.2 Aim

To assess the expression of MAdCAM-1 in human tissues by reverse transcription – polymerase chain reaction.

4.1.3 Methods

A 100 μg fresh tissue of histologically normal colon tissue (samples 1 and samples 2) was snap frozen in liquid nitrogen and cryopreserved at –80^{o}C until RNA extraction. TRIzol^{R} Reagent (Invitrogen) was used for isolation of total RNA following manufacturer's instructions. Briefly, 100μg of tissue was homogenised in 2ml TRIzol^{R}, 400 μl of chloroform was added to 1ml of homogenate (in TRIzol^{R}) and centrifuged for 10 minutes at 12,000rpm in a microcentrifuge. The RNA partitions in the aqueous phase which is removed and RNA recovered by precipitation with an equal volume of

isopropanol incubated at –20^{0}C for 30 minutes and centrifuged for 15 minutes at 12,000rpm. The supernatant was removed and the pellet was washed with excess 70% ethanol and centrifuged at 12,000rpm for another ten minutes. The RNA pellet was then resuspended in 100µl RNase free H_2O. The total RNA was reverse transcribed to complementary DNA in a 50 µl reaction, allowing transcription top proceed at 37^{0}C for 2 hours. These experiments were carried out on 3 occasions using different normal colon tissue samples to confirm reproducibility.

4.1.3.1 Reverse Transcription

10 picomole of oligo dT primer was added to 20µl of RNA (DNase treated) and incubated at 65^{o}C for 5 minutes. This was then added to the reverse transcription mix as detailed below and incubated at 37 ^{o}C for 60 minutes.

	Volume
1st Strand Buffer	10
Moloney Murine leukaemia virus (MMLV) reverse transcriptase	4.0
Oligo d(T) Primer (10picomol)	1.0
dNTP (10mM)	2.5
RNase FreeH_2O	12.5
RNA	20
	50 µl

The reaction was terminated by heating to 70 ^{o}C for 15 minutes and the cDNA stored at 20^{o}C until use.

4.1.3.2 Polymerase Chain Reaction

The cDNA was then amplified by single round PCR using hot start Taq DNA polymerase kit (Hotstar, Qiagen, UK) to minimize amplification of non-specific product. The PCR consisted 15 minutes incubation at 95^{o}C to activate the Taq polymerase followed by 35 cycles each consisting of denaturation at 94 ^{o}C for 30seconds, primer annealing at 60^{o}C for 30 seconds and extension at 72^{o}C for 1 minute. The PCR reaction was set up as follows:

	Volume
HotStar Mix	25.0
Forward Primer	2.50
Reverse Primer	2.50
H_20	18.75
cDNA	1.25
TOTAL	50.0µl

Primer pairs were designed using the online program Primer 3 (http://frodo.wi.mit.edu/) and 3 sets designed as shown in Table 4.1.

Table 4.1 MAdCAM-1 Oligonucleotide Primers (f1,f3,f5-forward,r2, r4,r6-reverse)

Primer	**Amplicon Size (base pairs)**	**Primer Sequence (5'-3')**
MAdCAMf1 MAdCAMr2	117	5'-GAGAAGTGATCCCAACAGGC-3' 5'-AGAGGTGATACGTGGGCAAG-3'
MAdCAMf3 MAdCAMr4	240	5'-CAGCTCCTTGTGTACGCCTT-3' 5'-CTCTGTCACCCTGAACAGCA-3'
MAdCAMf5 MAdCAMr6	143	5'CGGGCCGCAGCGTCCTCAC-3' 5'TCCCCCTGTGAAAGCAAAAT-3'

4.1.3.3 Gel electrophoresis

Analysis of the PCR product was carried out by agarose gel electrophoresis. A 1.5% agarose gel in TBE buffer (0.89M Tris, 0.89M Boric acid, 0.02M EDTA) was prepared by melting the agarose in TBE in a microwave oven. After cooling to 50^{o}C 5µl of ethidium bromide solution (0.05µg/ml) was added and the gel cast in the perspex mould with a gel comb for well formation. After the gel had set, it was placed in the electrophoresis tank submerged in TBE buffer and the comb removed. 5µl of PCR product was mixed with 1µl gel loading buffer (15% Ficoll, 0.06% Bromophenol Blue, 30mM Tris/EDTA pH8.0). The PCR samples and appropriate MW markers were added to the wells and the gel electrophoresed at 10V/cm until the dye front had migrated 4/5 the length of the gel. The gel was then visualised by trans-illumination with UV light in a UVP EpiChem II Gel Documentation System (UVP Laboratory Products, USA) and a digital image acquired.

4.1.3.4 Gel extraction of PCR DNA

The DNA amplicon was extracted from the agarose gel using QIAquick Gel Extraction Kit (QIAGEN, UK). The DNA fragment was excised from the agarose gel three volumes of Buffer QG were added to 1 volume of gel. This was incubated at 50 ^{0}C for 10 minutes until the gel slice had completely dissolved. To increase the yield of DNA fragments one volume of isopropanol was added and mixed thoroughly. The mixture was loaded onto a QIAquick spin column and centrifuged for 1minute at 13000 rpm. The flow-through was discarded and a further 0.5 ml of Buffer QG Buffer was added and centrifuged for a further 1 minute to remove all traces of agarose. 0.75 ml of Buffer PE was added to the column and centrifuged again for 1minute at 13,000 rpm. The flow-through was discarded and the column centrifuged for an additional 1minute at 13,000 rpm to ensure complete removal of wash buffer. The column was placed into a clean 1.5ml-microcentrifuge tube and the DNA eluted with 30µL 10mM Tris pH 7.4. The DNA was stored at -20^{o}C until used.

4.1.3.4 DNA sequencing

The amplicon was directly sequenced using forward and reverse primers by The Sequencing Service (School of Life Sciences, University of Dundee, Scotland, www.dnaseq.co.uk) using Applied Biosystems Big Dye Ver 3.1 chemistry and an Applied Biosystems 3730 automated capillary sequencer.

4.1.4 Results (figure 4.3 to 4.4)

Human MAdCAM-1 may be extensively alternatively spliced, creating an array of at least four variant forms that lack all or part of the second immunoglobulin domain, including all or part of the major mucin domain. Our results do not show splicing variants of MAdCAM-1 in histologically normal large bowel. We have demonstrated a single band using newly designed forward primer F1 (5'-GAGAAGTGATCCCAACAGGC-3') and reverse primer R2 (5'-AGAGGTGATACGTGGGCAAG-3') to nucleotides 980-999 and 1096-1115 respectively, with amplification of a 117 bp product subsequently identified by sequence analysis *(figure 4.3 and 4.4)*.

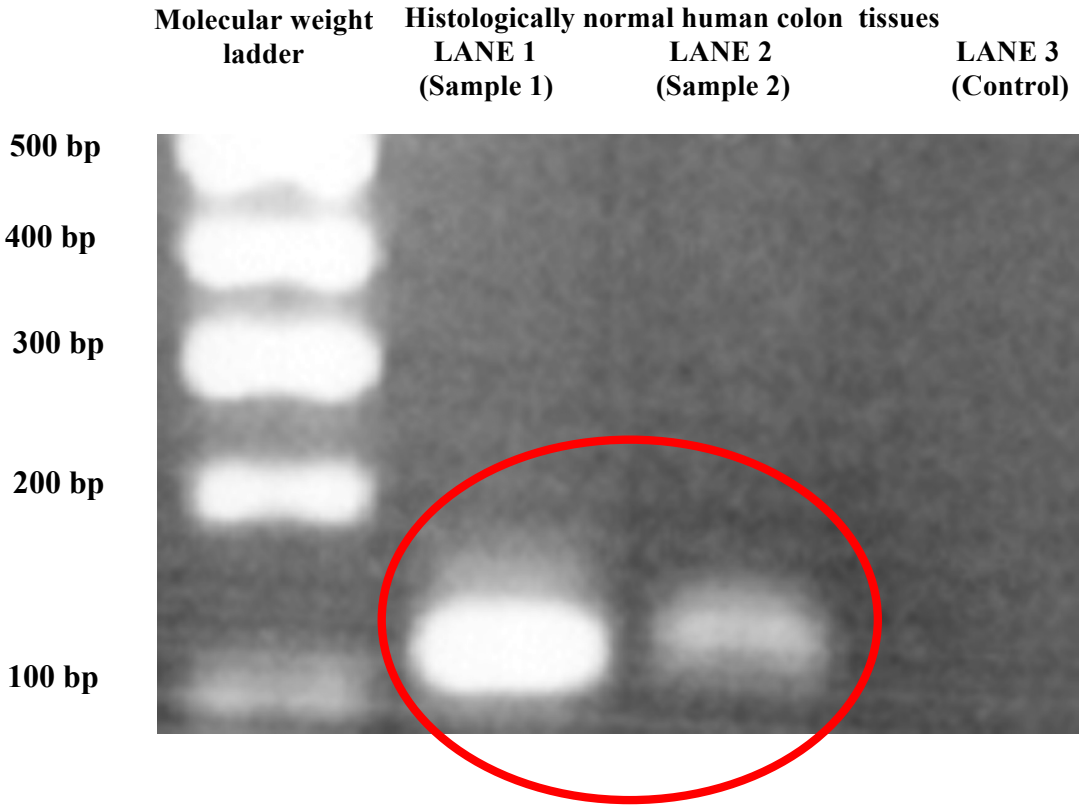

Figure 4.3 Identification of human MAdCAM-1. MAdCAM-1 cDNA was amplified from reverse transcribed human colon RNA(Sample 1 and 2) using PCR primer sequences directed to nucleotides 980-999,1096-1115 and subsequent amplification of a 117 base pair(bp) product.

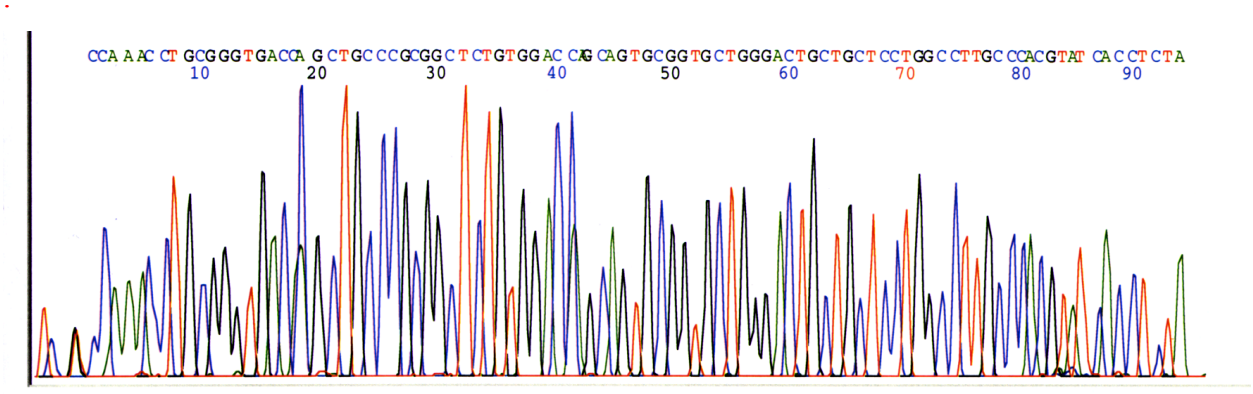

Figure 4.4 Electrophoretogram and sequence of human MAdCAM-1 using specific PCR primer sequences and amplified cDNA transcribed from RNA extracted from histologically normal large bowel, indicating consensus between sequenced material and MAdCAM-1 sequence information from GenBank.i.e presense of constitutive MAdCAM-1 in normal colon.

4.1.5 Discussion

We set out to develop methods to assess MAdCAM-1 expression so as to enable its quantification in future experiments with different tissue samples e.g. liver . Using RT-PCR technology our results confirm MAdCAM-1 expression in gut tissue e.g. histologically normal colon tissue.

The conditions required for the generation of sensitive and specific RT-PCR assays from gut tissue samples required optimisation. There were a number of PCR optimising strategies that we used to alter the specificity characteristics of the PCR reaction:

1. Primer design

As well as the specific considerations relevant to the MAdCAM-1 primer design given in all the methods, there are some general considerations that are relevant. The two primers are generally 20-30 base pair long, contain a relatively balanced GC vs AT content (e.g. 45-55% GC) with no long stretches of one base (prevents secondary structures). The primary pairs should not have more than 2 adjacent complimentary base pairs (especially at the 3'end) to avoid primer dimer formation.

2. Magnesium concentration

The specificity of the PCR reaction can be increased by decreasing the Mg2+ concentration in the reaction mix. The magnesium concentration must therefore be optimised for an efficient PCR reaction to occur, as a concentration too low may result in no product forming and a concentration too high may result in a variety of unwanted products.

3. Annealing characteristics

The annealing temperature is particularly important in determining the specificity of the PCR reaction. At lower temperatures the specificity of primer binding is reduced, resulting in the formation of multiple non-specific products. The ideal annealing temperature is at or just below the melting point (Tm) of the primer/DNA hybrid i.e. when half of the mixture is double stranded and half dissociated. We were able to optimise the annealing temperature to obtain a single band on the gel, a critical requirement for an accurate quantification during the PCR.

4. Template considerations

The efficiency of the MAdCAM-1 PCR was also critically dependant on the presence of Qiagen solution Q in the PCR reaction mix. This is a solution that reduces template secondary structure and is particularly useful in templates with high GC content.

5. Reducing nonspecific background products

We used HotStar Taq DNA Polymerase, a modified form of Taq DNA Polymerase which is inactive at ambient temperatures thus reducing mis-primed products and primer-dimers at low temperatures. It is activated by a 15-minute incubation period at 95^{o}C, which was incorporated into our thermal-cycler programs.

4.2 Experiment 2: Developing a real time RT-PCR method to quantify MAdCAM-1 mRNA in gut and liver tissue

4.2.1 Introduction - Real time PCR

4.2.1.1 Quantitation

There is a quantitative relationship between the relative amounts of starting target sample and PCR product at any given cycle number. Real time PCR aims to estimate the amount of input DNA by real time monitoring of the accumulation of amplicons during the reaction. Traditional PCR is measured at the End-Point (plateau), while Real Time PCR collects data in the exponential growth phase combining the amplification and detection into one step. The detection of amplicons is generally measured using a fluorescent based methodology and the first point at which the fluorescence rises above background in related to the amount of target DNA. This value is referred to as the cycle threshold or C_t, so the sooner a signal is generated i.e. a lower C_t the greater the starting DNA.

There are many different chemistries which have been utilised for the detection of amplicons most of which are based on fluorescence and instruments have been developed which are able to carry out the PCR reaction and accurately measure the fluorescence of each sample at the end of each cycle. Popular among detection methods are DNA binding dyes, hybridization probes, hydrolysis probes, Molecular Beacons and Scorpion probes. In this study I have used methodology based on SYBR Green, a DNA binding dye which benefits from being relatively inexpensive and easy to set up.

SYBR Green emits fluorescence when bound to DNA and as the DNA accumulates then the signal increases and is proportional to the concentration. The DNA binding is non-specific and therefore can also bind to other non-specific DNA species which are present and or accumulating during the PCR from sources such as Primer-Dimers, contaminant DNA or misannealed primers. For this reason careful optimization of the PCR conditions is required in order to avoid false positive signals. Each PCR run was accompanied by a melt curve analysis which identifies the Tm or dissociation temperature of the amplicon. Well optimized reactions with no contaminants should give a single peak for Tm.

Quantification of the amount of starting material (target DNA) in the qPCR reaction and by inference the amount of mRNA in the sample may be determined by absolute or relative methods. In this study we used absolute quantitation where known standards are used to generate a standard curve. The standard curve of Ct versus log input DNA is plotted which gives a linear relationship. The unknowns are derived from this based on their Ct values.

The gene expression data requires normalisation to correct for sample to sample variation in terms of cell number, RNA quality, etc. The real time PCR results are normalized against a control gene which is expressed constantly in different tissue types, throughout development and irrespective of treatment. Generally housekeeping genes e.g. GAPDH, β-actin or ribosomal RNA are used for this purpose. In this study 18S rRNA was used to normalize the real time PCR data.

4.2.2 Quantitation of Mouse tissue MAdCAM-1 mRNA by Real-Time RT-PCR

4.2.2.1 Isolation of Total RNA from mouse tissue

A variety of tissue samples (including brain, colon, heart, lung, liver, ileum and spleen) were obtained from CALB/Rk strain mice. The CALB/Rk mouse strain was used as this was the most accessible and easily available. The mouse experiments were performed once.

The samples were cut into small pieces (approx 20mg), snap frozen in liquid nitrogen immediately after removal, and stored at -80^{o}C until use. Total RNA was isolated using the Qiagen RNeasy Mini Kit (QIAGEN Ltd, Crawley, UK) using the manufacturer's instructions. Briefly, frozen tissue was powdered in a pestle and mortar under liquid nitrogen and transferred to a microcentrifuge tube to which 600µl of lysis buffer was added. The lysate was then homogenised by repeatedly passing through a 21 G needle attached to a sterile syringe during which the high molecular DNA is sheared. The homogenate was then cleared by centrifugation at maximum speed in a microcentrifuge, the supernatant transferred to a new tube, and 600µl of 70% ethanol added. The RNA

was bound to the silica-gel based membrane by centrifugation of the lysate through the RNeasy spin column and contaminants removed by several wash spins. The RNA was then eluted into sterile microcentrifuge tubes in 50µl of RNase-free water and stored at -80^{o}C.

4.2.2.2 Reverse Transcription

cDNA was prepared using the Sensiscript Reverse Transcription kit (Qiagen Ltd, Crawley, UK). 10µl of RNA was added to 10µl reaction mix containing 1x RT buffer, 0.5mM dNTP's, 10µM random hexamer primers, 40U RNaseOUT (Invitrogen, UK), and 1µl M-MLV reverse transcriptase. The reaction was incubated at 37^{o}C for 60 minutes and finally heated at 93^{o}C for 5 minutes to inactivate the enzyme.

4.2.2.3 Quantitative Polymerase Chain Reaction

Primers RTMC1 (5'-GACACCAGCTTGGGCAGTGT) and RTMC2 (5'-CAGCAT GCCCCGTACAGAG) designed as described for qualitative PCR were used for real-time quantitation of MAdCAM-1 mRNA utilizing Sybr Green reagents. A standard curve was included in each run comprising DNA copies of the PCR product in the range 10^3 – 10^8 per reaction. Reaction conditions were: 5µl DNA, 1x buffer, 5mM $MgCl_2$, 0.2mM dNTP's, 1µM each Primer, Sybr Green (1/75000), 1U Platinum Taq DNA polymerase (Invitrogen, UK) in a final volume of 25µl. Thermal cycling and data acquisition was carried out on a Rotor-Gene RG-3000 (Corbett Research, Mortlake, Australia) using the following conditions: 95^{o}C for 15 minutes; 44 cycles of 94^{o}C 30 seconds, 60^{o}C 30 seconds, 72^{o}C 60 seconds. Melt curve analysis was carried out between 50^{o}C - 99^{o}C. All samples were analysed in duplicate. Standard curves were constructed by regression analysis and unknowns calculated using Rotor-Gene software. Sample copy numbers were normalized for 18S RNA by carrying out real-time RT-PCR on each sample as described using 18S RNA primers (sense,5'GTATTGCGCCGCTAGAGGTG;anti-sense, 5'CTGAACGCCACTTGTCCCTC) and comparative amounts calculated against a standard RNA included in each run. Normalized copies were calculated by dividing measured values by comparative 18S RNA value. Relative expression could then be determined by comparing the normalised copies.

4.2.3 Results (table 4.2, figure 4.5)

We used real time PCR to quantify the levels of mouse MAdCAM-1 per unit 18S ribosomal RNA in a variety of murine tissue samples. There was increased constitutive expression of MAdCAM-1 in spleen and ileum with relatively poor expression in liver and heart.

	A	B	C	D	E
	Mouse				
	TISSUE	MAdCAM-1 COPIES	RELATIVE 18S RNA	CORRECTED MAdCAM-1	RELATIVE EXPRESSION MAdCAM-1
1	Brain	314	0.71	442	0.42
2	Colon	207	1.26	164	0.16
3	Heart	25	4.6	5.4	0.005
5	Lung	508	3.55	143	0.14
6	Liver	148	2.35	63	0.06
7	Ileum	671	0.64	1048	1
8	Spleen	5215	1	5215	5

Table 4.2 Real time RT-PCR methodology to quantify levels of mouse MAdCAM-1/18S RNA expression in different mouse tissues. The results have been expressed as the ratio of MAdCAM-1/18S (n=1)

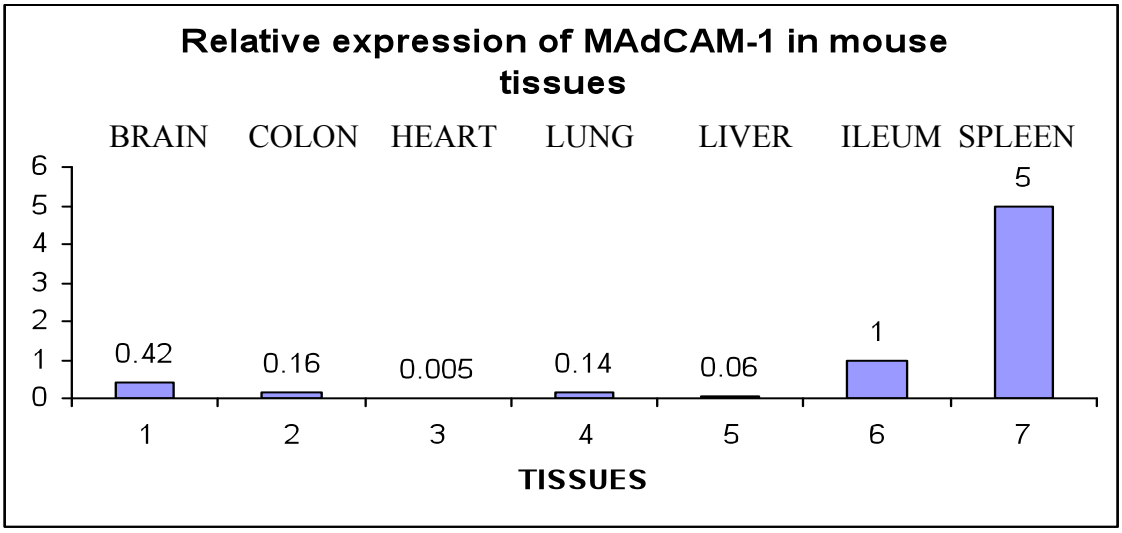

Figure 4.5 Relative expression of MAdCAM-1 in mouse tissues. The highest level of MAdCAM-1 expression was observed in splenic and ileum tissues with the lowest in heart samples and relatively weaker MAdCAM-1 levels in brain, colon, lung and liver(n=1)

4.2.4 Discussion

The ability to effectively quantify MAdCAM-1 in tissues has thus far been challenging, hindering significant progress to explore its modulation. The results from our first series of experiments in this chapter confirm the ability to detect and quantitatively assess MAdCAM-1 mRNA in normal mouse tissues.

Using real-time PCR the relative expression of MAdCAM-1 in normal murine tissues showed it to be raised in spleen and ileum compared with relatively low levels in the heart and liver. The constitutive expression of MAdCAM-1 in histologically normal mouse tissues has previously been described using semiquantitative immunohistochemical data. In support of this, MAdCAM-1 transcripts have previously been described, expressed predominantly in the small intestine, mesenteric lymph nodes, colon, spleen, pancreas and brain.

There is greater expression of MAdCAM-1 in the mouse spleen from our experiments compared to the other organs. This confirms its importance in this organ. Unfortunately whilst these experiements show differences in the expression of mouse MAdCAM-1 in different organs, the mouse experiments were only performed once and different numbers of tissue samples from the same organ were not used. The natural limitations of reproducibility are clear and unfortunately time constraints did not allow repeat.

It is noteworthy to report that high endothelial venules are constitutively absent in the spleen; expression has been described from immunohistochemical and electron microscopy analysis to be immunolocalised to the cells in the marginal zone between red and white pulp where expression is restricted to the sinus lining cells close to the lymphoid white pulp (Kraal *et al.* 1995). Specifically, MAdCAM-1 plays a critical role in the organisation of the marginal sinus around the splenic white pulp nodules. This may be a pre-requisite for unimpaired migration and segregation of B and T cells to and within the spleen i.e. proper trafficking of cells from the marginal zone to the white pulp particularly after a microbial challenge. Steiniger *et al* (2001) reported that fibroblasts with an unusual phenotype located in the perifollicular zone, the outer marginal zone and the T-cell zone of the splenic white pulp are immunoreactive to MAdCAM-1. Each of the latter studies were carried out with two different monoclonal antibodies anti-

MAdCAM-1 mAb 10A6 and 10G3 developed by the Briskin group *laboratory* has the ability to detect MAdCAM-1 in frozen sections but poorly (or not at all) in formalin fixed sections. Thus, the intriguing expression of MAdCAM-1 on fibroblasts, which have not previously been known to express MAdCAM-1, might suggest that these monoclonal antibodies cross-react with an unrelated determinant. However, it has also been reported that MAdCAM-1 is expressed by NIH 3T3 fibroblasts following activation with TNFα. The epitope recognised by the 314G8 monoclonal antibody may be labile in the spleen, duodenum and colon, but this seems unlikely given that the 314G8 mAb recognises MAdCAM-1 in paraffin-embedded sections. A possible explanation is that MAdCAM-1 is alternatively spliced at specific anatomic sites, such that different functional domains are represented. Thus, MAdCAM-1 in the colon, duodenum, and on fibroblast-like splenic cells may represent differentially spliced forms that lack the first immunoglobulin domain of MAdCAM-1 and hence are not recognised by the 314G8 monoclonal antibodies.

We observed MAdCAM-1 to be poorly expressed in mouse brain tissue. MAdCAM-1 expression has been reported in astrocytes surrounding blood vessels in lesions from animals displaying chronic relapsing experimental autoimmune encephalomyelitis (EAE), where it appears to play a contributory role in the progression of chronic EAE and is a potential therapeutic target for the treatment of demyelinating disease e.g. multiple sclerosis. Functional blockade of MAdCAM-1 has been shown to effectively prevent the development of a progressive, non-remitting form of EAE. It is interesting to note that treatment with anti-VCAM-1, anti-MAdCAM-1 and anti-ICAM-1 antibodies induced a more rapid remission than the anti-MAdCAM-1 treatment alone (Karwar *et al* 2000).

Lung Alpha-4 integrins and VCAM-1, but not MAdCAM-1, are essential for recruitment of mast cell progenitors to the inflamed lung. The lung is an important tertiary lymphoid organ and many lung diseases are associated with disordered lung immunity. Unlike the gut, α4β7 (binding to MAdCAM-1) the molecular pathways controlling lymphocyte migration to the lung are unclear.

A distinctive and important observation arising from immunohistochemical analysis and real time data is the faint expression of MAdCAM-1 in the normal liver. This is likely to

reflect its inactive role in normal liver. Additional mRNA analysis by Northern blot or in situ hybridization would also be useful in validating the presence of MAdCAM-1 mRNA in liver tissue. An interesting possibility could be that this MAdCAM-1 exists in a non-functional state. Under inflammatory conditions, a conformational change and increased expression results in increased functional MAdCAM-1 that leads to the recruitment of lymphocytes to liver tissues. It is plausible that MAdCAM-1 is present in normal liver where it exists with a divergent structural folding. This divergent could explain the relatively low expression of MAdCAM-1 detection.

As MAdCAM-1 is a marker of high endothelial venules which are induced at chronically inflamed sites, tissue MAdCAM-1 could be a useful immunological marker diagnostically in monitoring and therefore managing the progression of a variety of major chronic inflammatory diseases with which it is linked, either alone, or in combination with other soluble adhesion molecules. Therefore, increased levels of circulating MAdCAM-1 as outlined earlier could be a marker for the presence or progression of chronic inflammatory disease (Leung *et al* 2004).

4.3 Development and use of a Real Time PCR assay to quantify MAdCAM-1 mRNA in human disease

4.3.1 Isolation of Total RNA from human tissue

Fresh liver tissues n=20 (4 normal, 3 PBC cirrhosis, 3 PSC cirrhosis, 2 ALD cirrhosis, 1 autoimmune hepatitis, 2 cryptogenic cirrhosis, 2 secondary biliary cirrhosis, 2 non-cirrhotic portal hypertension, 1 fulminant liver failure (secondary to paracetmaol overdose and treated with GCSF) were cut into small pieces (50-100 mg), snap frozen in liquid nitrogen immediately after removal and stored at -80^{o}C until use. Total RNA was isolated using the Qiagen RNeasy Mini Kit (QIAGEN Ltd, Crawley, UK) as described previously. The RNA was stored at -80^{o}C until use.

4.3.2 Reverse Transcription

cDNA was prepared using the Sensiscript Reverse Transcription kit (Qiagen Ltd, Crawley, UK). 10µl (approximately 50ng) of RNA was added to 10µl reaction mix containing 1x RT buffer, 0.5mM dNTP's, 1µM random hexamer primers, 1U RNase Inhibitor and 1µl Sensiscript reverse transcriptase. The reaction was incubated at 37^{o}C for 60 minutes and finally heated at 95^{o}C for 5 minutes to inactivate the enzyme. cDNA was stored at -20^{o}C until use.

4.3.3 Quantitative Polymerase Chain Reaction

Primers MAdCAM F5 and R6 designed as described for qualitative PCR were used for real-time quantitation of MAdCAM-1 mRNA utilizing Sybr Green reagents. A standard curve was included in each run comprising DNA copies of the PCR product in the range 10^3 – 10^8 per reaction. Reaction conditions were: 5µl cDNA, 1x buffer, 5mM $MgCl_2$, 0.2mM dNTP's, 1µM each Primer F5 and R6, Sybr Green (1/75000), 1U Platinum Taq DNA polymerase (Invitrogen) in a final volume of 25µl. Thermal cycling and data acquisition was carried out on a Rotor-Gene RG-3000 (Corbett Research, Mortlake, Australia) using the following conditions: 95^{o}C for 15 minutes; 44 cycles of 94^{o}C 30 seconds, 60^{o}C 30 seconds, 72^{o}C 60 seconds and a melt curve between 50^{o}C - 99^{o}C. All

samples were measured in duplicate. Standard curves were constructed by regression analysis and unknowns calculated using Rotor-Gene software.

Sample copy numbers were normalized for 18S RNA by carrying out real-time RT-PCR on each sample as described using 18S RNA primers (sense, 5'GTATTGCGCCGCTAGAGGTG; anti-sense, 5'CTGAACGCCACTTGTCCCTC) and comparative amounts calculated against a standard RNA included in each run. Normalized copies were calculated by dividing measured values by comparative 18S RNA value.

We initially set out to verify the accuracy of real time PCR in measuring MAdCAM-1 DNA levels. We can duplicate samples on serial dilutions of standard MAdCAM-1 DNA to establish the reproducibility and accuracy *(figure 4.6 and 4.7)* of the assay. The assay for the standard 18s internal controls had previously been verified by Oswell, Southampton, UK. We tested standard concentrations of 18S RNA in number of PCR reactions provided by the manufacturer to verify the accuracy of the 18S internal controls prior to testing our samples. To establish the accuracy of this real time PCR protocol in quantifying MAdCAM-1DNA we used the biogene software to generate a standard curve for serial dilutions *(figure 4.7)*.

4.3.4 Results (figure 4.6 to 4.8 and table 4.3)

I used real time PCR to quantitify levels of MAdCAM-1 mRNA perunit 18S ribosomal RNA in our liver samples.There were varying levels of MAdCAM-1 expression in the human liver tissues from a a range of liver diseases, grouped into normal liver, cirrhotic liver explants, non-cirrhotic portal hypertension and fulminant liver failure (secondary to paracetamol overdose treated with GCSF). The latter case was associated with the highest MAdCAM-1 level recodered with the lowest levels of MAdCAM-1 expression in autoimmune hepatitis related cirrhosis.

There was significant upregulation of MAdCAM-1 expression in the cirrhotic liver (n=14) $p<0.011$ as compared to normal liver (n=4)

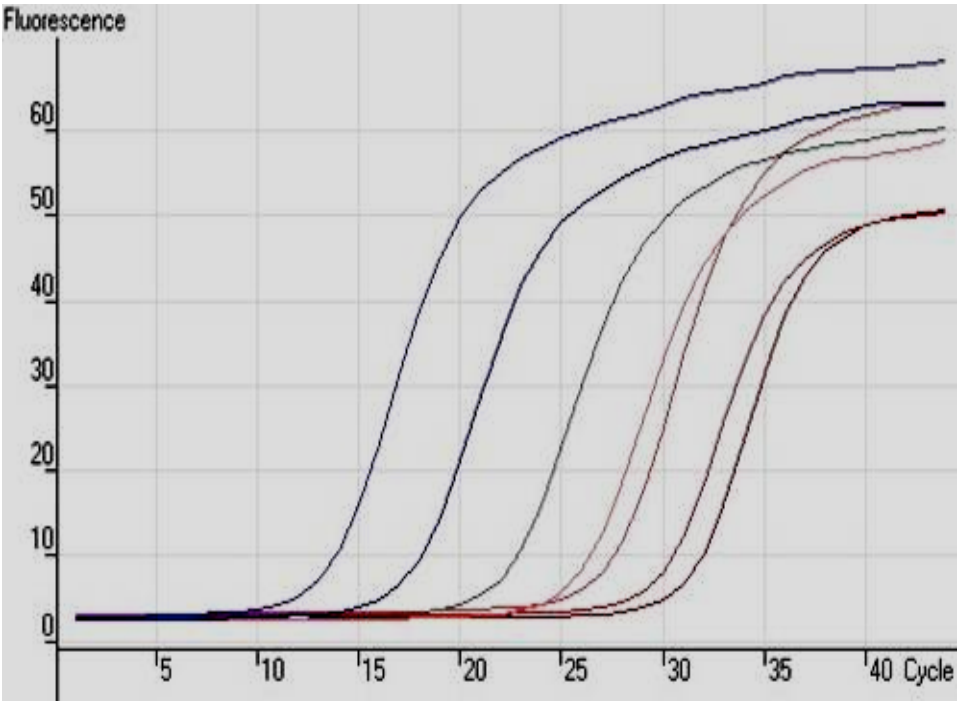

a Human MAdCAM-1 = 10^8 copies/reaction

b Human MAdCAM-1 = 10^7 copies/reaction

c Human MAdCAM-1 = 10^6 copies/reaction

d Human MAdCAM-1 = 10^5 copies/reaction

e Human MAdCAM-1 = 10^4 copies/reaction

f Human MAdCAM-1= 10^3 copies/reaction

g PCR Negative Control=water

Figure 4.6 The fluorescence profile for the standard concentrations of Human MAdCAM-1 DNA using real time PCR. The fluorescence profile follows the classical sigmoidal shape (reproducibility) and a serial drop in threshold Ct value representing each dilution (log 10).

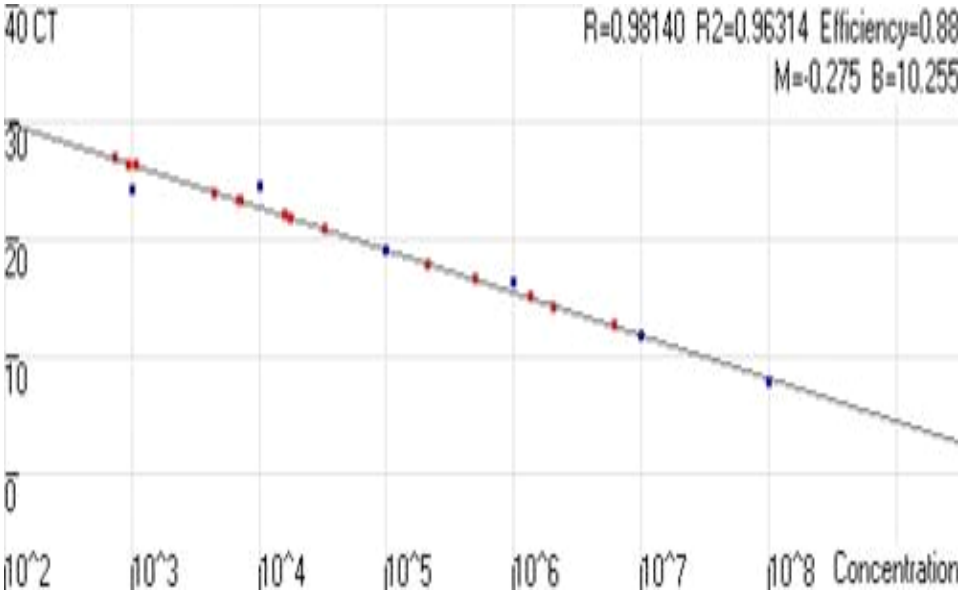

Figure 4.7 A standard curve was generated for the serial dilutions of MAdCAM-1. The blue dots (MAdCAM-1) are standards and reds are the unknowns.

PATIENT	DIAGNOSIS	COPIES MAdCAM-1 mRNA/unit 18S RNA	MEAN ± SE COPIES MAdCAM-1
1	NORMAL	$4.7X10^6$	$3.6X10^6 \pm 2.18X10^6$
2	NORMAL	$9.3X10^6$	
3	NORMAL	$0.32X10^6$	
4	NORMAL	$0.083X10^6$	
5	SECONDARY BILIARY CIRRHOSIS	$2.2X10^6$	
6	NON CIRRHOTIC PORTAL HYPERTENSION	$1.1X10^6$	
7	CRYPTOGENIC CIRRHOSIS	$65X10^6$	$42X10^6 \pm 23X10^6$
8	CRYPTOGENIC CIRRHOSIS	$19X10^6$	
9	FULMINANT LIVER FAILURE SECONDARY TO PARACETAMOL OVERDOSE TREATED WITH GCSF	$23000X10^6$	
10	AIH CIRRHOSIS	$0.064X10^6$	
11	ALD CIRRHOSIS	$67X10^6$	$41X10^6 \pm 14.5X10^6$
12	ALD CIRRHOSIS	$11X10^6$	
13	ALD CIRRHOSIS	$64X10^6$	
14	ALD CIRRHOSIS	$21X10^6$	
15	PSC CIRRHOSIS	$34X10^6$	$32X10^6 \pm 5.9X10^6$
16	PSC CIRRHOSIS	$41X10^6$	
17	PSC CIRRHOSIS	$21X10^6$	
18	PBC CIRRHOSIS	$2.3X10^6$	$8.3X10^6 \pm 4.5X10^6$
19	PBC CIRRHOSIS	$17X10^6$	
20	PBC CIRRHOSIS	$5.6X10^6$	

Table 4.3 Human hepatic MAdCAM-1 cDNA assay from normal liver tissues and from a range of liver conditions(Total n=20).

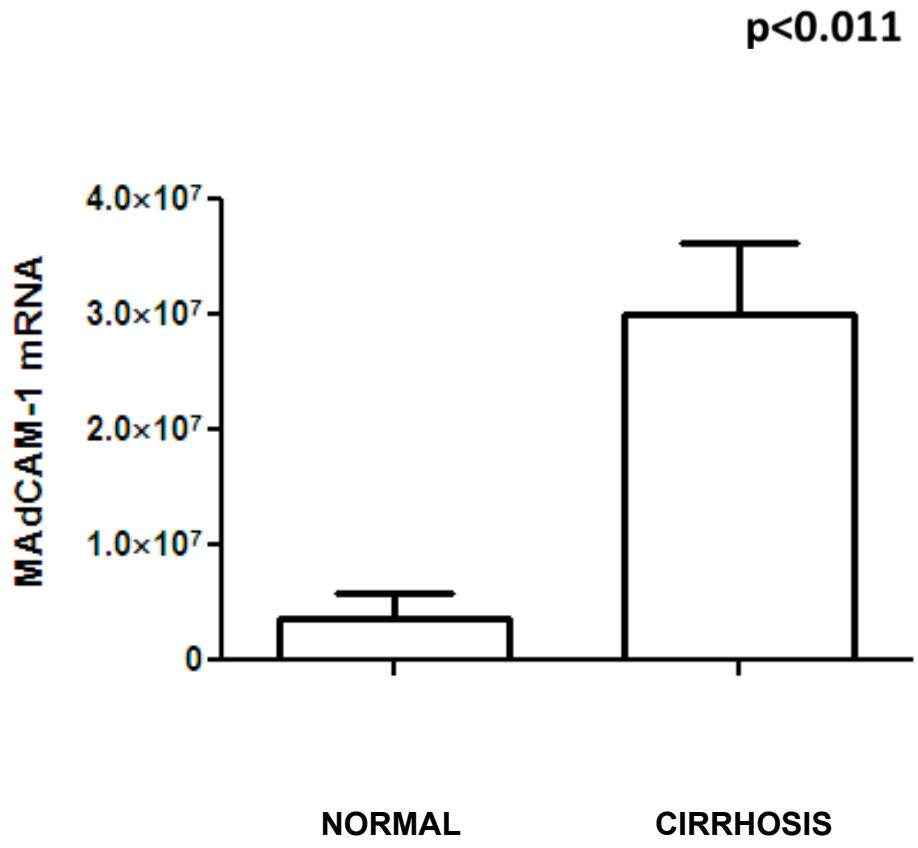

Figure 4.8 Expression of MAdCAM-1 mRNA in the human liver as determined by real-time PCR. *The figure shows significant upregulation of MAdCAM-1 in cirrhotic liver (n=14) p<0.011 as compared to normal liver(n=4).*

4.3.5 Discussion

The expression of MAdCAM-1 has previously been reported in human livers in a variety of liver diseases which are linked to IBD e.g. PSC and AIH. Our aims in this section was to confirm our findings from MAdCAM-1 immunohistochemistry and determine whether MAdCAM-1 is expressed in the liver as mRNA was examianed specifically looking to see if detection was possible in both normal and diseased livers. I found sequence analysis of mRNA from a normal liver revealed complete alignment with the MAdCAM-1 gene provided by GeneBank validating the presence of MAdCAM-1. Additional mRNA by Northern blot or insitu hybridisation would also have been useful in validating the presence of MAdCAM-1 in human liver tissue as would MAdCAM-1 protein using Western Blot analysis.

Our current experiments thus far, from chapter 2 and 4 have demonstrated our ability to detect and effectively quantify MAdCAM-1 in fresh human tissues e.g. liver. Using real time analysis (qPCR), I have shown the significant upregulation of MAdCAM-1 mRNA in advanced liver disease($p<0.011$), confirming the findings from my immunohistochemical analysis. Specifically, in the immunohistochemical work from Chapter 2, I found no evidence of MAdCAM-1 in non-cirrhotic portal hypertension, normal liver and pre-cirrhotic PBC, HCV. This compares to my findings of MAdCAM-1 upregulation, in cirrhotic liver disease from immunohistochemistry and confirmed by real time PCR. Unfortunately, whilst further liver tissues samples at different disease stages for PBC and HCV i.e. pre-cirrhosis were not available to allow MAdCAM-1 real time measurement, there was no doubt of its absence in the pre-cirrhotic immunohistochemical studies and upregulation in the cirrhosis. We hypothesise that the pre-cirrhotic real time samples would have shown relative paucity in MAdCAM-1 RNA, with a rising trend in expression compared from normal tissues. Clearly, this would be important future work to study this.

It was worthy of note that the lowest levels of MAdCAM-1 expression in human liver was found in autoimmune hepatitis related cirrhosis, albeit in one sample. This level was even lower than those taken from normal liver tissues. Whilst drug history from the autoimmune explant was not available, it is certainly possible that this patient is likely to have been on immunomodulatory drugs e.g prednisolone and/or azathiporine at the

time of orthotopic liver transplantation. The level of MAdCAM-1 may therefore reflect the downregulation effect from immunosuppression.

It is clear from our experiments *(table 4.3)* that MAdCAM-1 is present constitutively in normal human liver, all be it in relatively small quantities, where it probably exists with a divergent structural folding. This contrasts with the mouse real-time analysis where we found almost nonexistent levels of MAdCAM-1*(table 4.2 and figure 4.5)*. This divergence in human MAdCAM-1 could explain the relatively low expression levels of MAdCAM-1 in some studies (Grant *et al* 2002 using monoclonal antibodies) and absence in others (Ala *et al*, using polyclonal antibodies). Currently, the epitope where the monoclonal antibody binds is not known, but as it acts as a function-blocking antibody it is likely that it recognises an epitope in either of the two extracellular domains. In the normal liver setting the non-functional folded state cannot support lymphocyte recruitment, where as in inflammatory conditions the local release of TNFα could induce further expression of MAdCAM-1.It is possible that another stimulatory agent(s) e.g. chemokines in combination with the already expressed MAdCAM-1 acquires a functional confirmation, thus being allowed to recognise leukocyte-integrin recognition and binding. There would certainly be merit in exploring this further. Specifically, additional protein nuclear magnetic resonance spectroscopy (NMR) and X-ray crystallography experiments would provide important topographical details and folding of the ligand – binding domains of the MAdCAM-1 protein in not only basal but also inflammatory conditions.

The goal of most quantitative RT-PCR methods is to use PCR product yield as a measure of relative differences in mRNA template abundance. As the efficiency of the RT reaction has been assumed to be constant, the quantitative capacity of the PCR has been the prime focus of debate. Early on the chapter, the feasibility of the quantitative PCR was questioned because of two theoretical constraints. Firstly, given the exponential nature of the process small tube variations in efficiency would grossly affect the field yield of the PCR products. Secondly, the PCR product yield would not only provide a valid measure of template input during the exponential phase of amplification. The development of competitive PCR methods allows investigators to address such theoretical concerns experimentally. To date the pre-requisites to allow quantitative RT-PCR appear to be:

1. PCR product yield is determined using the exponential phase of amplification (figure 4.6).
2. A standard curve demonstrates the range over which PCR product yield provides a measure of mRNA input (figure 4.7).

We have already discussed the importance of MAdCAM-1 in Chapter 2 having shown `immunohistochemical upregulation in end stage liver disease. The real-time PCR protocol with the appropriate samples allowed us to show a significant MAdCAM-1 mRNA upregulation in human cirrhotic livers (figure 4.8).

It is interesting to note the GCSF treated patient from paracetamol induced fulminant liver failure was associated with the highest MAdCAM-1 levels *(table 4.3)*. Whilst this is an isolated case it certainly allows us to postulate the aetiologies. The effect of MAdCAM-1 is unlikely to be secondary to the acute liver failure per se, as we have previously shown the absence of MAdCAM-1 in earlier stages and grades of liver disease. Certainly, the direct effect of GCSF on adhesion molecules is not well described. We can hypothesize that GCSF leads to the upregulation of TNFα, which as we have previously shown may induce the expression on MAdCAM-1.

Chapter 5

Modulation of MAdCAM-1 expression

5.1 Background

The hypothesis underlying this chapter is that MAdCAM-1 is amenable to modulation, an ability which can be confirmed by quantification. The expression of MAdCAM-1 is achieved using an *in vitro* model as described in Chapter 3. Interactions can be prevented by reducing or masking expression of leukocyte antigens, vascular adhesion molecules, or both. Experimentally, in animals and man, both approaches have been tried. Following the positive therapeutic effect of anti-α4, (Podolosky *et al* 1993) α4β7 (Hesterberg D *et al* 1996) or β7 (Kanai T *et al 2003*) antibodies against leukocyte integrins in experimental colitis, humanised monoclonal antibody natalizumab to α4 integrin IgG4 in active Crohn's disease showed therapeutic benefits in controlled trials (Targan *et al* 2007). In respect of reducing adhesion molecule expression, as discussed above there are a number of adhesion molecules that are upregulated in diseased bowel- e.g. E-Selectin, ICAM-1 and our own findings from MAdCAM-1 (Briskin *et al* 1997*)* (Ala *et al* 2003) and the particular attraction of MAdCAM-1 as a target due to its mucosal specificity has been discussed. In particular, an anti-MAdCAM-1 antibody has been used in experimental colitis with some therapeutic effect (Kato S *et al* 2000).

Whilst we have discussed the use of blocking antibodies, the use of such agents, particularly on repeated occasions, has potential disadvantages associated with sensitization to foreign proteins (even with extensively humanised antibodies) or the development of anti-idiotype responses. An alternative strategy is the prevention of the synthesis of endogenous proteins, which can be specifically achieved by the use of antisense oligonucleotides. Indeed, the potential application of this general approach has already been explored in Crohn's disease, using antisense to the vascular adhesion molecule ICAM-1 (Yacyshyn *et al* 1998) (Yacyshyn *et al* 2002). Here, the results were negative for efficacy and therapeutic value, though the general safety of the approach was demonstrated in patients with IBD. We have already commented that we believe ICAM-1 is a less appropriate target than MAdCAM-1. Thus, the *specific hypothesis* underlying this chapter is that modulation of MAdCAM-1 expression may be achieved and can be subsequently quantified.

5.2 Experiment 1: Effect of modulating MAdCAM-1 using an *in vitro* model

5.2.1 Introduction

Having established our endothelial cell culture model there is potential to investigate the effects of modulating MAdCAM-1 expression on SVEC 4-10 cells. Therefore, our cell culture model has important implications relating to both clinical applications and the mechanism for studying MAdCAM-1 expression. I have already shown the effect of TNFα stimulation and quantifying this endothelial expression. Our aim is to follow a logical sequence from our *in vitro* cell culture work, which began with a dose response experiment studying the effects of TNFα on a monolayer of endothelial cells. This system was developed to study the effect of stimulation with other pro-inflammatory agents such as bacterial endotoxin LPS, and IL-1β. As a result, subsequent inhibition of MAdCAM-1 expression may also be achieved as a potential therapy, by designing strategies and testing them *in vitro*. TNFα has already been shown in Chapter 1 to stimulate the transcription of genes encoding endothelial cell adhesion molecules including E-selectin, ICAM-1 and VCAM-1. Specifially, we have found maximal MAdCAM-1 to occur at a dose of 20ng/ml as the target dose of choice for TNFα following stimulation of SVEC4-10 endothelial cells.

We have chosen to modulate MAdCAM-1 in view of our own interesting observations from chapter two on the expression of MAdCAM-1 in the liver (Ala *et al* 2003), gut (Ala *et al* 2002) and pancreas. Previously, our laboratory chose to modulate E-selectin expression because as we have already shown, using plasma levels, tissue immunohistochemistry, and *in vivo* studies in patients using radiolabelled antibodies, that E-selectin is strongly upregulated in active but not inactive ulcerative colitis and Crohn's disease. (Bhatti *et al* 1998). Potential strategies include administration of steroids, mesalasine, anti-inflammatory cytokines such as IL-10 (which may act directly, or indirectly via inhibition of pro-inflammatory cytokines) and the use of specific agents e.g. anti-sense oligonucleotide sequences (Anti-S) to inhibit expression of MAdCAM-1.

These observations will explore the hypothesis that the ability of endothelial cells to express MAdCAM-1 in response to different pro-inflammatory stimuli (bacterial endotoxin LPS, IL-1β, and TNFα). can be consistantly quantified and that this system could then be further developed to investigate inhibition of MAdCAM-1 expression as a potential therapy. We shall then be in a position to design strategies to downregulate MAdCAM-1 expression, and test them *in vitro.*

5.2.2 Methods

Our aim was to follow a logical sequence from our *in vitro* cell culture work, building on the study of the effects of TNFα on a monoloayer of SVEC 4-10 cells. I utilised the *in vitro* model already developed and described in chapter 3. The SVEC 4-10 cells were seeded at 20,000 cells/cm^2 and used immediately after confluency. I stimulated the cells for 24hrs with IL-1(1-100ng/ml), LPS(1-500ng/ml) and made comparisons with a fixed dose of 20ng/ml of TNFα, which I have already shown to have given maximal surface expression of MAdCAM-1 in dose dependant studies. The endothelial monolayers were pre-treated with Dexamethasone(0.001-1.00mM), 5-aminosalicylic acid(1uM-2mM of 5-ASA), hydrocortisone(0.001-10mM), interleukin-10(1-100ng/ml). prior to transfection with TNFα. In MAdCAM-1 induction assays, the endothelia were treated with IL-10 (20 ng/ml), dexamethasone (10μm) or 5-ASA (400μm), 1 hour prior to TNFα (20ng/ml) stimulation. The percentage inhibition of MAdCAM-1 was calculated having taking into account the negative control and the observed values of the flourscence intensity. Values are mean ± standard error. Data were analysed by one-way ANOVA. Significance was set at $p < 0.05$. All data were the mean of three experiments.

5.2.3 Results (figure 5.1 to 5.3)

The first experiments were a simple series of dose response studies to study the effects of stimulating a monolayer of SVEC4-10 cells with LPS, IL-1 compared to 20ng/ml TNFα for 24 hours. As expected, there were greater variations in responses with co-culture IL-1 and LPS compared to the dose reponse study of TNFα already established in chapter 3. The greatest inhibition of MAdCAM-1 was observed with Hydrocortisone *(Figure 5.2).*

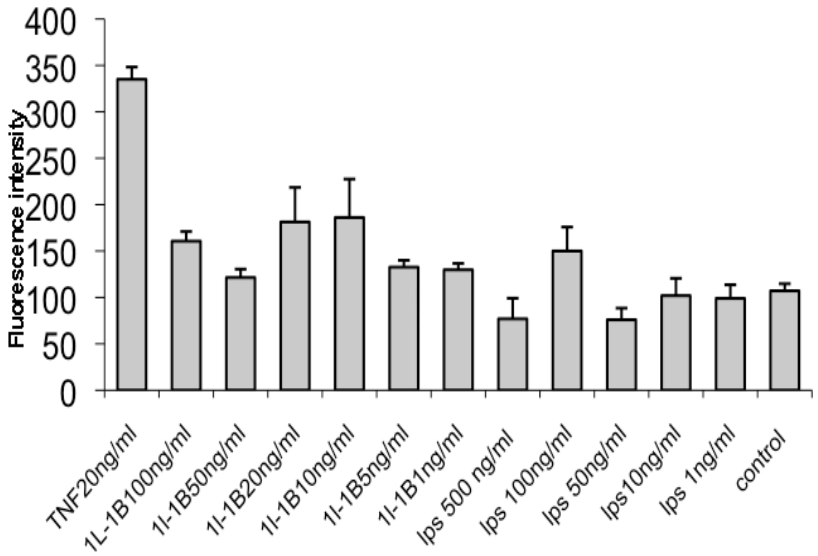

Figure 5.1 The dose response studies on the effect of stimulating a monolayer of SVEC4-10 cells with Interleukin 1L-1β(1-100ng/ml) or LPS (1-500ng/ml) compared to 20ng/ml TNFα over a 24hr period. (n=9). Like LPS, there are also variations in doses of IL-1β . There were greater variations in responses with LPS doses, compared to the dose response study of TNFα already established in chapter 3.

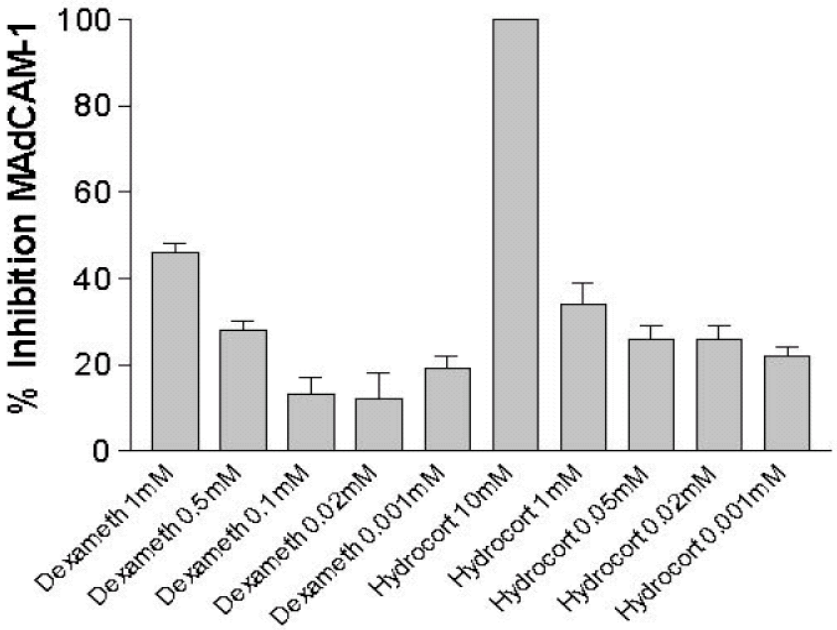

Figure 5.2 The effect of different doses of dexamethasone and hydrocortisone on mouse SVEC4-10 cells pre-stimulated with 20ng/ml mouse TNFα in vitro (n=9) and results expressed as mean ± S.D. The results are shown as percentage inhibition of TNFα. There is a dose dependant increase in MAdCAM-1 inhibition using hydrocortisone at cencentrations varying from 0.001mM to 10mM. The effect from Dexamethasone is less predicatable however, with the highest concentrations (1mM Dexamethasone) leading to over 40% inhibition in MAdCAM-1 expression($p<0.01$) and the greatest inhibition with 10mM of Hydrocortisone at 98%($p<0.001$)

In the next set of experiments (Figure 5.3) I characterised the effects of IL-10 and 5-ASA. I assessed if IL-10 at five different doses between 1ng/ml and 100ng/ml affects inhibition of MAdCAM-1. I also determined if 5-ASA at five different doses between 1μM and 2Mm had an effect. I found whilst the effect of 1L-10 was dose dependant, the overall inhibition of MAdCAM-1 was not significant, although lower doses of IL-10(1ng/ml) appeared to have slightly greater levels of inhibition of MAdCAM-1. The effect of 5-ASA on MAdCAM-1 inhibition was more substantive with the greatest level of inhibition being demonstrated by a dose of 2mM($p<0.05$)

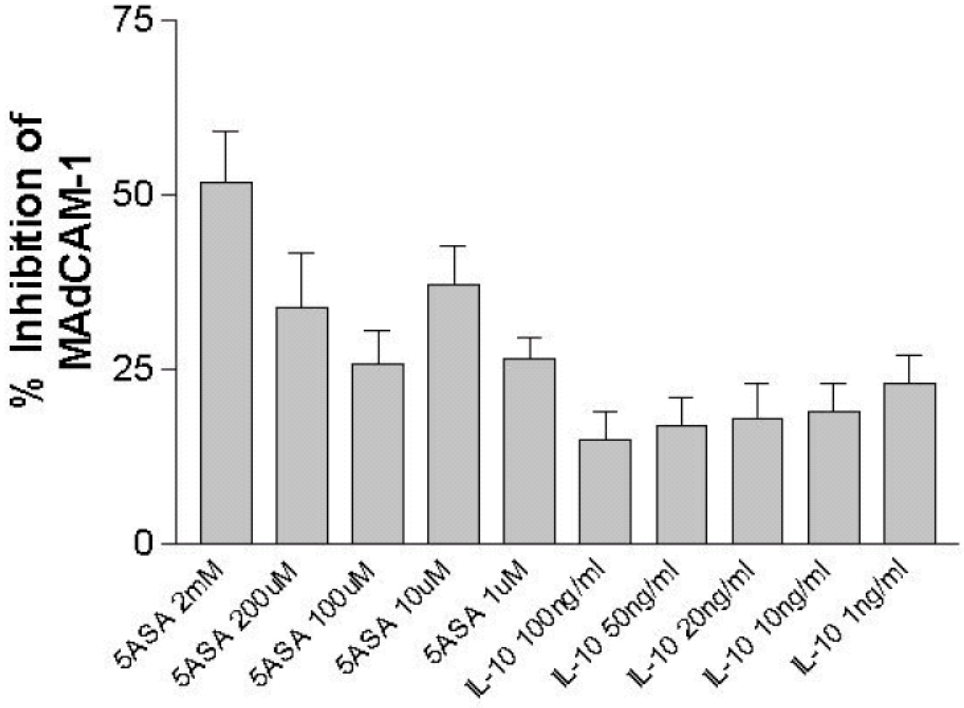

Figure 5.3 The effect of 5-ASA and IL-10 on SVEC4-10 endothelial cells stimulated with 20ng/ml TNFα in vitro(n=9). Pre-incubation of monolayers with 5-ASA and IL-10, prevented TNFα induced MAdCAM-1 expression to varying extents. Whilst there was no evidence of a significant effect of MAdCAM-1 with dose related IL-10, there was still a degree of inhibition using 5-ASA ($p<0.05$)

5.2.4 Discussion

We have shown that mouse endothelial cells express MAdCAM-1 upon stimulation with pro-inflammatory cytokines TNF-α, LPS and IL-1 to varying degrees. The expression can be consistently quantified. We have seen a consistent dose dependant increase in MAdCAM-1 with TNFα contrasting with greater variations in responses with co-culture IL-1 or LPS. It is for this reason that TNFα was used to stimulate the SVEC-40 cells for further study into modulating the expression of MAdCAM-1.This system has further been developed to show that modulation of MAdCAM-1 can be effectively achieved. In particular, we demonstrated that glucocorticoids e.g. hydrocortisone, and 5-ASA cause the most significant effect on MAdCAM-1 expression.

In our *in vitro* model, whilst MAdCAM-1 expression was certainly downregulated with IL-10 and dexamethasone, it was not so to a signifiant level (Ala *et al* 2003). There was a step wise dowregulation of IL-10 (100ng/ml to 10ng/ml). Curiously, the greatest percentage of MAdCAM-1 inhibition being achieved with the small doses of IL-10 (10ng/ml). It is therefore likely that the clinical efficacy of these agents can be related to the direct affects on MAdCAM-1, whilst IL-10 may promote MAdCAM-1 independent effects on IBD. These findings appear to be in contrast to the study by Oshima *et al* (2001a), showing that 1L-10 can exert significant therapeutic activity in IBD with reduced TNFα-induced MAdCAM-1 protein, mRNA and also a functional lymphocyte adhesion. However, in these experiments neither 5-ASA, sulphasalazine, nor 6-MP blocked MAdCAM-1 induction.

The biology of IL-10 is highly complex. It is a regularity cytokine which inhibits both antigen presentation and subsequent pro-inflammatory cytokine release e.g. 1L-1, 1L-6, 1L-12, IFN-α, TNFα and the chemokine IL-8. Finally, IL-10 induces the production of cytokine inhibitors, such as 1L-1 receptor antagonist and the release of soluble TNFα receptors. The pivotal role played by IL-10 within the mucosal immune system is demonstrated by the chronic ileitis that develops in gene-targeted interleukin-10 knock-out mice and by its therapeutic efficacy in animal models of colitis. However, the therapeutic efficacy of IL-10 in patients with Crohn's disease is less clear cut. *In vitro* studies have shown that exogenous 1L-10 will down-regulate the enhanced pro-

inflammatory cytokine release from lamina propria mononuclear cells isolated from patients with Crohn's disease (Schreiber *et al* 1995)

Direct immunoregulatory effects exerted by the 5-ASA include the delicate balance of pro-inflammatory mechanisms during active inflammation as seen in inflammatory bowel disease. Such effects are the inhibition of peripheral and intestinal B lymphocyte immunoglobulin secretion and inhibition of pro-inflammatory cytokine production and their binding to receptors. Some of these immunoregulatory effects appear to be mediated by an inhibition of the activation of the nuclear factor kappa B (NFκB) transcription factor family by steroids and5-ASA. Activation of NFκB appears to be pivotal for the sustained upregulation of inflammation molecule expression in many inflammatory diseases. It seems, therefore, most likely that the enormous therapeutic potency of steroids, as well as the anti-inflammatory properties of 5-ASA, are not achieved by a single action of the drug.

There have been other agents which have been shown to attenuate modulatory effects on MAdCAM-1 expression and therefore have a therapeutic use in IBD. Most notably here they include melatonin but which have have been pre-stimulated with lower doses of TNFα e.g. 1ng/ml, over 24 hours (Sasaki *et al* 2002) . This affect may have therapeutic activity thorough its ability to inhibit NFκB dependent induction of MAdCAM-1.

Nitric oxide is a key modulator of adhesion molecule expression in both acute and chronic inflammatory states. Specifically both reactive oxygen and nitrogen metabolites participate in regulating adhesion molecule expression in response to TNF-α with the ability to influencing the course of inflammatory bowel disease. Nitric oxide can function both as an oxidant or antioxidant depending on the availability of reactive oxygen species. It has been reported that inhibition of endothelial nitric oxide synthases (using the non-selective NOS inhibitor L-NAME), induces endothelial adhesion molecules (ICAM-1 and VCAM-1) in human umbilical vein cell culture. In a study by Oshima *et al* (2001b), the investigators show how MAdCAM-1 expression in cultured endothelial cells is altered by NO donors and by NO synthase inhibitors. The study explains the affect of cytokines and NO-modifying agents which control adhesion of α4β7-expressing mouse lymphocytes in response to TNFα stimulation. It was observed

that both a short and long-acting NO donor significantly reduce TNF-α-induced expression of MAdCAM-1 expression in lymphatic endothelial cells. The effects of NO donors appear to reflect their ability to prevent the nuclear translocation of NFkB and as we have discussed in Chapter 4, the MAdCAM-1 promoter is strategivcally positioned for this action by its inherent NFkB binding sites, which are necessary to induce MAdCAM-1 expression.

Despite the clinical problems associated with blocking antibodies, they have been used in clinical practise to varying extents. Future experiments using our invitro cell culture model to study the effect of using MAdCAM-1 antibodies and its α4β7 receptor woud be the next logical step in exploring this further.

5.3 Experiment 2: Modulating mouse MAdCAM-1 expression using speciifc antisense oligonucleotides

5.3.1 Introduction

I have described that the use of blocking antibodies, particularly on repeated occasions has potential disadvantages associated with sensitisation of foreign proteins (even with humanised antibodies) or the development of anti-idiotype responses. An alternative strategy is the prevention of the synthesis of endogenous proteins by the use of anti-sense oligonucleotides. Indeed, the potential application has already been explored in Crohn's disease, using antisense to the vascular adhesion molecule ICAM-1 (Schreiber *et al* 2001) (Yacyshyn *et al* 2007). Here the results were negative for therapeutic value, although the safety of the approach was demonstrated in patients with IBD. We have already commented that we believe ICAM-1 is a less appropriate target than MAdCAM-1. The *specific hypothesis* is that antisense oligonucleotides can be targeted to MAdCAM-1 to allow modulation of its expression.

Antisense oligonucleotides (Anti-S) are sequences of nucleotides targeted at the messenger RNA (mRNA) which then prevents the production of protein (Crooke *et al*

1999**).** They have the potential to specifically turn off the production of any protein in cells which may be used for therapeutic gain, in contrast to the majority of agents currently in use which modulate the activity of specific proteins involved in inflammation and immune regulation.

Several strategies are available to regulate gene expression using oligonucleotides. Antisense therapy is different to gene therapy, in that the target is mRNA rather than the specific gene of interest. Anti-S drugs exert their effect by two separate mechanisms:

5.3.1.1 Binding to complementary mRNA

Knowledge of the targeted sequence and steric interference with mRNA binding shows that inhibition of key steps in mRNA processing or function are important in anti-sense therapy e.g. 5'-capping, splicing, and initiation of translation **(**Walton *et al* 2002) (Mahara *et al* 2003**).**

5.3.1.2 Utilization of *Rnase H*

Rnase H is a family of ubiquitous enzymes that cleave the mRNA strand of the DNA-RNA heterodimer formed during normal DNA transcription, leaving the Anti-S intact and allowing released oligonucleotides free to bind to other target mRNA's (Galarneau *et al* 2005)

5.3.1.3 Intracellular Anti-S degradation

A number of nucleases exist naturally within cells to breakdown native DNA/RNA. Several strategies have been used to help prevent degradation of Anti-S. The first Anti-S to enter clinical trials were phosphorothioate oligodeoxynucleotides (Ghosh *et al* 1993) (Dagle 1991), which differ from normal oligonucleotides by the substitution of a sulphur atom for one of the non-bridging oxygen atoms at each of the phosphodiester linkages.

Chemical modifications to Anti-S have been shown to increase stability in biological systems, specificity to potential targets and reduced level of toxicity **(**De Mesmaeker *et al* 1995) (Sanghvi *et al* 1993**).** Such modifications are mostly to the backbone, sugar

moiety or base of the nucleotide. However, some modifications reduce the subsequent action of *Rnase H.* Perhaps the most promising modification involves the 2' position of the ribose ring to form the 2'-O-(2-methoxy) ethyl (2'- MOE) moiety **(**Prakash *et al* 2002) (Prakash *et al* 2004) (Vickers 2003) this modification has shown significantly improved pharmacological profiles *in vitro,* when compared to phosphorothioate oligonucleotides. Clinical experience with MOE oligonucleotides has so far revealed some dose limiting toxicities but also increased potency, prolonged duration of action and a lack of neutralising antibody production, which allows repeated administration (Geary *et al* 2001).

5.3.1.4 Non-antisense effects

The advantages conferred by chemical modifications are offset by important non-antisense activities e.g. immune stimulation such as B-cell proliferation and inhibition of viral entry into cells (Boggs *et al* 1997). Confirmation of the biological effects of Anti-S critically relies upon differentiating specific from non-specific antisense effects. This includes the use dose-response, time course experiments and evaluating effects on functionally related and structurally distinct proteins whilst employing housekeeping gene products. Furthermore, specific sequences associated with non-specific effects such as C-G pairs and G-quartets should be avoided in designing Anti-S. It is not known whether the response elicited by Anti-S is due to the interaction of Anti-S with its target RNA, or other nucleic acids/proteins.

5.4 Methods

5.4.1 Generation and design of antisense oligonucleotides

The following antisense oligonucleotides were generated and designed**:**

MAdCAM-1 ANTISENSE 1 5'AGGATGGATTCCATGCCTGC 3' (40-21)

MAdCAM-1 ANTISENSE 2 5'GTTCACCTGGAAGGACTGTCCT3' (107-86)

MAdCAM-1 ANTISENSE 3 5'TCTGTACACTGCCCAAGCTG3'(234-215)

MAdCAM-1 ANTISENSE 4 5'ATCCTGCAGCTGGTCACTCT3' (864-843)

SCRAMBLED OLIGO'S 5'GCCTGGTCGCACAGATGTAT3'

Phosphorothioate oligonucleotides were synthesized using phosphoramidite chemistry, purified by high-performance liquid chromatography, and lyophilised to dryness before use *(Oswel Research Products, Southampton, UK)*. The specificity of sequences of oligonucleotides used in this study were checked by using BLAST analysis.

We initially designed a 20 mer phosphorothioate oligonucleotide spanning the *translation initiation codon* of mouse MAdCAM-1, 5'AGGATGGATTCCATGCCTGC 3' (40-21), which would also target known alternative splicing variants of MAdCAM-1's mucin domain. 5'GTTCACCTGGAAGGACTGTCCT3'(107-86) to target the 3 -untranslated sequences immediately 3 to the *translation termination codon*, 5'TCTGTACACTGCCCAAGCTG3'(234-215) to the 3 *-untranslated region,* 5'ATCCTGCAGCTGGTCACTCT3'(864-843) to target the 3 *-untranslated sequences immediately 3 to the polyadenylation signal* and 5'GCCTGGTCGCACAGATGTAT3' as a scrambled oligonucleotide.

Initially a fully phosphorothioated oligonucleotide (molecular weight 6453.0518mono-isotropic and average 6455.88) *(Oswel)* was obtained. We used a concentration of 250nmol/l mixed with lipofectin, to pretreat near confluent SVEC4-10 cells prior to stimulation with TNF-alpha. A scrambled oligonucleotide was used as negative control. These initial experiments were carried out to confirm the effectiveness of this specific Anti-S; if down regualtion was not achieved then further experiemnts were to be performed including the use of fluorinated oligonucleotides to confirm cell pernetration. In all, a total of four different 20-mer oligonucleotides were synthesized as described.

To minimise the potential non-specific toxicity observed with phosphorothioate oligonucleotides we used oligonucleotides with a normal phosphodiester backbone and two terminal phosphorothioate linkages at the 3' and 5' terminal. The oligonucleotide was purified by high-performance liquid chromatography and analysed by mass spectrometry.

5.4.2 Oligonucleotide treatment

The SVEC4-10 cells were seeded on to the gelatin coated 8 chamber wells as described in chapter 4 and grown to near confluence. Cells were treated with oligonucleotides by first washing in a serum free medium. Opti-MEM containing 10ug/ml DOTAMA/DOPE solution was added to the cells followed by the indicated concentration of oligonucleotides. The cells were incubated for 4 hours at 37 degrees and the medium was replaced by normal growth medium. TNF-alpha was added 0-4 hours after removal of serum-free medium. To determine whether Anti-S could inhibit *MAdCAM-1* expression, SVEC4-10 cells were incubated with *MAdCAM-1* antisense oligonucleotides and then stimulated with TNFα.

5.4.3 Oligonucleotide Uptake in endothelial cells

The need to achieve adequate intracellular concentrations of Anti-S has led to the use of extremely large amounts of Anti-S (up to 100μmol/L) in some *in vitro* studies (Manoharan *et al* 1992). To target intracellular RNA sequences, Anti-S should ideally traverse cellular membranes easily but in fact they do this rather poorly due to their low lipid solubility, and inherent negative charge. They appear to enter cells via adsorptive and fluid phase endocytosis **(**Loke *et al* 1989**).** The identity of cell membrane proteins implicated in binding Anti-S is unclear, although a number of heparin binding proteins e.g. fibroblast growth factors, vascular endothelial growth factors have been implicated, suggesting that Anti-S may be preferentially taken up by activated leukocytes **(**Pirruccello *et al* 1994) (Hawley *et al.* 1996**).** Thus, following the stability in biological medium and their weak intracellular penetration, colloidal drug carriers e.g.nanoparticles have been useful in the delivery of Anti-S **(**Zhu 2004**).** It has been shown that oligonucleotides associated to nanoparticles appear to be protected against

degradation thus improving Anti-S stability **(**Arnedo 2002**)** Also, the use of cationic lipids to facilitate delivery of Anti-S in tissue culture have allowed experiments to be performed with concentrations of less than 1 micromol/L (Zhi 2004), allowing entry into different types of cells effectively and efficiently, thus avoiding aptameric effects.

The lack of effect of some Anti-S may be explained by poor distribution inside the cell. In order to be active, Anti-S should be delivered to the nuclei of cells. The oligonucleotides used in the experiments were labelled with fluorescein isothiocyanate (FITC) at the 5'end in order that the uptake of oligonucleotides could be confirmed by fluorescence microscopy. All of the oligonucleotides were phosphorothioated. I attempted to improve the intracellular distribution of the anti-S by transfection with lipofectin. I also used varying concentrations of antisense oligonucleotides to study its effect on MAdCAM-1 inhibition.

5.4.4 Quantifying the effect of different oligonucleotides and varying concentrations on MAdCAM-1 expression

The SVEC4-10 cells were seeded onto gelatin coated 96 well plates as described in chapter 4. To determine if varying the concentration of the different Anti-S compounds could effectively influence *MAdCAM-1* expression, SVEC4-10 cells were incubated with different *MAdCAM-1* antisense oligonucleotides, including scrambled negative control antisense oligonucleotides of the same length and then stimulated with TNFα and TNF peptide. Prior to analysis of results the background fluorescence was subtracted from all values. The experiments were performed on six occasions.

5.5 Results (figure 5.4 to 5.5)

Using the gelatin coated 8 chamber wells at 12 hours the Anti-S mostly exhibited a dot like appearance with most fluorescence detected in vesicles without significant cytoplasmic or nuclear diffusion of the ASO. There was clear uptake and intracellular localisation of antisense oligonucleotide (Antisense 1, 2, 3, 4). Figure 5.4 depicts the intracellular localisation of the these antisense oligonucleotides, proving that all cross the plasma membrane with the potential to exert their effects.

Fluorescence microscopy results from the cells transfected with lipofectin coupled FITC-Anti S indicated that the oligonucleotides internalisation with the ideal oligonucleotides /lipofectin ratio (0.5uM oligonucleotides and 15ug/L lipofectin) promoted a diffuse staining of the nucleus and cytoplasm. We found that when the oligonucleoitide/lipofectin ratio increased the oligonucleotides uptake assumed a vesicular pattern. The green staining is due to the strong fluorescence observed in the agglomeration of vesicles, which resemble the Golgi complex.

Using the 96 well plates, I studied the effect of varying concentration of MAdCAM-1 antisense oligonucleotides of the same length. The experiments were performed on 6 occasions. The only oligonucleotides to show significant inhibition of MAdCAM-1 expression were AS1 2ug ($p<0.05$) and AS4 2ug ($p<0.005$), with 2ug AS3 nearer the limit of significance at $p<0.06$ *(figure 5.5)*. The other concentrations of the same oligonucleotides, both concentrations of AS2 and the scrambled antisense oligonucleotides showed no major inhibitory activity. In most cases, higher doses of antisense oligonucleotides appeared to achieve lesser favourable MAdCAM-1 inhibition statistics (all numbers have blank subtracted).

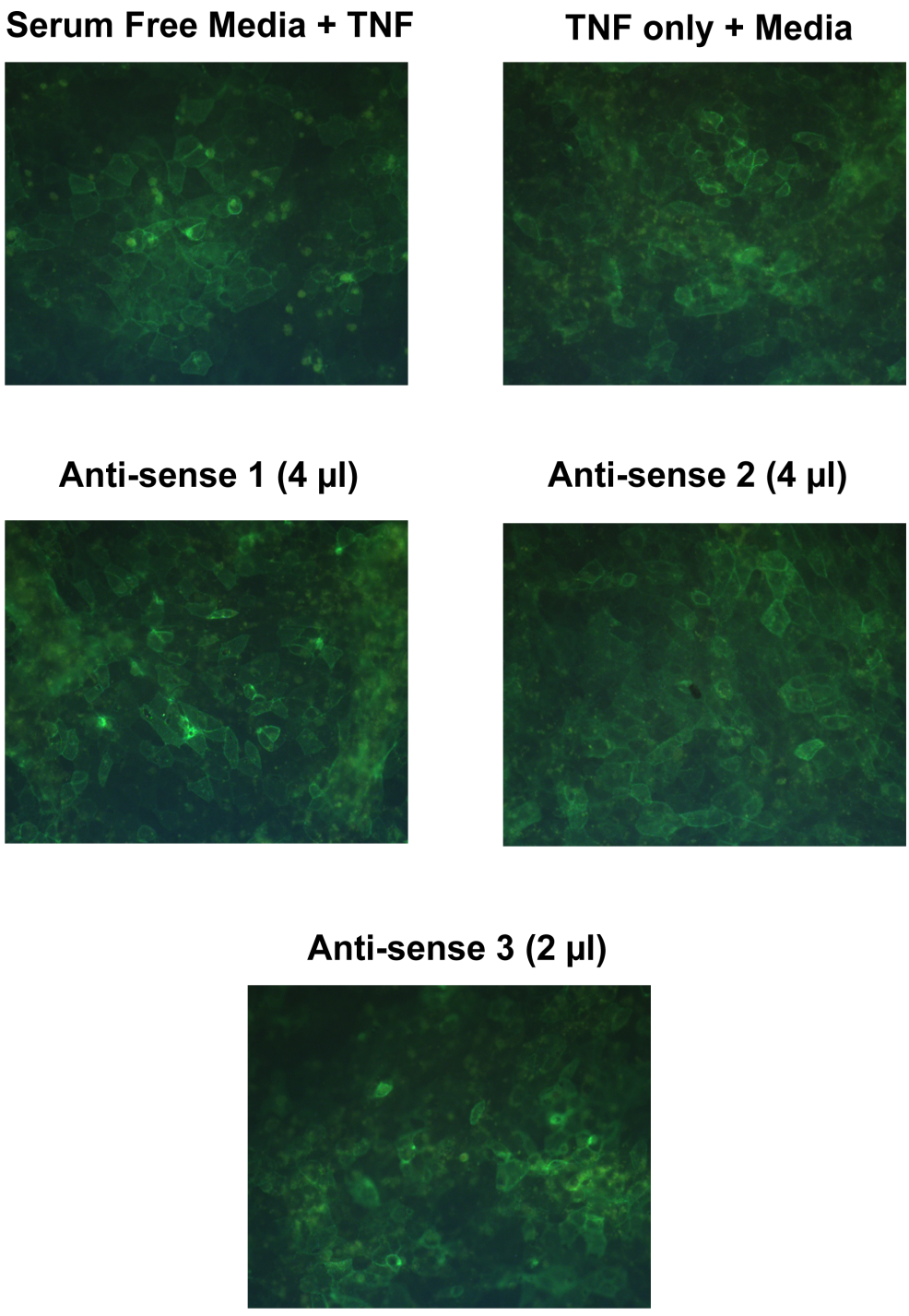

Figure 5.4: Uptake and intracellular localisation of antisense oligonucleotide (Antisense 1, 2, 3). The diagram depicts the intracellular localisation of the antisense oligonucleotides with the ability to cross the plasma membrane so as to exert their effects.

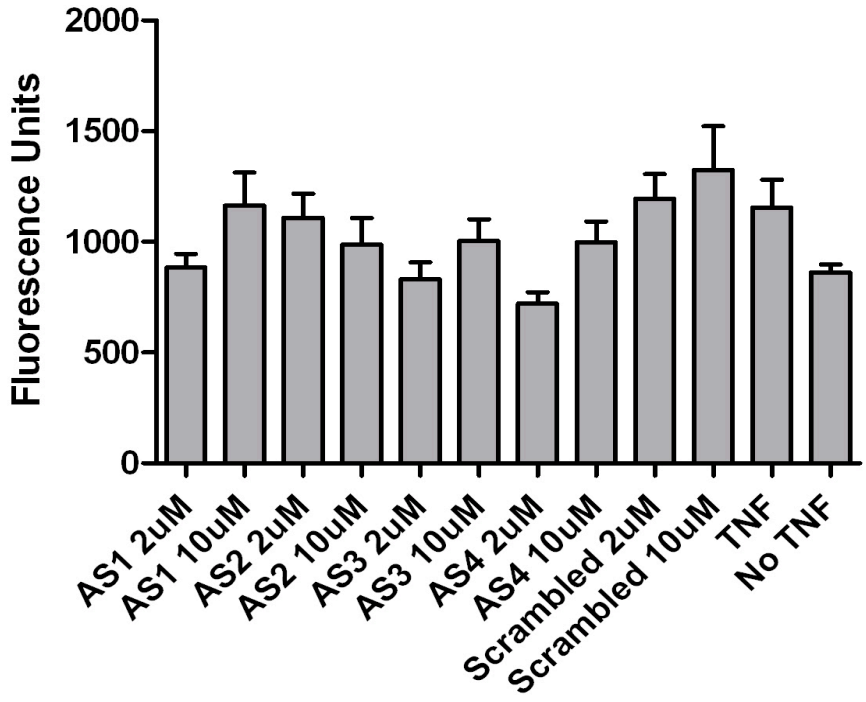

Figure 5.5 The effect of Antisense Oligonucleotides on MAdCAM-1 expression. This graph shows the inhibition of MAdCAM-1 expression by various antisense oligonucleotides with a scrambled antisense oligonucleotide included as a control. The experiments were performed on 6 occasions. The only oligonucleotides to show significant inhibition of MAdCAM-1 expression were AS1 2ug ($p<0.05$) and AS4 2ug ($p<0.005$), with 2ug AS3 nearer the limit of significance at $p<0.06$. The other concentrations of the same oligonucleotides, both concentrations of AS2 and the scrambled antisense oligonucleotides showed no major inhibitory activity.

5.6 Discussion

At the time of our initial observations this was the first study to report the effects of antisense on MAdCAM-1. We designed and tested antisense molecules in an *in vitro* setting, assessed effective penetration and efficacy at modulating the expression of MAdCAM-1.

We have seen that in order to maintain activity, antisense oligonucleotides should ideally be delivered to the nuclei of cells. The apparent lack of effect of some antisense oligonucleotides may be explained by poor distribution within cells. Specifically, we found the successful uptake and intracellular localisation of our antisense oligonucleotides targeted to MAdCAM-1 (Antisense 1, 2, 3, 4) within endothelial cells i.e. the ability of these antisense oligonucleotides to negotiate the plasma membrane of these appeared to be effective. It is widely accepted that most cell types efficiently exclude oligonucleotides *in vitro* and require specific delivery systems, such as cationic lipids, to enhance uptake and subsequent antisense effects. One of the fundamental problems associated with antisense technology is that of delivery of oligonucleotides into the intracellular compartments of intact cells *in vitro*. Uptake generally proceeds by incorporation of exogenously applied antisense effectors into endocytotic vesicles. The ideal Anti-S agent should therefore maintain stability and cellular penetration whilst retaining hybridizing capabilities. We hypothesised that observed biological effects in our antisense experiments had been as a result of antisense effects or non–sequence specific effects.

Phosphorothioated oligonucleotides were utilised due to their stability in cells and tissues. Specifically, this involves the substitution of sulphur for a non-bridging oxygen (at each phosphorus in the oligonucleotide chain), which retains the charge and solubility of the phosphodiester oligomer, as well as its crucial ability to hybridise with target mRNAs but is much more resistant to degradation by intracellular nucleases.

Very high concentrations (usually $\geq$ 20 μM) of naked oligonucleotides have been reported to be required for “antisense” efficacy i.e. without carrier. At such high concentrations, tremendous non–sequence specific activity will be seen at least in part because of the adsorption of the oligonucleotides to cell-surface heparin-binding

proteins. Therefore, the delivery of such naked oligonucleotides should be avoided and any putative evidence for antisense effects obtained in this manner is thought to be highly suspect. Oligonucleotides may be delivered instead using any one of a number of commercially available carriers, including the cationic lipids, Lipofectin, Lipofectamine 2000 (both, Life Technologies Inc., Grand Island, New York, USA), and Cytofectin (Glen Research, Herndon, Virginia, USA), as well as polyamines. Surprisingly, we found there was little effect of lipofectamine on the delivery of antisense oligonucleotides into our cells.

I explored the effect of appropriate controls using endothelial cell lines stimulated with TNFα peptides. These are capable of binding TNF-alpha under physiological conditions and can include but are not limited to portions of TNF-alpha receptor and/or portions or structural analogs of anti-TNF antibody antigen binding regions or variable regions. I found no significant effect on endothelial cell stimulation with TNF-alpha peptides.

I further explored the effect of antisense oligonucleotides on MAdCAM-1 expression. After performing the experiments on six occasions and using different antisense oligonucleotides (including scrambled controls) our study showed a reduction in fluorescence using AS1–AS4 *(figure 5.5)*. Specifically, there were significant differences on MAdCAM-1 expression between the various antisense oligonucleotides and their concentrations. In particular, the only oligonucleotides to show significant inhibition of MAdCAM-1 expression were AS1 2ug ($p<0.05$) and AS4 2ug ($p<0.005$) with 2ug AS3 nearer the limit of significance at $p<0.06$. The other concentrations of the same oligonucleotides, both concentrations of AS2 and the scrambled antisense oligonucleotides showed no major inhibitory activity. I found the greatest MAdCAM-1 inhibition was obtained with relatively low dose antisense concentrations. This intriguing observation is different to our expected outcome from higher concentrations leading to increased efficacy of antisense products.

Since my original novel observations (Ala *et al* 2003), Goto *et al* (2006) reported *in vivo* antisense therapy using mouse MAdCAM-1 targeting the translational initiation codon. Unlike my own experiments utilising the more representative endothelial cell line SVEC4-10 cells, these authors used b.End.3 cells stimulated with TNFα. Among the 5 oligonucleotides tested, including the control, MAd 19 reproducibly demonstrated

the strongest inhibitory effect on TNFα induced MACAM-1 expression, which reached an average of only 17.3% of MAdCAM-1 expression with MAdCAM-1 in 3 independent experiments, compared to our experiments showing relatively higher levels of TNFα inhibition with levels of MAdCAM-1 varying from 24% to 39%. These authors chose MAd 19 for further evaluation of its efficacy *in vivo* and went on to inject antisense MAdCAM-1 oligonucleotides into mice at 1.5 mg/kg/day for seven consecutive days from the first day of a trinitrobenzene sulfonate(TNBS) enema. MAdCAM-1 antisense oligonucleotides significantly suppressed the development of TNBS colitis clinically and histopathologically compared with controls. Immunohistochemistry and semi quantitative reverse-transcription polymerase chain reaction of the colon tissues revealed that MAdCAM-1 protein and mRNA expression were lower in antisense-treated mice than in controls. MAdCAM-1 antisense treatment reduced the number of $\alpha4\beta7^+$ lymphocytes in the inflamed colonic mucosa suggesting that antisense suppression of MAdCAM-1 can attenuate recruitment of lymphocytes bearing $\alpha4\beta7^+$ integrin to the inflamed colon. The accumulation level of FITC-labelled oligonucleotides found in the colon from TNBS-treated mice was higher than that from normal mice, indicating that inflammation appeared to promote the accumulation of oligonucleotides in the colon.

These results fit with the studies on ICAM-1 by Bennett *et al* (1997) and others, supporting the use antisense therapy for IBD (Rijcken *et al* 2002). Taken together, these results are compatible with those of previous studies using an anti-MAdCAM-1 (Kato *et al* 2000) or anti-α4-specific antibody in experimental colitis (Lee *et al* 2005). It is possible since our own set of antisense oligonucleotides achieved higher levels of antisense modulation than those used by Goto *et al* (2006).

I have demonstrated that administration of antisense oligonucleotides can inhibit MAdCAM-1 in SVEC4-10 cells, with the ability to significantly suppress its expression in the inflamed gut at both mRNA and protein levels, allowing simultaneous suppression in the development of wasting disease and histological inflammation in TNBS-induced colitis. There exists at least 2 levels of possible silencing effects of antisense oligonucleotides either at the transcriptional or posttranscriptional level; the former targets the AUG translation initiation codon, thereby interrupting ribosome

activity by masking the ribosome recognition site of MAdCAM-1; the latter is RNase H activation, which degrades the RNA strand of an RNA-DNA heteroduplex.

Chapter 6

General Discussion

6.1 Role and expression of MAdCAM-1 in tissues

Following the initial description of MAdCAM-1 by Briskin *et al* in 1993, there have been relatively few articles published related to the subject, compared with other adhesion molecules such as VCAM-1 and ICAM-1. This is probably due to the expression of MAdCAM-1 being apparently limited to relatively fewer tissues, paucity of *in vitro* systems in which to study MAdCAM-1 and the apparent lack of evidence implicating MAdCAM-1 with any disease process other than IBD.

The work in this thesis has characterised MAdCAM-1 expression in tissues and cell culture systems. The data presented here confirms the expression of MAdCAM-1 using a variety of techniques developed in our laboratory including immunohistochemical methods, cytofluorometry, RT-PCR and quantitative real-time RT-PCR technology. Using these techniques, I confirmed the presence of MAdCAM-1 and quantified its expression in mouse cell lines (SVEC4-10) and tissues from both murine and humans. I developed a reproducible *in vitro* model which was used to study factors governing MAdCAM-1 expression. In particular, using this system I explored the concept of modulating MAdCAM-1 expression by a variety of agents including anti-sense oligonucleotides targeted to mouse MAdCAM-1. I showed using immunohistochemistry that MAdCAM-1 is absent in the normal human liver and upregulated in end stage chronic liver disease, where it immuno-localises mainly to the peribiliary plexus and lymphoid aggregates. However, using Real Time PCR analysis I found evidence apparently contradicting these initial set of observations. Specifically, I found MAdCAM-1 to be present constitutively in normal human liver, albeit in relatively small quantities and upregulated in end stage liver disease. In the setting of IBD, I confirmed MAdCAM-1 expression and upregulation in active disease from paraffin fixed tissues and further extended this observation to show its localisation within the transmural wall in chronic Crohn's disease, an observation later validated by Arihiro *et al* 2002, using monoclonal antibodies.

The expression and upregulation of MAdCAM-1 on chronically inflamed endothelia especially high endothelial venules, is consistent with the hypothesis that MAdCAM-1 has a key role in recruitment of lymphocytes during inflammatory processes. In addition to the expression of MAdCAM-1 on vascular endothelium MAdCAM-1 was also

detected on immune cells with the morphology of dendritic cells. Having performed double staining techniques we found focal staining with S100, CD68 and CD21 but these did not correspond to the pattern seen for MAdCAM-1. Expression of MAdCAM-1 has been reported on the dendritic processes within human Payer's patches (Briskin *et al* 1997). Such hepatic expression could serve as a signal for retention α4β7 lymphocytes in the liver. It is interesting to note that isolated follicular dendritic cells have been reported to express VCAM-1 and could present an antigen clustering with α4β1 and LFA-1 expressing B cells, leading to maturation and differentiation of B cells into memory cells (Freedman 1990). Thus, if MAdCAM-1 is expressed on dendritic cells with in the liver then it might have the same function but ultimately may play a broader role than just acting as an addressin in chronic liver disease.

We found the distinct absence of MAdCAM-1 on the hepatocytes of all the liver tissues we examined. This contrasts with the findings of Grant *et al* (2001) where in some samples there was weak MAdCAM-1 immunoreactivity localised to the hepatocyte cytoplasm. However, MAdCAM-1 has been demonstrated to be integral in the progression of Type 1 diabetes mellitus in the NOD mouse, having also shown to be expressed not only on the endothelia but also epithelial cells of the choroid plexus in chronic relapsing experimental autoimmune encephalomyelitis (Faveeuw *et al* 1994) (Steffen *et al* 1996) which supports lymphocyte adhesion. We can postulate that in the observations by Grant *et al* that hepatocyte MAdCAM-1 may also have this role. There are no published studies reporting the expression of MAdCAM-1 on hepatocytes. It is also plausible that since hepatocytes take up molecules by pinocytosis and endocytosis and can engulf other cell types, so MAdCAM-1 within the hepatocyte might be a reflection of uptake and degradation of protein produced from other cells.

Our original hypothesis was that MAdCAM-1 acts as a local addressin at different sites using the vessel endothelium e.g. PBP, HEV crucial for lymphocyte egress and effective in re-circulatory pathways to areas of inflammation, such as those around bile ducts and lamina propria which I have described in Chapter 2. The possibility that this egress occurs in capillaries is interesting because this lymphocyte-endothelium interaction could occur in low velocity flow states. In agreement with previous studies Hillan *et al* (1999) using polyclonal antibodies and Grant *et al* (2001) using monoclonal antibodies we detected MAdCAM-1 in a variety of liver disease associated with IBD e.g. PSC, as

well as in non IBD associated liver disease (HCV, ALD, PBC), although in normal liver MAdCAM-1 was undetectable by immunostaining which contrasted with its significant RNA expression in end stage liver disease, not just limited to PSC. The real time PCR protocol with the appropriate samples allowed us to show for the first time a trend that MAdCAM-1 mRNA is upregulated in human cirrhotic livers. Sequence analysis of cDNA from a normal liver revealed complete alignment with the MAdCAM-1 gene sequence thus validating the presence of MAdCAM-1. Constitutive mouse MAdCAM-1 was present in normal liver although this was at a relatively lower level. Despite the strong data from increased mRNA in human and mouse tissue work and the immunohistochemical data from human MAdCAM-1 we were disappointingly unsuccessful in detecting MAdCAM-1 protein in Western blot studies of stimulated SVEC4-10 cells, even when reversing the monoclonal with polyclonal anti-MAdCAM-1 during the immunoprecipitation phase of the experiments or using alternative SVEC4-10 cells from The Alexander Group (Oshima *et al* 2001).

It is interesting to note from chapter 4 that the GCSF treated patient from paracetamol induced fulminant liver failure was associated with the highest recorded MAdCAM-1. The effect of MAdCAM-1 was unlikely to be secondary to acute liver failure shown by the absence of MAdCAM-1 in earlier stages and grades of liver diseases. Clearly more samples are required to make a satisfactory statistical conclusion. We can hypothesize that GCSF leads to TNFα which may induce expression of MAdCAM-1. Our established *in vitro* model in future studies is well placed to test this hypothesis

6.2 Other observations on MAdCAM-1

Since our earlier observations describing the expression of MAdCAM-1 on SVEC4-10 cells, there have been further reports confirming our findings and exploring other cell lines linked with MAdCAM-1 expression (Ando *et al* 2005). These groups have studied colon microvascular endothelium cell line MJC-1. This technique has involved cloning microvascular endothelial cells from primary colon cultures using ImmortoMice whose cells express a temperature-sensitive SV40 large T antigen, H-2Kb-tsA58 mice. They found that *in vitro* MAdCAM-1 can be induced on colon endothelial cells by TNFα

stimulation and may represent a useful model to study microvascular injury in the murine large intestine.

It is off interest to note that the MAdCAM-1 gene and its protein expression has also been shown to be expressed in primary cultures of human intestinal microvascular endothelial cells (HIMEC) which have not previously been demonstrated in human umbilical vein endothelial cells. Similar to ICAM-1 and E-selectin expression, MAdCAM-1 gene expression in HIMEC is upregulated by inflammatory cytokines e.g. TNF-α, IL-1, or LPS activation. However, in contrast to ICAM-1 or E-selectin expression, MAdCAM-1 mRNA and protein expression in HIMEC is dependent on culture duration and/or cellular density. This suggests a prominent role for cell-cell interaction among these endothelial cells on the surface expression of MAdCAM-1. In the studies by Ogawa *et al* (2005), MAdCAM-1 expression is dependent on NF-kappa B activation which is similar to the regulated expression of ICAM-1 and E-selectin. However, unlike the expression of these ubiquitous endothelial cell adhesion molecules, MAdCAM-1 expression is also dependant on PI3-K/Akt signaling and the degree of activation of this signaling pathway is directly linked to endothelial cell-cell contact. These data suggest that PI3-K/Akt is involved in the gut-specific differentiation of HIMEC, which contributes to the expression of MAdCAM-1. Thus, density-dependant activation appears to reflect a PI3-K mediated Akt activation, which is maximal at higher cell densities and therefore related to particular phases of inflammation, with relatively higher levels of MAdCAM-1 in the chronic inflammatory state which is typical of IBD.

Therefore, the ability of MAdCAM-1 to be induced by inflammatory stimuli is increased by cell-cell contact and may be reciprocally regulated compared to other endothelial adhesion molecules. There are several possible implications of such regulation suggesting that the differentiation of gut specific endothelial cells is governed by different factors. Firstly, there may be repeated cycles of angiogenesis accompanying the extensive intestinal tissue remodeling during inflammation. Secondly, adhesion molecule expression as a characteristic of culture differentiation is controlled not only by the number, but also the type of cell-cell junctional contacts which are proportional to cell densities. These factors control cytoplasmic second messages and affect cell responses to cellular signaling. The demonstration of MAdCAM-1 in isolated human

microvascular endothelial cells has previously been limited. It is possible that the factors responsible for prolonged culture duration and increased cell densities in HIMEC monolayers necessary for the demonstration of MAdCAM-1 gene and protein expression may be have been partly responsible for the previous challenges in its detection.

Particular variants of MAdCAM-1 gene transcription may affect structure and expression of the MAdCAM-1 protein. A number of single nucleotide polymorphisms (SNP's) have recently been described in the human MAdCAM-1 gene (Bowlus *et al* 2006). Reports on the analysis of SNP's in PSC patients compared to ulcerative colitis with healthy controls were published exploring the frequency of polymorphisms in MAdCAM-1 and ICAM-1 variants. There was no difference found in the frequency of seven alleles between any of these groups, concluding that neither the specific variants of ICAM-1 e.g. G241R nor the K469E, play a role in PSC development suggesting that the lack of polymorphism within this gene is associated with these two diseases.

It has been hypothesised that MAdCAM-1 contributes to the recruitment of donor T cells into the mucosal tissues of recipients after allogeneic hematopoietic stem cell transplantation (aHSCT). Supporting this hypothesis was an important study demonstrating the relationship between selected SNPs of the MAdCAM-1 gene and the development of serious complications following aHSCT (Ambruzova Z *et al* 2009). Specifically, three MAdCAM1 gene single nucleotide polymorphisms (rs758502 C/T, rs2302217 A/G, rs3745925 G/T) were genotyped by polymerase chain reaction in Czech HLA-identical donor-recipient aHSCT pairs. Specifically, MAdCAM-1 rs2302217 AA homozygous recipients developed chronic GVHD more frequently than patients with other genotypes These workers went onto demonstrate that MAdCAM-1 rs2302217 AA genotype in recipients was not only an independent factor associated with the development of acute Graft Versus Host Disease (GVHD) but also decreased overall survival, suggesting that MAdCAM-1 gene polymorphisms may be associated with the risk of developing chronic GVHD and thereby affecting mortality related to aHSCT.

6.3 Detection of MAdCAM-1 expression in fluids

Circulating soluble forms of cell adhesion molecules including ICAM-1 and VCAM-1 have been shown to be elevated in inflammatory, infectious and malignant diseases. Levels of these soluble cellular adhesion molecules reflect cellular expression and have been shown to correlate with disease activity and may provide useful markers to monitor and confirm the results of therapy.

Leung *et al* (2004) developed the first ELISA model for soluble MAdCAM-1 in body fluids. The group demonstrated the presence of MAdCAM-1 in the serum and urine of healthy individuals, at similar levels to ICAM-1 and VCAM-1. As we have discussed in chapter 1 some soluble cellular adhesion molecules are thought to be released from the cell-surface by proteolytic cleavage, whilst others are secreted as alternatively spliced forms lacking a transmembrane domain, or even anchored to the cell surface by a glycosyl-phosphatidyl-inositol protein and which could be released by phosphatidyl-inositol-specific phospholipase C.

6.4 Potential of imaging MAdCAM-1 expression in inflammation

Targeting MAdCAM-1 so as to non-invasively image Crohn's ileitis underlies its importance in diagnosing and monitoring disease activity. Using a novel intravascular ultrasound contrast agent targeting MAdCAM-1 in experimental small bowel inflammation, there is potential not only for the detection but quantification of intestinal inflammation. An image-enhancing ultrasound (US) contrast agent, consisting of encapsulated gaseous microbubbles (MB) was developed specifically to bind mucosal MAdCAM-1 (Bachmann *et al* 2006). MAdCAM-1-targeted MB were tested for binding specificity on MAdCAM-1 protein and TNFα stimulated SVEC4-10 endothelial cells using a combination of (i) *in vitro* flow chamber assay, for their ability to detect and quantify ileitis by intravital microscopy and (ii) trans-abdominal ultrasound. Specifically, the authors used conjugated rat anti-mouse antibodies detecting MAdCAM-1 to the external surface of lipid-shelled MB to produce a targeted contrast agent for use with ultrasound to detect experimental ileitis. Therefore, the targeted

imaging strategy presented here forms the basis of pursuing similar technologies that have the potential to provide a cost-effective, non-invasive means to improve the diagnosis, clinical care, and management of patients with IBD.

6.5 MAdCAM-1 as a therapeutic target

MAdCAM-1 remains an important target to modulate and different strategies have been described which are capable of modulating its expression. It still remains to be shown whether the effect of modulation can be translated effectively and efficiently for clear therapeutic benefit. As the pathways in controlling the expression of MAdCAM-1 become better characterised future strategies will clearly need to be developed to focus on new therapeutic targets.

6.5.1 Modulating MAdCAM-1 and α4β7 axis.

The ability to modulate adhesion molecule expression by means of monoclonal antibodies may have potential for therapeutic benefit. The results of a placebo-controlled study assessing the effects of monoclonal antibodies against α4 integrin e.g. Natalizumab *(Biogen Idec),* in patients with mild to moderately active Crohn's disease demonstrated that the reduction in Crohn's disease activity index, and the proportion of patients achieving remission at week two, was significantly higher in patients receiving Natalizumab than in those treated with placebo (Ghosh S *et al* 2003). In a pilot study, administration of Natalizumab resulted in clinical improvement in 6 out of 10 treated patients with active ulcerative colitis (Gordon F *et al* 2002). Since Natalizumab is an anti-α4 (95% human–derived) monoclonal antibody, it blocks both α4β7 and α4β1 integrins and in the process, therefore all VCAM-1 and MAdCAM-1 mediated leukocyte-endothelial cell interactions.

Natalizumab was initially approved in 2004, for induction and maintenance of moderate to severe Crohn's disease, but later on it was withdrawn from the market after three patients developed progressive multifocal leukoencephalopathy (Targan *et al* 2007, Van Assche *et al* 2005). This is a consequence of defective immune surveillance of the central nervous system (CNS) because α4β1 is required for T cell trafficking to the

CNS. Natalizumab has returned to the market in the United States, where it is used for the treatment of patients with Crohn's disease.

A limitation in interpreting negative findings with monoclonal antibodies is the uncertainty regarding whether blocking doses are actually achieved *in vivo*. Target levels are generally based on the minimum concentration required to achieve maximal inhibition of leukocyte adhesion *in vitro*. Experience gained from open-labelled clinical trials indicates that blocking doses are more difficult to achieve *in vivo* than those predicted from *in vitro* leukocyte binding assays. Another potential limitation of prolonged monoclonal antibodies usage, at least in chronic models of inflammation, is immunogenicity. This limitation has fostered the search for alternative approaches to block adhesion molecule function.

MLN-02 is a humanised immunoglobulin G1 (IgG1) monoclonal antibody which blocks $\alpha_4\beta_7$-integrin/MAdCAM-1 interaction and selectively inhibits leukocyte adhesion in the gastrointestinal mucosa. Fc receptor recognition and binding has been detected, thus eliminating complement fixation and cytokine release. In a randomised placebo controlled trial in 185 patients with mild to moderately active Crohn's disease treated with placebo, MLN-02 led to remission significantly more than placebo (Fegan *et al* 2008) as was the case in patients with ulcerative colitis. In both studies, apart from one patient with infusion reaction and angioedema, no significant adverse events were noted. MLN-02 appears to be an effective therapy especially for active ulcerative colitis, but further trials are warranted to confirm the efficacy of MLN-02 therapy for IBD.

It would be interesting to study the effect of antibodies affecting the MAdCAM-1/$\alpha 4\beta$ described in the clinical studies e.g. Natalizumab, first generation anti-MAdCAM-1 antibodies (MECA-367), PF-00547659 in our own *in vitro* model. Specifically, we will study if the effects of modulation are functionally active.

Using adhesion assays, the Adams laboraratory (Miles *et al* 2007) have studied effects of blocking antibodies against the α_4-, β_7-, and β_1-integrin subunits and L-selectin (for adhesion to MAdCAM-1 only), or an isotype-matched control antibody. In a series of antibody experiments targeted against the MAdCAM-1/$\alpha_4\beta_7$, they found blockade of lymphocyte L-selectin had no significant effect on rolling or static adhesion on

MAdCAM-1 because the recombinant MAdCAM-1 was not glycosylated and therefore lacked L-selectin ligands. This allowed further study of integrin-mediated adhesion without any specific interference from L-selectin. Blockade of α_4-integrin completely abolished rolling and reduced static adhesion on MAdCAM-1. On the other hand, treatment with β_7 antibodies reduced rolling and static adhesion to minimal levels, whereas antibody blockade of β_1-integrin had no effect on either rolling or static adhesion. In contrast, antibody blockade of lymphocyte α_4-integrin abolished rolling on VCAM-1 and reduced static adhesion, whereas anti-β_7-integrin had no significant effect on rolling or static adhesion. Blockade of the β_1-integrin subunit significantly reduced both rolling and static adhesion on VCAM-1. Adhesion to immobilized MAdCAM-1 was therefore $\alpha_4\beta_7$ dependent, without contribution from $\alpha_4\beta_1$, whereas $\alpha_4\beta_1$ mediated rolling and static adhesion on VCAM-1.

6.5.2 Modulating MAdCAM-1 using Anti-MAdCAM-1 antibodies

First generation rat anti-mouse MAdCAM-1 monoclonal antibodies e.g. MECA-367 have unfortunately not been found to be therapeutically beneficial in human patients. MECA-367 binds mouse MAdCAM-1 but does not show significant affinity for the human MAdCAM-1 molecule. In addition to being a rat antibody it leads to an immune response in human patients and therefore may not be suitable for therapeutic intervention. Mouse monoclonal antibodies, directed against human MAdCAM-1 have been described (WO 96/24673) but these are also likely to be immunogenic in humans.

Recently, therapeutically useful fully human anti-human MAdCAM-1 antibodies with specificity and affinity to human and primate MAdCAM-1 have been developed e.g. WO2005/067620. An inhibitor of the interaction between MAdCAM-1 and $\alpha_4\beta_7$ integrin such as a blocking anti-MAdCAM-1 antibody, or an antibody to $\alpha_4\beta_7$ integrin (MLN02, which is humanised Act-1, described in WO 01/078779) has been postulated to be useful in the treatment of IBD. However, it has now been found that inhibitors of this interaction including blocking antibodies to MAdCAM-1 are also useful in the treatment of coeliac disease and tropical sprue. Currently the use of anti-MAdCAM-1 antibodies for the treatment of coeliac disease and tropical sprue are currently being explored.

PF-00547,659 is the first highly specific, fully human blocking anti-MAdCAM-1 IgG_2 monoclonal antibody from Pfizer which has recently been described, identified and fully characterised in Phase 1 multicentre trials to study the induction and maintenance of remission of ulcerative colitis and Crohn's disease (Pullen *et al* 2009) (Vermeire *et al* 2009). It selectively binds to MAdCAM-1 and reduces homing of specific lineages of leukocytes to the gastrointestinal tract without impairing normal CNS immune surveillance. The study results show that single and multiple doses of PF-00547659 were safe and well tolerated with no evidence of immunogenicity. Thus, this reagent it has been suggested represents a better therapeutic approach for treatment of IBD than other available antibodies. Specifically, *in vitro* studies using functional assays by Pullen *et al* (2009) demonstrate PF-00547659 blocks the binding of MAdCAM-1 expressing cells to lymphocyte Peyer's patch adhesion molecule integrin $\alpha_4\beta_7$ (LPAM) and is highly specific for cynomolgus and human MAdCAM-1 over other homologous cell adhesion molecules. A blocking rat anti-mouse MAdCAM mAb MECA-367 was also used in these *in vitro* experiments the role of MAdCAM in inflammatory processes. While there are currently no defined criteria to approve surrogate antibodies for use in safety testing, *in vitro* and *in vivo* pharmacological evaluation of MECA-367 to determine its suitability as a surrogate antibody to support the clinical development of PF-00547659.

6.5.3 Modulating MAdCAM-1 protein synthesis: applications of oligonucleotides-silencing MAdCAM-1 RNA

The modulation of the MAdCAM-1/α4β7 axis has received an enormous degree of interest due to its possible beneficial effects on gut and liver tissue inflammation. I have shown that the expression of MAdCAM-1 *in vitro* can be subject to modulation by different agents including for the first time antisense oligonucleotides. Unfortunately, unpredictable interactions, toxicity and variability in silencing different target genes coupled with poor *in vivo* stability have been major drawbacks in their use as therapeutic agents thus far. Considerable progress however has been achieved in the clinical application of antisense technology. First generation Anti-S has advanced logically to Phase III trials in the treatment of gastrointestinal disease such as colorectal malignancy and IBD (van Deventer *et al* 2004). Whilst the above examples concern the use of blocking antibodies, the use of such agents, particularly on repeated occasions, as

we have seen has potential disadvantages associated with sensitisation to foreign proteins (even with extensively humanised antibodies) or the development of anti-idiotype responses. An alternative strategy is the prevention of the synthesis of endogenous proteins, which can be specifically achieved by the use of antisense RNA oligonucleotides. Certainly, the use of antisense oligonucleotides over in mild to moderately active distal ulcerative colitis, antisense inhibitor of ICAM-1 in enema formulation has been found to be safe and efficacious at 1,3 and 6 months following administration (van Deventer *et al* 2004). Improved antisense chemistry with second generation Anti-S will enhance the utilisation of antisense drugs offering the potential of less frequent dosing although still at the detriment of the expense of Anti-S. Careful assessment of future controlled studies is needed to confirm antisense mediated down regulation of the target proteins in a larger number of patients. A sound proof of principle is virtually impossible in a clinical trial because of the limitations posed by the lack of future controls. The potential of antisense technology depends on the design of multiple drugs based on our increasing knowledge of genes implicated in disease pathogenesis.

There are other alternatives to oligonucleotides as therapy. They include silencing RNA (siRNA), immune modulators, and triple helix oligonucleotides. It is possible that the relatively new area of RNA interference may offer better ways of silencing genes involved in pathogenic processes. It appears to be a more promising system than knockout mice because groups of genes can be simultaneously rendered ineffective.

Although RNAi strategies are reliant on a high degree of specificity there are some, potential non-specific effects as siRNA's may have broad and complicated effects beyond the selective silencing of target genes when transfected into cells.

Transfection of 21-bp double stranded siRNA regularly used to induce specific gene silencing also result in interferon mediated activation of the Jak-STAT signalling pathway and up-regulation of IFN-stimulated genes. This effect is mediated by the dsRNA-dependant protein kinase.

The transition from an *in vitro* setting into an appropriate animal based model has remained an enormous challenge, to many workers in the field of RNAi technology. Xia

et al (2004) appeared to have overcome this problem by using short hairpin RNA's (shRNAs). These sequences are themselves processed intracellular into siRNA's of approximately 21 nucleotides. An initial assessment of the potential use of shRNAs may be studied using appropriate cell culture techniques. This highlights the need to test many RNAi-mediating molecules in vitro so as to assess efficacy and specificity of RNAi. These workers studied RNA interference in the fatal brain related neurodegenerative condition spinocerebellar ataxia type 1 (SCA1). In this model mice express a mutant SCA1 transcript in the Purkinje cells of the cerebellum and which may be the target of choice by RNAi. The SCA1 gene encodes a mutant ataxin-1 protein containing an expanded poly-glutamine repeats. An RNAi approach may offer an advantage by reducing gene expression. Thus, the neurotoxic effect of the mutant protein may therefore be restricted whilst allowing sufficient wild-type protein to remain for normal functioning. In this study the authors chose an AAV (adeno-associated virus) vector because of its ability to efficiently transfect a broad range of cell types (particularly neurons) and express transgenes over a sustained period.

Modifications to siRNA may be introduced to prolong stability *in vivo* as has been shown from observations where siRNA may be targeted to conserved sites in the hepatitis B virus (HBV).

The transformation of siRNAs from a functional genomic tool into a new therapeutic modality could be assisted by effective systems for systemic administration. I postulate that further work on siRNA directed against MAdCAM-1 could be used to explore the modulation of MAdCAM-1 in this respect. Overall, a total of 14 RNAi therapeutic programs have entered clinical trials in the last decade involving local/topical delivery to the eye, respiratory tract and skin. No data have emerged to suggest serious adverse events linked to siRNA. The conduct of large phase 3 studies using siRNA is awaited.

6.5.4 Chemokines and emerging relationships with MAdCAM-1 and its modulation

Chemokines trigger $\alpha4\beta7$and $\alpha4\beta1$ integrin mediated adhesion to VCAM-1 and MAdCAM-1 through emerging pathways, a number of such critical pathways which have been recently identified. Specifically, the immobilised CC-chemokine ligand CCL25 and CCL28 are both been found to trigger $\alpha4\beta7$ dependent lymphocyte arrest

on MAdCAM-1 under shear, highlighting a potential role for these chemokines in the arrest of lymphocytes on gut postcapillary venules. Furthermore, immobilised CCL21 and CXC-chemokine ligand (CXCL) 12 convert rolling cell adhesion to static arrest on MAdCAM-1 by activating lymphocyte integrins. Thus, the α4β1/VCAM-1 and α4β7/MAdCAM-1 operate independently to support lymphocyte adhesion and flow. Chemokines which may act in concert with one set of chemokines triggering integrin-mediated arrest and a second set of chemokine promoting motility and transendothelial migration. The receptor for CCL28 is CCR10; its presence on IgA secreting B cells in the small and large intestine is crucial and underlies the importance of CCL28 in B cell localisation to these sites.

Another important related chemokine CXCL13 is expressed on a substantial proportion of HEV's in lymph nodes and Peyer's patches (Kanemitsu *et al* 2005). CXCL13 induces B-cell adhesion to MAdCAM-1 by activating GTPase critically involved in α4β7 so supporting its role as an arrest chemokine for B cells in HEV's and confirms its important role in B-cell entry into Peyer's Patches as well as MLN's.

I have described earlier the effective role of chemokines CCL21 (lymph node associated) and CCL25 (gut-associated) as important factors responsible for activation of lymphocyte adhesion to MAdCAM-1 and recruiting lymphocytes. Studies by Grant et al (2002) show the expression of chemokine CCL25 (thymus-expressed chemokine - TECK) to be also localised in PSC liver sinusoidal endothelium but absent in the liver in autoimmune hepatitis and primary biliary cirrhosis. A significant population of CCR9+ mucosal lymphocytes (i.e. the ligand for CCL25) has been detected infiltrating PSC liver tissue compared with controls and matched peripheral blood supporting the hypothesis of a T cell enterohepatic recirculation. The CCR9 lymphocytes also co-express the gut homing integrin α4β7. Therefore, CCL25 recruits CCR9+ lymphocytes to the liver in PSC by triggering adhesion to MAdCAM-1 and CCL25 which are upregulated in the liver in inflammatory liver diseases whereas previously they were thought to be restricted to the gut.

Emerging data from the Adams laboratory suggests that in addition to its specific role for CCL25 in PSC, CCL21 is also involved in the critical recruitment of T lymphocytes

into the portal tract. Specifically CCL21 or secondary lymphoid chemokine is noted for its strong up regulation on CD34(+) vascular endothelium in PSC portal associated lymphoid tissue. In contrast CCL21 is absent from LYVE-1(+) lymphatic vessel endothelium. The expression of CCL21 in association with MAdCAM-1 portal tracts in PSC may promote the recruitment and retention of CCR7(+) mucosal lymphocytes, leading to the establishment of chronic portal inflammation and the expanded portal-associated lymphoid tissue. This study provides further evidence for the existence of portal-associated lymphoid tissue and provides novel findings demonstrating ectopic CCL21 is associated with lymphoid neogenesis in human inflammatory disease.

Interesting therapeutic studies in the SAMp/Yit mice where targeting CCL25 or CCR9 have shown that this receptor/ligand is important during the early stages of induction of spontaneous chronic murine ileitis but not in late disease suggesting that in the late stage the recruitment process is less dependent on this chemokine/receptor pair (Rivera-Nieves *et al* 2006). To this effect TRAFICET-EN, an orally active pharmaceutical CCR9 inhibitor is currently being assessed for the treatment of Crohns disease (Eksteen *et al* 2010).

6.5.5 VAP and its emerging relationship in the expression MAdCAM-1

It is clear from our *in vitro* experiments that TNFα is pivotal in the initiation of MAdCAM-1. This has of course been effectively translated by the commercial use of anti-TNFα antibody which successfully reduces colonic injury and expression of adhesion molecules in IBD. Although VAP-1 is only expressed at low concentrations within vessels in the non-inflamed gut, it like MAdCAM-1 is upregulated in active IBD (Kurkiijarvi *et al* 1998) (Salmi *et al* 1993). Unlike MAdCAM-1 the factors that regulate the induction of VAP-1 in gut mucosa have not been well characterised. It has however been reported that VAP-1 dependant signaling induces production of soluble E-selectin which activates neutrophil β2 integrin and induction of ICAM-1 and VCAM-1 (Lalor *et al* 2007) (Jalkanen *et al* 2007). Increased levels of metabolic products released by catabolic activity of VAP-1/SSAO could curiously upregulate and induce functional expression of adhesion molecules such as MAdCAM-1, P-selectin and together with the

other adhesion molecules like properties of VAP-1 promote uncontrolled leukocyte recruitment in the gut mucosa in IBD.

6.5.6 Other MAdCAM-1 related targets

The importance of immunoglobulin A's secretory role in the intestinal lumen has been described in Chapter 1. Pivotal to this function is the role of B-lymphocytes which proliferate and differentiate into IgA-secreting plasma cells within lymphoid organs and migrate directly into the intestinal lamina propria. Studies on MAdCAM-1-deficient mice have specifically explored the B-cell compartment of the GI-associated lymphoid tissue. These studies provide *in vivo* evidence of MAdCAM-1's critical role in the localisation and function of IgA-secreting plasma cells in the intestine (Schippers *et al* 2009). The authors found that in MAdCAM-1 deficient mice the size of Peyer's patches is significantly reduced when compared with that of wild-type mice. This significant finding is detectable as early as three days post partum, indicating that MAdCAM-1 is not only critical for embryonic Peyer's patch development but also strategically positioned to facilitate recruitment of lymphocytes into these lymphoid organs at later stages (Salmi *et al* 2001a).

It is intriguing to note that enteral feeding has also been found to affect MAdCAM-1 expression. Complete MAdCAM-1 blockade reduces GALT lymphocytes to PN levels but the effect of chow feeding stimulus preserves IgA and early antibacterial resistance implying the existence of non-MAdCAM-1 mechanisms to preserve mucosal immunity. That is, chow does not eliminate mucosal immunity. Protection against an infectious challenge is preserved in spite of that blockade. Experimentally lack of enteral stimulation decreases GALT cell mass, reduces intestinal and respiratory tract IgA levels, and impairs established mucosal immunity to specific pathogens.

These experiments quantify the effects of the route and type of nutrition on the magnitude and/or kinetics of MAdCAM-1 expression and the response of GALT cell populations to MAdCAM-1 blockade. Current work demonstrates that lack of enteral feeding rapidly reduces expression of MAdCAM-1 responsible for directing cells into the PP, thereby resulting in lymphocyte depletion, which rapidly recovers with enteral

feeding. The cause and effect is confirmed by reducing GALT cell populations to the level of PN-fed mice by administering MECA-367 which blocks all MAdCAM-1. This blockade reduces GALT cell populations but IgA levels in the respiratory and GI tract are preserved with chow feeding.

One recent study explored the interesting hypothesis that MAdCAM-1 is regulated via angiotensin II type 1 receptor (AT1R) (Mizushima *et al* 2010). The role of AT1R in the expression of MAdCAM-1 in SVEC and MJC-1 (a mouse colonic endothelial cell) was examined following cytokine stimulation. Whilst NF-κB translocation was inhibited into the nucleus by these treatments, angiotensin receptor blockade significantly suppressed MAdCAM-1 expression induced by TNFα but did not inhibit phosphorylation of p38 MAPK or of IκB, which has already been been shown to modulate MAdCAM-1 expression. These investigators went on to investigate in a murine colitis model induced by DSS. They found that the degree of colitis as judged by weight loss, histological damage and the disease activity index, was much milder in AT1R-/- than in wild-type mice and that the expression of MAdCAM-1 was also significantly lower in AT1R-/- than in wild type mice. These results suggest that AT1R regulates the expression of MAdCAM-1 under colonic inflammatory conditions through the regulation of the translocation of NF-κB into the nucleus and inhibition of AT1R ameliorates colitis in a mouse colitis model. Therefore, AT1R might be one of the new future therapeutic targets of inhibition e.g. IBD, end stage liver disease via the regulation of MAdCAM-1.

Mucosal vaccination has been shown to upregulate MAdCAM-1 expression. Using oral cholera vaccine, the endothelial expression of MAdCAM-1 is increased in the gastric and upper small intestinal mucosa after immunisation through the different local routes of administration compared to rectal immunisation (Lindholm *et al* 2004). Specifically the vaccine component cholera toxin B subunit (CTB) increased MAdCAM-1 expression on endothelial cells in cultured human gastric explants, an effect which is mediated by TNFα. This strongly supports the involvement of MAdCAM-1 in the preferential homing of mucosal lymphocytes to their original site of activation. That is, the mucosal homing of antigen-specific lymphocytes after vaccination, which is dependent on a regionally increased expression of the addressin and TNFα mediates vaccine-induced MAdCAM-1 expression in the human gastrointestinal mucosa.

6.6 Future work

1. Functionality and further MAdCAM-1 modulation

We will determine functionality by using adhesion assays to observe the ability of gut and liver derived lymphocytes to bind to MAdCAM-1 under normal or inflammatory conditions. We will study the effect of GCSF and antibodies affecting the MAdCAM-1/α4β7 system described in the clinical studies e.g. Natalizumab, first generation anti-MAdCAM-1 antibodies(MECA-367), PF-00547659 in our *in vitro* model. Specifically, we will study if the effects of modulation are functionally active.

2. Quantitation of MAdCAM-1

The assay developed to measure MAdCAM-1 could be used to quantitiate expression in a variety of mouse and human tissues e.g. precirrhotic liver samples at different stage and grade of disease. The development of an ELISA would be useful for the measurement of secreted MAdCAM-1 in tissue lysate.

3. Identifying the natural cleavage of MAdCAM-1

By using single amino acid mutagenesis we can elucidate the 'hot spot' for MAdCAM-1 and α4β7 interaction, which is critical in drug design. The options are small sequence specific molecule inhibitors, peptide inhibitors, molecular modelling e.g. docking studies, to determine the biological sequele of modulation. Further studies investigating the structural conformation of MAdCAM-1 in normal and diseased livers using site directed mutagenesis of the residues responsible for integrin recognition and binding might help to develop therapies targeting functionally active MAdCAM-1 thus diminuting the side effects when widely used pathways are blocked.

4. Small interfering RNA

We would like to design sequence specific siRNA targeted to mouse MAdCAM-1 and use our established *in vitro* model to assess penetration and effect of modulation. We will choose an adenovirus-associated virus vector to deliver siRNA into a colitis mouse model and study the affect of MAdCAM-1 inhibition within this system.

References

Adams DH, Hubscher SG, Shaw J, Rothlein R, Neuberger JM. 1989. Intercellular adhesion molecule 1 on liver allografts during rejection. *Lancet* 2:1122-5.

Adams DH, Hubscher SG, Shaw J, Johnson GD, Babbs C, Rothlein R, Neuberger JM. 1991. Increased expression of intercellular adhesion molecule 1 on bile ducts in primary biliary cirrhosis and primary sclerosing cholangitis. *Hepatology* 14:426-31.

Adams DH, Mainolfi E, Burra P, Neuberger JM, Ayres R, Elias E, Rothlein R. 1992. Detection of circulating intercellular adhesion molecule-1 in chronic liver diseases. *Hepatology* 16:810-4.

Adams DH, Burra P, Hubscher SG, Elias E, Newman W. 1994. Endothelial activation and circulating vascular adhesion molecules in alcoholic liver disease. *Hepatology* 19:588-594.

Ala A, Standish R, Khan K, Hillon K, Dhillon AP, Hodgson HJF. 2002. Mucosal addressin cell adhesion molecule-1 and podoplanin localisation in primary sclerosing cholangitis and primary biliary cirrhosis. MAdCAM-1 in PSC and PBC. *Journal of Hepatology*. 36(1).

Ala A, Stubbs M, Coward S, Brown D, Hodgson HJ. 2003. Characterisation of mucosal addressin cell adhesion molecule in inflammatory bowel disease. Gut 52;suppl i;A121

Ala A, Brown D, Stubbs M, Jacobs R, Hodgson HJ. 2003. Mucosal addressin cell adhesion molecule in chronic liver disease and development of an *in vitro* model to investigate therapeutic modulation. *Hepatology* 38; suppl.i, 648A.

Ambruzova Z, Mrazek F, Raida L, Stahelova A, Faber E, Indrak K, Petrek M.2009. Possible impact of MADCAM1 gene single nucleotide polymorphisms to the outcome of allogeneic hematopoietic stem cell transplantation. *Hum Immunol* 70:457-60.

Ando T, Jordan P, Joh T, Wang Y, Jennings MH, Houghton J, Alexander JS. 2006.

Isolation and characterization of a novel mouse lymphatic endothelial cell line: SV-LEC. *Lymphat Res Biol* 3:105-15.

Ando T, Jordan P, Wang Y, Itoh M, Joh T, Sasaki M, Elrod JW, Carpenter A, Jennings MH, Minagar A, Alexander JS. 2005. MAdCAM-1 expression and regulation in murine colonic endothelial cells in vitro. *Inflamm Bowel Dis* 11:258-64.

Arao S, Masumoto A, Otsuki M. 2000. Beta 1 integrins play an essential role in adhesion and invasion of pancreatic carcinoma cells. *Pancreas* 20:129-37.

Arihiro S, Ohtani H, Suzuki M, Murata M, Ejima C, Oki M, Kinouchi Y, Fukushima K, Sasaki I, Nakamura S, Matsumoto T, Torii A, Toda G, Nagura H. 2002. Differential expression of mucosal addressin cell adhesion molecule-1 (MAdCAM-1) in ulcerative colitis and Crohn's disease. *Pathol Int* 52:367-74.

Arnedo A, Espuelas S, Irache JM. Albumin nanoparticles as carriers for a phosphodiester oligonucleotide. 2002. *Int J Pharm* 244:59-72.

Auth MK, Keitzer RA, Scholz M, Blaheta RA, Hottenrott EC, Herrmann G, Encke A, Markus BH. 1993. Establishment and immunological characterisation of cultured human gallbladder epithelial cells. *Hepatology* 18:546-555.

Ayres RC, Neuberger JM, Shaw J, Joplin R, Adams DH. 1993. Intercellular adhesion molecule-1 and MHC antigens on human intrahepatic bile duct cells: effect of pro-inflammatory cytokines. *Gut* 34:1245-9.

Bachmann C, Klibanov AL, Olson TS, Sonnenschein JR, Rivera-Nieves J, Cominelli F, Ley KF, Lindner JR, Pizarro TT. 2006. Targeting mucosal addressin cellular adhesion molecule (MAdCAM)-1 to noninvasively image experimental Crohn's disease. *Gastroenterology* 130:8-16.

Baker BF, Monia BP. 1999. Novel mechanisms for antisense-mediated regulation of gene expression. *Biochim Biophys Acta* 1489:3-18.

Bennett CF, Kornbrust D, Henry S, Stecker K, Howard R, Cooper S, Dutson S,Hall W, Jacoby HI. 1997. An ICAM-1 antisense oligonucleotide prevents and reverses dextran sulfate sodium-induced colitis in mice. *J Pharmacol Exp Ther.* 280:988-1000.

Berg EL, McEvoy LM, Berlin C, Bargatze RF, Butcher EC. 1993. L-selectin-mediated lymphocyte rolling on MAdCAM-1. *Nature* 366:695-8.

Berlin C, Berg EL, Briskin MJ, Andrew DP, Kilshaw PJ, Holzmann B, Weissman IL, Hamann A, Butcher EC. 1993. Alpha 4 beta 7 integrin mediates lymphocyte binding to the mucosal vascular addressin MAdCAM-1. *Cell* 74:185-5.

Berman AE, Kozlova NI. 2000. Integrins: structure and functions. *Membr Cell Biol* 13:207-44.

Bevilacqua MP, Stengelin S, Gimbrone MA Jr, Seed B. 1989. Endothelial leukocyte adhesion molecule 1: an inducible receptor for neutrophils related to complement regulatory proteins and lectins. *Science* 243:1160-5.

Bhatti M, Chapman P, Peters M, Haskard D, Hodgson HJ. 1998. Visualising E-selectin in the detection and evaluation of inflammatory bowel disease. *Gut* 43:40-7.

Bloom S, Fleming K, Chapman R. 1995. Adhesion molecule expression in primary sclerosing cholangitis and primary biliary cirrhosis *Gut* 36:604-609.

Bo X, Broome U, Remberger M, Sumitran-Holgersson S. 2001. Tumour necrosis factor alpha impairs function of liver derived T lymphocytes and natural killer cells in patients with primary sclerosing cholangitis. *Gut* 49:131-41.

Boggs RT, McGraw K, Condon T, Flournoy S, Villiet P, Bennett CF, Monia BP.1997. Characterization and modulation of immune stimulation by modified oligonucleotides. *Antisense Nucleic Acid Drug Dev* 7:461-71.

Braasch DA, Liu Y, Corey DR. 2002. Antisense inhibition of gene expression in cells by oligonucleotides incorporating locked nucleic acids: effect of mRNA target sequence and chimera design. *Nucleic Acids Res* 30:5160-7.

Breiteneder-Geleff S, Matsui K, Soleiman A, Meraner P, Poczewski H, Kalt R, Schaffner G, Kerjaschki D. 1997. Podoplanin, novel 43-kd membrane protein of glomerular epithelial cells, is down-regulated in puromycin nephrosis. *Am J Pathol* 151:1141-52.

Briskin MJ, McEvoy LM, Butcher EC. 1993. MAdCAM-1 has homology to immunoglobulin andmucin-like adhesion receptors and to IgA1.*Nature* 363:461-4.

Briskin MJ, Rott L, Butcher EC. 1996. Structural requirements for mucosal vascular addressin binding to its lymphocyte receptor alpha 4 beta 7. Common themes among integrin-Ig family interactions. *J Immunol* 156:719-26.

Briskin M, Winsor-Hines D, Shyjan A, Cochran N, Bloom S, Wilson J, McEvoy LM, Butcher EC, Kassam N, Mackay CR, Newman W, Ringler DJ. 1997. Human mucosal addressin cell adhesion molecule-1 is preferentially expressed in intestinal tract and associated lymphoid tissue. *American Journal of Pathology* 151: 97-110.

Broome U, Hultcrantz R, Scheynius A. 1993. Lack of concomitant expression of ICAM-1 and HLA-DR on bile duct cells from patients with primary sclerosing cholangitis and primary biliary cirrhosis. *Scand J Gastroenterol* 28:126-30.

Bowlus CL, Karlsen TH, Broomé U, Thorsby E, Vatn M, Schrumpf E, Lie BA, Boberg KM.2006. Analysis of MAdCAM-1 and ICAM-1 polymorphisms in 365 Scandinavian patients with primary sclerosing cholangitis. *J Hepatol* 45:704-10.

Bujan J, Gimeno MJ, Prieto A, Pascual G, Bellon JM, Alvarez-Mon M. 1999. Modulation of PECAM-1 (CD31) expression in human endothelial cells: effect of IFN gamma and IL-10. *J Vasc Res* 36:106-13.

Burt AD, Portmann BC, Ferrell LD. 2007. Macsween's Pathology of the liver. 5th Edition. Churchill Livingstone

Butcher EC.1991. Leukocyte-endothelial cell recognition: three (or more) steps to specificity and diversity. *Cell* 67:1033-6.

Collett C, Munro JM. 1999. Functional distribution and further characterization of human endothelial ligand for cellular L-selectin. *Tissue Cell* 31:39-44.

Crooke ST. 1999. Molecular mechanisms of action of antisense drugs. *Biochim Biophys Acta* 1489:31-44.

Dagle JM, Andracki ME, DeVine RJ, Walder JA. 1991. Physical properties of oligonucleotides containing phosphoramidate-modified internucleoside linkages. *Nucleic Acids Res* 19:1805-10.

Danese S. 2008. Negative regulators of angiogenesis in inflammatory bowel disease:thrombospondin in the spotlight. *Pathobiology* 75:22-4

Dando J, Wilkinson KW, Ortlepp S, King DJ, Brady RL. 2002. A reassessment of the MAdCAM-1 structure and its role in integrin recognition. *Acta Crystallogr D Biol Crystallogr* 58:233-41.

De Mesmaeker A, Altmann KH, Waldner A, Wendeborn S. 1995. Backbone modifications in oligonucleotides and peptide nucleic acid systems. *Curr Opin Struct Biol* 5:343-55.

Diacovo TG, Puri KD, Warnock RA, Springer TA, von Andrian UH. 1996. Platelet-mediated lymphocyte delivery to high endothelial venules. *Science;* 273:252-5.

Dietsch MT, Smith VF, Cosand WL, Damle NK, Ledbetter JA, Linsley PS, Aruffo A. 1993. Bispecific receptor globulins, novel tools for the study of cellular interactions. Preparation and characterization of an E-selectin/P-selectin bispecific receptor globulin.

J Immunol Methods 162:123-32.

Dogan A, Du M, Koulis A, Briskin MJ, Isaacson PG. 1997. Expression of lymphocyte homing receptors and vascular addressins in low-grade gastric B-cell lymphomas of mucosa-associated lymphoid tissue. *Am J Pathol* 151:1361-9.

Doukas J, Pober JS. 1990. IFN-gamma enhances endothelial activation induced by tumour necrosis factor but not IL-1. *J Immunol* 145:1727

Dulkanchainun TS, Goss JA, Imagawa DK, Shaw GD, Anselmo DM 1998. Reduction of hepatic ischaemia/reperfusion injury by a soluble P-selectin glycoprotein ligand-1. *Ann Surg* 227:832-40.

Dryselius R, Aswasti SK, Rajarao GK, Nielsen PE, Good L. 2003. The translation start codon region is sensitive to antisense PNA inhibition in Escherichia coli. *Oligonucleotides* 13:427-33.

Eksteen B, Adams DH. 2010. GSK-1605786, a selective small-molecule antagonist of the CCR9 chemokine receptor for the treatment of Crohn's disease. *Drugs* 13:472-781.

Erle DJ, Briskin MJ. Butcher E. 1994. Expression and function of the MadCAM-1 Receptor Integrin α4β7 on Human Leukocytes. *The Journal of Immunology* 517-528.

Evans SS, Collea RP, Appenheimer MM, Gollnick SO. 1993. Interferon-alpha induces the expression of the L-selectin homing receptor in human B lymphoid cells. *J Cell Biol* 123:1889-98.

Faveeuw C, Gagnerault MC, Lepault F. 1994. Expression of homing and adhesion molecules in infiltrated islets of Langerhans and salivary glands of nonobese diabetic mice. *J Immunol* 152:5969-78.

Feagan BG, Greenberg GR, Wild G, Fedorak RN, Paré P, McDonald JW, Cohen A,Bitton A, Baker J, Dubé R, Landau SB, Vandervoort MK, Parikh A.2008. Treatment

of active Crohn's disease with MLN0002, a humanized antibody to the alpha4beta7 integrin. *Clin Gastroenterol Hepatol.*6:1370-7.

Feuerer M, Beckhove P, Mahnke Y, Hommel M, Kyewski B, Hamann A, Umansky V, Schirrmacher V. 2004. Bone marrow microenvironment facilitating dendritic cell: CD4 T cell interactions and maintenance of CD4 memory. *Int J Oncol* 25:867-76.

Freedman AS. 1990. Immunobiology of chronic lymphocytic leukemia. *Hematol Oncol Clin North Am 4*:405-29.

Fries JW, Williams AJ, Atkins RC, Newman W, Lipscomb MF, Collins T.1993. Expression of VCAM-1 and E-selectin in an in vivo model of endothelial activation. *Am J Pathol.* 143:725-37.

Galarneau A, Min KL, Mangos MM, Damha MJ. 2005. Assay for evaluating ribonuclease H-mediated degradation of RNA-antisense oligonucleotide duplexes. *Methods Mol Biol* 288:65-80.

Garcia-Monzon C, Sanchez-Madrid F, Garcia-Buey L, Garcia-Arroyo A, Garcia-Sanchez A, Moreno-Otero R. 1995. Vascular adhesion molecule expression in viral chronic hepatitis: evidence of neoangiogenesis in portal tracts. *Gastroenterology* 108: 231-41.

Geary RS, Watanabe TA, Truong L, Freier S, Lesnik EA, Sioufi NB, Sasmor H, Manoharan M, Levin AA. 2001. Pharmacokinetic properties of 2'-O-(2-methoxyethyl)-modified oligonucleotide analogs in rats. *J Pharmacol Exp Ther* 296:890-7.

Girard JP, Springer TA. 1995. High endothelial venules (HEVs): specialized endothelium for lymphocyte migration. *Immunol Today* 16:449-573.

Ghosh MK, Ghosh K, Dahl O, Cohen JS. 1993. Evaluation of some properties of a phosphorodithioate oligodeoxyribonucleotide for antisense application. *Nucleic Acids Res* 21:5761-6.

Ghosh S, Goldin E, Gordon FH, Malchow HA, Rask-Madsen J, Rutgeerts P, Vyhnálek P, Zádorová Z, Palmer T, Donoghue S. 2003. Natalizumab Pan-European Study Group. Natalizumab for active Crohn's disease. *N Engl J Med* 348:24-32.

Goggins MG, Goh J, O'Connell MA, Weir DG, Kelleher, D, Mahmud N. 2001. Soluble adhesion molecules in inflammatory bowel disease. *Ir J Med Sci* 179:107-11.

Gordon FH, Lai CW, Hamilton MI, Allison MC, Srivastava ED, Fouweather MG, Donoghue S, Greenlees C, Subhani J, Amlot PL, Pounder RE. 2001. A randomized placebo-controlled trial of a humanized monoclonal antibody to alpha4 integrin in active Crohn's disease. *Gastroenterology* 121:268-74.

Gordon FH, Hamilton MI, Donoghue S, Greenlees C, Palmer T, Rowley-Jones D, Dhillon AP, Amlot PL, Pounder RE. 2002. A pilot study of treatment of active ulcerative colitis with natalizumab, a humanized monoclonal antibody to alpha-4 integrin. *Aliment Pharmacol Ther* 16:699-705.

Goto A, Arimura Y, Shinomura Y, Imai K, Hinoda Y. 2006. Antisense therapy of MAdCAM-1 for trinitrobenzenesulfonic acid-induced murine colitis. *Inflamm Bowel Dis* 12:758-65.

Gotsch U, Jager U, Dominis M, Vestweber D. 1994. Expression of P-selectin on endothelial cells is upregulated by LPS and TNF-alpha in vivo. *Cell Adhes Commun 2:7-14.*

Grabsch H, Takeno S, Noguchi T, Hommel G, Gabbert HE, Mueller W. 2001. Different patterns of beta-catenin expression in gastric carcinomas: relationship with clinicopathological parameters and prognostic outcome. *Histopathology* 39:141-9.

Grant AJ, Lalor PF, Hubscher SG, Briskin M, Adams DH. 2001. MAdCAM-1 expressed in chronic inflammatory liver disease supports mucosal lymphocyte adhesion to hepatic endothelium (MAdCAM-1 in chronic inflammatory liver disease). *Hepatology* 33:1065-72.

Grant AJ, Lalor PF, Salmi M, Jalkanen S, Adams DH. 2002. Homing of mucosal lymphocytes to the liver in the pathogenesis of hepatic complications of inflammatory bowel disease. *Lancet* 359:150-7.

Grimwood J, Gordon LA, Olsen A, Terry A, Schmutz J, Lamerdin J, Hellsten U,Goodstein D, Couronne O, Tran-Gyamfi M, Aerts A, Altherr M, Ashworth L, Bajorek E, Black S, Branscomb E, Caenepeel S, Carrano A, Caoile C, Chan YM, ChristensenM, Cleland CA, Copeland A, Dalin E, Dehal P, Denys M, Detter JC, Escobar J, Flowers D, Fotopulos D, Garcia C, Georgescu AM, Glavina T, Gomez M, Gonzales E,Groza M, Hammon N, Hawkins T, Haydu L, Ho I, Huang W, Israni S, Jett J, Kadner K,Kimball H, Kobayashi A, Larionov V, Leem SH, Lopez F, Lou Y, Lowry S, Malfatti S, Martinez D, McCready P, Medina C, Morgan J, Nelson K, Nolan M, Ovcharenko IPitluck S, Pollard M, Popkie AP, Predki P, Quan G, Ramirez L, Rash S, Retterer J,Rodriguez A, Rogers S, Salamov A, Salazar A, She X, Smith D, Slezak T, Solovyev V, Thayer N, Tice H, Tsai M, Ustaszewska A, Vo N, Wagner M, Wheeler J, Wu K, Xie G, Yang J, Dubchak I, Furey TS, DeJong P, Dickson M, Gordon D, Eichler EE, Pennacchio LA, Richardson P, Stubbs L, Rokhsar DS, Myers RM, Rubin EM, Lucas SM. 2004. The DNA sequence and biology of human chromosome 19. *Nature* 428:529-35.

Gunn MD, Tangemann K, Tam C, Cyster JG, Rosen SD, Williams LT. 1998. A chemokine expressed in lymphoid high endothelial venules promotes the adhesion and chemotaxis of naive T lymphocytes. *Proc Natl Acad Sci USA* 95:258-63.

Handschel J, Prott FJ, Sunderkotter C, Metze D, Meyer U, Joos U. 1999. Irradiation induces increase of adhesion molecules and accumulation of beta2-integrin-expressing cells in humans. *Int J Radiat Oncol Biol Phys* 45:475-81.

Hänninen A, Jaakkola I, Jalkanen S. 1998. Mucosal addressin is required for the development of diabetes in nonobese diabetic mice. *J Immunol* 160:6018-25.

Haraldsen G, Kvale D, Lien B, Farstad IN, Brandtzaeg P. 1996. Cytokine-regulated expression of E-selectin, intercellular adhesion molecule-1 (ICAM-1), and vascular cell

adhesion molecule-1 (VCAM-1) in human microvascular endothelial cells. *J Immunol* 156:2558-65.

Hayasaka H, Taniguchi K, Fukai S, Miyasaka M. 2010. Neogenesis and development of the high endothelial venules that mediate lymphocyte trafficking.Cancer Sci 101:2302-8.

Heckmann M, Douwes K, Peter R, Degitz K. 1998. Vascular activation of adhesion molecule mRNA and cell surface expression by ionizing radiation. *Exp Cell Res* 238: 148-54.

Hesterberg D, Winsor-Hines M, Briskin, D, Soler-Ferran C, Merrill, C, Mackay W, Newman D, Ringler DJ. 1996. Rapid resolution of chronic colitis in the cotton-top tamarin with an antibody to a gut-homing integrin alpha 4 beta 7. *Gastroenterology* 111:1373-1380.

Hillan KJ, Hagler KE, MacSween RN, Ryan AM, Renz ME, Chiu HH, Ferrier RK, Bird GL, Dhillon AP, Ferrell LD, Fong S. 1999. Expression of the mucosal vascular addressin, MAdCAM-1, in inflammatory liver disease. *Liver* 19:509-18.

Horie Y, Wolf R, Miyasaka M, Anderson DC, Granger DN. 1996. Leukocyte adhesion and hepatic microvascular responses to intestinal Ischemia/reperfusion in rats. *Gastroenterology* 111:666-73.

Huang GT, Eckmann L, Savidge TC, Kagnoff MF. 1996. Infection of human intestinal epithelial expression and neutrophil adhesion. *J Clin Invest* 98:572-83.

Iizuka T, Tanaka T, Suematsu M, Miura S, Watanabe T, Koike R, Ishimura Y, Ishii H, Miyasaka N, Miyasaka M. 2000. Stage-specific expression of mucosal addressin cell adhesion molecule1during embryogenesis in rats. *J Immunol* 164:2463-71.

Jalkanen S, Karikoski M, Mercier N, Koskinen K, Henttinen T, Elima K, Salmivirta K, Salmi M.2007. The oxidase activity of vascular adhesion protein-1 (VAP-1) induces endothelial E- and P-selectins and leukocyte binding. *Blood* 110:1864-70.

Jayaraman A, Walton SP, Yarmush ML, Roth CM. 2001.Rational selection and quantitative evaluation of antisense oligonucleotides. *Biochim Biophys Acta* 1520:105-14.

Kanai T, Totsuka T, Uraushihara K, Makita S, Nakamura T, Koganei K, Fukushima T, Akiba H, Yagita H, Okumura K, Machida U, Iwai H, Azuma M, Chen L,Watanabe M. 2003. Blockade of B7-H1 suppresses the development of chronic intestinal inflammation. *J Immunol* 172:4156-63.

Kanemitsu N, Ebisuno Y, Tanaka T, Otani K, Hayasaka H, Kaisho T, Akira S, Katagiri K, Kinashi T, Fujita N, Tsuruo T, Miyasaka M. 2005. CXCL13 is an arrest chemokine for B cells in high endothelial venules. *Blood* 106:2613-8.

Kanwar JR, Kanwar RK, Wang D, Krissansen GW. 2000. Prevention of a chronic progressive form of experimental autoimmune encephalomyelitis by an antibody against mucosal addressin cell adhesion molecule-1, given early in the course of disease progression. *Immunol Cell Biol* 78:641-5.

Kato S, Hokari R, Matsuzaki K, Iwai A, Kawaguchi A, Nagao S, Miyahara T, Itoh K, Ihii H, Miura S. 2000. Amelioration of murine experimental colitis by inhibition of mucosal addressin cell adhesion molecule-1. *J Pharmacol Exp Ther* 295:183-9.

Kelleher D, Murphy A, Lynch S, O'Farrelly C. 1994. Adhesion molecules utilized in binding of intraepithelial lymphocytes to human enterocytes. *Eur J Immunol* 24: 1013-6.

Kobatashi S, Nakanuma Y, Matsui O. 1994. Intrahepatic peribiliary vascular plexus in various hepatobiliary diseases: a histological survey. *Hum Pathol* 259:940-6.

Koda W, Harada K, Tsuneyama K, Kono N, Sasaki M, Matsui O, Nakanuma Y.2000. Evidence of the participation of peribiliary mast cells in regulation of the peribiliary vascular plexus along the intrahepatic biliary tree. *Lab Invest* 80:1007-17.

Komatsu S, Berg RD, Russell JM, Nimura Y, Granger DN. 2000. Enteric microflora contribute to constitutive ICAM-1 expression on vascular endothelial cells. Am J *Physiol Gastrointest Liver Physiol* 279:G186-91.

Koopman G, Parmentier HK, Schuurman HJ, Newman W, Meijer CJ, Pals ST. 1991. Adhesion of human B cells to follicular dendritic cells involves both the lymphocyte function-associated antigen 1/intercellular adhesion molecule 1 and very late antigen 4/vascular cell adhesion molecule 1 pathways. *J Exp Med* 173:1297-304

Kraal G, Schornagel K, Streeter PR, Holzmann B, Butcher EC.1995. Expression of the mucosal vascular addressin, MAdCAM-1, on sinus-lining cells in the spleen. *Am J Pathol* 147:763-71.

Kratz A, Campos-Neto A, Hanson MS, Ruddle NH. 1996. Chronic inflammation caused by lymphotoxin in lymphoid neogenesis. *J Exp Med* 183:1461-72.

Kunkel EJ, Campbell JJ, Haraldsen G, Pan J, Boisvert J, Roberts AI, Ebert EC, Vierra MA, Goodman SB, Genovese MC, Wardlaw AJ, Greenberg HB, Parker CM, Andrew DP, Agace WW. 2000. Lymphocyte CC chemokine receptor 9 and epithelial thymus-expressed chemokine-expressed chemokine (TECK) expression distinguish the small intestinal immune compartment: epithelial expression of tissue-specific chemokines as an organizing principle in regional immunity. *J Exp Med* 192:761-68.

Kurkijarvi R, Adams DH, Leino R, Mottonen T, Jalkanen S, Salmi M. 1998. Circulating form of human vascular adhesion protein-1 (VAP-1): increased serum levels in inflammatory liver diseases. *J Immunol* 161:1549-57.

Kurkijarvi R, Yegutkin GG, Gunson BK, Jalkanen S, Salmi M, Adams DH. 2000. Circulating soluble vascular adhesion protein 1 accounts for the increased serum monoamine oxidase activity in chronic liver disease. *Gastroenterology* 119:1096-103.

Lalor PF, Edwards S, McNab G, Salmi M, Jalkanen S, Adams DH. 2002. Vascular adhesion protein-1 mediates adhesion and transmigration of lymphocytes on human hepatic endothelial cells. *J Immunol* 169:983-92.

Lalor PF, Sun PJ, Weston CJ, Martin-Santos A, Wakelam MJ, Adams DH. 2007. Activation of vascular adhesion protein-1 on liver endothelium results in an NF-kappa B-dependent increase in lymphocyte adhesion. *Hepatology* 45:465-74.

Lasky LA. 1995. Selectin-carbohydrate interactions and the initiation of the inflammatory response. *Annu Rev Biochem* 64:113-39.

Lee J, Lee EN, Kim EY, Park HJ, Chang CY, Jung DY, Choi SY, Lee SK, Lee KW, Kwon GY, Joh JW, Kim SJ. 2005. Administration of agonistic anti-4-1BB monoclonal antibody leads to the amelioration of inflammatory bowel disease. *Immunol Lett* 101:210-6.

Lefkowitch J. 2010. *Scheuer's Liver Biopsy Interpretation.* Sixth Edition. WB. Saunders.

Leung E, Berg RW, Langley R, Greene J, Raymond LA, Augustus M, Ni J, Carter KC, Spurr N, Choo KH, Krissansen GW. 1997. Genomic organization, chromosomal mapping, and analysis of the 5' promoter region of the human MAdCAM-1 gene. *Immunogenetics* 46:111-9.

Leung E, Kanwar RK, Kanwar JR, Krissansen GW. 2003. Mucosal vascular addressin cell adhesion molecule-1 is expressed outside the endothelial lineage on fibroblasts and melanoma cells. *Immunol Cell Biol* 81:320-7.

Leung E, Lehnert KB, Kanwar JR, Yang Y, Mon Y, McNeil HP, Krissansen GW. 2004. Bioassay detects soluble MAdCAM-1 in body fluids. *Immunol Cell Biol* 82:400-9.

Lidington EA, Moyes DL, McCormack AM, Rose ML. 1999. A comparison of primary endothelial cells and endothelial cell lines for studies of immune interactions. *Transpl Immunol* 7:239-46.

Lindholm C, Naylor A, Johansson EL, Quiding-Järbrink M. 2004. Mucosal vaccination increases endothelial expression of mucosal addressin cell adhesion molecule 1 in the

human gastrointestinal tract. *Infect Immun* 72:1004-9.

Lindor KD, Wiesner RH, LaRusso NF, Homburger HA. 1987. Enhanced autoreactivity of T-lymphocytes in primary sclerosing cholangitis. *Hepatology* 7:884-8.

Loke SL, Stein CA, Zhang XH, Mori K, Nakanishi M, Subasinghe C, Cohen JS, Neckers LM. 1989. Characterization of oligonucleotide transport into living cells. *Proc Natl Acad Sci* USA 86:3474-8.

Luna-Casado L, Diez-Ruiz A, Gutierrez-Gea F, Santos-Perez JL, Rico-Irles J, Wachter H, Fuchs D. 1997. Increased peripheral mononuclear cells expression of adhesion molecules in alcoholic cirrhosis: its relation to immune activation. *Hepatology* 27:477-83.

Mahara A, Iwase R, Sakamoto T, Yamaoka T, Yamana K, Murakami A. 2003. Detection of acceptor sites for antisense oligonucleotides on native folded RNA by fluorescence spectroscopy. *Bioorg Med Chem* 11:2783-90.

Manoharan M, Johnson LK, McGee DP, Guinosso CJ, Ramasamy K, Springer RH, Bennett CF, Ecker DJ, Vickers T, Cowsert L, Cook PD. 1992. Chemical modifications to improve uptake and bioavailability of antisense oligonucleotides. *Ann N Y Acad Sci* 660:306-9.

Martelius T, Salaspuro V, Salmi M, Krogerus L, Höckerstedt K, Jalkanen S, Lautenschlager I. 2004. Blockade of vascular adhesion protein-1 inhibits lymphocyte infiltration in rat liver allograft rejection. *Am J Pathol* 165:1993-2001.

Masumoto A, Arao S, Otsuki M. 1999. Role of beta1 integrins in adhesion and invasion of hepatocellular carcinoma cells. *Hepatology* 29:68-74.

Matsuzaki K, Tsuzuki Y, Matsunaga H, Inoue T, Miyazaki J, Hokari R, Okada Y, Kawaguchi A, Nagao S, Itoh K, Matsumoto S, Miura S. 2005. In vivo demonstration of T lymphocyte migration and amelioration of ileitis in intestinal mucosa of SAMP1/Yit mice by the inhibition of MAdCAM-1. *Clin Exp Immunol* 140:22-31.

Miles A, Liaskou E, Eksteen B, Lalor PF, Adams DH. 2008. CCL25 and CCL28 promotealpha4 beta7-integrin-dependent adhesion of lymphocytes to MAdCAM-1 under shearflow. *Am J Physiol Gastrointest Liver Physiol* 294:G1257-67.

Miyasaka M, Tanaka T. 2004. Lymphocyte trafficking across high endothelial venules: dogmas and enigmas. *Nat Rev Immunol* 4:360-70.

Mizushima T, Sasaki M, Ando T, Wada T, Tanaka M, Okamoto Y, Ebi M, Hirata Y, Murakami K, Mizoshita T, Shimura T, Kubota E, Ogasawara N, Tanida S, Kataoka H, Kamiya T, Alexander JS, Joh T. 2010. Blockage of angiotensin II type 1 receptor regulates TNF-alpha-induced MAdCAM-1 expression via inhibition of NF-kappaB translocation to the nucleus and ameliorates colitis. *Am J Physiol Gastrointest Liver Physiol* 298:G255-66.

Mora JR, Bono MR, Manjunath N, Weninger W, Cavanagh LL, Rosemblatt M, Von Andrian UH. 2003. Selective imprinting of gut-homing T cells by Peyer's patch dendritic cells. Nature 424:88-93.

Mueller AR, Platz KP, Haak M, Undi H, Muller C, Kottgen E, Weidemann H, Neuhaus P. 1996. The release of cytokines, adhesion molecules, and extracellular matrix parameters during and after reperfusion in human liver transplantation. *Transplantation* 62:1118-26.

Nielson OH, Brynskov J, Vainer B. 1996. Increased mucosal concentrations of soluble intercellular adhesion molecule-1 (sICAM-1), sE-selectin, and interleukin-8 in active ulcerative colitis. *Dig Dis Sci* 41:1780-5.

Nielsen OH, Vainer B. 2000. Beta 2 integrins inhibit ICAM –1 induced neutrophil locomotion in ulcerative colitis. *Gastroenterology* 118 suppl 12,1879.

Nummer D, Suri-Payer E, Schmitz-Winnenthal H, Bonertz A, Galindo L, Antolovich D, Koch M, Büchler M, Weitz J, Schirrmacher V, Beckhove P. 2007. Role of tumor

endothelium in CD4+ CD25+ regulatory T cell infiltration of human pancreatic carcinoma. *J Natl Cancer Inst* 99:1188-99.

Obata T. 2006. Diabetes and semicarbazide-sensitive amine oxidase (SSAO) activity: a review. *Life Sci.* 79:417-22.

Ogawa H, Binion DG, Heidemann J, Theriot M, Fisher PJ, Johnson NA, Otterson MF,Rafiee P. 2005. Mechanisms of MAdCAM-1 gene expression in human intestinal microvascular endothelial cells. *Am J Physiol Cell Physiol* 288:C272-81.

Ohara H, Isomoto H, Wen CY, Ejima C, Murata M, Miyazaki M, Takeshima F, Mizuta Y, Murata I, Koji T, Nagura H, Kohno S. 2003. Expression of mucosal addressin cell adhesion molecule 1 on vascular endothelium of gastric mucosa in patients with nodular gastritis. *World J Gastroenterol* 9:2701-5.

Oshima T, Pavlick KP, Laroux FS, Verma SK, Jordan P, Grisham MB, Williams L, Alexander JS. 2001a. Regulation and distribution of MAdCAM-1 in endothelial cells in vitro. *Am J Physiol Cell Physiol* 281:C1096-105.

Oshima T, Jordan P, Grisham MB, Alexander JS, Jennings M, Sasaki M, Manas K. 2001b.TNF-alpha induced endothelial MAdCAM-1 expression is regulated by exogenous, not endogenous nitric oxide. *BMC Gastroenterol* 1:5.

Pachynski RK, Wu SW, Gunn MD, Erle DJ. 1998. Secondary lymphoid-tissue chemokine (SLC) stimulates integrin alpha 4 beta 7-mediated adhesion of lymphocytes to mucosal addressin cell adhesion molecule-1 (MAdCAM-1) under flow. *J Immunol* 161:952-6.

Palmer HG, Gonzalez-Sancho JM, Espada J, Berciano MT, Puig I, Baulida J, Quintanilla M, Cano A, de Herreros AG, Lafarga M, Munoz A. 2001. Vitamin D(3) promotes the differentiation of colon carcinoma cells by the induction of E-cadherin and the inhibition of beta-catenin signaling. *J Cell Biol* 154:369-87.

Panes J, Anderson DC, Miyasaka M, Granger DN. 1995. Role of Leucocyte endothelial cell adhesion in radiation microvascular dysfunction in rats. *Gastroenterology* 108:1761-1769.

Patel RT, Pall AA, Adu D, Keighley MR. 1995. Circulating soluble adhesion molecules in inflammatory bowel disease. *Eur J Gastroenterol Hepatol* 7:1037-41.

Picarella DE, Kratz A, Li CB, Ruddle NH, Flavell RA. 1993.Transgenic tumor necrosis factor (TNF)-alpha production in pancreatic islets leads to insulitis, not diabetes. Distinct patterns of inflammation in TNF-alpha and TNF-beta transgenic mice. *J Immunol* 150:4136-50.

Pirruccello SJ, Perry GA, Bock PJ, Lang MS, Noel SM, Zon G, Iversen PL. 1994. HIV-1 rev antisense phosphorothioate oligonucleotide binding to human mononuclear cells is cell type specific and inducible. *Antisense Res Dev* 4:285-9.

Podolsky DK, Lobb R, King N, Benjamin CD, Pepinsky B. 1993. E-selectin in-situ expression correlates with clinical, endoscopic and histological activity and outcome. Attenuation of colitis in the cotton-top tamarin by anti-alpha 4 integrin monoclonal antibody *J Clin Invest 92:372*-80.

Polzien F, Ramadori G. 1996. Increased intercellular adhesion molecule-1 serum concentration in cholestasis. *J Hepatol* 25:877-86.

Prakash TP, Johnston JF, Graham MJ, Condon TP, Manoharan M 2004. 2'-O-[2-[(N,Ndimethylamino)oxy]ethyl]-modified oligonucleotides inhibit expression of mRNA in vitro and in vivo. *Nucleic Acids Res* 32:828-33.

Prakash TP, Manoharan M, Kawasaki AM, Fraser AS, Lesnik EA, Sioufi N, Leeds JM, Teplova M, Egli M. 2002. 2'-O-[2-(methylthio)ethyl]-modified oligonucleotide: an analogue of 2'-O-[2-(methoxy)-ethyl]-modified oligonucleotide with improved protein binding properties and high binding affinity to target RNA. *Biochemistry* 41:11642-8.

Pullen N, Molloy E, Carter D, Syntin P, Clemo F, Finco-Kent D, Reagan W, Zhao S, Kawabata T, Sreckovic S.2009. Pharmacological characterization of PF-00547659, an anti-human MAdCAM monoclonal antibody. *Br J Pharmacol* 157:281-93.

Rescigno M, Urbano M, Valzasina B, Francolini M, Rotta G, Bonasio R, Granucci F, Kraehenbuhl JP, Ricciardi-Castagnoli P.2001. Dendritic cells express tight junction proteins and penetrate gut epithelial monolayers to sample bacteria. *Nat Immunol* 2:361-7.

Rijcken E, Krieglstein CF, Anthoni C, Laukoetter MG, Mennigen R, Spiegel HU, Senninger N, Bennett CF, Schuermann G.2002. ICAM-1 and VCAM-1 antisense oligonucleotides attenuate in vivo leucocyte adherence and inflammation in rat inflammatory bowel disease. *Gut* 51:529-35.

Rivera-Nieves J, Ho J, Bamias G, Ivashkina N, Ley K, Oppermann M, Cominelli F. 2006. Antibody blockade of CCL25/CCR9 ameliorates early but not late chronic murine ileitis. *Gastroenterology* 131:1518-29.

Rong G, Zhou Y, Xiong Y, Zhou L, Geng H, Jiang T, Zhu Y, Lu H, Zhang S, Wang P, Zhang B, Zhong R. 2009. Imbalance between T helper type 17 and T regulatory cells in patients with primary biliary cirrhosis: the serum cytokine profile and peripheral cell population. Clin Exp Immunol 156:217-25.

Salmi M, Alanen K, Grenman S, Briskin M, Butcher EC, Jalkanen S. 2001a. Immune cell trafficking in uterus and early life is dominated by the mucosal addressin MAdCAM-1 in humans. *Gastroenterology* 121:853-64.

Salmi M, Hellman J, Jalkanen S. 1998. The role of two distinct endothelial molecules, vascular adhesion protein-1 and peripheral lymph node addressin, in the binding of lymphocyte subsets to human lymph nodes. *J Immunol* 160:5629-36.

Salmi M, Jalkanen S. 1992. A 90-kilodalton-endothelial cell molecule mediating lymphocyte binding in humans. *Science* 257:1407-9.

Salmi M, Jalkanen S. 2001b. Human leukocyte subpopulations from inflamed gut bind to joint vasculature using distinct sets of adhesion molecules. *J Immunol* 166:4650-7.

Salmi M, Kalimo K, Jalkanen S. 1993. Induction and function of vascular adhesion protein-1 at sites of inflammation. *J Exp Med* 178:2255-60

Salmi M, Smith DJ, Bono P, Leu T, Hellman J, Matikainen MT, Jalkanen S. A. 1997. A mouse molecular mimic of human vascular adhesion protein-1. Mol Immunol.34:1227-36.

Salmi M, Tohka S, Berg EL, Butcher EC, Jalkanen S. 1997. Vascular adhesion protein 1 (VAP-1) mediates lymphocyte subtype-specific, selectin-independent recognition of vascular endothelium in human lymph nodes. *J Exp Med* 186:589-600.

Sampaio S, Li, X, Takeuchi M, Mei C, Francke, U, Butcher, EC, Briskin, MJ. 1995. Organization, regulatory sequences, and alternatively spliced transcripts of the mucosal addressin cell adhesion molecule-1 (MAdCAM-1) gene. *J Immunol* 155:2477–2486.

Sanghvi YS, Hoke GD, Freier SM, Zounes MC, Gonzalez C, Cummins L, Sasmor H, Cook PD. 1993. Antisense oligodeoxynucleotides: synthesis, biophysical and biological evaluation of oligodeoxynucleotides containing modified pyrimidines. *Nucleic Acids Res* 21:3197-203.

Sasaki M, Jordan P, Joh T, Itoh M, Jenkins M, Pavlick K, Minagar A, Alexander SJ. 2002. Melatonin reduces TNF-a induced expression of MAdCAM-1 via inhibition ofNF-kappaB. *BMC Gastroenterol* 2:9.

Schreiber S, Heinig T, Thiele HG, Raedler A. 1995. Immunoregulatory role of interleukin 10 in patients with inflammatory bowel disease. *Gastroenterology* 108:1434-44.

Schippers A, Leuker C, Pabst O, Kochut A, Prochnow B, Gruber AD, Leung E, Krissansen GW, Wagner N, Müller W. 2009. Mucosal addressin cell-adhesion

molecule-1 controls plasma-cell migration and function in the small intestine of mice. *Gastroenterology* 137:924-33.

Schon MP, Arya A, Murphy EA, Adams CM, Strauch UG, Agace WW, Marsal J, Donohue JP, Her H, Beier DR, Olson S, Lefrancois L, Brenner MB, Grusby MJ, Parker CM.1999. Mucosal T lymphocyte numbers are selectively reduced in integrin alpha E (CD103)-deficient mice. *J Immunol* 162:6641-9.

Schreiber S, Nikolaus S, Hampe J. 1998. Activation of nuclear factor kappa B inflammatory bowel disease *Gut* 42:477-84.

Schreiber S, Nikolaus S, Malchow H, Kruis W, Lochs H, Raedler A, Hahn EG, Krummenerl T, Steinmann G; German ICAM-1 Study Group. 2001. Absence of efficacy of subcutaneous antisense ICAM-1 treatment of chronic active Crohn's disease. Ga*stroenterology* 120:1339-46.

Schweighoffer T, Tanaka Y, Tidswell M, Erle DJ, Horgan KJ, Luce GE, Lazarovits AI, Buck D, Shaw S.J. 1993. Selective expression of integrin alpha 4 beta 7 on a subset of human CD4+ memory T cells with Hallmarks of gut-trophism. *Immunol* 151:717-29.

Shepley MP, Racaniello VR. 1994. A monoclonal antibody that blocks poliovirus attachment recognizes the lymphocyte homing receptor CD44. *J Virol* 68:1301-8.

Shimizu Y, Shaw S, Graber N, Gopal TV, Horgan KJ, van Seventer GA. 1991. Activation-independent binding of human memory T cells to adhesion molecule ELAM-1. *Nature* 349:799-802.

Sigal A, Bleijs DA, Grabovsky V, van Vliet SJ, Dwir O, Figdor CG, van Kooyk Y,Alon R.2000. The LFA-1 integrin supports rolling adhesions on ICAM-1 under physiological shear flow in a permissive cellular environment. *J Immunol.* 165:442-52.

Sikorski EE, Hallmann R, Berg EL, Butcher EC. 1993. The Peyer's patch high endothelial receptor for lymphocytes, the mucosal vascular addressin, is induced on a

murine endothelial cell line by tumor necrosis factor-alpha and IL-1. *J Immunol* 151: 5239-50.

Sitrin RG, Pan PM, Blackwood RA, Huang J, Petty HR. 2001. Cutting edge: evidence for a signalling partnership between urokinase receptors (CD87) and L-selectin (CD62L) in human polymorphonuclear neutrophils. *J Immunol* 166:4822-5.

Soriano A, Salas A, Salas A, Sans M, Gironella M, Elena M, Anderson DC, Piqué JM, Panés J.2000. VCAM-1, but not ICAM-1 or MAdCAM-1, immunoblockade ameliorates DSS-induced colitis in mice. *Lab Invest* 80:1541-51.

Souza HS, Elia CC, Spencer J, MacDonald TT. 1999. Expression of lymphocyte-endothelial receptor-ligand pairs, alpha4beta7/MAdCAM-1 and OX40/OX40 ligand in the colon and jejunum of patients with inflammatory bowel disease. *Gut* 45:856-63.

Springer T. Adhesion receptors of the immune system. 1990. *Nature* 346:425-34.

Stagg AJ, Kamm MA, Knight SC. 2002. Intestinal dendritic cells increase T cell expression of alpha4beta7 integrin. *Eur J Immunol* 32:1445-54.

Steeber DA, Green NE, Sato S, Tedder TF 1996. Lyphocyte migration in L-selectin-deficient mice. Altered subset migration and aging of the immune system. *J Immunol* 157:1096-106.

Steffen BJ, Breier G, Butcher EC, Schulz M, Engelhardt B. 1996. ICAM-1, VCAM-1, and MAdCAM-1 are expressed on choroid plexus epithelium but not endothelium and mediate binding of lymphocytes in vitro. *Am J Pathol* 148:1819-38.

Steiniger B, Barth P, Hellinger A. 2001. The perifollicular and marginal zones of the human splenic white pulp : do fibroblasts guide lymphocyte immigration? *Am J Pathol* 159:501-12.

Steven W. Martin, Matts O. Magnusson, Ivan T. Matthews, Gary Burgess, Wojciech Niezychowski. 2009. Mechanistic Population Pharmacokinetics (PK) Model of PF-

0054659, a Fully Human IgG2 Anti-MAdCAM-1 Antibody, in Ulcerative Colitis Patients: Results of a First in Human (Fih) Study. *Gastroenterology* 136:A-641.

Streeter PR, Berg EL, Rouse BT, Bargatze RF, Butcher EC. 1988. A tissue-specific endothelial cell molecule involved in lymphocyte homing, *Nature* 331:41-6.

Sturgess RP, Macartney JC, Makgoba MW, Hung CH, Haskard DO, Ciclitara PJ. 1990. Differential upregulation of intercellular adhesion molecule-1 in coeliac disease. *Clin Exp Immunol* 82:489-92.

Sumpter TL, Abe M, Tokita D, Thomson AW. 2007. Dendritic cells, the liver, and transplantation. *Hepatology* 46:2021-31.

Szabo MC, Butcher EC, McEvoy LM. 1997. Specialisation of mucosal follicular dendritic cells revealed by mucosal addressin-cell adhesion molecule-1 display. *J Immunol* 158:5584-8.

Takasaki S, Hano H. 2001. Three-dimensional observations of the human hepatic artery (Arterial system in the liver). *Journal of Hepatology* 34:455-466.

Takei Y, Kadomatsu K, Matsuo S, Itoh H, Nakazawa K, Kubota S, Muramatsu T. 2001. Antisense oligodeoxynucleotide targeted to Midkine, a heparin-binding growth factor, suppresses tumorigenicity of mouse rectal carcinoma cells. *Cancer Res* 61:8486-91.

Takeuchi M, Baichwal VR. 1995. Induction of the gene encoding mucosal vascular addressin cell adhesion molecule 1 by tumor necrosis factor alpha is mediated by NF-kappa B proteins *Proc Natl Acad Sci* USA 92:3561-5.

Tan K, Casasnova JM, Liu JH, et al. 1998. The structure of immunoglobulin superfamily domains 1 and 2 of MAdCAM-1 reveals novel features important for integrin recognition. *Structure* 6:793-801.

Taraszka KS, Higgins JM, Tan K, Mandelbrot DA, Wang JH, Brenner MB. 2000 Molecular basis for leukocyte integrin alpha (E) beta (7) adhesion to epithelial (E)-cadherin. *J Exp Med* 191:1555-67.

Targan SR, Feagan BG, Fedorak RN, Lashner BA, Panaccione R, Present DH, Spehlmann ME, Rutgeerts PJ, Tulassay Z, Volfova M, Wolf DC, Hernandez C, Bornstein J, Sandborn WJ. 2007. International Efficacy of Natalizumab in Crohn's Disease Response Natalizumab for the treatment of active Crohn's disease: results of the ENCORE Response and Remission (ENCORE) Trial Group. *Gastroenterology* 132:1672-83.

Thies A, Mauer S, Fodstad O, Schumacher U. 2007. Clinically proven markers of metastasis predict metastatic spread of human melanoma cells engrafted in scid mice. 2007. *Br J Cancer* 96:609-16.

Tian L, Yoshihara Y, Mizuno T, Mori K, Gahmberg CG. 1997.The neuronal glycoprotein telencephalin is a cellular ligand for the CD11a/CD18 leukocyte integrin. *J Immunol* 158:928-36.

Vainer B, Nielsen OH. 2000. Changed colonic profile of P-selectin, platelet-endothelial cell adhesion molecule-1 (PECAM-1), intercellular adhesion molecule-1 (ICAM-1), ICAM-2, and ICAM-3 in inflammatory bowel disease. *Clin Exp Immunol* 121:242-7.

Van Assche G, Van Ranst M, Sciot R, Dubois B, Vermeire S, Noman M, Verbeeck J, Geboes K, Robberecht W, Rutgeerts P. 2005. Progressive multifocal leukoencephalopathy after natalizumab therapy for Crohn's disease. *N Engl J Med* 353:362-8.

Van der Feltz MJ, de Groot N, Bayley JP, Lee SH, Verbeet MP, de Boer HA. 2001. Lymphocyte homing and Ig secretion in the murine mammary gland. *Scand J Immunol* 54:292-300.

van Deventer SJ, Tami JA, Wedel MK. 2004. A randomised, controlled, double blind, escalating dose study of alicaforsen enema in active ulcerative colitis. *Gut* 53:1646-51.redirect polyadenylation. *Nucleic Acids Res* 29:1293-9.

Vermeire S, Ghosh S, Panes J, Dahlerup J, Luegering A, Sirotiakova J, Strauch U, Burgess G, Spanton J, Niezychowski W. 2009. Safety and Efficacy of Pf-00547659 a Fully Human Anti-MAdCAM-1 Antibody in Ulcerative Colitis. Results of a first in Human Study. *Gastroenterology* 136, A-132.

Vickers TA, Wyatt JR, Burckin T, Bennett CF, Freier SM. 2001. Fully modified 2' MOE oligonucleotides redirect polyadenylation. *Nucleic Acids Res* 29:1293-9.

Vidal-Vanaclocha F, Rocha MA, Asumendi A, Barbera-Guillem E. 1993. Role of periportal and perivenous sinusoidal endothelial cells in hepatic homing of blood and metastatic cancer cells. *Semin Liver Dis* 13:60-71

Volpes R, van den Oord JJ, Desmet VJ. 1990. Immunohistochemical study of adhesion molecules in liver inflammation. *Hepatology* 12:59-65.

Wagner N, Lohler J, Kunkel EJ, Ley K, Leung E, Krissansen G, Rajewsky K, Muller W. 1996. Critical role for beta7 integrins in formation of the gut-associated lymphoid tissue. *Nature* 382:366-70.

Waidmann M, Allemand Y, Lehmann J, di Genaro S, Bücheler N, Hamann A, Autenrieth IB. 2002. Microflora reactive IL-10 producing regulatory T cells are present in the colon of IL-2 deficient mice but lack efficacious inhibition of IFN-gamma and TNF-alpha production. *Gut* 50:170-9.

Walton SP, Stephanopoulos GN, Yarmush ML, Roth CM. 2002. Thermodynamic and kinetic characterization of antisense oligodeoxynucleotides binding to a structured mRNA. *Biophys J* 82:366-77.

Weller A, Isenmann S, Vestweber D. 1992. Cloning of the mouse endothelial selectins. Expression of both E- and P-selectin is inducible by tumor necrosis factor alpha. *J Biol Chem* 267:15176-83

Whiteside T, Lasky S, Si L, Van Thiel D. Immunologic analysis of mononuclear cells in liver tissues and blood of patients with primary sclerosing cholangitis. Hepatology 1985;5:468-74.

Wong J, Johnston B, Lee SS, Bullard DC, Smith CW, Beaudet AL, Kubes P. 1997. A minimal role for selectins in the recruitment of leukocytes into the inflamed liver microvasculature. *J Clin Invest* 99:2782-90

Xia H, Mao Q, Eliason SL, Harper SQ, Martins IH, Orr HT, Paulson HL, Yang L, Kotin RM, Davidson BL. 2004. RNAi suppresses polyglutamine-induced neurodegeneration in a model of spinocerebellar ataxia. *Nat Med* 10:816-20.

Yacyshyn BR, Bowen-Yacyshyn MB, Jewell L, Tami JA, Bennett CF, Kisner DL, Shanahan WR Jr.1998 A placebo-controlled trial of ICAM-1 antisense oligonucleotide in the treatment of Crohn's disease. *Gastroenterology* 114:1133-42

Yacyshyn BR, Chey WY, Goff J, Salzberg B, Baerg R, Buchman AL, Tami J, Yu R,Gibiansky E, Shanahan WR; ISIS 2302-CS9 Investigators. 2002. Double blind, placebo controlled trial of the remission inducing and steroid 1sparing properties of an ICAM-1 antisense oligodeoxynucleotide, alicaforsen (ISIS 2302), in active steroid dependent Crohn's disease. *Gut* 51:30-6.

Yacyshyn B, Chey WY, Wedel MK, Yu RZ, Paul D, Chuang E. 2007. A randomized, double-masked, placebo-controlled study of alicaforsen, an antisense inhibitor of intercellular adhesion molecule 1, for the treatment of subjects with active Crohn's disease. *Clin Gastroenterol and Hepatology* 5:215-20.

Yamada G, Hyodo I, Tobe K, Mizuno M, Nishihara T, Kobayashi T, Nagashima H.1986. Ultrastructural immunocytochemical analysis of lymphocytes infiltrating bile duct epithelia in primary biliary cirrhosis. *Hepatology* 6:385-91.

Yasoshima M, Nakanuma Y, Tsuneyama K, Van de Water J, Gershwin ME. 1995. Immunohistochemical analysis of molecules in the micro-environment of portal tracts in relation to aberrant expressin of PDC-E2 and HLA-DR on the bile ducts in primary biliary cirrhosis. *J Pathol* 175:319-25.

Zhu SG, Xiang JJ, Li XL, Shen SR, Lu HB, Zhou J, Xiong W, Zhang BC, Nie XM, Zhou M, Tang K, Li GY.2004. Poly (L-lysine)-modified silica nanoparticles for the delivery of antisense oligonucleotides. *Biotechnol Appl Biochem* 39:179-87.

Zouki C, Ouellet S, Filep JG.2000. The anti-inflammatory peptides, antiflammins, regulate the expression of adhesion molecules on human leukocytes and prevent neutrophil adhesion to endothelial cells. *FASEB J* 14:572-80.